

Asymmetric Synthesis of 1,2,3-Triazoles Utilising the Copper-Catalysed Azide-Alkyne Cycloaddition

By

William David George Brittain



UNIVERSITY OF
BIRMINGHAM

A thesis submitted to

The University of Birmingham

For a degree of

DOCTOR OF PHILOSOPHY

School of Chemistry

College of Engineering and Physical Sciences

University of Birmingham

March 2017

UNIVERSITY OF
BIRMINGHAM

University of Birmingham Research Archive

e-theses repository

This unpublished thesis/dissertation is copyright of the author and/or third parties. The intellectual property rights of the author or third parties in respect of this work are as defined by The Copyright Designs and Patents Act 1988 or as modified by any successor legislation.

Any use made of information contained in this thesis/dissertation must be in accordance with that legislation and must be properly acknowledged. Further distribution or reproduction in any format is prohibited without the permission of the copyright holder.

Abstract

The copper-catalysed azide-alkyne cycloaddition (CuAAC) is a highly efficient reaction and is the cornerstone of “click” chemistry. However, unlike many common metal-mediated transformations asymmetric CuAAC variants are relatively sparse. This thesis details asymmetric “click” reactions with Chapter 1 introducing the CuAAC and the asymmetric variants already present in the literature. Chapter 2 outlines research demonstrating the first example of kinetic resolution of an alkyne *via* a CuAAC reaction. Selectivity factors of up to 22.1 ± 0.5 were obtained and triazoles and alkynes were obtained in $\leq 80\%$ enantiomeric excess (*ee*). This chapter also contains a study on the simultaneous kinetic resolution of azides and alkynes; azides were obtained in $>30\%$ *ee*, alkynes in $>40\%$ *ee* and a triazolic diastereomeric product was obtained in up to 90% *ee*. In Chapter 3 the Bull-James three-component boronic acid assembly is successfully employed for the kinetic resolution of primary amine alkynes with selectivity factors of up to 4.1 obtained. The principle behind the assembly is also elaborated upon in this chapter leading to its use in both dynamic combinatorial chemistry and as a pedagogical tool. Chapter 4 details work on atropisomerism in triazolic systems. A series of novel triazoles, iodotriazoles and triazolium salts were successfully synthesised and their atropisomeric stability probed. Chapter 5 presents feasibility studies towards the asymmetric synthesis of 5,5'-bis(triazoles) and ruthenium olefin metathesis catalysts in the formation of 1,5-triazoles.

Acknowledgements

I think out of the entirety of writing this thesis trying to convey in this section all of the people who have helped me along the way is the most difficult task of all. Acknowledging all the friends, family and co-workers who have helped me in getting to this point is a mammoth task, I am going to try my best though.

Firstly, great thanks must go to my supervisors during the last 3 (ish) years. My main supervisor John Fossey has been a great mentor, allowing me to chase my own ideas and allowing me fantastic opportunities to visit places such as China and the USA. I always enjoyed the afternoon meetings where multiple structures would be drawn and redrawn on the whiteboard for hours normally to the conclusion of “well give it a go, what’s the worst that could happen”. He has helped greatly in proof reading of this thesis and also the myriad of dubious quality paper drafts I have sent him over the last few years. His guidance and support has been fantastic and I am very grateful for it. Ben Buckley has also been fantastic, always happy to skype at 5pm on a Friday! Big thanks go to him for looking after me in Utah and again I would like to say thanks for all the guidance, support and proof reading over the course of my PhD. I must say a huge thankyou to Eric Anslyn for looking after me during my two stints in Texas. He was a fantastic mentor always there for advice when I needed it. I really enjoyed being the UK expert within the group, I think my personal favourite moment was during group meeting where Eric put his new mug with the queen’s face proudly on the desk before saying “so Will, what do you think of that?”.

A big debt of gratitude goes out to all the people in the Fossey group who I have had the pleasure to work alongside. I would like to thank a few group members in particular, Mark taught me many of my synthetic skills during my masters project in the group and was always a source of excellent practical advice. I think his teaching style of frenetic dancing to

hypertronic dance music whilst throwing pipette fillers at me was pretty much the best way I could have learned. Dan was also a big help in making this thesis possible, we did a lot of projects together, some of them good some of them better left to never see the light of day. I would like to thank him for all the practical help, proofreading and most of all, lifts to Frankie and Benny's to eat family feasts. Rama, thanks for listening to me go on and on about nonsense, you were always there to listen to my problems. Wenlei, you were always a pleasure to work with, nothing ever too much trouble, I am extremely grateful for your help on many of the projects in this thesis. The other members of the group during my time have also been fantastic, Akina, Yiming, Xingjian, Mariwan, Glenn and Huy I wished I could write a section for each one of you but I think it might be longer than the thesis.

Masters and project students, even though at times you have been trying, must also be acknowledged for the massive contributions you have made. I will quickly list all the students I have had the pleasure to work with, Matt, Aisha, Lisa, Rob, Ethan, Kyle, Jack, Amy, Jordan, Nick, Andy, Samantha, Winter, Lizzie, Elliot, Ryan and Alex, all of you were great young scientists and I hope you go on to achieve big things in the future. I would like to especially thank three project students, firstly Nick thanks for help with submission of compounds and thanks for helping with other students over the summer it was much appreciated, I hope your PhD in the Grainger group goes well. Winter thanks so much with the help on the crystallisation work, without you and your exacting approach to science the absolute structure of those materials may never have been calculated. Finally, a massive thanks to Andy, without you much of chapter 2 simply wouldn't exist, the work on the sim KR project was vital in getting it to the point it is today. I really hope the PhD in Bristol goes well, I'm sure you are destined for big things.

I also need to acknowledge the members of the Anslyn group who were extremely warm and friendly to me during my time(s) in Texas, you treated me like one of the group from day one. Big thanks go to all the group members I shared an office with, Brette, Maggie, Igor, Rogelio, Logan, Brendan, Sam, Katharine and John, there was always something crazy going on in that office normally involving foam swords, blow up hammers (Brette I know it's called a whomp it) and suba seals. All the other members were also great and you guys really made me feel at home. Also thanks to Matt Sigman and all the Sigman group for making me feel at home in Utah and special thanks to Nick for looking after me.

I would also like to thank the Preece, Davies, Simpkins, Pikramenou and Grainger groups for their help with finding chemicals and equipment, I hope I wasn't too annoying. The members of the analytical facility are amazing, always willing to help. I would like to thank Louise Male for teaching me XRD, always being friendly and patient with me even when I had no idea what I was doing. Both Neil Spencer and Cécile Le Duff for help with NMR, both always happy to have a chat (mainly about broken spectrometers) and do some phenomenal spectroscopic work. Chi Tsang, John Snelling and Pete Ashton for running all my mass specs, especially big thanks to Chi for never turning me away even on the day I came down with 110 samples. Also, big thanks to Chi and Allen Bowden for help with chromatography.

All the friends I have made during my seven years in Birmingham have been amazing. I would like to name check a few but there are too many to be listed so if you're not here please don't be offended. Big thanks to John, Greg, Shani, Owen, Dennis, George, Pete, Louise, Ashleigh and Siobhan for being great friends over the years and for putting up with me.

I would like to say a special thankyou to Brette, you have been a constant source of support and I am very lucky to have met you. You are the best proof reader in the business (absolutely

deadly with a comma or hyphen) along with being an amazing co-worker and friend.

Thankyou (and Bonnie) for being there always, even if at times we were far apart.

Finally, my family have been pivotal in getting me to this point, Mom and Dad you are the best parents anyone could hope for. Even though you don't understand what I do, you are always happy to listen to me and try to understand, I am very grateful for that. You have helped me with guidance and support all the way from Claverley *via* Oldbury Wells to this point, I simply could not have got here without you.

Abbreviations

Ac	Acetyl
AMS	Angstrom Molecular Sieves
Ar	Aryl
BINAP	2,2'-Bis(diphenylphosphino)-1,1'-binaphthyl
BINOL	2,2'-Dihydroxy-1,1'-binaphthyl
Bn	Benzyl
Boc	<i>tert</i> -Butoxycarbonyl
Cat	Catalyst
CD	Circular Dichroism
CM	Cross Metathesis
COD	1,5-Cyclooctadiene
conv.	Conversion
Cp*	Pentamethylcyclopentadiene
CuAAC	Copper-Catalysed Azide-Alkyne Cycloaddition
Cy	Cyclohexyl
DBU	1,8-Diazabicyclo[5.4.0]undec-7-ene
DCE	Dichloroethane
DCM	Dichloromethane
DFT	Density Functional Theory
DIPEA	Diisopropylethylamine
DMAP	4-Dimethylaminopyridine
DMF	<i>N,N</i> -Dimethylformamide
DMSO	Dimethylsulfoxide

DNA	2-Deoxyribonucleic Acid
DPPA	Diphenylphosphoryl Azide
<i>dr</i>	Diastereomer Ratio
<i>E</i>	Entgegen
<i>ee</i>	Enantiomeric Excess
equiv.	Equivalents
ESI	Electrospray Ionisation
Et	Ethyl
<i>et al.</i>	<i>et alia</i>
FBDD	Fragment-Based Drug Discovery
FPBA	2-Formylphenylboronic acid
GC	Gas Chromatography
h	Hour(s)
HPLC	High-Performance Liquid Chromatography
HTS	High-Throughput Screening
<i>i</i> Pr	Isopropyl
<i>i</i> Pr-PHOX	[2-(Diphenylphosphino)phenyl]-4-isopropyl-4,5-dihydrooxazole
IUPAC	International Union of Pure and Applied Chemistry
KR	Kinetic Resolution
L	Ligand
<i>M</i>	Minus
M	Molar
Me	Methyl

Me-DUPHOS	1,2-Bis-[2,5-dimethylphospholano]benzene
min	Minute(s)
mol	Mole(s)
MW	Microwave
N	Normal
NaAsc	Sodium Ascorbate
NBS	<i>N</i> -Bromosuccinimide
"Bu	Butyl
NHC	<i>N</i> -Heterocyclic Carbene
NLE	Non-linear Effect
NMP	<i>N</i> -Methyl-2-pyrrolidone
NMR	Nuclear Magnetic Resonance
NORPHOS	2,3-Bis(diphenylphosphino)bicyclo[2.2.1]hept-5-ene
P	Primitive
<i>P</i>	Plus
Ph	Phenyl
ppm	parts per million
PyBox	Pyridine Bis(oxazoline)
<i>R</i>	Rectus
<i>rac</i>	Racemic
RCEYM	Ring Closing Ene Yne Metathesis
RCM	Ring Closing Metathesis
ROM	Ring Opening Metathesis
rt	Room Temperature

RuAAC	Ruthenium-Catalysed Azide Alkyne Cycloaddition
<i>S</i>	Sinister
<i>s</i>	Selectivity Factor
S _N 2	Nucleophilic Substitution Second Order
SPAAC	Strain-Promoted Azide Alkyne Cycloaddition
SPS	Solvent Purification System
TBAF	Tetrabutylammonium fluoride
TBTA	Tris[(1-benzyl-1 <i>H</i> -1,2,3-triazol-4-yl)methyl]amine
^t Bu	tertiary-Butyl
TCE	1,1,2,2-Tetrachloroethane
TEA	Triethylamine
Tf	Trifluoromethanesulfonyl
TFA	Trifluoroacetic acid
THF	Tetrahydrofuran
TLC	Thin Layer Chromatography
TMS	Trimethylsilane / Trimethylsilyl
Tol	Tolyl
UV	Ultraviolet
VT	Variable Temperature
v/v	Volume/volume
w/v	Weight/volume
XRD	X-ray diffractometry
Xyl	3,5-dimethylphenyl
Z	Zusammen

Table of Contents

Contents

1	Introduction	1
1.1	Click Chemistry	1
1.2	Types of Click Reactions	2
1.2.1	Nucleophilic Opening of Strained Rings	2
1.2.2	“Protecting Group” Reactions	3
1.2.3	The “Thiol Ene” Reaction	3
1.3	The Azide-Alkyne Cycloaddition	4
1.3.1	Thermally Promoted Azide-Alkyne Cycloaddition	4
1.3.2	Copper-Catalysed Azide-Alkyne Cycloaddition	6
1.4	Asymmetric CuAAC	18
1.5	Kinetic Resolution	27
1.6	Triazoles	30
1.6.1	Triazoles in drug development	31
1.6.2	Triazoles in other applications	34
1.7	Conclusion	34
2	Kinetic Resolution of Terminal Alkynes via Copper-Catalysed Azide-Alkyne Cycloadditions	36
2.1	Kinetic Resolution of Quaternary Oxindoles via CuAAC	39
2.1.1	Summary	57
2.2	Simultaneous Kinetic Resolution of Azides and Alkynes via Copper-Catalysed Azide-Alkyne Cycloadditions	57
2.3	Summary	69
3	Three-Component Boronic Acid Assemblies, Applications in Asymmetric Catalysis, Combinatorial Chemistry and Pedagogy	70
3.1	High-Throughput Screening for ee Determination	70
3.2	The Bull-James Assembly for Use in Asymmetric Catalysis	73
3.2.1	Summary	85
3.3	Three-Component Boronic Acid Assemblies in Water and Potential Application in Dynamic Combinatorial Chemistry	86
3.3.1	Summary	96
3.4	The Bull-James Assembly Application in Pedagogy	96
3.4.1	Experimental Design	97
3.4.2	Assessment and Feedback	102

3.4.3	Summary	103
4	Atropisomeric Triazoles and Triazoliums Designed for Use as Chiral N-Heterocyclic Carbenes	104
4.1	Synthesis of Novel Atropisomeric Triazolium Salts	104
4.1.1	Summary	123
4.2	Chiral 4-Dimethylaminopyridine Derivatives Synthesised by CuAAC and Attempted Kinetic Resolution of Secondary Alcohols	124
4.2.1	Summary	130
5	Studies Toward Asymmetric 5,5'-Bis(triazole) Formation and The Use of Ruthenium-Based Olefin Metathesis Catalysts in the Synthesis of 1,5-Triazoles	131
5.1	Studies Toward Asymmetric 5,5'-Bis(triazole) Formation	131
5.1.1	Summary	137
5.2	The Use of Ruthenium-Based Olefin Metathesis Catalysts in the Synthesis of 1,5-Triazoles	137
5.2.1	Summary	147
6	Conclusion and Future Work	148
7	Appendix 1 Experimental	154
7.1	General	154
7.2	Experimental for Chapter 2	155
7.2.1	Synthesis	155
7.2.2	Screening Tables for Kinetic Resolution of Compound 85	168
7.2.3	Chromatography for Chapter 2	171
7.2.4	Experimental for the Kinetic Resolution of Quaternary Oxindoles	172
7.2.5	Kinetic Resolution of Quaternary Oxindoles Chromatography	187
7.2.6	Simultaneous Kinetic Resolution of Azides and Alkynes	191
7.2.7	Simultaneous Kinetic Resolution Chromatography	208
7.3	Experimental Chapter 3	215
7.3.1	Experimental for the Kinetic Resolution of Primary Amine Alkynes	215
7.3.2	Experimental for Boronic Acid Assemblies in Aqueous Environments	223
7.3.3	Chapter 3 Chromatography	227
7.4	Chapter 4 Experimental	233
7.4.1	Synthesis	233
7.4.2	Chromatography Chapter 4	261
7.5	Experimental Chapter 5	264
7.5.1	Synthesis	264
7.5.2	Chromatography Chapter 5	268

8	Appendix 2 Crystal Structure Data	270
9	Appendix 3 Undergraduate Experiment Supporting Documents	283
9.1	Student Experimental Procedure	283
9.2	Student Proforma	293
10	References	299

1 Introduction

1.1 Click Chemistry

The area of “click chemistry” was defined by K. B. Sharpless in 2001.^[1] Click chemistry is a set of reactions which must satisfy a set of core principles. To fulfil these, a reaction should give the product in extremely high yields, excellent purity and require no chromatographic purification. Due to these properties, click chemistry has become increasingly popular and papers published with the topic “click reaction” have shown an upward trend during the period of 2001-2016 (Figure 1).

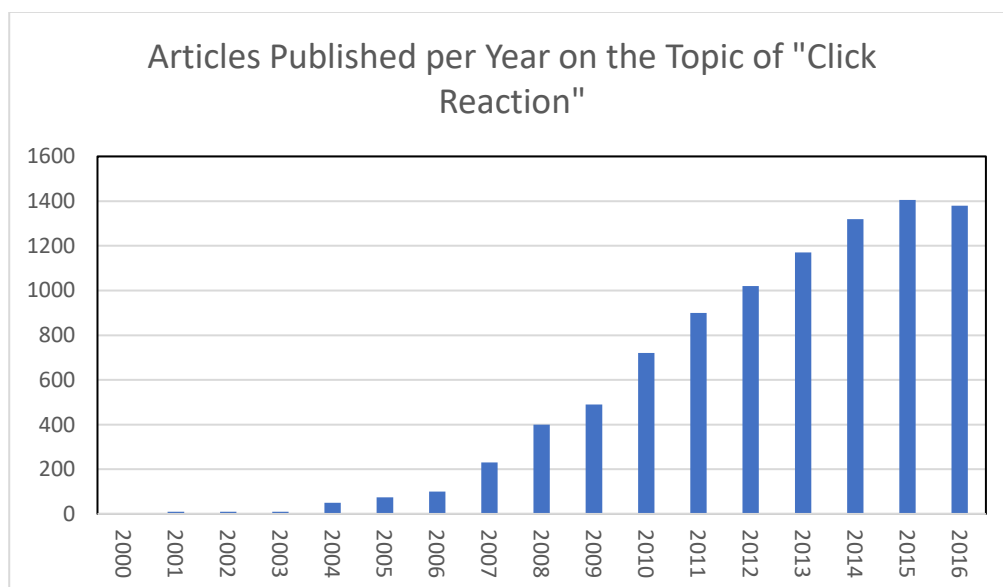


Figure 1 Items published on the topic of "click reaction" in the period 2000-2016 (Data from Web of Science Thomas Reuters 2017)

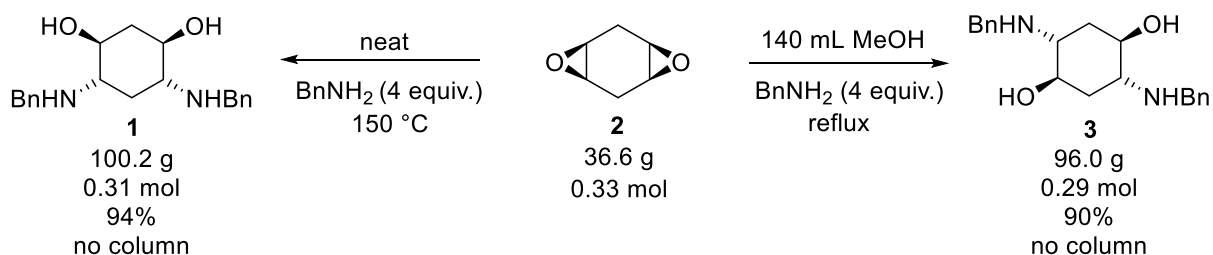
Click reactions allow molecular complexity to be built up rapidly and in a modular way. This lends click a flexibility few other reactions possess; diverse functionalities and molecular structures can be achieved in a synthetically straightforward manner. This convenience and reproducibility has undoubtedly led to the increasing popularity of click chemistry over recent years.

1.2 Types of Click Reactions

1.2.1 Nucleophilic Opening of Strained Rings

Strained-ring systems are highly reactive species. Three-membered rings such as epoxides, aziridines, cyclic sulfates, cyclic sulfamidates, aziridinium ions and episulfonium ions are all electrophilic systems which are prone to opening.

The thermodynamic stability of ring-opened products means they can often be recovered in close to quantitative yields and with good purity. Products are obtainable chemoselectively due to the stereochemical disfavouring of possible elimination pathways. For example, taking the diepoxide **2** and exposing it to two differing sets of conditions can yield two diastereoisomers **1** and **3** with high efficiency (Scheme 1). This reaction therefore epitomises the idea of click chemistry. It should also be noted that these reactions can usually be carried out neat or in water/alcohol mixtures (benign solvent systems are another feature of click chemistry) and in the case of some ring openings, water can actually promote the process.^[2]



Scheme 1 Diepoxide opening to give diastereoisomers dependent on reaction conditions

The “spring-loaded” nature of three-membered rings is due to their inherent strain, which is relieved upon ring-opening. A common feature to all click reactions is that they have a high thermodynamic driving force pushing the reaction to a single product. The thermodynamics

of click reactions thus inform their characteristics of being highly efficient and chemoselective with minimal amounts of purification required.

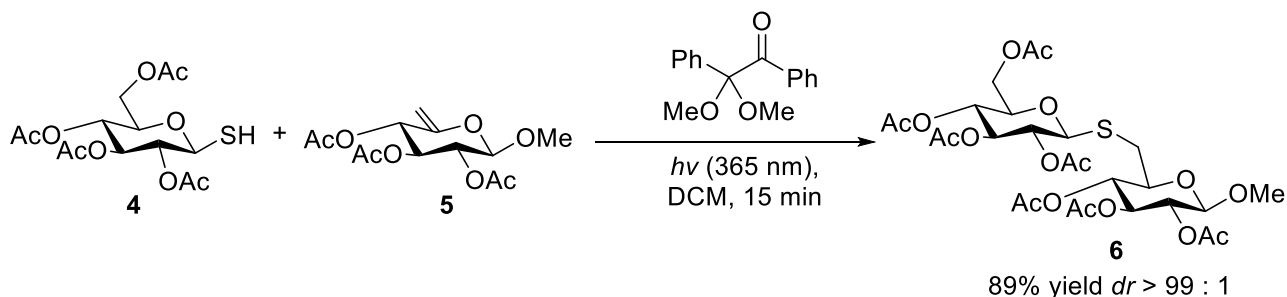
1.2.2 “Protecting Group” Reactions

Sharpless argues that reactions many view as only useful in protecting other moieties are a way to form medically relevant heterocyclic compounds in a highly efficient manner.^[1] Acetal and ketal formation along with their aza-analogues are ways of protecting diol functionality, but it can be argued that in addition they afford these biologically relevant heterocycles.^[3] Bioavailability of these systems can be good if they are tuned to be stable at physiological pH, adding further weight to Sharpless’s argument concerning the drug-like nature of these compounds and their inclusion under the umbrella of click products.^[4]

1.2.3 The “Thiol Ene” Reaction

Since the outlining of click chemistry in 2001, the thiol-ene reaction has become considered by many to fulfil Sharpless’s criteria of a click reaction. The thiol-ene coupling sees the reaction of a thiol and an alkene through a free radical or Michael addition catalyst to form a thioether. The coupling can garner products in quantitative yields, requiring low catalytic loading with benign catalysts in environmentally benign solvents, without sensitivity to air or water and with versatility of application.^[5]

One such application is in the synthesis of thiodisaccharides, Dondoni and co-workers utilised photoinduced thiol-ene couplings to form a range of disaccharides (Scheme 2) in a quick and highly efficient manner with excellent selectivity observed.^[6]



Scheme 2 Synthesis of thiodisaccharides, Dondoni and co-workers.^[6]

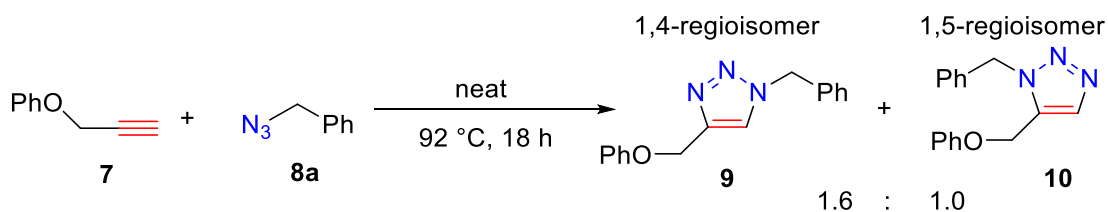
The thiol-ene reaction has seen extensive use in polymer- and dendrimer-based chemistry.^[5] For example, using a thermally promoted thiol-ene reaction, Heidecke and Lindhorst were able to form spaced glycodendrons.^[7] These dendrimers were tested for biological activity and were found to be active inhibitors of type 1 fimbriae-mediated bacterial adhesion. Using the thiol-ene reaction, large dendrimers and polymers can be synthesised efficiently in high yields with potent biological activity, thus exemplifying the ideology behind click chemistry.

1.3 The Azide-Alkyne Cycloaddition

The azide-alkyne cycloaddition is without doubt the reaction most think of when the topic of click chemistry is mentioned. This is with good cause; Sharpless himself refers to the copper-catalysed version as the “cream of the crop” of click reactions.^[1] The reaction between an azide and an alkyne is a Huisgen 1,3-dipolar cycloaddition with the product being a 1,2,3-triazole. The reaction can be quantitative with high purity products, in water and with very mild reaction conditions if the correct catalysts are employed. The variants of the azide-alkyne cycloaddition are discussed below.

1.3.1 Thermally Promoted Azide-Alkyne Cycloaddition

The azide-alkyne cycloaddition can be carried out without the use of any catalyst under thermal conditions. Heating the two starting materials **7/8a** in the absence of solvent will afford the triazolic product as a mixture of 1,4- and 1,5- regioisomers **9/10**. The regiochemical control of the thermally promoted reaction is poor, with a 1.6:1.0 mixture of the 1,4- and 1,5- regioisomers **9/10**, respectively (Scheme 3). This is due to the HOMO-LUMO energy gap of the two possible regiochemical pathways being too close in energy for regioselectivity to be achieved with thermal promotion alone.

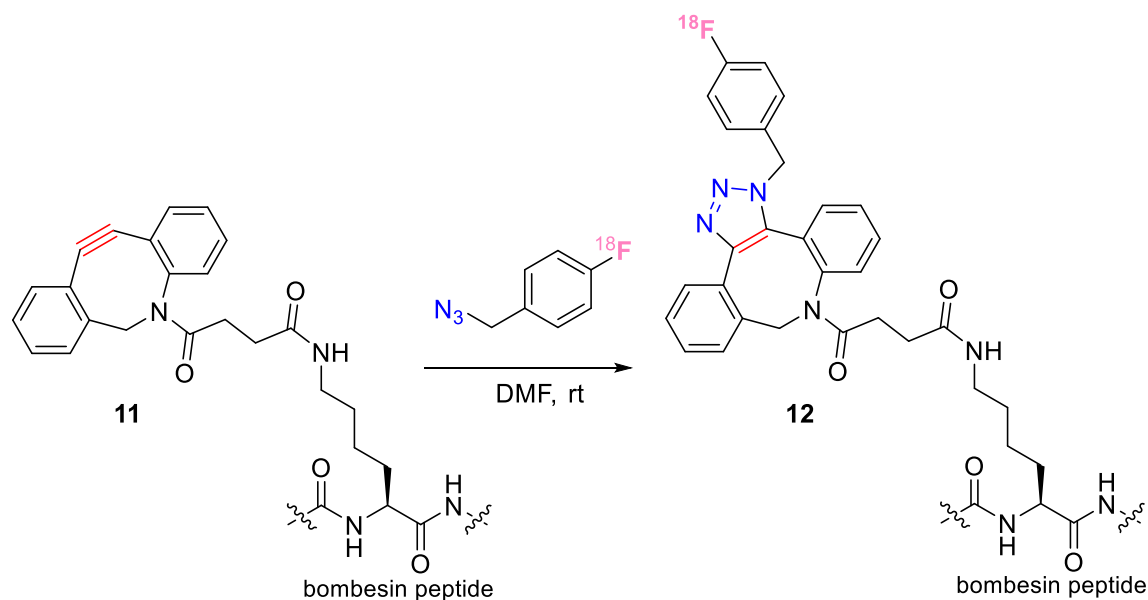


Scheme 3 Thermally promoted azide-alkyne cycloaddition

Even though the thermal azide-alkyne cycloaddition is regiochemically unpredictable, it has still been used in a variety of applications,^[8] mainly in strain-promoted situations and where regioisomeric control is not important.

The combination of thermal promotion along with the reactivity of strained alkynes has led to the development of the strain-promoted azide-alkyne cycloaddition (SPAAC). Removal of ring strain from cyclic alkynes (e.g. Sondheimer diynes) greatly decreases the activation energy required for triazole formation, and SPAACs can often be carried out at room temperature.^[8b] Strain-promoted thermal reactions are especially attractive for *in vivo* applications. The absence of transition metal catalysts, which are often used to promote triazole formation, allows SPAACs to be used within the body without unwanted interactions with metal catalysts *i.e.* copper within the CuAAC. For example, Feringa and co-workers used the SPAAC for ¹⁸F radioactive labelling of bombesin, a protein which is over-expressed in cancer cells (Scheme 4).^[8c] This allows for the imaging of bombesin, which was tested on

human prostate cancer cells, thus further cancer treatments can be applied in a targeted manner.



Scheme 4 ^{18}F Radioactive labelling of bombesin peptides through SPAAC, Feringa and co-workers^[8c]

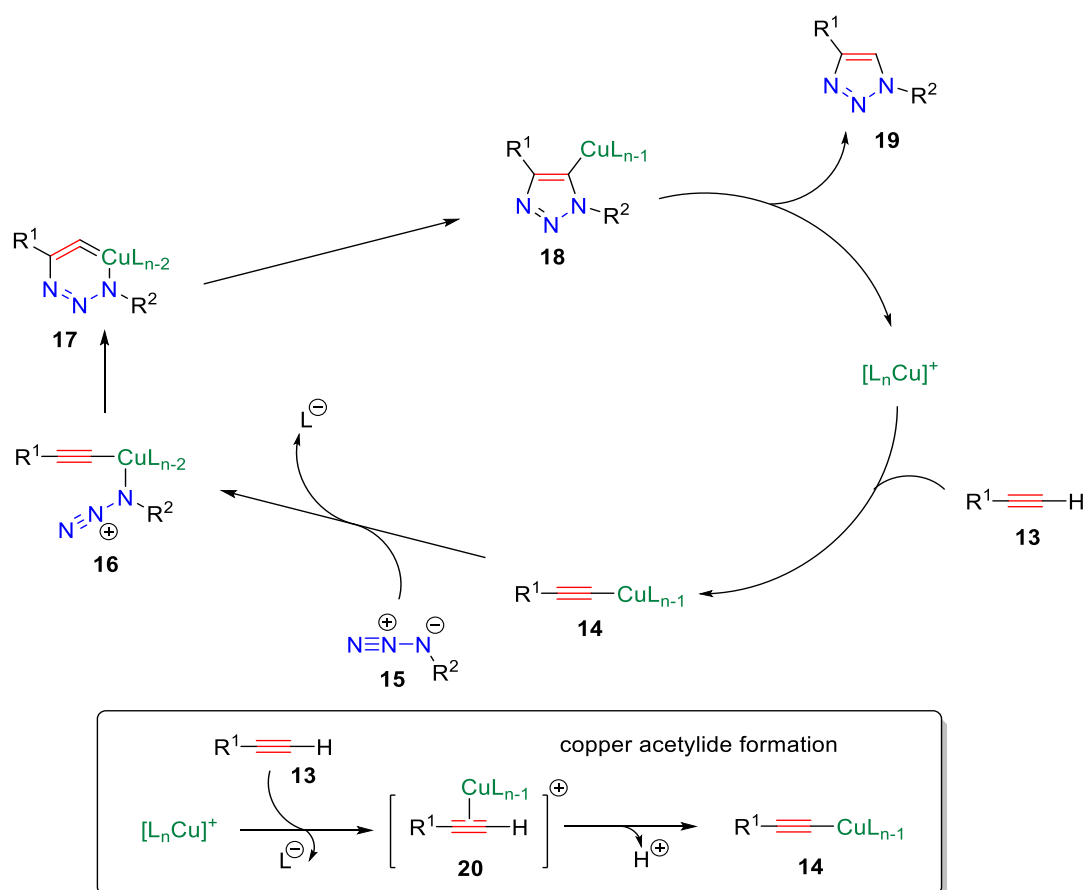
1.3.2 Copper-Catalysed Azide-Alkyne Cycloaddition

First reported by both Tornøe *et al.* and Sharpless and co-workers in 2002, the copper-catalysed variant of the azide-alkyne cycloaddition has become known as “the click reaction”.^[9] The introduction of a copper(I) catalyst dramatically decreases the activation energy required to form the triazole compared with thermal promotion only (an increase in seven orders of magnitude in the rate of reaction between copper-catalysed and thermal) and thus very mild reaction conditions can be used. The triazolic product from the click reaction is a very thermodynamically stable entity, according to the calculated energy potentials.^[1, 10]

1.3.2.1 The Catalytic Cycle

Despite the ubiquitous nature of the CuAAC, the precise nature of its catalytic cycle has been debated since its original discovery. Using density functional theory (DFT) calculations,

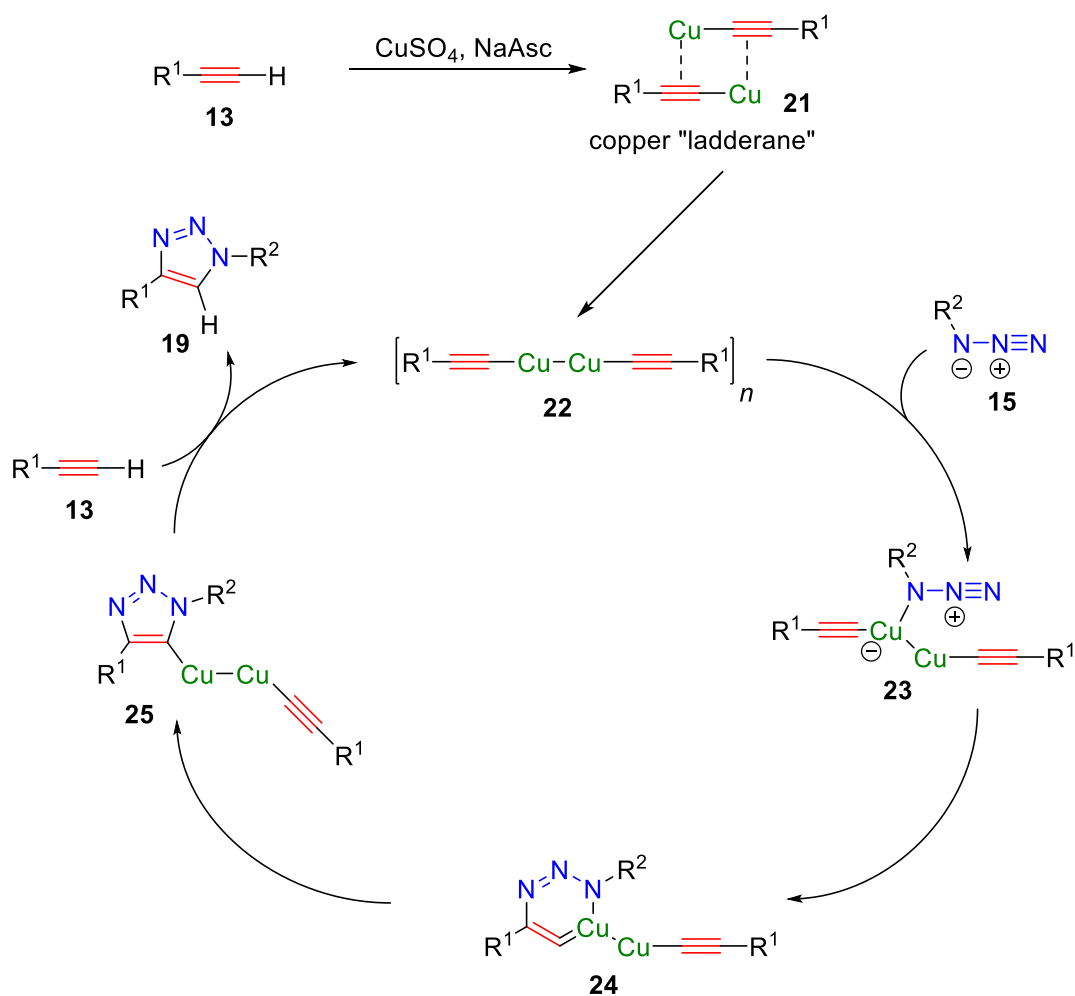
building on preliminary proposals in 2002, Sharpless and co-workers proposed the first iteration of the cycle in 2005 (Scheme 5).^[11] It was proposed that the cycle begins with the formation of a copper acetylide species **14** which is also observed in C-C bond-forming copper-catalysed reactions (e.g. Glaser and Castro-Stephens couplings).^[12] After the formation of the copper acetylide, the azide also coordinates to the same copper centre **16**. Finally, the formation of a six-membered metallocyclic intermediate **17** and subsequent protonation garners the triazole as the 1,4-regioisomer **19**.



Scheme 5 Proposed CuAAC catalytic cycle, utilising a single catalytically active copper centre, Himo *et al.*^[11]

The catalytic cycle depicted in Scheme 5 appeared to explain both the massive increase in rate compared with the thermal reaction (due to lowering of the activation barrier of the rate-determining step), but also the regioselectivity observed (due to the coordination and

orientation of the alkyne to azide in proposed intermediate **16**). However, copper acetylides are complicated species; they seldom exist as discrete entities. It was questioned if the simplistic modelling of the acetylenic species was accurate, or whether a multinuclear copper species was taking part.

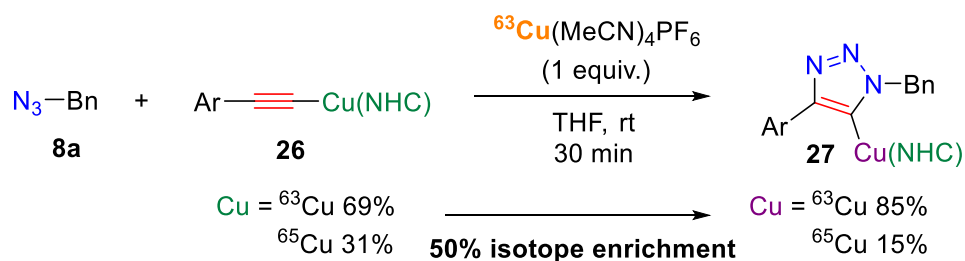


Scheme 6 Proposed mechanism of the CuAAC involving copper ladderanes, Buckley *et al.*^[13]

The multinuclear hypothesis was supported by experimental evidence: Rodinov *et al.* found that the CuAAC process was second order with respect to copper, which did not fit with the outlined copper acetylide model.^[14] Other researchers have also evidenced that more than one copper centre is needed for catalytic turnover. Buckley *et al.* showed through preforming a binuclear copper “ladderane” complex **21**, the formation of triazolic species was subsequently

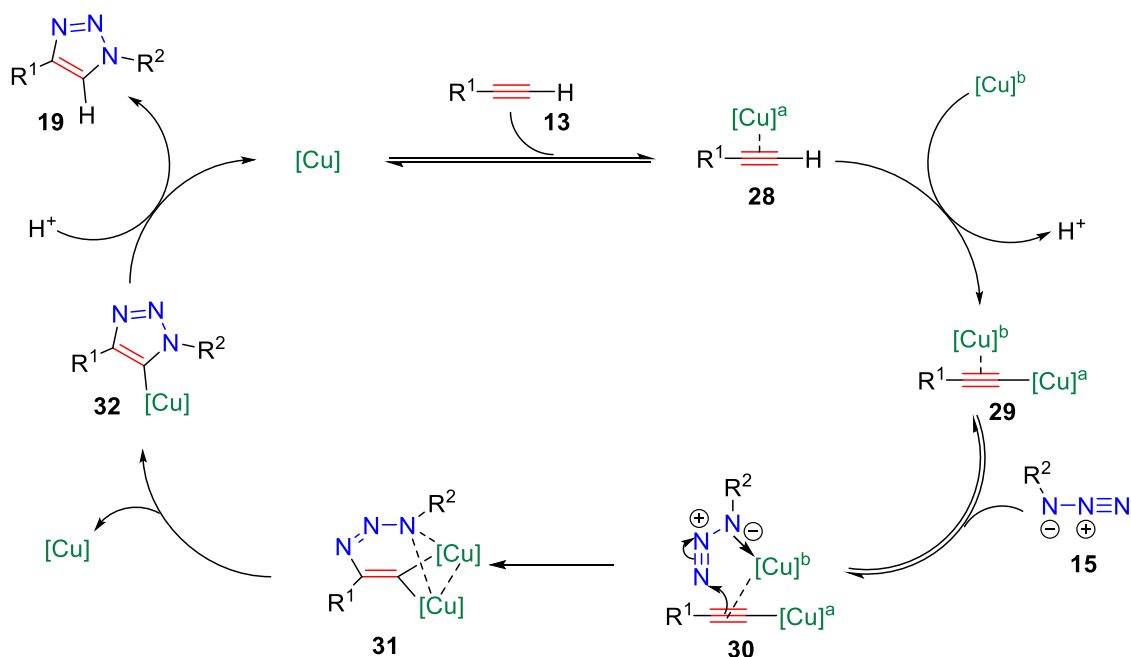
possible, and from this determined that dinuclear alkynylcopper(I) species **22** could be responsible for catalysis (Scheme 6).^[13] Modelling by Ahlquist and Fokin would lend further evidence to a non-monomeric copper species being responsible for catalysis.^[15] By modelling potential dinuclear copper acetylides and transition states using DFT, it was found that the activation barrier towards the cycloaddition reaction was significantly lowered compared with the previously proposed monomeric species. They proposed that the formation of the metallocyclic intermediate **17** was the rate determining step. Calculating the transition state energies during cycloaddition and for the proposed metallocyclic intermediate **17** for a combination of σ and π coordinating copper atoms, they calculated that the rate of reaction when using a dimeric copper species should be several orders of magnitude greater than that of a monomeric copper species.

This new evidence led to the revisiting of the proposed catalytic cycle to incorporate multiple copper centres. Thus, several revisions have been made in the intervening years. A proposed cycle by Worrell *et al.* (2013) incorporates two active copper centres per alkyne (Scheme 7).^[16] They proposed that the two copper centres fulfil specific and separate roles: one as a strong σ -bound ligand and one interacting only through weak π interactions. Using a copper isotope enrichment crossover study, which took advantage of the stability of copper *N*-heterocyclic carbene (NHC) triazolide species, they saw that the isotopic distributions between the starting copper acetylide **26** and the resulting CuNHC-triazolide complex **27** were not the same (Scheme 7). This showed that the copper atoms can cross between σ and π complexation.



Scheme 7 Isotope enrichment study, Worrell *et al.*^[16]

From this observed isotopic distribution, it was questioned at which point during the CuAAC reaction could isotopic enrichment take place. Using control experiments, they ruled out the possibility for the switchover to take place in either the copper acetylide **26** or copper NHC-triazolide species **27**. Therefore, the enrichment must take place during the cycloaddition steps. From these findings, a new catalytic cycle was proposed (Scheme 8). First, a copper acetylide species is formed with a second copper centre coordinating in a π fashion across the alkyne **29**. An azide coordinates to the second copper atom **30**, forming a metallocyclic intermediate, in which both copper centres are σ -bonded in intermediate **31**. At this stage, as there is no bias towards ejecting one copper centre or the other to form the triazolide **32** (when using a CuNHC), thus explaining the observed isotopic enrichment seen in Scheme 7. There may be a bias to which copper atom is ejected, dependent upon the ligand employed; however, this has not been studied. In the cases in which NHC-based ligands have been used, there is no bias observed. Finally, the copper dissociates and the copper-triazole is protodemetalated to give product **19**.



Scheme 8 Proposed CuAAC catalytic cycle taking into account isotopic copper enrichment, Worrell *et al.*^[16]

The Worrell *et al.* cycle has led to more work using stabilised copper NHCs to isolate the proposed dinuclear intermediates. In 2015, Iacobucci *et al.* used mass spectrometry to directly detect dinuclear copper intermediates for the first time.^[17] Through the combination of electrospray ionisation (ESI) and use of NHC-stabilised alkynes (such as those used by Worrell *et al.*) **26** they were able to record *m/z* peaks that related to dinuclear copper-alkyne-azide complexes, thus lending evidence to the hypothesis that indeed two copper centres are present during the cycloaddition process.

Further detailed research has been carried out on the dinuclear catalytic hypothesis to lend supporting evidence to the proposals of Worrell *et al.* from 2013 (Scheme 8). Using the increased stability of NHC copper acetylide intermediates, Bertrand and co-workers were able to isolate and crystallise dinuclear CuAAC intermediates and showed that these could be used to generate triazoles (Figure 2).^[18] This finding, that two copper centres can successfully interact with a terminal alkyne at the same time, helps to confirm the previously postulated dinuclear nature of the catalytic cycle.

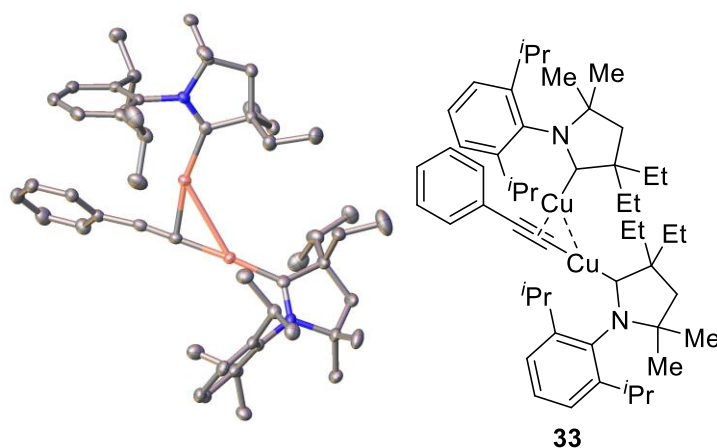
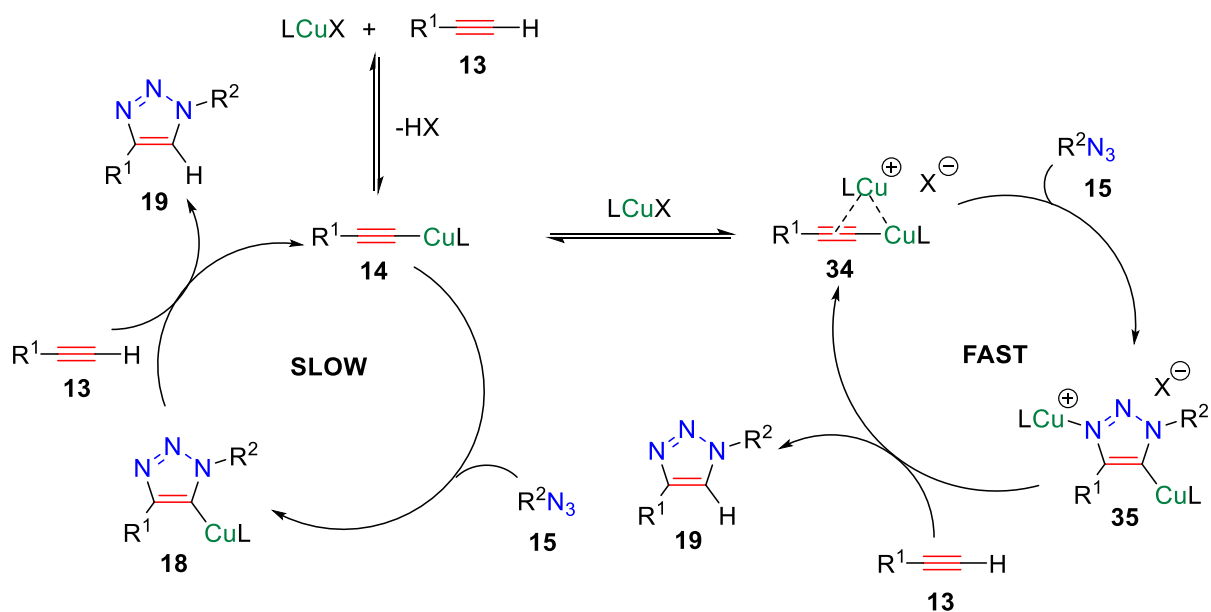


Figure 2 Crystal structure of a dinuclear copper NHC σ and π coordinated terminal alkyne, a proposed catalytic intermediate, Bertrand and co-workers^[18] Ellipsoids are drawn at the 50% probability level, protons are omitted for clarity.

Bertrand performed two different copper acetylides, the σ -coordinated only version, invoked in the mononuclear pathway, and the σ/π -coordinated species **33**, associated with the dinuclear pathway. The two copper acetylides were then used in a stoichiometric fashion as preformed catalysts in the reaction of benzyl azide and phenylacetylene. Both reactions proceeded, but it was found that there was a significant difference in the rate of triazole formation between the two preformed catalysts. It was found that triazole formation was faster when copper acetylide **33** was employed. This rate difference was attributed to the increased strain in the six-membered metallocyclic intermediate **17** compared with the intermediate **31** proposed in the dinuclear cycle. Thus, a new catalytic cycle was proposed, this featured both possible (mono and multinuclear) pathways. It was proposed that the multinuclear pathway is favoured (Scheme 9).



Scheme 9 Proposed catalytic cycle Bertrand *et al.*^[18]

This finding is supported by the work of Makaram *et al.*, in which tethered NHC ligands were used to form crystalline copper acetylide clusters **36** (Figure 3). These clusters exhibited the same forms of copper-alkyne complexation as observed by Bertrand (each alkyne had a σ and π coordinated copper centre associated with it). Upon addition of acid, the clusters became extremely catalytically active (the CuAAC reaction had proceeded to quantitative conversion before an NMR spectrum could be taken).

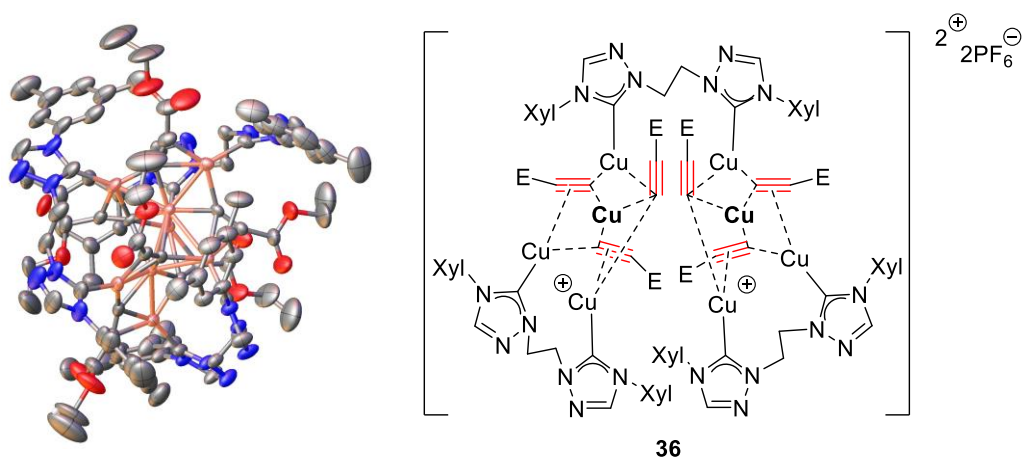


Figure 3 Copper acetylide cluster crystallised by Makaram *et al.*^[19] E = COOEt, Xyl = 3,5-dimethylphenyl. Ellipsoids are drawn at the 50% probability level, protons and counterions are omitted for clarity.

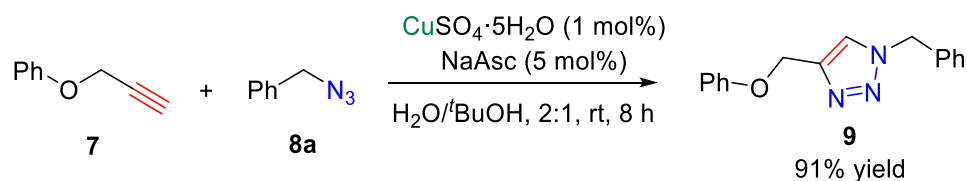
The mechanistic aspects of the CuAAC have been shown to be more complicated than originally thought. Considering the complex nature of copper acetylide species, a fuller picture of the working of the CuAAC is beginning to emerge. There is still much investigation to be carried out in the pursuit of a definitive catalytic cycle for the CuAAC.

1.3.2.2 Synthetic Considerations

1.3.2.2.1 Copper Sources

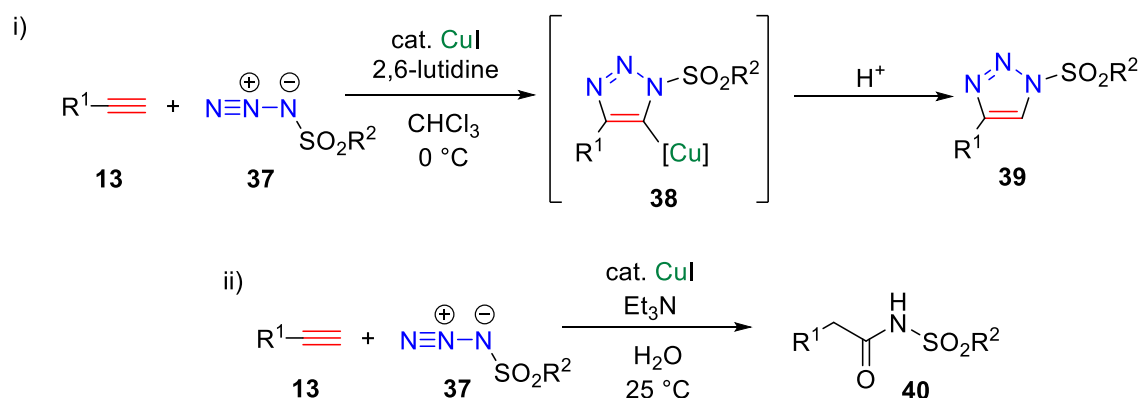
As with any reaction there are certain synthetic considerations which must be considered when employing a CuAAC. The choice of copper source is one aspect that requires planning. The CuAAC is a copper(I)-catalysed process and therefore only certain copper sources will work straight from the reagent bottle.

Copper(II) sulfate is the most widely reported choice (according to tabulated data by Meldal *et al.*^[20]) and was identified as a possible copper source by Fokin and Sharpless. The use of copper(II) sulfate has become ubiquitous and some have come to refer to these reaction conditions as “the Sharpless-Fokin protocol” (Scheme 10).^[13] Copper(II) sulfate requires a reducing agent (typically sodium ascorbate (NaAsc)) in order to become catalytically active. NaAsc is water-soluble and therefore copper(II) sulfate-catalysed reactions are often carried out in mixtures of alcohol and water, which are considered environmentally friendly, “green” solvents. The use of a slight excess of NaAsc prevents the formation of alkyne homocoupling products (e.g. through Glaser coupling) which are sometimes seen when copper and alkynes are present together.^[11] Due to the wide range of reaction conditions (solvents, temperatures and ligands) that can be employed, copper(II) sulfate is often seen as the first choice when it comes to carrying out the CuAAC.



Scheme 10 Sharpless-Fokin protocol for CuAAC

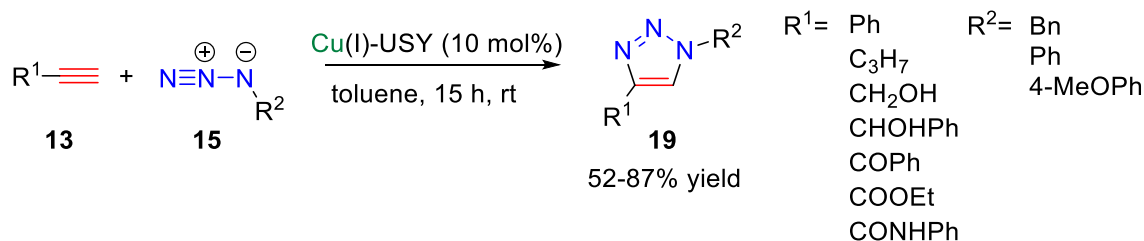
Copper (I) iodide is another popular choice for click reactions, as it is air-stable, easy to handle and commercially available at an economical price. It has been found that additives such as nitrogen-containing bases (diisopropylethylamine (DIPEA) or triethylamine (TEA)) or strongly coordinating ligands can help to increase the rate of reaction when CuI is employed as a catalyst for a CuAAC.^[21] Copper(I) iodide can be used in specialist anhydrous examples too, where the substrates may not be stable in the classical water/alcohol mixtures employed when Copper(II) sulfate is utilised as a catalyst. For example, Yoo *et al.* used copper(I) iodide for the formation of *N*-sulfonyl-1,2,3-triazoles **39** (Scheme 11).^[22] Prior work had shown that when water was used as the reaction medium, with sulfonyl azides, triazole formation did not occur, and instead copper-catalysed hydrative amide formation **40** was observed (Scheme 11).^[23]



Scheme 11i) Synthesis of *N*-sulfonyl-1,2,3-triazoles Yoo *et al.*^[22] ii) Copper-catalysed hydrative amide formation Cho *et al.*^[23]

While copper(II) sulfate and copper(I) iodide are widely used for CuAAC, researchers have also developed a range of other copper catalysts. Copper(0) sources (wire, turnings and chips) have been successfully used in CuAAC reactions, but they show a latency period before catalytic turnover occurs. Addition of a copper(II) source can improve reactivity due to the disproportionation chemistry of copper.^[24] An advantage of using copper(0) sources is that the majority of the inactive metallic copper(0) can often be simply filtered out, facilitating product recovery.^[25] Copper(0) sources, whilst being catalytically active, have not been employed widely due to their latency period and need in many cases to include a copper(II) source anyway.

Other, non-commercially available copper-containing species have also been successfully used in CuAACs. For example, Chassaing *et al.* successfully developed a range of copper(I) exchanged zeolites and examined these for catalytic activity.^[26] It was found that a copper(I)-USY zeolite catalyst offered the best isolated yield of triazolic products **19**. They were also able to carry out a range of CuAAC reactions with tolerance to various functional groups (Scheme 12). Other solid-supported copper sources have also seen use: cross-linked polymers,^[27] activated charcoal,^[28] alumina,^[29] aluminium oxyhydroxide fibres^[30] and silica^[31] have all been used as copper supports for CuAAC reactions.



Scheme 12 Triazole formation utilising a Cu(I) zeolite catalyst, Chassaing *et al.*^[26]

From the above examples, it has been shown that a wide selection of copper sources can be used to effect a CuAAC. This flexibility means that the experimentalist can choose the correct copper source to fit with his/her synthetic conditions.

1.3.2.2.2 Solvents

To satisfy the definition laid out by Sharpless, a click reaction must be able to be carried out in “*benign (such as water) or easily removed*” solvents. The CuAAC is extremely tolerant to a wide range of solvents, many of which fit with Sharpless’s definition.

The majority (according to tabulated data by Meldal *et al.*)^[20] of CuAACs are carried out in water or alcohol mixtures. The classic copper(II) sulfate-NaAsc reaction is carried out in a water:^tBuOH mixture. The reaction can be performed in almost any solvent, but, technically, once a non-benign solvent is used, the reaction cannot be classed as a click reaction.

1.3.2.2.3 Ligands

A common addition to CuAAC reactions is a ligand for the copper catalyst. It has been shown that the CuAAC is susceptible to the ligand acceleration effect.^[21] Ligands within CuAAC reactions can fulfil multiple roles in order to increase the rate of reaction. The coordination of chelating ligands to copper(I) atoms helps decrease the ability for the reaction solvent to competitively bind to the catalytic metal centre, thus preventing strongly coordinating solvents (e.g. DMSO, DMF or NMP) from inhibiting the reaction. Ligands can also help to preorganise two copper atoms into a highly reactive species and lead to increased rates of reaction. Many ligands exist for the CuAAC reaction (too many to fully discuss here), and several were developed by Finn and co-workers based upon multiple nitrogen-containing heterocycles such as the widely used tris[(1-benzyl-1*H*-1,2,3-triazol-4-yl)methyl]amine (TBTA) ligand **41** (Figure 4).^[21] These were found to greatly increase the rate of reaction of the CuAAC compared with reactions without ligands by decreasing competitive binding with

coordinating solvents and by binding two copper atoms, therefore preorganising the catalytically active metal centres towards reaction. There are also a wide range of nitrogen-containing asymmetric ligands which are discussed in Sections 1.4 and 2.1.

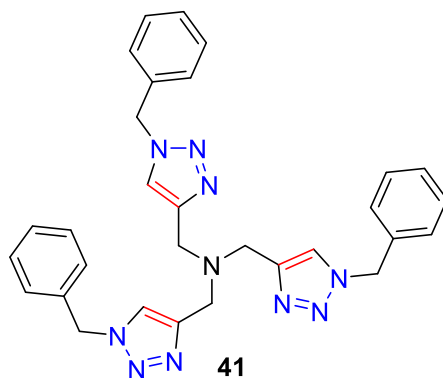


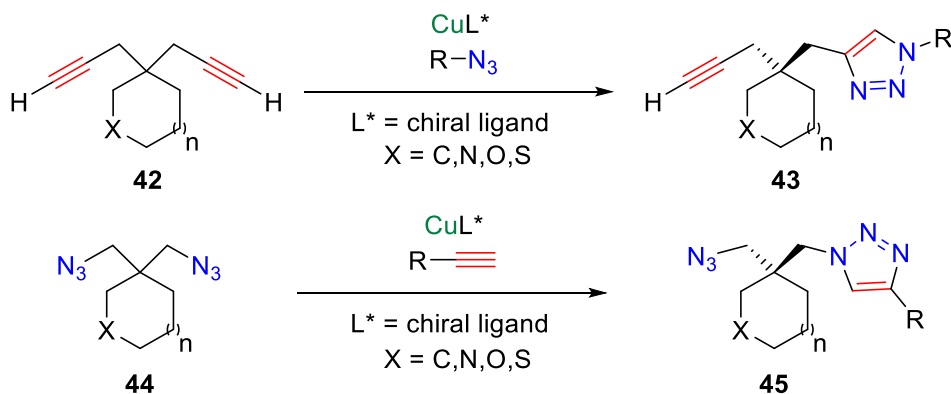
Figure 4 Tris[(1-benzyl-1H-1,2,3-triazol-4-yl)methyl]amine (TBTA)

1.4 Asymmetric CuAAC

Despite the ubiquity of the CuAAC, there are relatively few examples of asymmetric variants. Installing triazoles with stereochemical control to form defined stereocentres could be important for many applications (applications of triazoles are detailed in Section 1.6). Researchers have tried several different approaches to influence the stereochemical outcome of the CuAAC.

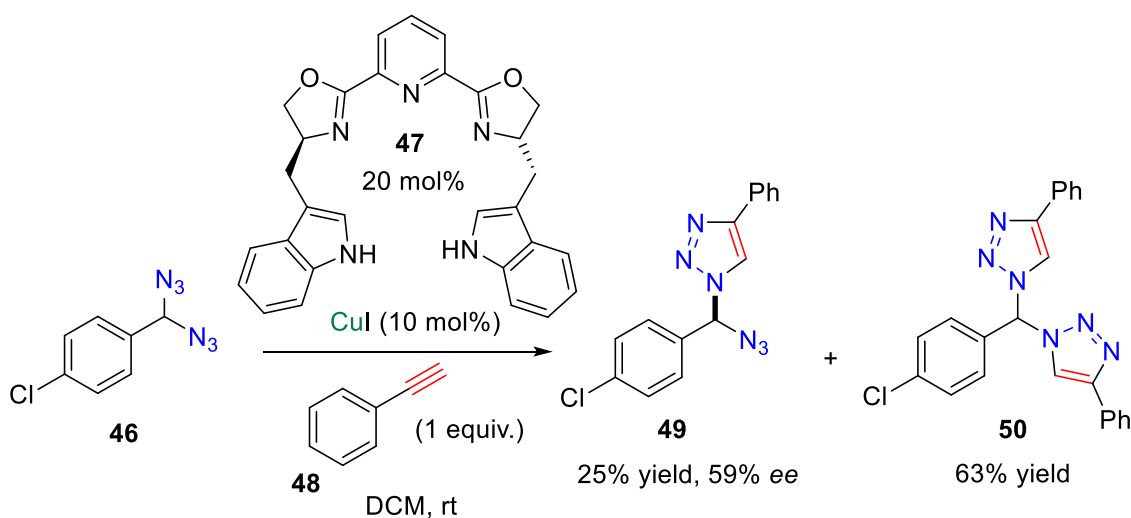
Desymmetrisation is one strategy which has been targeted. Desymmetrisation is defined by the International Union of Pure and Applied Chemistry (IUPAC) as “*the modification of an object which results in the loss of one or more symmetry elements, such as those which preclude chirality (mirror plane, centre of inversion, rotation-reflection axis), as in the conversion of a prochiral molecular entity into a chiral one*”. This strategy is particularly attractive to the synthetic chemist because a desymmetrisation reaction can take a racemic starting material and produce a single isomer of product with a quantitative theoretical maximum yield. In the case of the CuAAC, a starting material which contains two terminal

acetylenic groups **42** or two azides **44** could form a single isomer of product (**43** or **45**) through a selective triazole formation (Scheme 13).



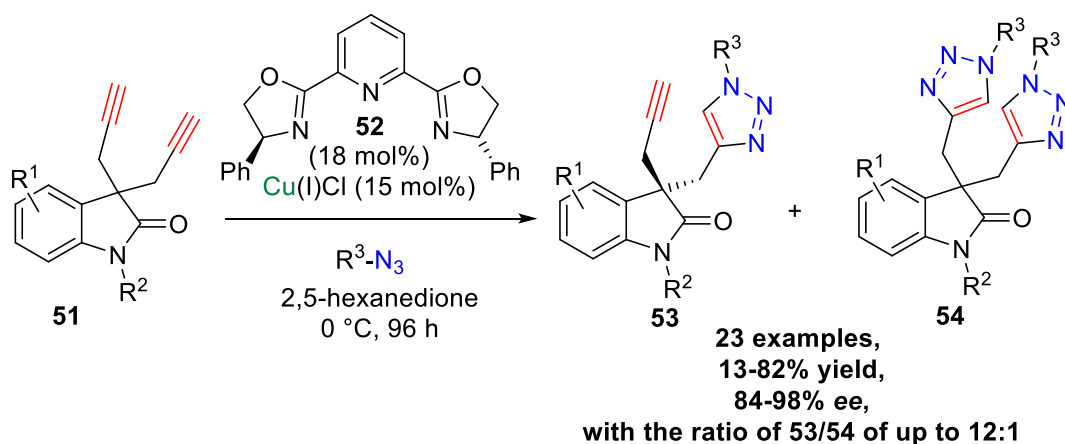
Scheme 13 General desymmetrization strategies where ($n \geq 1$)

The first desymmetrisation using CuAACs was reported by Meng *et al.* in 2005.^[32] Using *gem*-diazides **46** and an indole-appended pyridine bis(oxazoline) (PyBox) ligand **47**, they were able to obtain a 25% yield of 59% *ee* desymmetrised product **49** (Scheme 14). The observed selectivity demonstrated that carrying out the CuAAC with some degree of stereo control was possible, and set the groundwork for future asymmetric triazole formations.



Scheme 14 Desymmetrisation of *gem*-diazides using CuAAC, Meng *et al.*^[32]

The desymmetrisation of bis(alkyne) systems through click chemistry was reported by Zhou *et al.* in 2013.^[33] In this pioneering piece of work, terminal alkyne-appended quaternary oxindoles **51** were successfully desymmetrised using a phenyl-appended PyBox ligand **52** to garner triazoles **53** in up to 98% *ee* (Scheme 15).^[33] Zhou found that using a dione (2,5-hexanedione) as a solvent for the reaction was critical for obtaining good selectivity. They noted that in general, carbonyl-containing solvents appeared to be the best for desymmetrisation after observing a leap in selectivity when moving from DCM (67% *ee*, 11% yield) to acetone (75% *ee*, 20% yield). A wide range of carbonyl-containing solvents were screened, and it was found that 2,5-hexanedione gave the best selectivity (90% *ee*, 32% yield). Even though no explanation was given for this observation, presumably the copper-coordinating ability that oxygen possesses toward copper could play a role in achieving selectivity. Further work on this system could be to examine the influence that the spacer length of the dione plays. For example, if the dione coordinates through one or both oxygen atoms and in turn if there is a preferred size of the copper chelation ring formed. One disadvantage to desymmetrisation methodology is that, due to the presence of two alkynes, there is a possibility of overreaction to the undesired bis(triazole). It was found that cooling the reaction to 0 °C for 96 h led to a ratio of up to 12:1 between the alkyne-triazole and the bis(triazole).



Scheme 15 Desymmetrisation of quaternary oxindoles Zhou *et al.*^[33]

Zhou and co-workers tentatively reported that a dinuclear copper-ligand complex is involved in the reaction. A negative non-linear effect (NLE) was observed between the *ee* of the product **53** and the enantiopurity of the ligand **52** employed. A non-linear effect is where the *ee* of a product does not increase linearly with the *ee* of the chiral catalyst employed. As depicted graphically in Figure 5, there are two possible non-linear effects: positive and negative. A positive NLE is one in which the *ee* of product is higher than the *ee* of the catalyst employed, and a negative NLE is one in which the product's *ee* is lower than the *ee* of the catalyst.

There are several ways to rationalise the observation of NLEs. Kagan developed several models for explaining non-linear effects. In a system where the active catalyst is hypothesised to be a dimeric species (one metal centre with two ligands) Kagan's (ML)₂ model can be employed.^[34] Using the (ML)₂ model, positive NLEs can be rationalised by the formation of a homo-dimer of catalyst, which is more selective than the corresponding hetero-dimer. In negative NLEs, the formed hetero-dimer is more selective than the corresponding homo-dimer (this was given as the explanation behind the observation of Zhou's negative NLE). Kagan also developed a model referred to as the "reservoir model"; in this case the active

catalyst is a monomeric species and the dimeric species formed are inactive. Using the reservoir model, a positive NLE is rationalised by the formation of a homo-dimer leaving high *ee* monomeric catalyst free in solution, leading to the higher than expected product *ee* as the undesired enantiomer of catalyst is sequestered by dimer formation.

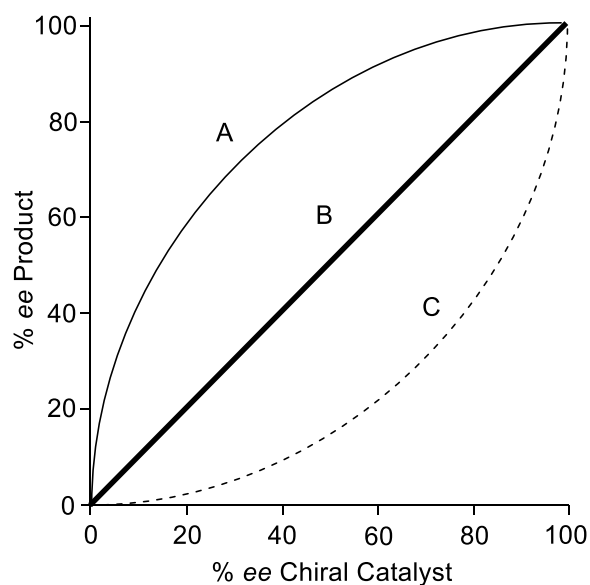
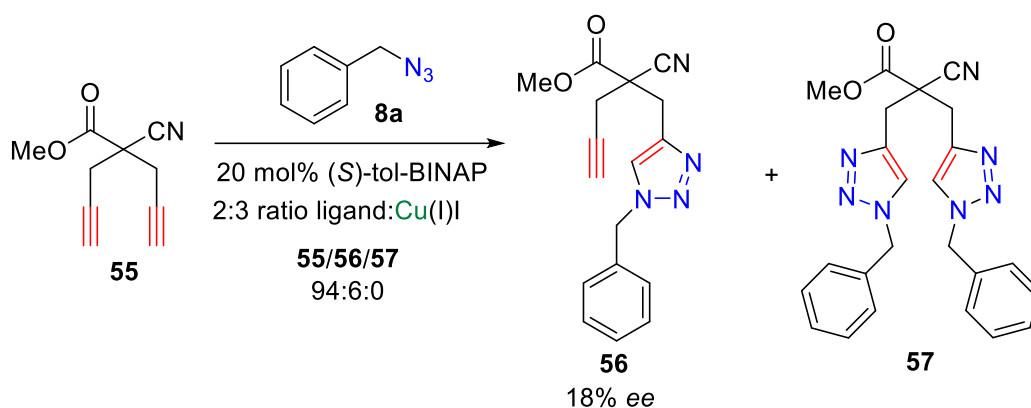


Figure 5 Graph of *ee* of product vs *ee* of chiral catalyst employed. A) A positive non-linear effect, the *ee* of product is higher than the corresponding *ee* of product. B) No non-linear effect, *ee* of product is equal to the *ee* of chiral catalyst across the range. C) A negative non-linear effect, *ee* of product is lower than the corresponding *ee* of product.

Investigations into desymmetrisation of non-heterocycle-containing bis(alkynes) was published by Stephenson *et al.* using prochiral 2,2-diynes **55**.^[35] They measured *via* chiral HPLC an *ee* of 18% in **56** when (*S*)-tol-BINAP was used as a chiral ligand (Scheme 16).

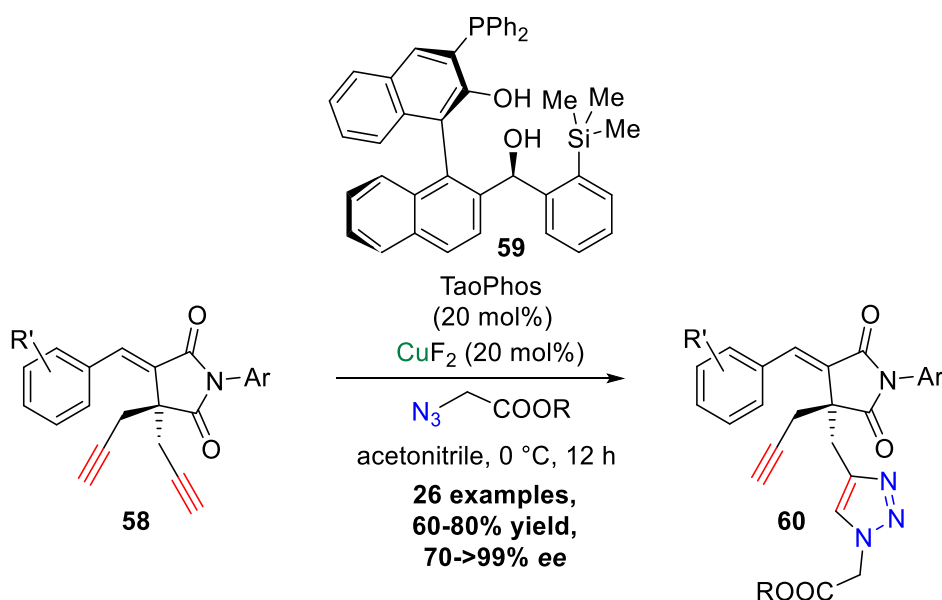


Scheme 16 Desymmetrisation of linear bis(alkyne) systems, Stephenson *et al.*^[35]

Stephenson and co-workers were unable to control overreaction to the bis(triazole) **57** effectively. For this reason, the reaction was only run until low conversion was observed, in this case a ratio of 94:6:0 (**55:56:57**), therefore much of the material remained as the bis(alkyne). This work showed that enantioenrichment can be achieved on linear systems through CuAAC desymmetrisation. It appears that the increased rotational freedom of linear systems makes obtaining high yields and enantiopurity more challenging than in conformationally restricted heterocyclic systems. It should be noted that the authors tried a range of ligands which had not been previously tried for asymmetric CuAACs, such as (*R,R*)-NORPHOS, (*S,S*)-Me-DUPHOS, (*R*)-tol-BINAP, (*R*)-xyl-BINAP and (*S*)-*i*-Pr-PHOX. However, as evidenced by the observed *ees*, none matched the *ees* previously achieved with PyBox-type ligand structures.^[32-33]

These observations made by Zhou and Stephenson led to the search for other ligands which could also asymmetrically influence the CuAAC. Song *et al.* developed a range of phosphine ligands.^[36] One in particular, TaoPhos, was successfully employed in the desymmetrisation of maleimide-based bis(alkynes) **58** (Scheme 17).^[37]

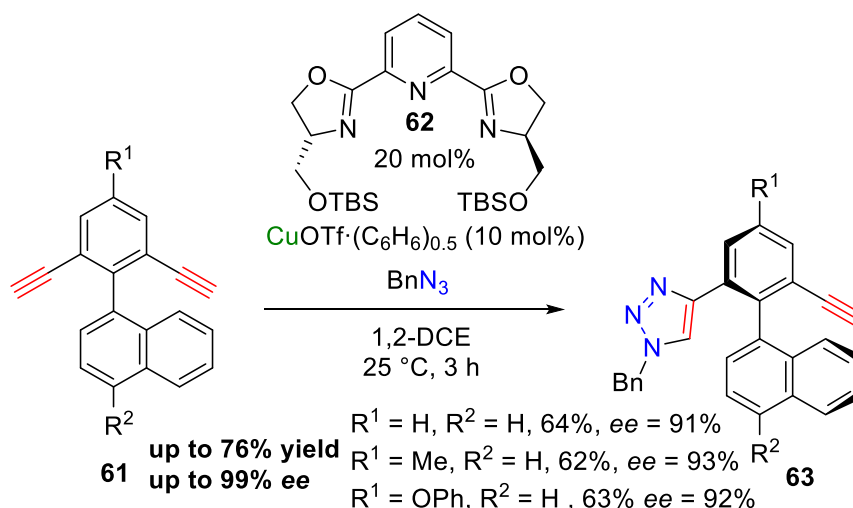
In their work, it was observed that a range of maleimides **58** were susceptible to desymmetrisation when a 1:1 ligand/ CuF_2 catalyst was employed. A range of conditions and additives were tested, and it was found that acetonitrile gave the best selectivity, with tetrahydrofuran (THF) being a close second (both with potential for coordination of copper). They also tried commonly used click additives; a study of the effect of the number equivalents of triethylamine (TEA) had on *ee* showed that it did help to boost the yield of the reaction, but with a loss in selectivity.



Scheme 17 Desymmetrisation of maleimide-based bis(alkynes), Song *et al.*^[37]

A nonlinear experiment was also carried out by Song *et al.*^[38] As was the case with Zhou *et al.*, a NLE was observed. As the *ee* of TaoPhos **59** was increased, the *ee* of the desymmetrised product **60** did not increase linearly. Instead, a positive NLE was noted thus, the increase in *ee* of the product was greater than the increase in the *ee* of the ligand **59**. Again, as in previous reports, this NLE suggests that the catalytic species is more complicated than a mono-nuclear one, and points towards a dimeric or multi-nuclear species being responsible for selectivity.^{[38-}

39]



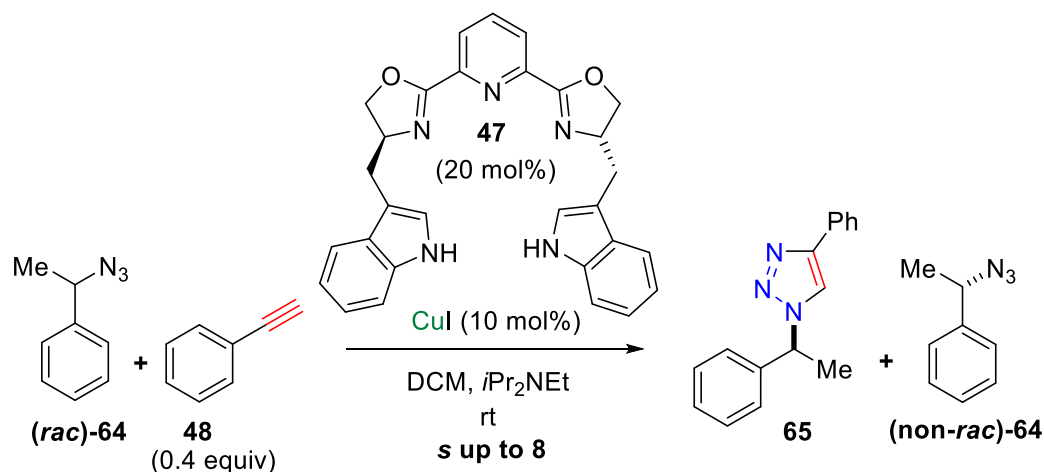
Scheme 18 Enantioselective CuAAC for construction of chiral biaryl derivatives, Osako and Uozumi^[40]

The ability for the CuAAC to be used to selectively form single atropisomers has also been studied by Osako and Uozumi (Scheme 18).^[40] Using a silyl-protected PyBox ligand **62**, they achieved up to 99% *ee* in **63**. However, they did note that they could not achieve good selectivity (<35% *ee*) with any azides other than benzyl azide.

Osako and Uozumi followed up their atropisomer-forming CuAAC reaction with a mechanistic study.^[41] By varying the number of equivalents of benzyl azide in the reaction, they noted that the enantioenrichment of the desymmetrised material changed (BnN₃ equiv. = 1, **63** = 80% *ee*; BnN₃ equiv. = 2, **63** = 97% *ee*). From these observations, it was concluded that two asymmetric processes were occurring. Firstly, a desymmetrisation to mono(triazole) **63** was occurring. This would then further react in a kinetic resolution process to the unwanted bis(triazole) by a further CuAAC with remaining benzyl azide. This increased the enantioenrichment of the remaining desymmetrised mono(triazole). This meant that increasing the number of equivalents of azide led to the minor enantiomer of mono(triazole) **63** being consumed faster than the major enantiomer, and this led to an increase in *ee* of the remaining major enantiomer of mono(triazole) **63**. In addition, an NLE study was carried out,

and, as in other asymmetric CuAACs, a positive nonlinear effect was observed, thus lending evidence to this reaction proceeding through a non-mononuclear catalytic species.

Another strategy that is employed in asymmetric click chemistry is to use kinetic resolution (KR) (the theory behind KR is discussed in Section 1.5). Thus far, there has only been one published example of kinetic resolution using CuAACs. Meng *et al.* reported the kinetic resolution of α -benzylic azides **64** utilising a Cu-PyBox complex in 2005.^[32] They obtained selectivity factors (*s*) of up to 8, but no *ee* values are reported for this resolution, so the level of enantioenrichment obtained is unknown (Scheme 19).



Scheme 19 Kinetic resolution of α -benzylic azide, Meng *et al.*^[32]

In addition to testing resolvable azides, Meng *et al.* also exposed a series of racemic alkynes to the resolution conditions. In the case of terminal alkynes, no resolution was observed (*s* = 1). At the time of publication, the dinuclear catalytic model for CuAACs had yet to be presented, and so Meng and co-workers proposed a reaction intermediate to explain the observed selectivity with only azides and not alkynes.^[32] They proposed a mononuclear intermediate in which the catalytically active copper centre occupied all three of the available coordination sites of the bis(oxazoline) PyBox ligand **66** (Figure 6). It was proposed that the copper acetylide forms, and due to the linear structure of alkynes, the resolvable stereogenic

centre is placed spatially distant from the ligand's chiral influence. This was presented as the reasoning behind terminal alkynes being resistant to resolution compared with azides, which were proposed to approach the ligand facially, allowing chiral relay to occur in this case. In the intervening years, greater understanding of PyBox copper complexes has shown that (in the solid state, at least) complexation does not occur as previously thought. This is discussed further in Chapter 2.

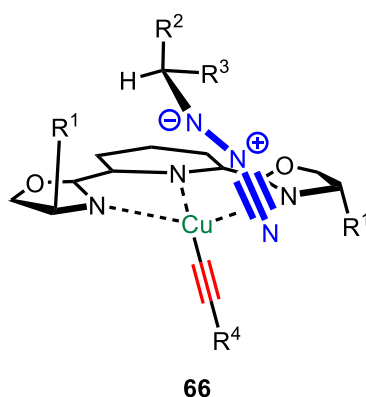


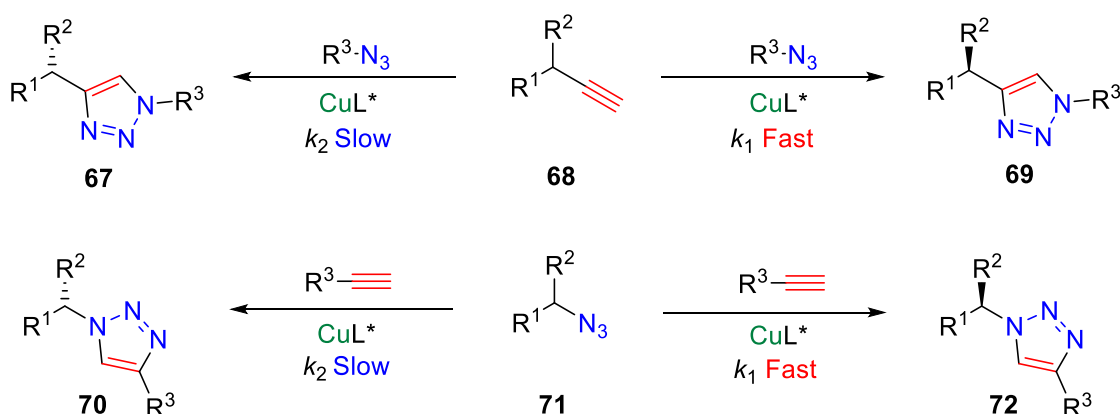
Figure 6 Proposed reaction intermediate in the kinetic resolution of α -benzylic azides, Meng *et al.*^[32]

As part of the projects detailed within this thesis, the author, along with Dr Fossey (UoB) and Dr Buckley (LU), published a review on the growing area of asymmetric CuAACs within in the journal *ACS Catalysis*.^[42]

1.5 Kinetic Resolution

Kinetic resolution is a strategy that can be used to access enantiopure materials from mixtures of enantiomers. A kinetic resolution takes a chiral starting material, and, through a kinetically selective reaction (*i.e.* one enantiomer of reactant reacts faster than the other), favours one of the enantiomers, thus bringing about enantioenrichment in the remaining starting material in the reaction mixture. KR is often used to recover an enantiopure starting material. However, due to its nature, one enantiomer of product also forms faster, giving an enantioenriched product in addition.

The mathematical underpinning of KR was developed by H. B. Kagan, which allows the quantitation and benchmarking of resolution processes.^[43] He used an expression he termed the selectivity factor to describe the efficiency of a resolution. The selectivity factor shows to what extent a system is kinetically favouring one enantiomer of reactant. The selectivity factor is defined as the ratio of the fast rate constant over the slow rate constant for the two enantiomers (Scheme 20, Equation 1). For example, if one enantiomer reacts 10 times faster than the other, the selectivity factor would be 10 ($s = 10$). Kagan developed a series of equations which related the conversion of the reaction (from starting material to product), the *ee* of either the recovered starting material or the product and the selectivity factor (Scheme 20, Equation 2).^[43]



$$\text{Equation 1 } \textit{Selectivity Factor } (s) = \frac{\textit{Rate of Fast Reacting Enantiomer}}{\textit{Rate of Slow Reacting Enantiomer}} = \frac{k_1}{k_2}$$

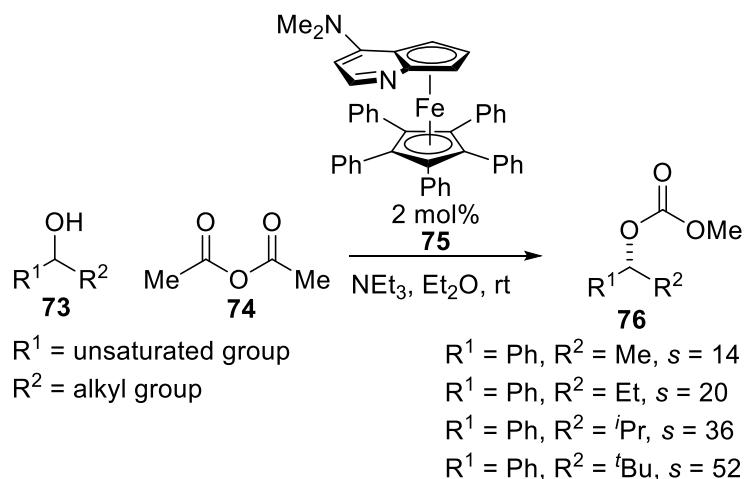
$$\text{Equation 2 } s = \ln[(1-c)(1-ee)] / \ln[(1-c)(1+ee)]$$

Scheme 20 Catalytic kinetic resolution of azides and alkynes. **Equation 1** Principle of selectivity factor. **Equation 2** Developed by H. B. Kagan where *ee* refers to the *ee* of the recovered starting material and *c* is conversion of starting material to product

In the case of applying KR to asymmetric CuAAC, a racemic azide **71** or alkyne **68** would be “clicked”, where one enantiomer of the starting material would react faster than the other, which would allow access to enantioenriched alkynes and azides. In addition, the reaction would also form enantioenriched triazoles.

The relationship between selectivity factor, conversion and *ee* will inform as to the conversion at which point one enantiomer of starting material would still remain within the reaction mixture. The best possible scenario for kinetic resolution would be one in which the reaction is fully selective for one enantiomer, and thus at 50% conversion, there is a single enantiomer of starting material remaining and a single enantiomer of product formed. In order to achieve this, a selectivity factor in excess of one thousand ($s = 1057$) is required. This is a number which enzymes can struggle to meet, but kinetic resolutions, due to their exponential nature (Scheme 20, Equation 2), can still be synthetically useful at lower s values. For example, if a reaction produces a selectivity factor of 10, then the conversion needed to recover a sample of enantiopure starting material is 72%; at this point only the slow reacting enantiomer would remain. Even at a selectivity factor of 10 it is possible to recover 28% of the chiral starting material in enantiopure form, which could still be useful in a synthetic setting.

Kinetic resolution is a field which has many existing literature examples. For instance, a way in which enzymes can produce single-enantiomer products is by kinetic resolution.^[44] Enzymes have extremely selective active sites which typically only allow for one enantiomer to successfully react. This leads enzymes to have very high selectivity factors. However, good selectivity has also been demonstrated through synthetic catalysts.^[45] For example, Fu and co-workers have championed the use of catalytic KR, especially on secondary alcohol substrates **73**.^[46] In 1997, Fu disclosed the KR of secondary alcohols using a planar chiral dimethylaminopyridine (DMAP) catalyst **75** (Scheme 21) with a selectivity factor of $s = 52$.^[47] This has been built upon by Fu and his group to give higher selectivity and, in addition, dynamic kinetic resolutions based on this work have been developed.^[48]



Scheme 21 Catalytic kinetic resolution of secondary alcohols, Fu and co-workers^[47]

Kinetic resolution has been shown to be a powerful technique, delivering a wide range of enantioenriched species such as amines,^[46, 49] alcohols^[47, 50] and thiols.^[51] The only drawback to kinetic resolution is that the maximum yield of enantiopure materials is 50%. Several methodologies have been developed to combat this: dynamic kinetic resolution^[52] and parallel kinetic resolution (see Section 2.2).^[53] Even with this limitation, the breadth of materials which have been shown to be applicable to kinetic resolution shows that it is a methodology which is useful and synthetically relevant.

1.6 Triazoles

A triazole is a heterocycle containing three nitrogens and two carbons in a five-membered ring. Triazoles have several regioisomers; in the case of copper-catalysed click chemistry, a 1,2,3-triazole substituted in a 1,4 pattern is formed, while in the case of ruthenium-catalysed click chemistry, a 1,2,3-triazole substituted in a 1,5 pattern is generated preferentially.

Triazoles formed *via* CuAAC reactions have come to be seen as a universal linkage moiety. The ability to couple azide- and alkyne-derivatised molecules in an efficient manner, in combination with the stability of triazoles makes this an attractive method for linking two or more desired moieties together. Triazoles have been shown to be resistant to acidic or basic

hydrolysis and oxidative/reductive environments. They also display a high dipole moment and can also take part in hydrogen bonding, dipole-dipole and π stacking interactions.^[54] These desirable attributes in addition to their ease of synthesis have helped triazoles garner a reputation as a linkage for a multitude of applications.

1.6.1 Triazoles in drug development

One area in which triazoles have seen widespread use is in the development of new drug compounds. Within drug development, triazoles have been used as both a linkage and as an integral moiety to deliver biological activity.

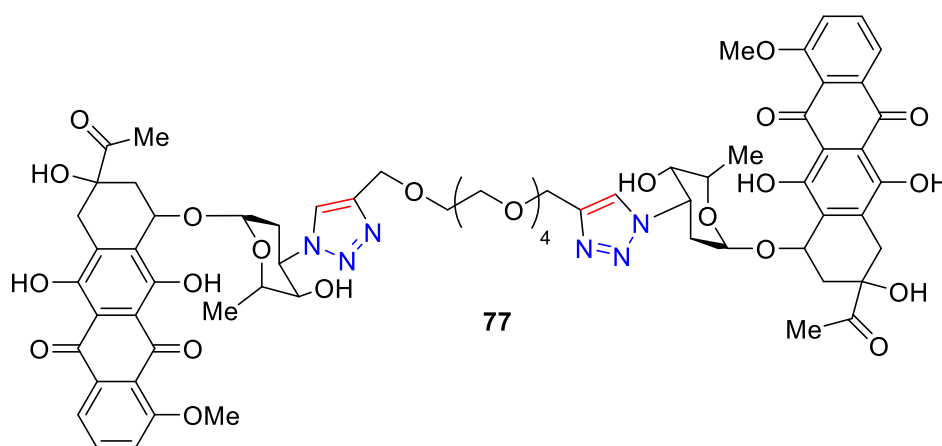


Figure 7 Anti-leukaemia compound synthesised via click chemistry, Zhang *et al.*^[55]

One strategy used in drug development is to couple multiple copies of the same active fragment together, which has been shown in some cases to increase potency. The binding of the first component to its target helps to spatially orientate the subsequent parts of the active compound to bind with its target, thus increasing a drug's potency. For example, Zhang *et al.* were able to form **77** which contains two of the same active fragment, and was shown to be biologically active towards leukaemia cells.^[55] They found that the length of the carbon linker attached to the triazole was critical in maintaining any activity towards the target (Figure 7). This dependence on the linker length shows that the orientation of the multiple active

components in relation to their targets is of paramount importance to obtaining good activity. The synthetic flexibility of click chemistry allows for this fine tuning of spatial orientation to maximise potency.

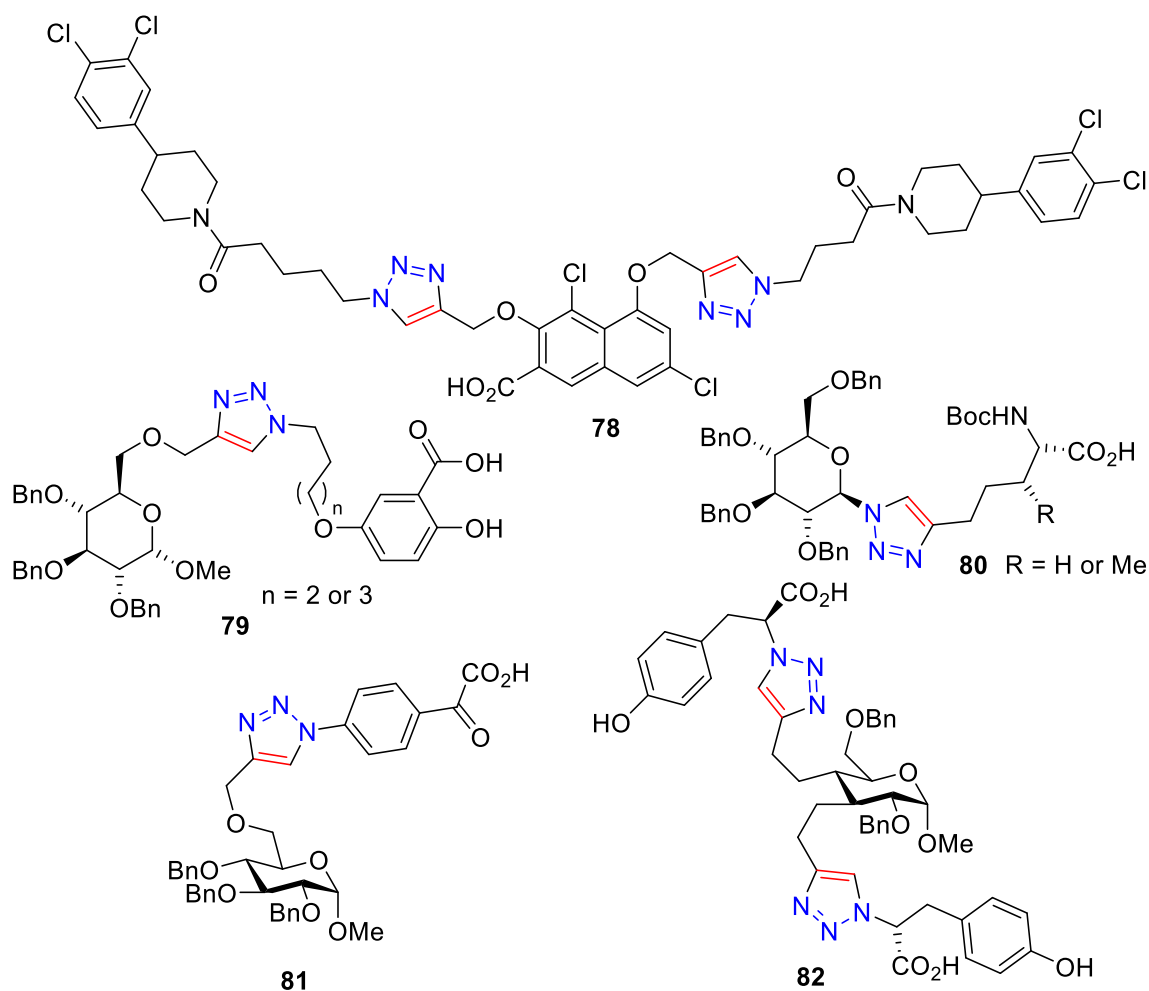


Figure 8 A range of protein phosphatase inhibitors synthesised *via* click chemistry

Taking the idea of using CuAACs as a manner of coupling has become a key method in fragment-based drug discovery (FBDD). FBDD is focused around identifying small molecules which exhibit some activity towards a target (this can just be weak activity) and then elaborating or combining fragments to achieve lead compounds with higher potency. Using click chemistry to combine these small molecules is a strategy employed to make a wide variety of drug-like molecules. Enzyme inhibitors, for example, are one area in which a

vast array of triazole-linked architectures have been developed using the FBDD approach.^[56] Shown in Figure 8, **78-82** are a very small selection of protein phosphatase inhibitors which have been developed in a modular fashion utilising click chemistry.^[57] A whole range of enzyme inhibitors with various targets have been synthesised using the combination of FBDD and CuAAC. Enzymes, however, are not the only target of click-synthesised drug compounds. A range of antitumour agents e.g. compound **83** have been developed using click linkage techniques along with antimicrobials **84** and antibiotics **85** (Figure 9).^[58] The widespread and successful use of triazole linkers shows the power of this approach and the value triazoles have in FBDD.

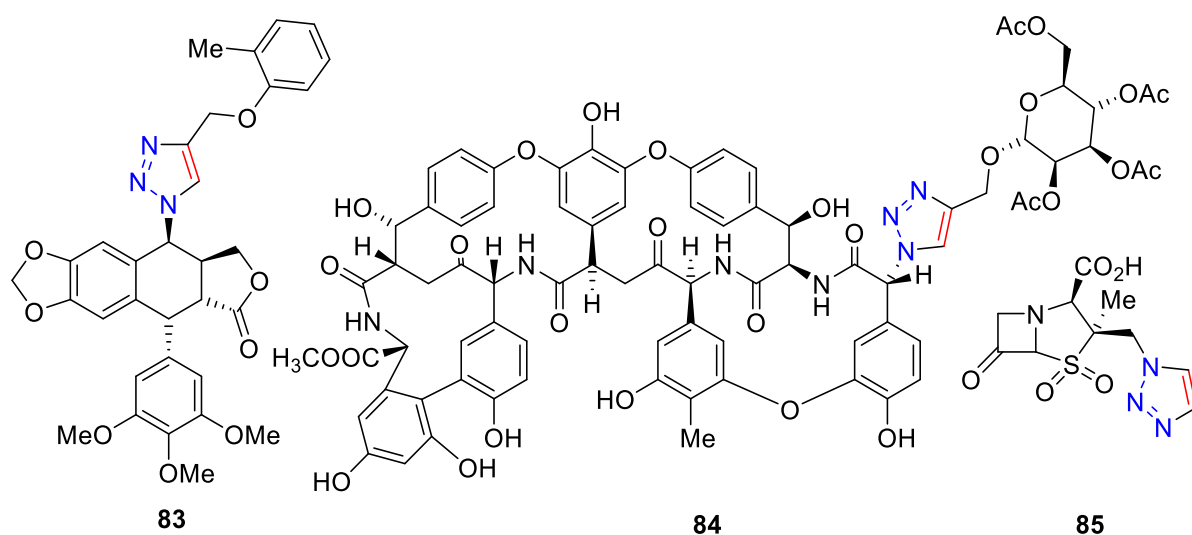


Figure 9 Antitumour, antimicrobial and antibiotic compounds synthesised using click chemistry

Another way CuAACs have been used for drug delivery is in the modification of DNA. The development of aqueous click chemistry has led to the ability to utilise triazole formation in biorthogonal labelling studies, in particular the labelling of RNA and DNA. Using alkyne-modified DNA bases in combination with click chemistry has led to highly functionalised and labelled sequences for the studying of nucleic acids and their intercellular roles.^[59] For example, click chemistry has been used to link fluorophores such as coumarin to nucleosides

and used to visualise DNA free in solution and also in DNA-protein complexes. This allows fluorophore-tagged DNA to be used in the visualisation of biomolecules *in vivo*, showing the roles and functions they can play in a biological environment.^[60] In some cases completely unnatural DNA backbones have been created through triazole linkages. Dondoni *et al.* synthesised unnatural click-constructed DNA sequences.^[61] In this work a triazolic “codon” of three bases was linked using a triazole backbone. As a first report, this showed the ability click chemistry has to modify DNA.

1.6.2 Triazoles in other applications

Triazoles have found many applications outside of the drug development community. The modularity of the CuAAC reaction means it has become a go-to reaction for fragment linking in a myriad of applications. Triazoles have found application in the linkage of receptors and reporters in the sensing community. Sugar sensing is one such arena where triazoles have been used effectively for the formation of sensors, which give a fluorescence response upon the detection of a sugar.^[62] New compounds for applications such as solar cells,^[63] polymers,^[64] supramolecular assemblies and chiral ligands^[65] have all been successfully synthesised through the CuAAC linkage approach.

1.7 Conclusion

The CuAAC has become a ubiquitous linkage reaction; its ease of use and predictability has seen it become a mainstay in areas such as FBDD and bioorthogonal labelling methodologies. The ability to efficiently link two molecular species together with relative operational simplicity has opened up new avenues of research for many biologists and biochemists, who are embracing the CuAAC for applications such as protein labelling.^[66]

Even though the CuAAC reaction has garnered much interest from researchers (evidenced by the number of published articles in the area each year (Figure 1)), asymmetric examples are

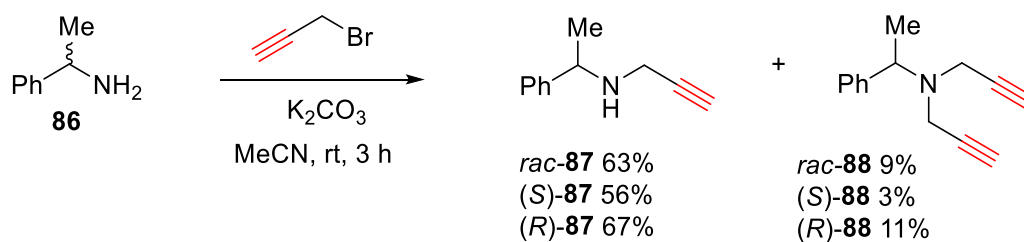
scarce. A handful of desymmetrisations and a single kinetic resolution are all that is present within the literature, and thus a need to develop new asymmetric methodologies is pressing. The experiments detailed in future chapters will show a range of attempted strategies to achieve asymmetric CuAAC. In addition, the ease of synthesis and modularity of triazoles make them an interesting structural motif for asymmetric applications. Work in later chapters within this thesis will detail the synthesis of new chiral triazoles along with the synthesis of bis(triazoles) and 1,5-substituted triazoles.

2 Kinetic Resolution of Terminal Alkynes *via* Copper-Catalysed Azide-Alkyne Cycloadditions

Kinetic resolution has been used to resolve a myriad of chiral species; amines,^[46, 49] alcohols^[47, 50] and thiols^[51] have all been shown to be susceptible to kinetic resolution. Terminal alkynes are a moiety for which kinetic resolution methodology has not been explored in detail. In fact, there are no literature reports describing the KR of chiral terminal alkynes, even though they are an extremely versatile moiety.^[67] The copper-catalysed azide-alkyne cycloaddition is a reaction which could be applied to kinetically resolve terminal alkynes (Scheme 20).

In 2005 Fokin and co-workers kinetically resolved α -benzylic azides using a PyBox-Cu catalyst in a CuAAC. However, when they tried to resolve a series of chiral terminal alkynes under the same conditions, they did not observe any resolution.^[32] Since then, several desymmetrisation reactions of terminal alkynes have been reported.^[35, 38, 40] In 2013 Zhou *et al.* desymmetrised bis(alkyne) systems *via* CuAAC using a PyBox-Cu catalyst.^[33] In light of this precedent, it was hypothesised that terminal alkynes should be susceptible to kinetic resolution.

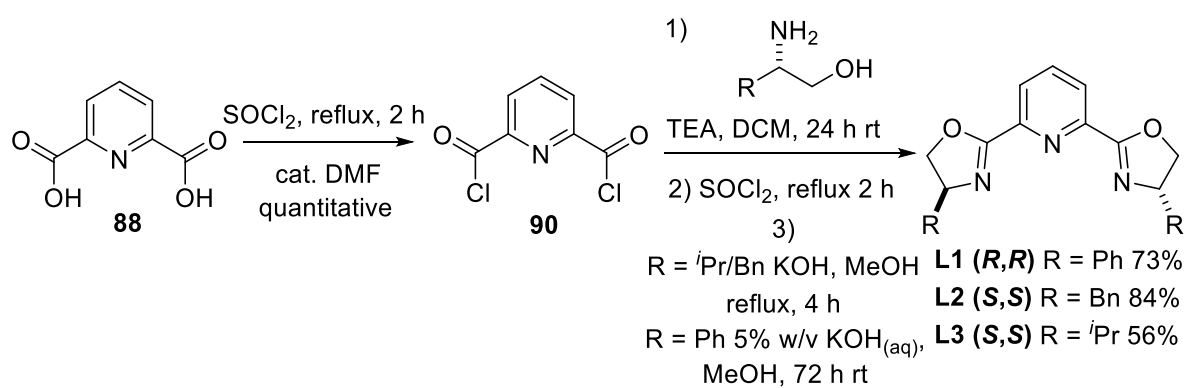
To test the hypothesis that KR of terminal alkynes could be achieved *via* CuAAC, a chiral terminal alkyne was needed. Alkylation of α -methylbenzylamine **86** with propargyl bromide was the first route chosen towards this aim. As both single enantiomers of the amine are commercially available, this would allow for straightforward analysis of any enantioenrichment gained through a kinetic resolution process.



Scheme 22 Synthesis of propargylated α -methylbenzylamine derivatives

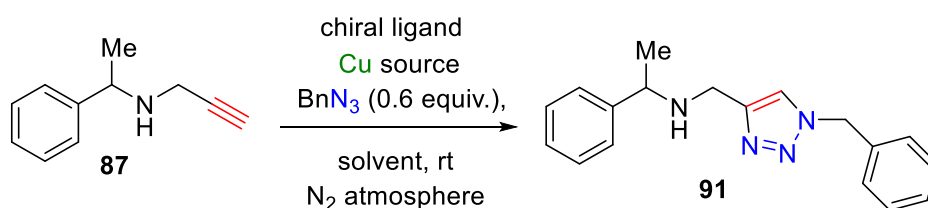
Alkylation of α -methylbenzylamine **86** with propargyl bromide afforded racemic alkyne **87** in 63% yield, (*R*)-**87** in 56% yield and (*S*)-**87** in 67% yield, but due to the increased nucleophilicity of the secondary amine product, over-alkylation did occur to give bis(alkyne) **88** (Scheme 22).

With an appropriate alkyne in hand, a series of ligands based around the PyBox motif were targeted due to their prevalence in the literature.^[32-33, 40] Using a synthetic procedure reported by Gao and co-workers, benzyl- and isopropyl-appended ligands (**L2** and **L3**, respectively) were successfully formed (Scheme 23).^[68] Ligand **L1** was synthesised using a slightly modified synthetic route developed by Nishiyama and co-workers in 73% yield.^[69]



Scheme 23 Synthesis of PyBox ligands

In order to quantify any enantioenrichment obtained using alkyne **87**, conditions needed to be developed to separate the enantiomers of starting material **87**. It was found that chiral gas chromatography (GC) allowed for separation of the two enantiomers of alkyne **87**. Using enantiopure samples of each of the alkynes of known configuration, assignment of the absolute stereochemistry of the alkyne responsible for each GC peak could be made (see Section 7.2.3)



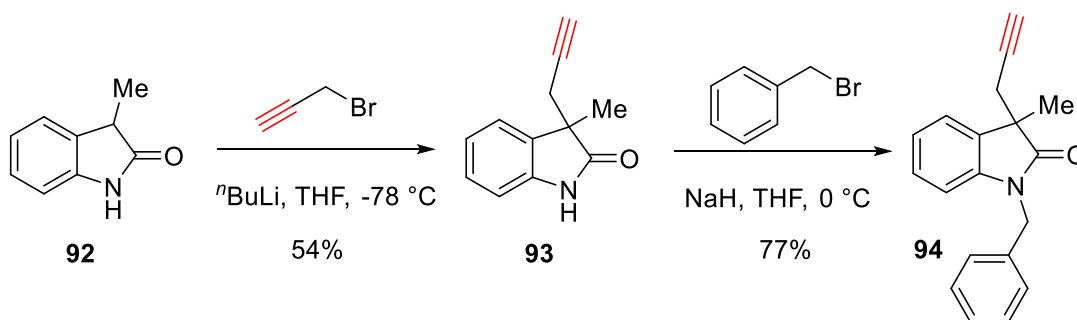
Scheme 24 General reaction scheme for the attempted kinetic resolution of alkyne **87**

With separation conditions in hand, several resolution conditions were applied to the reaction. Reaction conversion was not monitored during this phase of the project, because the main goal at this time was to identify a ‘hit’ with some level of enantioenrichment. Two phosphoramidite ligands were purchased from commercial sources and applied to the reaction in addition to the synthesised PyBox ligands (**L1**, **L2**, **L3**). Phosphoramidites have been shown to be effective in other copper-catalysed asymmetric transformations and have been shown to have a ligand acceleration effect in the CuAAC,^{91,92} so were deemed potentially useful for KR applications.^[70] A range of copper sources (CuSO₄, CuI and Cu(OTf)₂) and solvents (acetonitrile, THF, toluene and acetone) were screened. After 70 hours and 96 hours, aliquots of the reaction mixture were injected directly into the chiral GC and the *ee* was measured. No enantioenrichment was observed by chiral GC with any combination of conditions (for detailed screening tables see Section 7.2.2).

These results mirrored the findings by Fokin and co-workers.^[32] This did pose a question: if bis(alkynes) had been shown to be desymmetrisable by asymmetric CuAAC,^[33, 37, 40] why was alkyne **87** resistant to kinetic resolution? It was decided that it was worth pursuing KR of alkynes further.

2.1 Kinetic Resolution of Quaternary Oxindoles via CuAAC

After the failure to resolve alkyne **87**, it was decided that continuing with this substrate was not a productive pathway. Taking inspiration from the report by Zhou *et al.* on the desymmetrisation of quaternary oxindoles,^[33] an alkyne-appended quaternary oxindole was targeted. Due to the acidity of the 3-position of oxindoles, it was believed that it would be possible to append an alkyne to the oxindole framework *via* propargyl bromide in the presence of ⁿBuLi. Treating commercially available 3-methyl-2-oxindole **92** with propargyl bromide in the presence of ⁿBuLi led to successful addition of the desired terminal alkyne moiety to give the quaternary oxindole **93** in 54% yield (Scheme 25).



Scheme 25 Synthesis of quaternary oxindole **94**

The formation of oxindole **93** was unequivocally confirmed through single-crystal X-ray diffractometry (XRD) (Figure 10i). As chiral high performance liquid chromatography (HPLC) separation of the unprotected oxindole **93** was found to be troublesome, the oxindole was protected with a benzyl group in 77% yield (Scheme 25), and the crystal structure of compound **94** was also obtained (Figure 10ii). Using a chiral stationary phase (Phenomenex

Cellulose 3) it was established that the optimal HPLC separation conditions were reverse phase with water and acetonitrile (50:50) as the mobile phase.

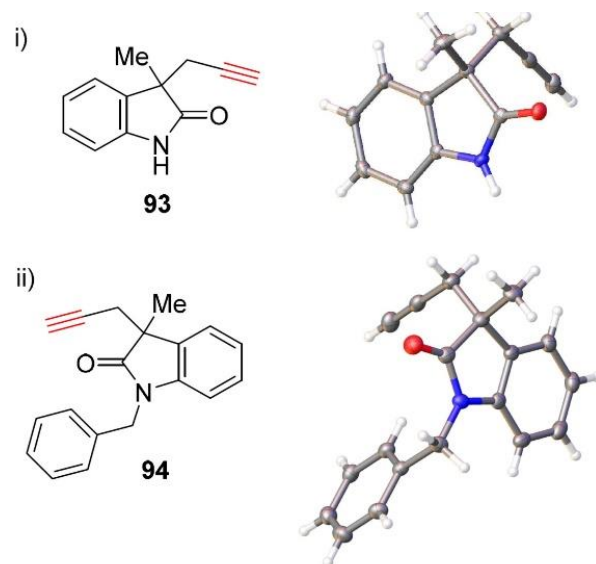
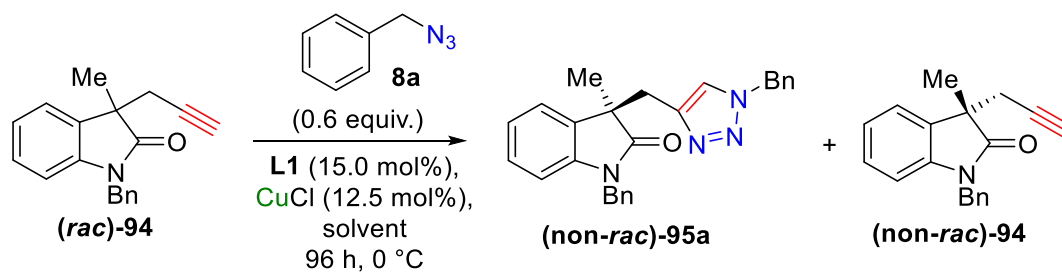


Figure 10 i) Crystal structure of racemic **93**. Ellipsoids are drawn at the 50% probability level, space group = $P2_1/c$ **ii)** Crystal structure of racemic **94**. Ellipsoids are drawn at the 50% probability level, space group = $P2_1/c$

Table 1 Solvent screening in the kinetic resolution of oxindole **94**

Entry	Solvent	Conv. (%) ^a	<i>ee</i> 92 (%) ^b	<i>s</i> ^c
1	2,5-Hexanedione	46	72	23.2 ^d
2	Acetone	34	35	5.3
3	Acetonitrile	14	1	1.1
4	DMF	0	-	-
5	DMSO	44	18	1.9
6	1,4-Dioxane	17	6	1.9
7	^t BuOH	34	7	1.4
8	^t BuOH/H ₂ O	13	0	1.0
9	H ₂ O	6	-	-
10	Toluene	5	-	-
11	2-Butanone	0	-	-
12	THF	37	46	8.7
13	1:10 Acetone/2,5-Hexanedione	61	56	3.5
14	NMP	4	-	-
15	Cyclohexanone	0	-	-
16	2,3-Butandione	34	18	1.1

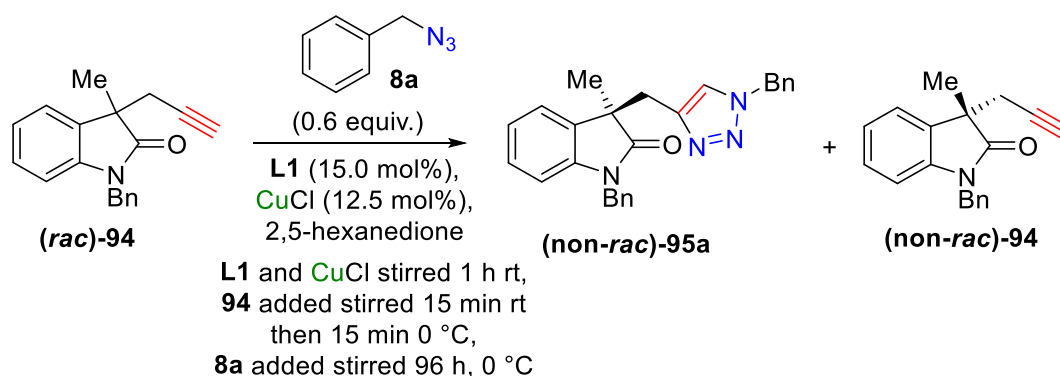
17	Furan	3	1	2.0
19	THF/2,5 Hexanedione 100:1	23	12	2.6
20	THF/2,5 Hexanedione 1:1	30	15	2.4

^a Conversion determined by inspection of ¹H NMR spectra (see ESI); ^b *Ee* of recovered starting material (HPLC); ^c $s = \ln[(1-c)(1-ee)]/\ln[(1-c)(1+ee)]$; ^d Average of three $s = 22.1 \pm 0.5$, best unique case $s = 23.2$. All other reactions were carried out once.

When oxindole **94** was treated with 0.6 equivalents of benzyl azide in the presence of 12.5 mol% CuCl and 15.0 mol% (*R,R*)-PhPyBox **L1** in acetone, a selectivity factor of $s = 5.3$ was realised (Table 1, entry 2). This was very pleasing, but it was hoped that this figure could be improved through screening. A wide range of solvents were probed, and the first leap in selectivity came in the case of tetrahydrofuran (THF), improving the selectivity to $s = 8.7$ (Table 1, entry 12). From this observation, it was decided that focusing on solvents with the ability to coordinate copper could be the key to achieving high selectivity. Discussion with the Zhou group led to trying 2,5-hexanedione, as they had noticed a large increase in selectivity in their asymmetric CuAAC studies with this solvent.^[33] Running the resolution reaction in 2,5-hexanedione led to a large increase in selectivity, giving $s = 23.2$. As dione functionality had been shown to improve selectivity, it was decided to test what effect altering the length of carbon chain between the ketones would have. Thus, the reaction was attempted in 2,3-butanedione, which after 96 h, gave a conversion of 34% and an *ee* of 18%, giving an overall selectivity factor of $s = 1.1$. This showed that the distance between the two ketone moieties was critical in obtaining good selectivity.

Even though good selectivity factors were obtainable using 2,5-hexanedione, the reaction was not consistent; conversion was extremely variable and some reactions set up with identical conditions gave zero conversion to a triazolic product. To begin with, it was assumed that

these screening reactions were homogeneous (so no stirring was necessary), and thus they were carried out in a fridge without stirring. However, the large variance in reaction conversion led to questioning if the homogeneous assumption was indeed correct, and whether these reactions were proceeding in a heterogeneous fashion. Therefore, it was believed that stirring the reactions could have an impact on the consistency of the outcome. In order to test this, a cool box was constructed which could hold its temperature at 0 °C for extended periods and could be placed on a stir plate. The stirring did improve the reproducibility slightly, but it was still observed that in some cases no conversion would occur. As no catalytic turnover was being observed it was concluded that the catalytically active species may not be forming. This led to the hypothesis that forming an initial copper acetylide (between the oxindole alkyne **94** and CuPyBox) may be a crucial first step in achieving catalytic turnover. Therefore, the reaction setup was altered, originally CuCl (12.5 mol%) and PhPyBox **L1** (15.0 mol%) were stirred at room temperature for an hour, at which time the reaction mixture was cooled in ice to 0 °C and **94** was added. This would then be stirred for a further 30 minutes before an azide was added. It was thought that addition of the alkyne **94** at room temperature would form the catalytically active copper acetylide more efficiently. Therefore, after the initial copper complexation, the alkyne was added and the mixture stirred at room temperature for 15 minutes before subsequent cooling in ice for a further 15 minutes before any azide was added. This procedure made the reaction much more reliable, giving consistent conversions within 4% error (Table 2).

Table 2 Repetition of kinetic resolution of **94**

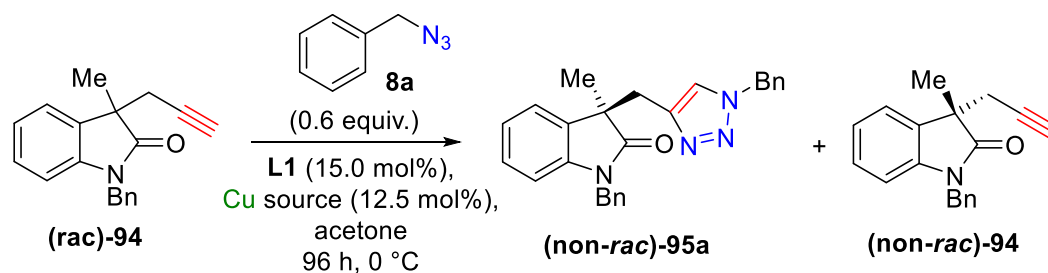
Entry	Conv. (%) ^a	<i>ee</i> 92 (%) ^b	<i>s</i> ^c
1	42	61	21.6
2	46	72	23.2
3	49	77	21.6
	Standard Deviation	0.92	
	Error	0.53	
	Value (<i>s</i>)	22.2 ± 0.5	

^a Conversion determined by inspection of ¹H NMR spectra (see ESI); ^b *Ee* of recovered starting material (HPLC); ^c *s* = ln[(1-*c*)(1-*ee*)]/ln[(1-*c*)(1+*ee*)].

With the best solvent and consistent conversion in hand, the copper source could be probed. Bertrand and co-workers have found that the counterion to copper can have a notable effect on the rate of the CuAAC when using ligated copper species.^{[71][71]} Due to this reported rate effect, a series of Cu(I), Cu(II) and Cu(0) species were tested. Previous screening reactions had shown that work-up when 2,5-hexanedione was employed could be problematic. Because the dione has a high boiling point (191 °C), it could not simply be removed under reduced pressure. In addition, the dione was found to react with silica during column chromatography (forming a bright orange compound which would elute over several tens of fractions) and to co-elute with the desired products. It is also light-sensitive, turning a dark brown colour over time after exposure to light. These problems could be overcome with several water washes to remove the bulk of the solvent, followed by flash column chromatography to remove any

trace amounts, but it was decided that carrying out the screening in acetone instead would significantly shorten the purification procedure and the best copper source could later be applied to the dione. This screening strategy assumed that the results obtained in acetone would be directly transferable to 2,5-hexanedione.

Table 3 Copper source screening in the kinetic resolution of **94**



Entry	Copper Source	Conv. (%) ^a	<i>ee</i> 94 (%) ^b	<i>s</i> ^c
1	CuCl	34	35	5.3
2	CuBr	14	8	3.2
3	CuI	51	26	2.1
4	CuSO ₄ , NaAsc	13	1	1.2
5	CuOTf·0.5Toluene	10	3	1.8
6	Cu(OTf) ₂	0	0	-
7	CuOAc	0	0	-
8	Cu(OAc) ₂	8	4	2.8
9	Cu Metal	0	0	-

^a Conversion determined by inspection of ¹H NMR spectra; ^b *Ee* of recovered starting material (HPLC); ^c $s = \ln[(1-c)(1-ee)]/\ln[(1-c)(1+ee)]$. All reactions were carried out once.

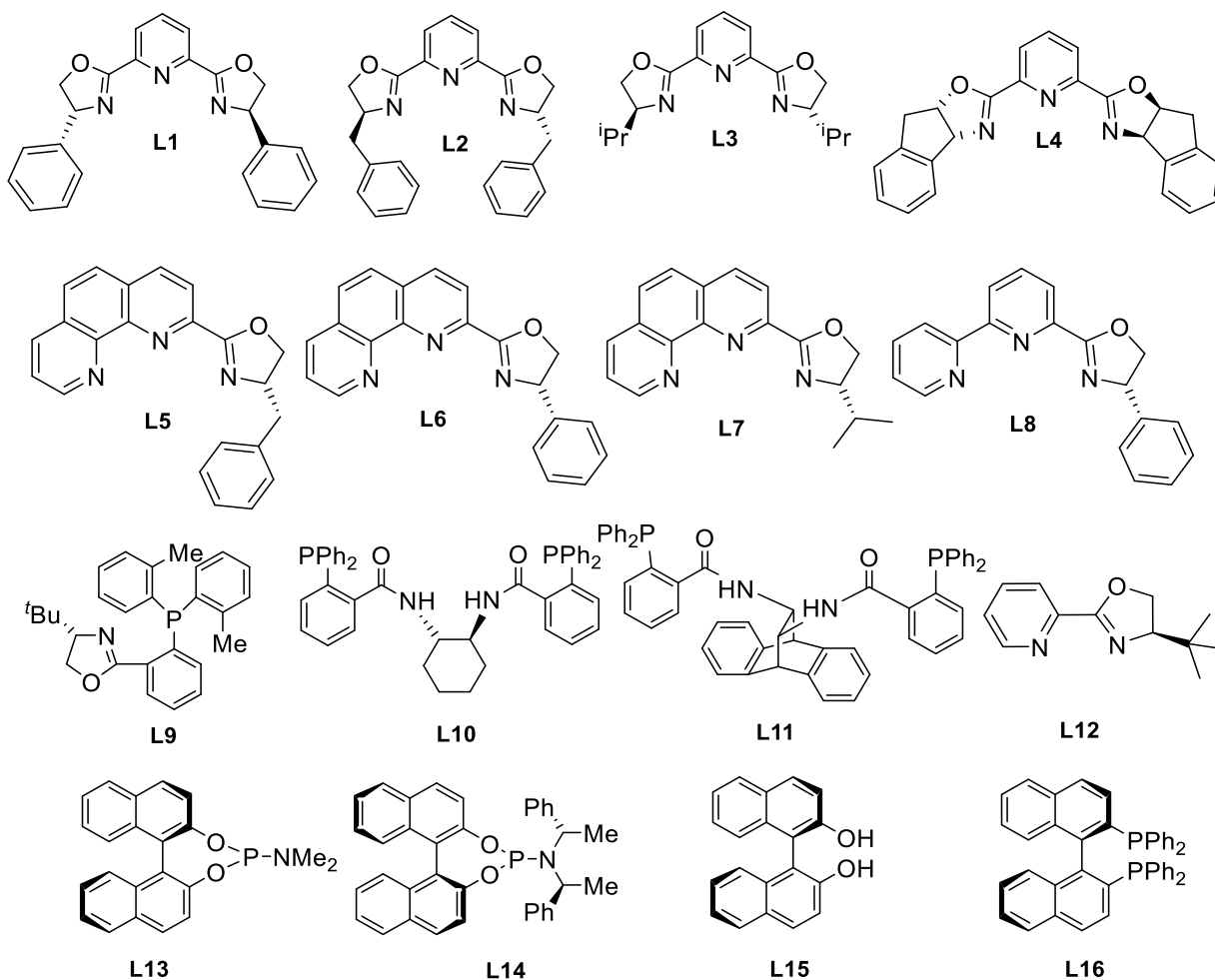
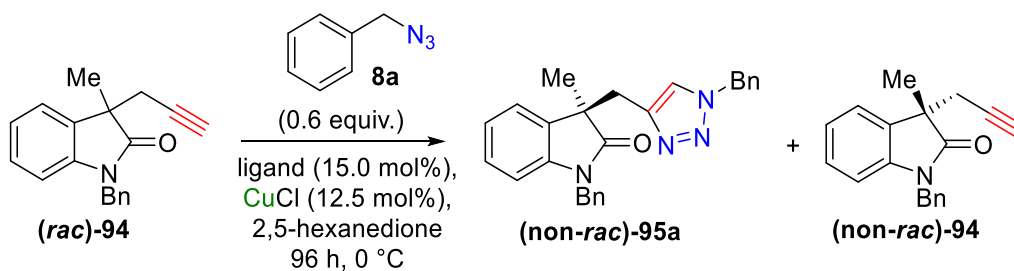


Figure 11 Ligands used during reaction optimisation

It was found that CuCl was the best choice for this resolution, giving reasonable conversion along with the best selectivity (conv. = 34 %, $s = 5.3$) (Table 3, entry 1). Moving to CuBr, both selectivity and conversion were decreased (conv. = 14 %, $s = 3.2$) (Table 3, entry 2) whilst CuI gave greatly improved conversion but with a concomitant loss of selectivity (conv. = 51% $s = 2.1$) (Table 3, entry 3). The other copper sources tested all gave both poor conversion and selectivity (Table 3, entries 4-9).

Table 4 Ligand screening in the kinetic resolution of **94**



Entry	Ligand	Conv.(%) ^a	ee 92 (%) ^b	<i>s</i> ^c
1	L1	46	72	23.2
2	L2	6	1	1.4
3	L3	0	-	-
4	L4	0	-	-
5	L5	0	-	-
6	L6	0	-	-
7	L7	0	-	-
8	L8	0	-	-
9	L9	0	-	-
10	L10	0	-	-
11	L11	0	-	-
12	L12	5	1	1.5
13	L13	0	-	-
14	L14	0	-	-
15	L15	4	0	1.0
16	L16	0	-	-

^a Conversion determined by inspection of ¹H NMR spectra; ^b *Ee* of recovered starting material (HPLC); ^c $s = \ln[(1-c)(1-ee)]/\ln[(1-c)(1+ee)]$. **L5-8** were synthesised by the group of Professor Matthew Sigman at the University of Utah. Reactions with **L1** were carried out in triplicate, best individual result displayed.

With the best copper source and solvent in hand (CuCl and 2,5-hexanedione respectively), along with a robust experimental procedure, it was decided to probe the ligand architecture in hopes of further improvement. A wide range of ligands spanning several families were tested under the optimised resolution conditions (Figure 11). In the majority of cases, no reaction was observed (**L3-L11**, **L13-L14** and **L16**). Benzyl-substituted PyBox **L2** gave a conversion of 6% and a selectivity factor of $s = 1.4$ (Table 4, entry 2). This outcome was much poorer than that observed for the phenyl case **L1** (Table 4, entry 1). The single oxazoline ligand **L12** also gave poor conversion at only 5%, as well as a poor selectivity factor of $s = 1.5$ (Table 4, entry 12). Finally, BINOL **L15** gave a conversion of 4% with no enantioenrichment observed (Table 4, entry 15). PhPyBox (**L1**) appears to be a privileged ligand architecture for this system.

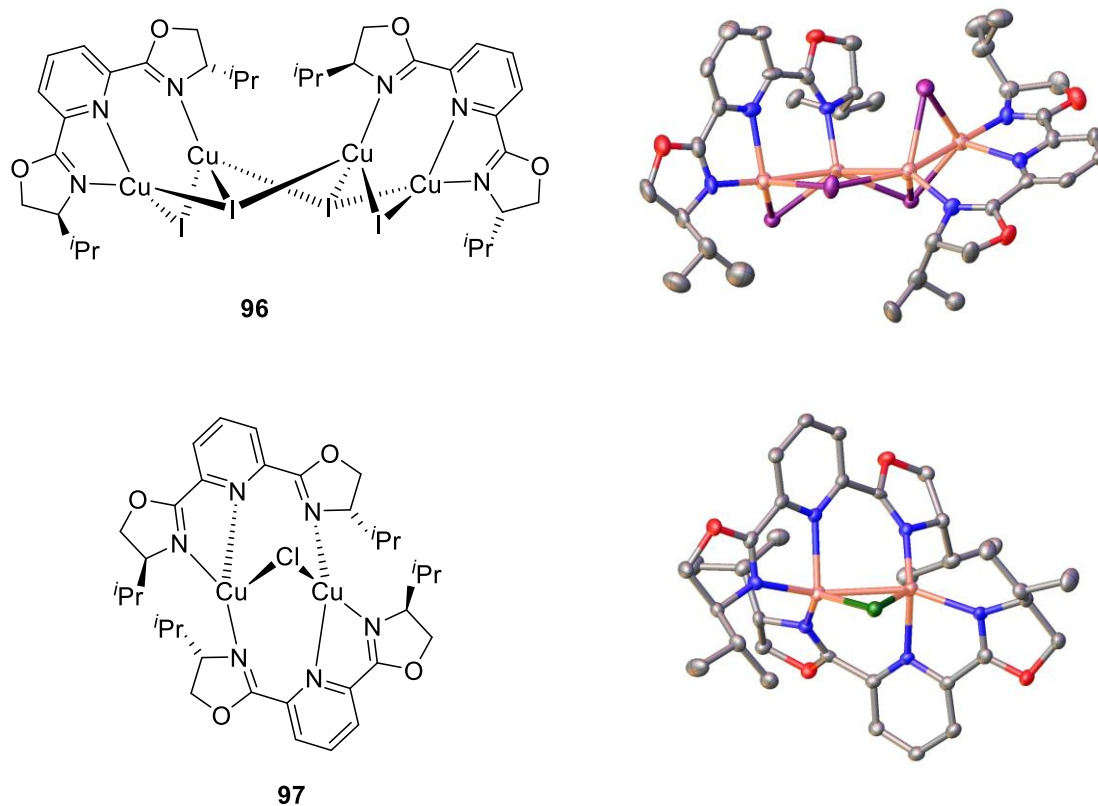
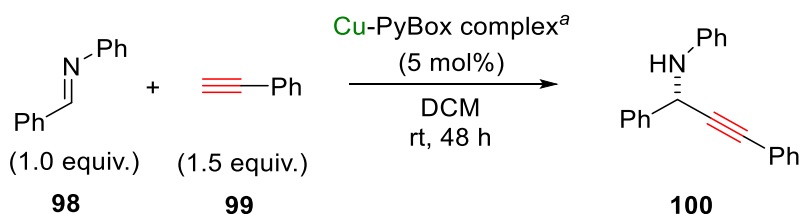


Figure 12 Crystal Structures of **L3** with CuI and CuCl reported by Panera *et al.*^[72] Thermal ellipsoids are shown at 20% probability. Hydrogen atoms and CuCl₂⁻ anion are omitted for clarity

Of the small range of examples of asymmetric CuAACs reported by Fokin *et al.*,^[32] Zhou *et al.*^[33] and Osako and Uozumi,^[41] pyridine bis(oxazolines) are superior in terms of selectivity compared with other common ligand families. Zhou *et al.* also reported that a negative non-linear effect (NLE) was observed when the enantiopurity of the ligand was altered. This points towards a non-monomeric species being responsible for selectivity in asymmetric CuAACs (see section 1.4). Work on crystallisation of PyBox complexes with various copper salts has been carried out by Panera and co-workers.^[72] They showed that mixing the ligands with various copper halides led to species **96** and **97**. The crystalline metal complexes were isolated and subjected to XRD where they were found to be dimeric in nature. For example, two distinctly different structures are seen when mixing **L3** with CuCl **97** or CuI **96** (Figure 12).

Panera and co-workers then used the isolated PyBox dimer species in the enantioselective synthesis of (1,3-diphenyl-2-propynyl)aniline **100**. They demonstrated that the reaction's yield and enantioselectivity was highly dependent upon the copper-PyBox species employed. For example, when a CuCl-based PhPyBox catalyst with a bridging chloride (see **97**) was utilised, yield (16%) and *ee* (7%) were poor (Table 5, entry 1). When CuI-based catalyst **96** was employed, no product was observed at all. This was in stark contrast to a CuBr-PyBox system which gave a high yield (89%), albeit with moderate selectivity (29% *ee*) (Table 5, entry 3). It should be noted that this reaction is different mechanistically to a CuAAC and therefore any direct comparison cannot be drawn.

Table 5 Enantioselective synthesis of 1,3-diphenyl-2-propynyl)aniline utilising isolated Cu-PyBox complexes Panera and co-workers^[72b]

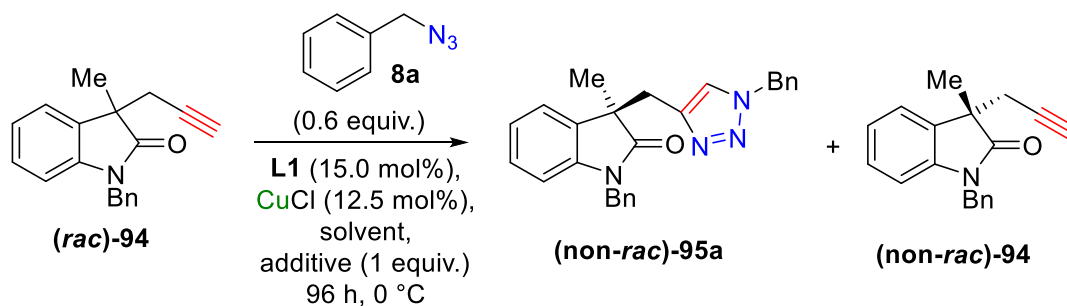


Entry	Catalyst	Isolated Yield (%)	Ee (%) ^b
1	$[\text{Cu}_2(\mu\text{-Cl})(\text{PhPyBox})_2][\text{CuCl}_2]$	16	7
2	$[\text{Cu}_4(\mu_3\text{-I})_2(\mu\text{-I})_2(\text{PhPyBox})_2]$	ND	ND
3	$[\text{Cu}_4(\mu_3\text{-Br})_2(\mu\text{-Br})_2(\text{PhPyBox})_2]$	89	29

^a Reactions were carried out using benzylideneaniline (0.4 mmol) in anhydrous DCM, under N₂ at rt for 48 h. ^b Ee determined by chiral HPLC, Chiracel OD-H

From Panera and co-workers' demonstration that the structure of the PhPyBox-derived metal complexes can be critical to obtaining good conversion and selectivity in asymmetric catalytic reactions (Table 5), it could be extrapolated that dimeric species could be important in the kinetic resolution of the quaternary oxindole **94**. It is worth noting, though, that the dimeric species obtained by Panera and co-workers are in the solid state, and the same structure and potentially conformations may not hold in solution.^[72b] Also, as mentioned by Panera,^[72b] it is unlikely that the PyBox copper complexes adopt a single structure in solution; a fluxional mixture of various structure and potentially conformations is much more likely.

Finally, it was decided that varying temperatures should be investigated, and common CuAAC additives should be tested to determine if selectivity could be further improved (Table 6, entries 1-13). Unfortunately, none of the conditions tested increased selectivity.

Table 6 Screening of temperature and additives in the kinetic resolution of **94**

Entry	Solvent	Additive	Copper Source	Temp (°C)	Reaction Time (h)	Conv (%) ^a	<i>ee</i> 94 (%) ^b	<i>s</i> ^c
1	THF		CuCl	50	24	45	8	1.3
2	Acetone		CuCl	50	24	46	24	2.3
3	^t BuOH		CuCl	50	24	7	0	1.0
4	Acetone		CuOTf·0.5 Toluene	50	24	51	11	1.4
5	Acetone		Cu(OAc) ₂	50	24	61	20	1.5
6	Acetone	NaAsc	CuOTf·0.5 Toluene	50	24	50	1	1.0
7	Acetone	NaAsc	Cu(OAc) ₂	50	24	53	16	1.5
8	DMSO		CuCl	50	24	38	4	1.2
9	DMF		CuCl	50	24	40	8	1.4
10	2,5-Hexanedione	NaAsc	CuCl	0	96	52	21	1.8
11	THF	NaAsc	CuCl	0	96	16	1	1.1
12	THF	DIPEA	CuCl	0	96	28	27	7.2
13	Acetone	DIPEA	CuCl	0	96	20	16	5.3

^a Conversion determined by inspection of ¹H NMR spectra; ^b *Ee* of recovered starting material (HPLC); ^c $s = \ln[(1-c)(1-ee)]/\ln[(1-c)(1+ee)]$. All reactions were carried out once.

Confident that all reaction variables had been probed, it was decided that testing this reaction with a range of azides might help to understand selectivity. To begin this process, a series of *in situ* azide formations were set up. As organic azides with low molecular weights and/or low C:N ratios can be explosive, it was deemed a safer option to identify selective azides before going to the lengths of isolation. In order to do this, a series of benzyl bromides was treated

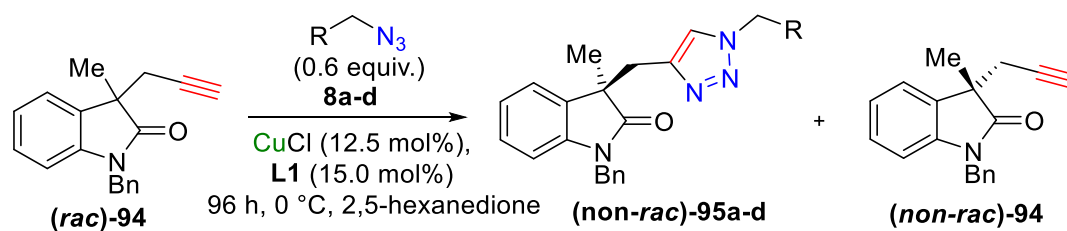
with sodium azide in acetone to form the corresponding benzyl azides **8a-g**. In a separate reaction vessel, the copper source and ligand were stirred at room temperature for an hour, and then alkyne **94** was added. The solution was stirred for 15 minutes at room temperature, then cooled to 0 °C for a further 15 minutes. The *in situ* azide formation reaction was monitored by TLC until consumption of the corresponding bromide was observed then transferred *via* syringe to the alkyne/catalyst mixture. This was then held for 96 h at 0 °C. This screening offered very poor conversions (Table 7, entries 1-6). In this set of experiments, the ratio of sodium azide to substituted benzyl bromide was 1.1:1.0, meaning that even with complete consumption of the bromide, there would still be 0.1 equivalents of inorganic azide in solution. It is well known that inorganic azides cannot undergo CuAAC reactions,^[73] so it is believed that the extra sodium azide in the reaction mixture was irreversibly binding to the chiral copper catalyst and deactivating it to further reaction. It should also be noted that the presence of bromide ions in solution may have led to the formation of copper bromide *in-situ*. Copper(I) bromide had already been shown to be inferior copper source to copper(I) chloride (Table 3, entries 1 and 2), therefore these reactions may have been carried out under less than optimal conditions.

Table 7 *In situ* formation and subsequent screening of benzylic azides in the kinetic resolution of oxindole **94**

Entry	Azide R	Conv. (%) ^a	<i>ee</i> 92 (%) ^b	<i>s</i> ^c
1	8b 2-PhC ₆ H ₄	13	14	35.2
2	8c 4-MeC ₆ H ₄	12	8	4.2
3	8d 3,5-CF ₃ C ₆ H ₃	12	7	3.3
4	8e 4-NO ₂ C ₆ H ₄	22	6	1.6
5	8f 4-ClC ₆ H ₄	12	6	2.7
6	8g 4-CF ₃ C ₆ H ₄	6	0	1

^a Conversion determined by inspection of ¹H NMR spectra; ^b *Ee* of recovered starting material (HPLC); ^c $s = \ln[(1-c)(1-ee)]/\ln[(1-c)(1+ee)]$. All reactions were carried out once.

Examining the conversions more closely, it does appear that the copper achieved around one catalytic turnover before deactivation. Using the selectivities observed, the best three were chosen for isolation. These were 2-PhC₆H₄N₃ **8b**, 4-MeC₆H₄N₃ **8c** and 3,5-CF₃C₆H₃N₃ **8d** (Table 7, entries 1-3). Looking at the selectivity factors, it appears as if the *in situ* formed 2-PhC₆H₄N₃ **8b** (Table 7, entry 1) was highly selective ($s = 35$), but due to the logarithmic nature of the selectivity factor equation, in combination with the inherent error in NMR (which is exaggerated at low conversions), the true selectivity of this reaction could be much lower.

Table 8 Isolated benzylic azide scope in the kinetic resolution of **94**

Entry	Azide R	Conv. (%) ^a	<i>ee</i> SM (%) ^b	<i>s</i> ^c
1	8a C ₆ H ₅	46	72	22.1 ^d
2	8b 2-PhC ₆ H ₄	45	67	17.5 ^e
3	8c 4-MeC ₆ H ₄	46	65	13.1 ^f
4	8d 3,5-(CF ₃) ₂ C ₆ H ₃	39	51	11.1 ^g

^a Conversion determined by inspection of ¹H NMR spectra; ^b *Ee* of recovered starting material (HPLC); ^c $s = \ln[(1-c)(1-ee)]/\ln[(1-c)(1+ee)]$; ^d Average of three $s = 22.1 \pm 0.5$, best unique case $s = 23.2$; ^e Average of three $s = 17.5 \pm 2.0$, best unique case $s = 19.8$; ^f Average of three $s = 13.1 \pm 1.7$, best unique case $s = 14.6$; ^g Average of three $s = 11.1 \pm 2.8$, best unique case $s = 14.4$.

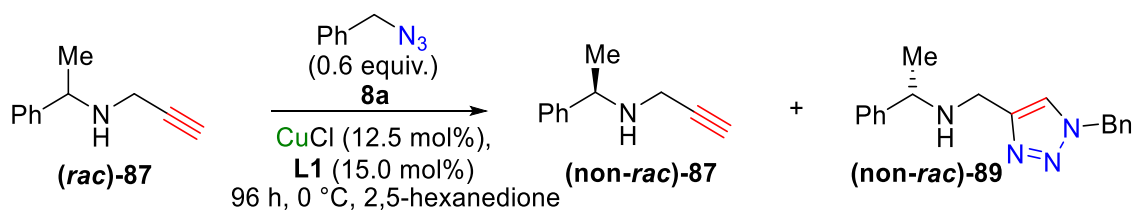
Taking the three azides with the best selectivity identified from the *in situ* screening, and isolating them before running the resolution reaction led to greatly increased conversion and good selectivity in all cases. With its electron-withdrawing trifluoromethyl groups, **8d** gave the poorest selectivity giving an average selectivity factor of $s = 11.1 \pm 2.8$ (Table 8, entry 4). Electron-donating methyl-containing **8c** gave $s = 13.1 \pm 1.7$ (Table 8, entry 3), **8b** with a bulky 2-phenyl substituent gave a good selectivity of $s = 17.5 \pm 2.0$ (Table 8, entry 2). However, none of the substituted benzyl azides could improve on the selectivity factor observed for simple benzyl azide **8a** ($s = 22.1 \pm 0.5$) (Table 8, entry 1). This mirrors findings of Osako and Uozumi; in their asymmetric CuAAC reaction (Scheme 18), benzyl azide was found to be superior to other benzyl azides in terms of *ee*.^[40] They reported *ees* of up to 99% when they used benzyl azide, but across a range of substituted benzyl azides the maximum enantioenrichment observed was only 35% *ee*.^[40]

Modification of the oxindole framework was also attempted to probe the scope of the alkyne component. Modification of the 3-position of oxindole was attempted through a Knoevenagel

condensation of oxindole with acetone in order to try to install an isopropyl group. Unfortunately, it was found that this material was inseparable from the starting oxindole. After multiple failed attempts to separate this material by column chromatography the compound and the project to modify the oxindole 3 position was abandoned. In addition to the 3-position, variation in the N-H protecting group was also attempted. Several N-protected oxindoles were synthesised (Boc, Cbz, Me), however enantiomer separation conditions of all variants were unable to be established.

Due to the nature of kinetic resolution, if the reaction of **94** with benzyl azide was run to a higher conversion, it is theoretically possible to obtain enantiopure recovered alkyne (to obtain 99% *ee* recovered alkyne with $s = 22.1$, conversion would need to be 61%). This was attempted, the reaction was conducted under the optimised conditions and left to react for 7 days, also a series of reactions with increased equivalents of benzyl azide were set up under the optimised conditions. It was found even with longer reaction times and greater equivalents of azide the reaction refused to proceed to above 50% conversion.

With effective resolution conditions for alkyne **94** obtained, it was hoped that they might be applicable to compound **87**. Applying the conditions developed for oxindole **94**, a selectivity factor of $s = 1.6 \pm 0.1$ was realised, with up to 27% *ee* noted in the recovered alkyne **87** following resolution (Table 9, entries 1-3). The absolute configuration at the alkyne **87** stereocentre was determined by comparison of retention times to enantiopure samples ((*R*)-**87**, (*S*)-**87**) in chiral GC analysis as (*R*)-**87**, thus the absolute configuration of the major triazole enantiomer could be assumed to be (*S*)-**89** (Table 9).

Table 9 Kinetic resolution of **87** under optimised reaction conditions

Entry	Conv. (%) ^a	87 <i>ee</i> (%) ^b	<i>s</i> ^c
1	59	21	1.49
2	50	15	1.53
3	58	27	1.88
Average <i>s</i>			1.63
Standard Deviation			0.21
Error			0.12

^a Conversion was determined by inspection of ¹H NMR spectra; ^b *Ee* of recovered starting material (GC); ^c $s = \ln[(1-c)(1-ee)]/\ln[(1-c)(1+ee)]$

Even though the selectivity factor for compound **87** was poor ($s = 1.6 \pm 0.1$), this result was still pleasing. Compared with all previous attempts, the dione-based reaction conditions were far superior, as the previous best *ee* realised was 4%, compared with 27% in the dione system. Looking at compound **87**, it is not surprising that the selectivity of the resolution is inferior to oxindole **94**. If it is assumed that copper acetylide formation is pivotal for the CuAAC to proceed, then the resolvable stereogenic centre is placed five bonds away from the catalytically active metal centre(s). Due to this connectivity, there is a great deal of conformational flexibility within the system. There are multiple C-C and C-N bonds within compound **87** which can freely rotate, thus making the relay of chiral information difficult to achieve. In contrast, the oxindole **94** possesses a quaternary stereogenic centre which is placed directly onto the aromatic framework, which may help to decrease flexibility in the system, thus leading to more efficient chiral relay and increased selectivity compared with the more flexible alkyne **87**.

The developed reaction conditions for the KR of **94** were also tested in the resolution of compounds which contain both primary amine and alkyne functionality, with no success, a detailed discussion of this can be found in Section 3.2.

2.1.1 Summary

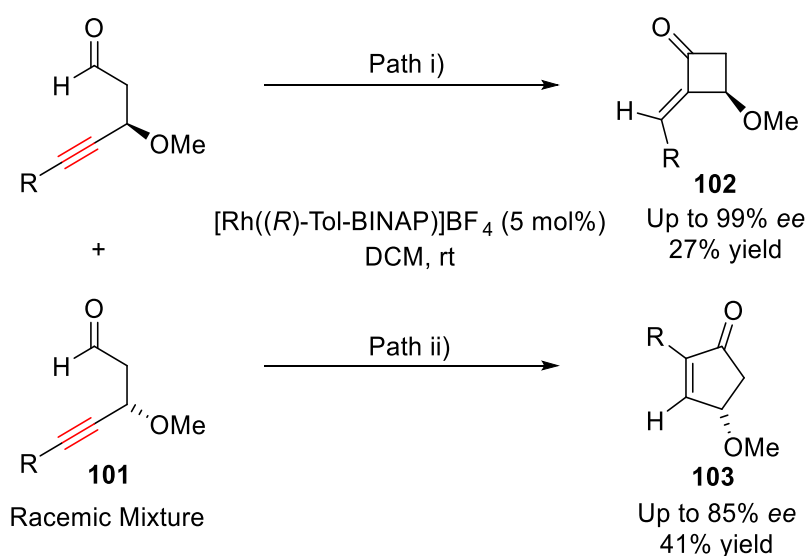
The studies detailed above demonstrate the first example of kinetic resolution of an alkyne *via* a CuAAC.^[74] Selectivity factors of up to 22.1 ± 0.5 were realised in the resolution of quaternary oxindole **94**, and enantioenriched alkynes and triazoles were obtained in greater than 80% *ee*. Optimisation of the reaction conditions was carried out and it was found that carbonyl-containing solvents gave superior selectivity. In addition, it was found that PhPyBox **L1** was a privileged ligand architecture for this reaction, with all other ligands tested being ineffective, both in terms of reaction conversion and selectivity. A range of substituted benzylic azides was shown to be compatible with the resolution conditions. Linear alkyne system **87** was resolvable using the optimised conditions, giving enantioenriched alkynes in up to 27% *ee*. These findings were reported in *Chemical Communications*.^[75] Experimental work was carried out by the author of this thesis, the primary investigators were Dr John Fossey (UoB) and Dr Benjamin Buckley (LU). This methodology was the basis for the work carried out in Sections 2.2 and 3.2.

2.2 ***Simultaneous Kinetic Resolution of Azides and Alkynes via Copper-Catalysed Azide-Alkyne Cycloadditions***

Azides, in addition to alkynes, have been shown to be susceptible to kinetic resolution methodologies. With this in mind, it was hypothesised that two kinetic resolutions could be carried out simultaneously. It was postulated that if PyBox ligand architectures could effect the successful kinetic resolution of alkynes and azides, then it may be possible to resolve both

simultaneously. This idea was conceived by the supervisors of this thesis and carried out jointly between the author of this thesis and a final-year masters project student.

Parallel kinetic resolution was outlined by Vedejs *et al.* in 1997.^[53b] In this type of KR, each enantiomer of a chiral substrate undergoes its own reaction to yield two enantioenriched products.⁵² For example, Fu and co-workers used rhodium catalysis in the parallel kinetic resolution of 4-alkynals **101** (Scheme 26).^[76] They found that in a racemic mixture of alkynals the (*R*) enantiomer reacts exclusively to form a cyclobutanone **102**, whilst the (*S*) enantiomer forms a cyclopentenone product **103**. Thus, the two starting enantiomers follow two reaction pathways leading to two enantioenriched products.^[53a]



Scheme 26 Parallel kinetic resolution of 4-alkynals, Fu and co-workers^[76] Path i) Reaction of (*R*)-**101** to form cyclobutanone product **102**. Path ii) Reaction of (*S*)-**101** to form cyclopentenone product **103**.

The simultaneous kinetic resolution of a racemic azide and a racemic alkyne to form a product as a single diastereomer would represent an unusual type of kinetic resolution in that most employ a single racemic starting material and form two separate products.

The concept of a simultaneous KR through CuAAC was to use a chiral racemic azide and a chiral racemic alkyne and allow them to react *via* a CuAAC to form one major diastereomer

of product. Due to the presence of two stereogenic centres in the triazole product, a set of four diastereoisomers would be formed, with the diastereomeric ratio dependent upon the ability to effect KR in the starting alkyne and azide. In addition, it was hoped that both enantioenriched alkyne and azide could be recovered at the end of the resolution, giving access to three enantioenriched materials from a single resolution process (Figure 13).

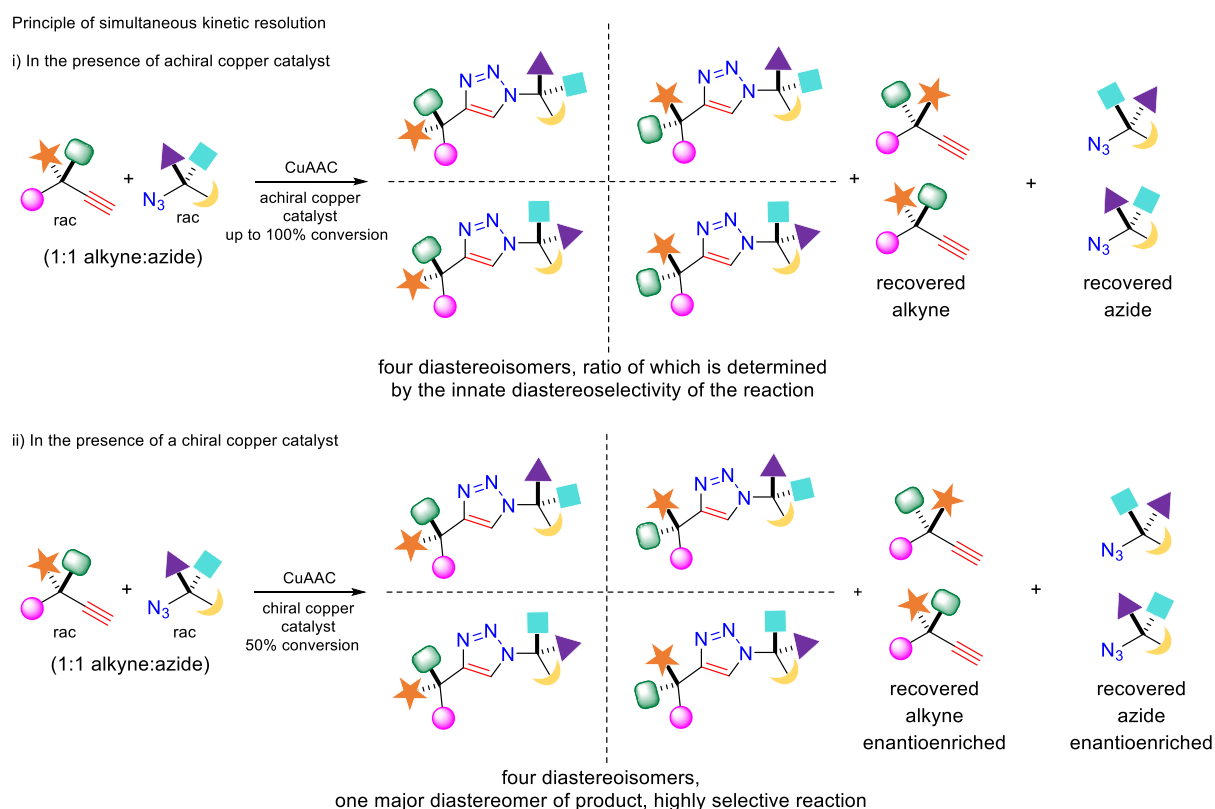
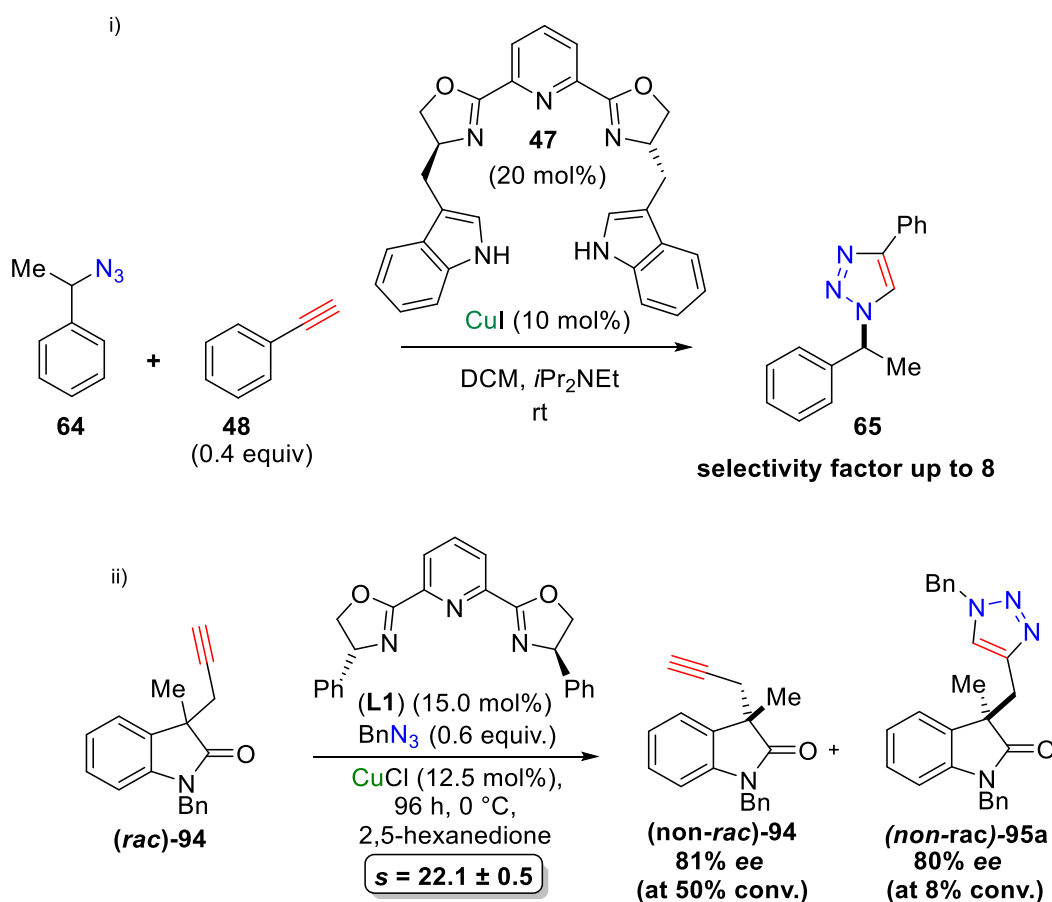


Figure 13 Principle of simultaneous kinetic resolution of a chiral azide and alkyne *via* a CuAAC reaction

In order to give the reaction the best chance of forming enantioenriched materials, literature precedents for known resolvable alkynes and azides were researched. Due to the literature precedent of Fokin and co-workers,^[32] **64** was chosen as the azide component in the simultaneous KR (Scheme 27). The alkyne component **94** was chosen due to the reaction development detailed earlier in this chapter (Section 2.1, Scheme 27).^[75] Both of these reaction components had been resolved using PyBox ligand architectures. Azide **64** has been

shown to be resolvable in DCM, but neither acetone nor 2,5-hexanedione were tested in this work. As the selectivity factor observed for the oxindole alkyne **94** had been shown to be higher ($s = 22$) than that of the literature value of azide **64** ($s = 8$), it was decided that the previously utilised resolution conditions for the alkyne would be applied to the simultaneous kinetic resolution. This meant that before the simultaneous process could be probed, the azide would need to be tested for compatibility in the solvents used for the alkyne KR.



Scheme 27 Previous work i) Kinetic resolution of azides, Meng *et al.*^[32] ii) Kinetic resolution of alkynes, Brittain *et al.*^[75]

Kinetic resolution of azide **64** with **L1** in 2,5-hexanedione and acetone were the first reactions carried out. Utilising the same reaction protocol as optimised in Section 2.1, the resolution was attempted using azide **64** and 0.5 equivalents of phenylacetylene **48**, with **L1** (15 mol%) and CuCl (12.5 mol%) catalyst in acetone or 2,5-hexanedione. A problem was encountered

during the work-up of these resolution reactions. It was found that following aqueous extraction, some azide was not being recovered and thus conversions greater than 50% were being measured (0.5 equivalent of alkyne was used; therefore, maximum conversion was 50%), further evidence of this was seen in the low mass recovery of these reactions. The reaction was then carried out in acetone- d_6 and the resolution monitored *in situ* via ^1H NMR spectroscopy. From this NMR experiment a selectivity of $s = 7.4$ was observed. Testing the resolution of azide **64** in 2,5-hexanedione was a more involved task because deuterated 2,5-hexanedione was not available at that time.^[77] Thus, the procedure used in the case of acetone- d_6 could not be used for this solvent. Following discussion with an NMR technician, it was decided that the conversion of the reaction could be garnered from running unlocked proton NMR spectroscopic analysis. This meant that the NMR spectrum of the reaction mixture could be obtained without the need for a deuterated solvent (Figure 14).

Comparing the resonances at 6.45 ppm (CH in triazole **104**) and 5.24 ppm (CH in azide **64**), a reaction conversion of 50% was determined (Figure 14). Chiral GC analysis of the same crude reaction mixture gave 60% *ee*, and from these figures a selectivity factor of $s = 7.1$ was calculated.

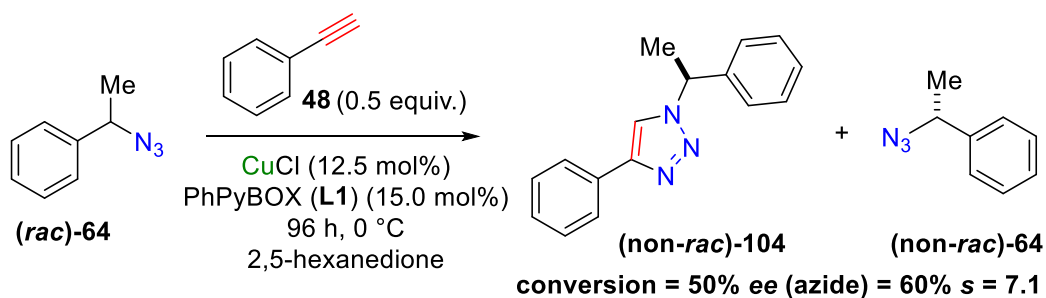
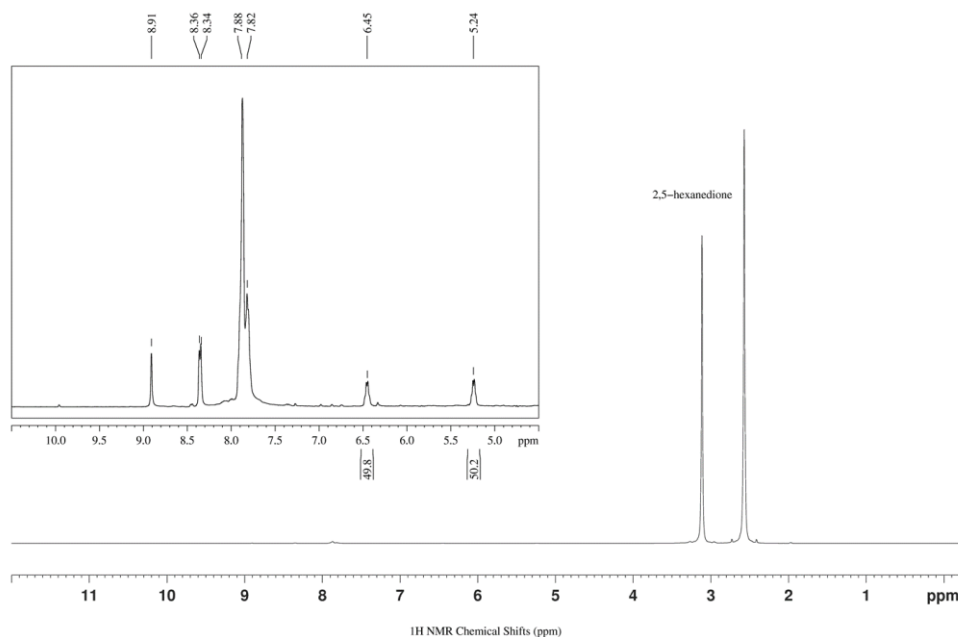


Figure 14 Unlocked NMR spectrum of the kinetic resolution of azide **64** to determine reaction conversion, *ee* determined by chiral GC analysis of remaining azide

Following successful resolution of azide **64** using the dione-based reaction conditions discussed earlier in this chapter (Section 2.1), the simultaneous resolution of both azide **64** and alkyne **94** could be tested. Chiral HPLC separation conditions for the diastereomeric products were developed (Figure 15). A sample of the triazole **105** was obtained through the reaction of racemic azide **64** (1.1 equiv.) with racemic alkyne **94** (1.0 equiv.) under standard click reaction conditions – CuI (5 mol%), TBTA (5 mol%) in acetone until full consumption of the starting alkyne was observed by TLC. This gave a chromatography trace showing four peaks in a 25:25:25:25 ratio. It should be noted that the reaction could have led to a ratio of diastereoisomers which was not 25:25:25:25 due to inherent diastereoselectivity.^[78] The

CuAAC of **64** with **94** was then carried out under the optimised conditions for the KR of **94** (2,5-hexanedione, 96 h, 0 °C, CuCl (12.5 mol%), TBTA (15.0 mol%) but with TBTA in the place of a chiral ligand, to measure any inherent diastereoselectivity within the CuAAC reaction under these conditions. A *dr* of 46:54 in the triazolic product **105** was observed, showing that the substrate diastereoselectivity in the presence of a non-chiral catalyst, under optimised reaction conditions was poor (Figure 15).

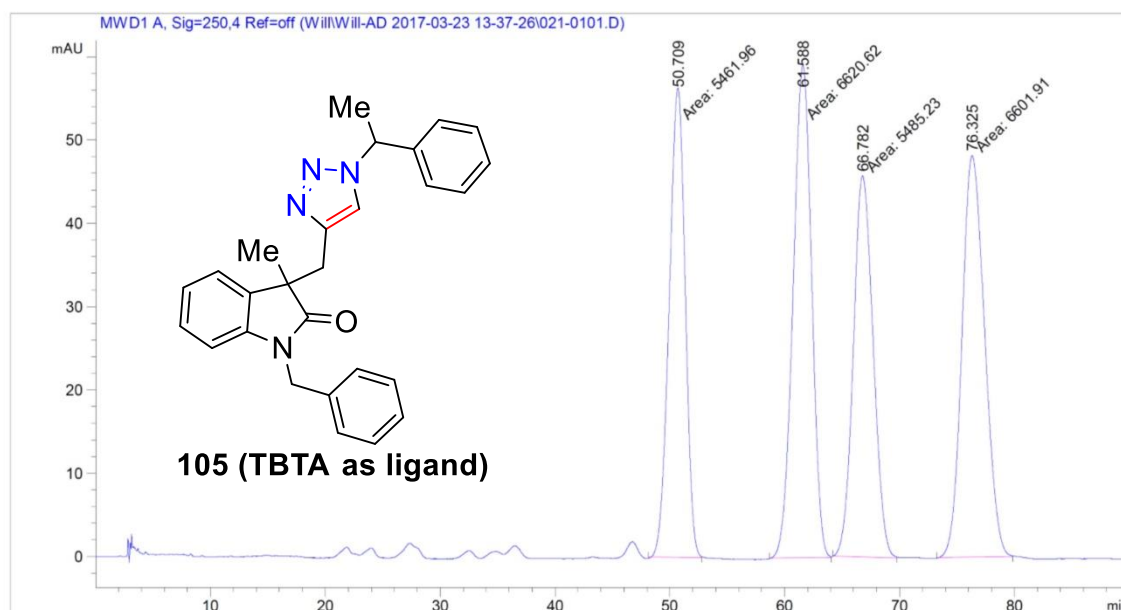
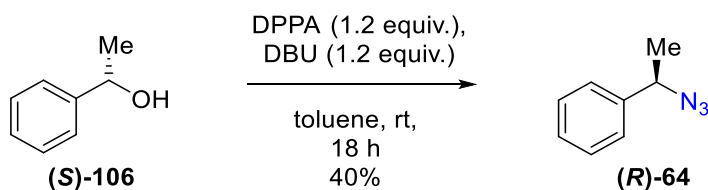


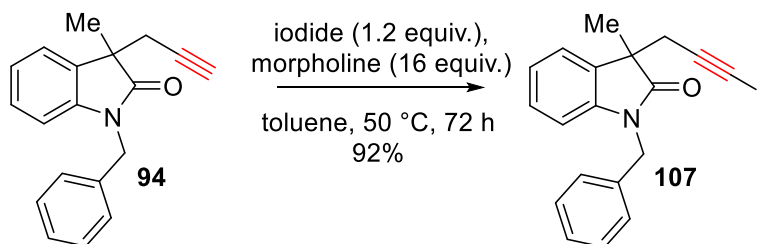
Figure 15 HPLC trace of triazole **105** in the absence of chiral catalyst. (*R,S*) 51 min, (*R,R*) 62 min, (*S,R*) 67 min, (*S,S*) 76 min. Ratio 23:27:23:27

In order to calculate which peaks in the HPLC traces referred to diastereomer pairs or enantiomer pairs several series of reactions were carried out. To identify which peaks in the HPLC traces were due to the diastereoisomeric pairs and which were enantiomeric pairs a series of resolutions were carried out using enantiopure starting alkyne and azide. Enantiopure (*R*)- and (*S*)-azides **64** were successfully synthesised using a literature method^[79] (Scheme 28) and the enantiopurity of each was determined by chiral GC analysis. Enantiopure alkyne **94** was obtained by chiral preparative HPLC of racemic alkyne **94**, and the isolated material was eluted through analytical HPLC to confirm its enantiopurity.



Scheme 28 Synthesis of enantiopure azide **64** from enantiopure alcohol **106**

To determine the absolute configuration of alkyne **94**, a study into the crystallisation of derivatives of alkyne **94** was carried out jointly between the author of this thesis and an international exchange project student. Assignment of the absolute configuration of the azide **64** (both recovered and consumed during the reaction) was relatively trivial due to existing literature of the enantiopure synthesis of the material.^[79] However, the assignment of the recovered and consumed enantiomers of alkyne **94** proved to be much more challenging. The strategy taken was to derivatise a single enantiomer of alkyne **94** with a heavy element. This would then allow the absolute stereochemistry to be determined by single-crystal XRD. It was originally hypothesised that forming a triazole with a benzyl azide derivative containing a heavy atom would be a straightforward way to introduce that said atom *via* a triazole. However, in all cases the triazoles formed could not be successfully crystallised. This led to the idea of using an iodoalkyne to achieve the aim.



Scheme 29 Synthesis of iodoalkyne **107**

Racemic alkyne **94** was successfully treated with iodine and morpholine to form iodoalkyne **107** in 92% yield (Scheme 29). (For further discussion of the synthesis of iodoalkynes, see Section 4.1.) Encouragingly, this material was a solid, and a single crystal of sufficient quality

for analysis was obtained by slow evaporation from acetonitrile. The single crystal XRD analysis showed that the racemic iodoalkyne was present (Figure 16). The space group of the crystal lattice was found to be $P2_1/c$, a centrosymmetric group, again proving that this was a racemic mixture.

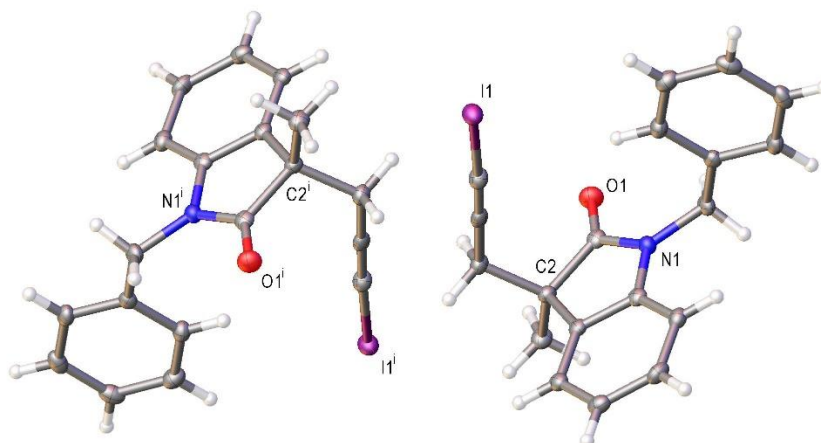


Figure 16 Selected molecules of oxindole **107** with ellipsoids drawn at the 50 % probability level. These molecules are related by an inversion centre and are thus opposite enantiomers. Symmetry codes used to generate equivalent atoms: i: 1-x, -y, -z

Utilising the same methodology used to form iodoalkynes, the reaction was repeated with a single enantiomer of the alkyne **94** (recovered following preparative chiral HPLC). This reaction garnered a single enantiomer of **107** in 74% yield. Evaporation from ethyl acetate led to the recovery of crystals suitable for XRD analysis. From the analysis, the stereogenic centre was determined to be (*R*) by anomalous dispersion with a Flack parameter of -0.018(3). In addition, the space group of the crystal lattice was found to be $P2_1$, a non-centrosymmetric space group, giving further evidence of a single enantiomer being present (Figure 17).

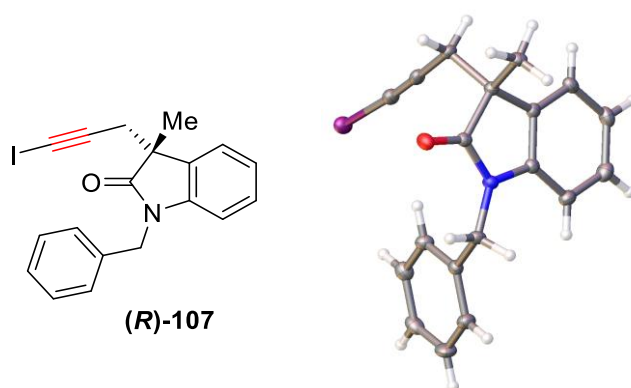
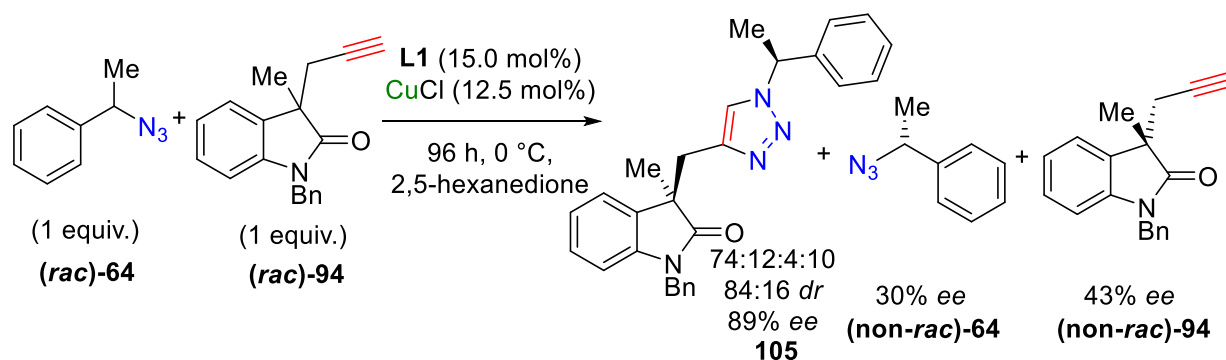


Figure 17 Single enantiomer crystal structure of iodoalkyne (**R**)-**107**. Ellipsoids are drawn at the 50% probability level, space group = P2₁ with a Flack parameter of -0.018(3).

This crucial crystal structure allowed the determination of absolute stereochemistry of the recovered alkyne for both the kinetic resolution of **94** with benzyl azide, but also in the simultaneous KR reaction. From knowing which enantiomer was being consumed slowly, it was straightforward to deduce the absolute stereochemistry of the oxindole stereogenic centre in triazoles **95** and **105**.

With both starting materials in their enantiopure forms and the crystal structure of **107**, it was possible to determine the stereochemical relationships between compounds giving rise to the peaks in the chiral HPLC traces. Reaction of enantiopure (*R*)-alkyne **94** with racemic azide **64** under the developed kinetic resolution conditions (see Table 10) showed two peaks in the HPLC trace, corresponding to the two fastest-eluting species in Figure 15. These species were therefore diastereoisomers of one another ((*R,S*) and (*R,R*)). Reaction of enantiopure (*S*)-azide **64** with racemic alkyne **94** under achiral conditions again led to two observed peaks. These peaks corresponded to the fastest-eluting and slowest-eluting species from Figure 15, and these were assigned as diastereoisomers of one another ((*R,S*) and (*S,S*)). With this knowledge, the four peaks within the HPLC trace could be assigned (Figure 15 and Figure 18).

The simultaneous kinetic resolution of alkyne **94** and azide **64** was next attempted. Pleasingly, it was found that a mixture of 1:1 **94** and **64** in the presence of **L1** (15 mol%) and CuCl catalyst (12.5 mol%) in 2,5-hexanedione gave product **105** with its diastereomers in a ratio that was not 23:27:23:27 (Figure 18). This showed that the reaction was kinetically resolving the two starting materials. Following resolution, the enantioenrichment of alkyne **94** was measured *via* chiral HPLC and that of the azide **64** by chiral GC; *ee* values of 43% and 30% were observed, respectively. The diastereomer ratio (*dr*) of the triazolic product was measured to show a ratio of 84:16 (with the ratio of the four diastereoisomers being 74:12:4:10), and the *ee* of the major diastereoisomer being 89% (Scheme 30). The favoured diastereoisomer of **105** was determined to be (*R,S*), and this confirmed by independently synthesising the compound from enantiopure (*R*)-**94** and (*S*)-**64**. The retention time of independently synthesised (*R,S*)-**105** matched that of the favoured diastereoisomer of the asymmetric catalytic reaction.



Scheme 30 Simultaneous kinetic resolution of alkyne **94** and azide **64**. *Ee* of compounds **105** and **94** were measured by chiral HPLC. *Dr* was measured by chiral HPLC. *Ee* of compound **64** was measured by chiral GC.

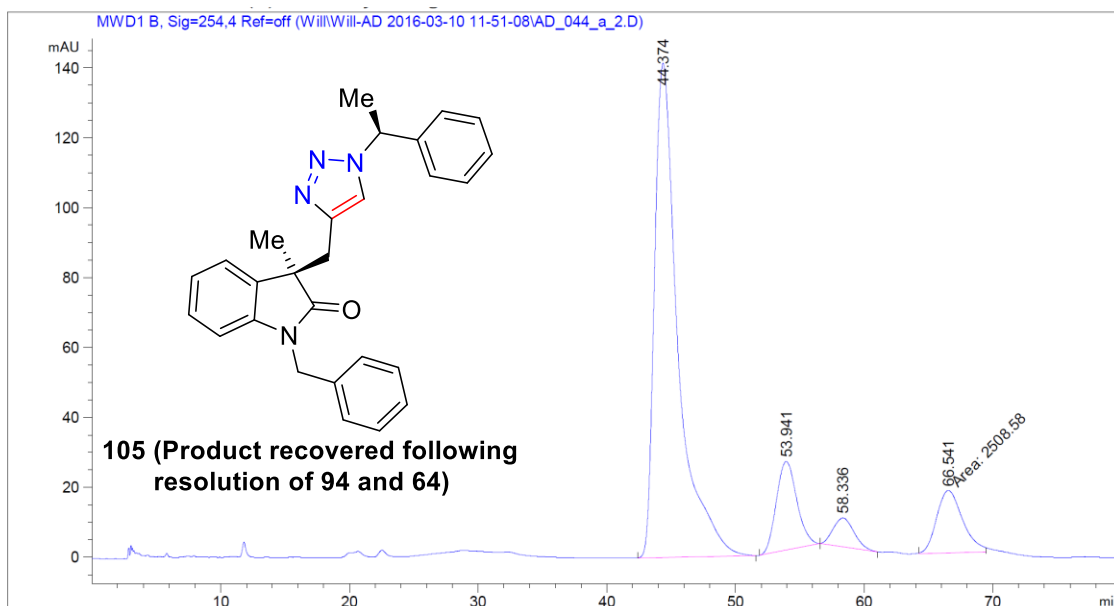
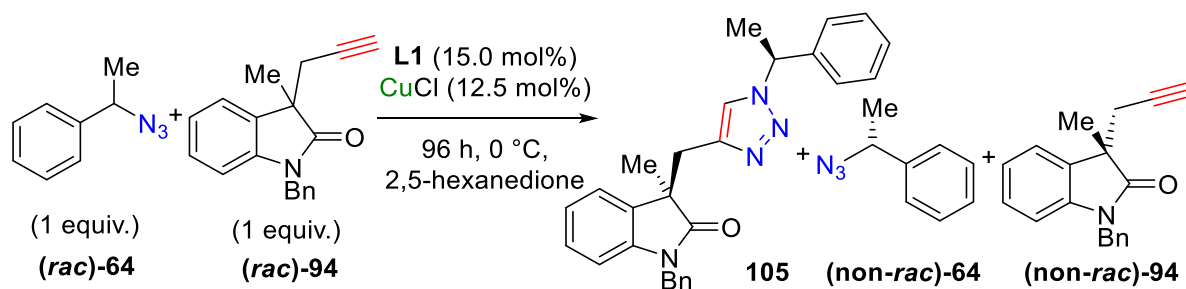


Figure 18 HPLC trace of triazole **105** recovered following simultaneous kinetic resolution of **94** and **64**. (*R,S*) 44 min, (*R,R*) 54 min, (*S,R*) 58 min, (*S,S*) 66 min. Ratio 74:12:4:10

The simultaneous kinetic resolution of **94** and **64** was carried out in triplicate as can be seen in Table 10. Enantioenriched alkynes and azides were observed in each case, showing that the reaction was reproducible.

Table 10 Simultaneous kinetic resolution of alkyne **94** and azide **64** carried out in triplicate



Entry	Conv. ^a (%)	<i>dr</i> 105 ^b	<i>ee</i> 105 ^c (%)	<i>ee</i> 64 ^d (%)	<i>ee</i> 94 ^e (%)
1	41	84:16	89	30	43
2	36	84:16	90	30	33
3	66	84:16	89	37	40

^a Conversion determined by ¹H NMR spectroscopy; ^b *dr* of **105** determined by HPLC; ^c *Ee* of major diastereoisomer determined by HPLC; ^d *ee* of **64** determined by GC; ^e *ee* of **94** determined by HPLC

2.3 Summary

A novel kinetic resolution process was developed within this section.^[80] Azides and alkynes were kinetically resolved simultaneously to favour one diastereoisomer in a mixture of diastereomeric triazole species. This is believed to be the only report of this type of reaction manifold. It is hoped that the underlying methodology developed in this section could be applicable to other types of reactions with other chiral materials. The ability to resolve multiple chiral species in a single process is attractive to the synthetic organic chemist, as it is more time-efficient and resource-efficient than running multiple single kinetic resolution reactions.

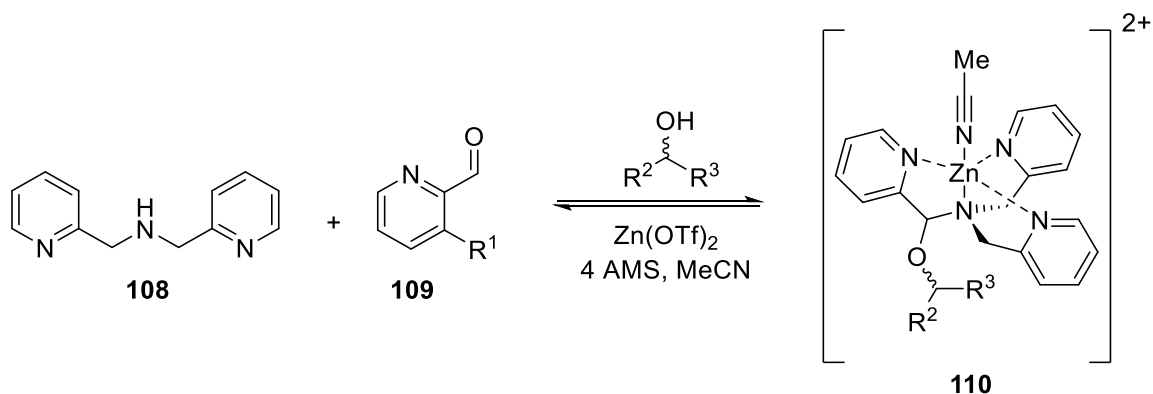
The kinetic resolution experimental work within this section was carried out jointly between the author of this thesis and Andrew Dalling. The work on crystallisation of oxindoles was carried out by Zhenquan Sun under the supervision of the author. Crystal structures were determined by the author along with Dr Louise Male (UoB) and unlocked NMR experiments were conducted by Dr Cécile Le Duff (UoB). The primary investigators were Dr John Fossey (UoB) and Dr Benjamin Buckley (LU).

3 Three-Component Boronic Acid Assemblies, Applications in Asymmetric Catalysis, Combinatorial Chemistry and Pedagogy

3.1 High-Throughput Screening for *ee* Determination

One of the bottlenecks in the analysis of asymmetric reaction outcomes is the enantiomeric excess determination by chiral HPLC analysis.^[81] The development of separation conditions for a pair of enantiomers, followed by often lengthy elution times, means that even a relatively fast reaction can require hours to properly analyse the enantiomeric makeup of the product. Therefore, the creation of high-throughput screening (HTS) techniques to determine *ee* is important, especially where hundreds to thousands of reactions need to be analysed swiftly.^[81-82]

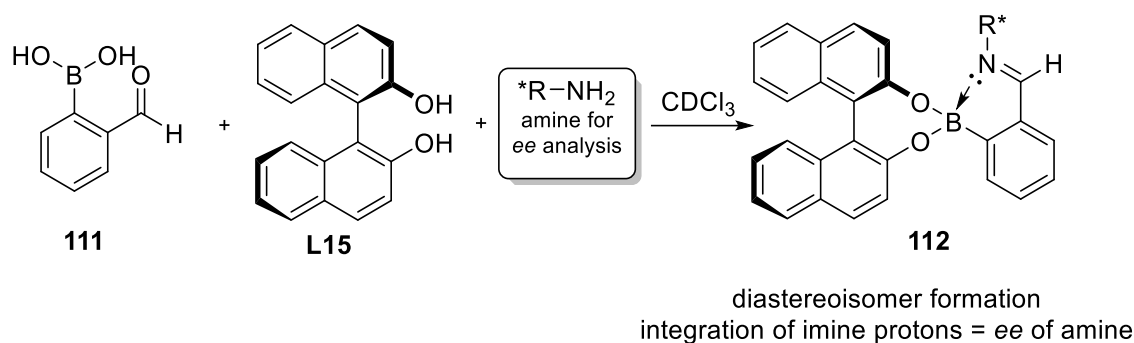
Many different strategies have been targeted to determine the enantiomeric makeup of mixtures without the need for chiral chromatography. Anslyn and his group have successfully designed assemblies which utilise circular dichroism (CD) to determine the *ee* of a scalemic mixture of enantiomers.^[81-83] For example, the group developed a zinc-based tripodal assembly for the *ee* determination of chiral alcohols (Scheme 31).^[84] Utilising hemiaminal formation, the assembly **110** takes on an M or a P twist in the presence of enantiomers, which is proportional to the enantiomeric makeup of the original sample, and this twist gives a CD signal which can be related to the *ee* of the chiral analyte. Previously, to accurately measure the *ee*, a calibration curve was required for each analyte tested. However, it has now been shown that using linear free-energy relationships, the *ee* of an analyte can be measured without the need for a calibration curve.^[85]



Scheme 31 Tripodal assembly for the rapid determination of *ee* of chiral diols, Anslyn and co-workers^[84]

NMR spectroscopy is another method that can be utilised in some cases as a HTS *ee* determination strategy. Proton NMR spectra can usually be obtained in less than five minutes, whereas HPLC runs often require approximately tens of minutes.^[86] The increased throughput in combination with circumvention of chiral chromatography method development makes ¹H NMR spectroscopy an attractive approach for HTS.^[87] One popular strategy is the use of chiral shift reagents, with the most common being relatively expensive lanthanide-based complexes, e.g. Eu(hfc)₃.^[88] A weakly paramagnetic chiral lanthanide complex forms an *in situ* mixture of diastereoisomers whose *dr* can be measured to determine the *ee* of the chiral analyte.^[88c]

Derivatisation of compounds to form distinguishable diastereoisomers is one strategy for indirect determination of *ee* *via* NMR spectroscopy.^[89] This technique was most notably employed by Mosher (Mosher's acid) for the analysis of enantiomeric ratios of chiral alcohols and amines.^[90] However, this method requires one to sacrifice a small amount of sample in order to carry out the analysis, and is therefore less than ideal for HTS applications.^[91]



Scheme 32 A three-component Bull-James boronic acid-based assembly for the determination of *ee* of chiral amines, Perez-Fuertes *et al.*^[92]

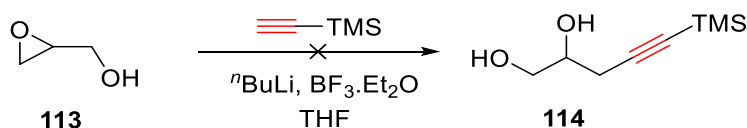
A boronic acid-based assembly for the ¹H NMR spectroscopic analysis of the enantiopurity of chiral amines and diols was developed by Bull, James and co-workers (Scheme 32).^[83, 92-93] This system takes advantage of the diastereomeric complexes formed from a boronic acid, chiral diol and a chiral primary amine. Using a stereo-defined amine component, the *ee* of a chiral diol could be analysed, and *vice versa*.^[92-93, 93f, 93h] The commercial availability and relatively inexpensive nature of the Bull-James assembly components gives it an economic edge over lanthanide-based chiral shift reagents.

The concept behind the Bull-James assembly has been used previously for a plethora of applications. Work between Bull, James and Anslyn used the three-component assembly, but applied CD to determine *ee* instead of NMR.^[83] As the three-component assembly forms, the twist angle of the BINOL changes and thus a CD signal is realised. CD is an attractive methodology for HTS applications, as it is quick to carry out and with specialised well plates up to 96 samples can be measured simultaneously. Work by Anslyn, Krische and co-workers would apply the zinc tripodal assembly **110** (Scheme 32) to a well plate system and show that asymmetric catalytic processes could be analysed very quickly with the enantioenrichment of 96 samples being calculated in under two hours.^[82]

The following work is based upon the three-component boronic acid-based system. It will demonstrate the system's applicability towards asymmetric click chemistry as well as dynamic combinatorial chemistry, and describe a way of teaching undergraduate students a method to determine *ee* of chiral amines.

3.2 The Bull-James Assembly for Use in Asymmetric Catalysis

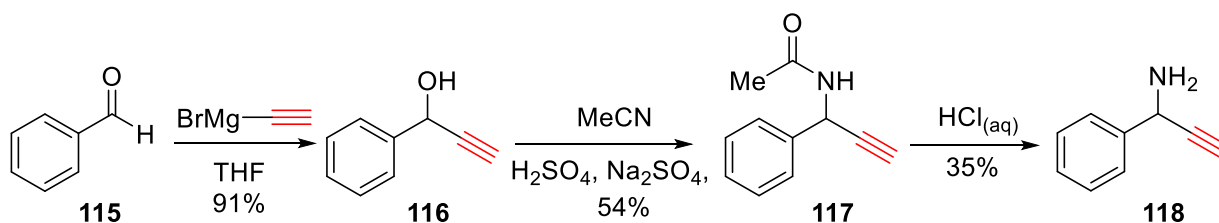
Using the Bull-James three-component assembly strategy, it was hypothesised that the enantioenrichment of a kinetic resolution could be analysed *in situ* using ^1H NMR spectroscopy. Due to previous expertise in kinetic resolution of alkynes through the CuAAC (Chapter 2) it was hypothesised this would be a challenging reaction to test and monitor *in situ* and thus it was ideal for testing a novel sensing regime. It was hoped that the kinetic resolution of a chiral diol or amine could be observed using this methodology. To test this hypothesis, originally a chiral diol substrate was targeted. Due to literature precedent it was postulated that the opening of epoxide **113** with TMS acetylene would lead to a chiral, kinetically resolvable diol **114** (Scheme 33).^[94] Unfortunately, this reaction always led to a complex, inseparable mixture of products. It was decided that effort should be refocused to the synthesis of a chiral primary amine alkyne.



Scheme 33 Attempted synthesis of diol **114**

A new substrate was designed to probe the assembly sensing hypothesis (Scheme 34). Substrate **118** was chosen due to the proximal nature of the amine and alkyne functionalities, which could be advantageous in obtaining good selectivity during KR. Ethynyl magnesium bromide was successfully added to benzaldehyde **115** to give secondary alcohol **116** in 91%

yield. A Ritter reaction using acetonitrile was then used to form the amide **117** in 54% yield. Due to the stability of this compound, the acid hydrolysis was not very efficient, giving only a 35% yield of the primary amine **118**. Even though the yield was moderate, this synthetic route gave enough of the desired material to determine if this would be a good substrate for KR and NMR spectroscopy analysis.



Scheme 34 Synthesis of amine alkyne **118**

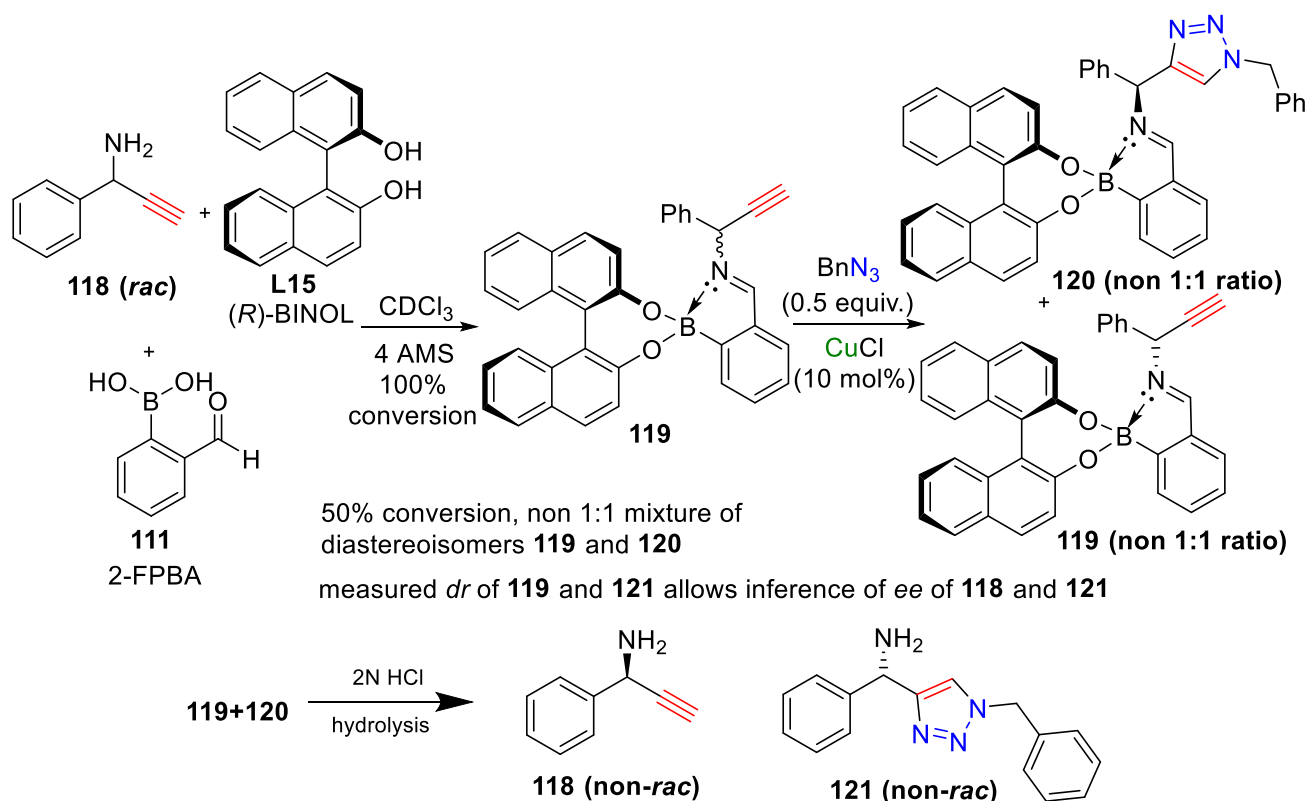
Immediately it was noticed that substrate **118** was self-reactive and not stable on silica during column purification attempts. Therefore, the material was used without further purification following acid-base extraction. It was found that compound **118** could be stored at $-20\text{ }^{\circ}\text{C}$ as a solution in chloroform.

Mixing a 1:1:1 ratio of amine **116**, (*R*)-BINOL **L15** and 2-formylphenylboronic acid (FPBA) **111** at 70 mM, a 1:1 integration of the imine protons of the formed diastereoisomers of assembly **119** was observed by ^1H NMR spectroscopy. The same analysis was carried out with the triazolic product **121** and again a 1:1 integration of the imine protons of the formed diastereoisomers of assembly **120** was observed. Crucially, these imine signals did not overlap with the signals resulting from the assembly formed with starting material **118**.

As assembly formation had been proven to give diastereoisomers with both starting material **118** and triazolic product **121**, and the imine resonances of assemblies **119** and **120** did not overlap with one another, it was time to probe whether the assembly methodology could be

applied to measuring the enantioenrichment of a kinetic resolution. To do this, a resolution reaction using amine **118** would be carried out. Once the resolution had finished, the other assembly components (**111** and **L15**) would be added and the ^1H NMR spectrum recorded. Unfortunately, when amine **118** was exposed to the PyBox-mediated resolution conditions developed in Chapter 2 (15.0 mol% PhPyBox **L1** and 12.5 mol% CuCl in 2,5-hexanedione), no amine or triazolic product (**118/121**) was recovered after the resolution process, and thus no NMR spectroscopic analysis could be carried out. Presumably, this was due to the self-reactivity noticed with substrate **118**.

Even though the initial hypothesis of using the Bull-James assembly to measure the enantioenrichment of a KR had been shown not to be viable, the reactivity issue encountered with **118** did lead to another train of thought. It was postulated that the three-component assembly could decrease the reactivity of **118** through imine formation. In addition, examining the enantiopure diol component of the assembly, it was proposed that the assembly could act as a chiral auxiliary and in turn could be able to influence the stereochemical outcome of the resolution reaction as well as monitor its enantioenrichment.

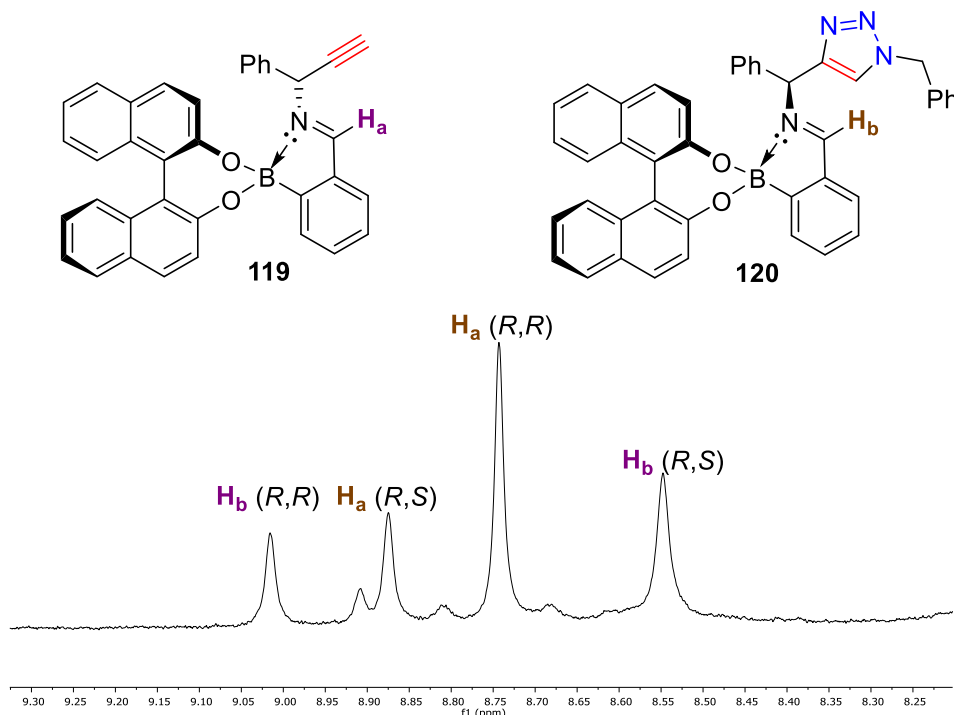


Scheme 35 Principle of utilising the Bull-James assembly as a dual-purpose chiral auxiliary and chiral shift reagent

From these ideas, it was hypothesised that the three-component assembly could be used for two simultaneous functions; it could act as a method of analysing the *ee* of both the starting material **118** and product **121** during kinetic resolution, as well as being a chiral auxiliary to influence the stereochemical outcome of said resolution (Scheme 35). To test this theory, a 1:1:1 ratio of amine **118**, (*R*)-BINOL **L15** and FPBA **111** were mixed together in chloroform-*d* and then 0.5 equivalents of benzyl azide was added. Finally, 10 mol% of CuCl was added as a catalyst.

Following the CuAAC reaction *via* ^1H NMR spectroscopy, it was found that indeed, the two resonances for the imine proton in the product assembly **120** did appear in a ratio which was not 1:1, and the two imine resonances for the starting alkyne assemblies **119** were no longer

1:1 (Figure 19). This was a very pleasing result as it appeared that the Bull-James assembly was acting as planned, as a dual-function chiral auxiliary and *ee* determination tool.

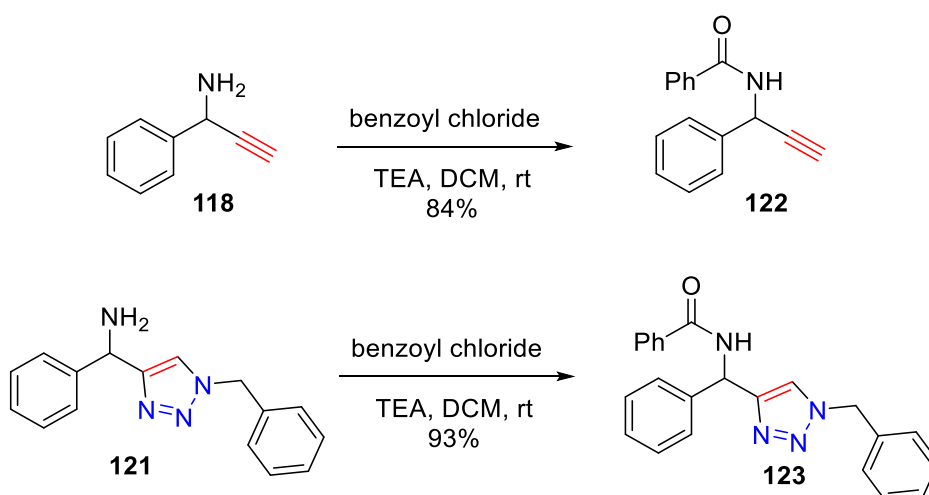


highlighted peaks at 8.87ppm and 8.74 corresponding to the imine proton of the mixture of diastereoisomers of complex **119** after kinetic resolution. Integration gives an inferred *ee* of 37%

Figure 19 Imine region of assembly ^1H NMR spectrum

For the dual-purpose assembly methodology to be useful, the enantioenriched alkynes and triazoles needed to be recovered from the assembly after resolution. It was hoped that the amine and assembly equilibrium could be forced back to the individual components through acid hydrolysis. It was found that stirring the mixture of assemblies **119/120** with 2 N $\text{HCl}_{(\text{aq})}$ and subsequent extraction with DCM led to a recovery of a mixture of FPBA **111** and BINOL **L15**. Basifying the aqueous phase to pH ~ 10 and then extraction gave back a clean mixture of the alkyne **118** and triazole **121**. Following on from the recovery of the desired materials, it was critical to find other means to analyse enantioenrichment of the compound recovered and measure the accuracy of the ^1H NMR spectroscopic determination.

Attempts at chiral HPLC analysis of the materials (alkyne **118** and triazole **121**) were at first fruitless; the primary amine functionality did not seem to be productive towards achieving good enantiomer separation (causing dragging on the analytical column). Therefore, a protection strategy of the amines **118** and **121** was targeted. The protection chosen had to be easy to carry out and protect both alkyne **118** and triazole **121** at the same time in the same pot. Therefore, benzoylation was targeted, this reaction could be carried out quickly and easily at room temperature. The rapidity of protection was key (>1 h), as it was imperative that the benzoylation would proceed more rapidly than self-reaction of **118** or **121** could occur.



Scheme 36 Benzoylation of **118** and **121**

Making pure reference samples of protected compounds was straightforward. Alkyne **118** and triazole **121** were treated with benzoyl chloride to form amides **122** and **123** in 84% and 93% yield, respectively (Scheme 36). The enantiomers of compounds **122** and **123** were separable by normal phase chiral HPLC, in stark comparison to **118**. Taking an assembly kinetic resolution reaction mixture which had been successfully hydrolysed and the solvent removed, the residue was taken up in DCM and benzoyl chloride was added. This mixture of protected materials was then subjected to chiral HPLC and non-racemic materials with matching

retention times to the pure samples of **122** and **123** were observed. The HPLC traces across several repeat reactions showed that the levels of enantioenrichment observed *via* the ^1H NMR spectroscopic assembly methodology were accurate to within $\pm 5\%$ of the values measured by HPLC.

It was then found that primary amine **118** was separable *via* chiral GC methodology without the need for protection. Another repeat of the CuCl-catalysed assembly kinetic resolution reaction was carried out and the material following hydrolysis was analysed. The resulting chiral GC trace showed that the level of enantioenrichment observed in the alkyne starting material **118** was within $\pm 3\%$ of the ^1H NMR spectroscopic analysis.

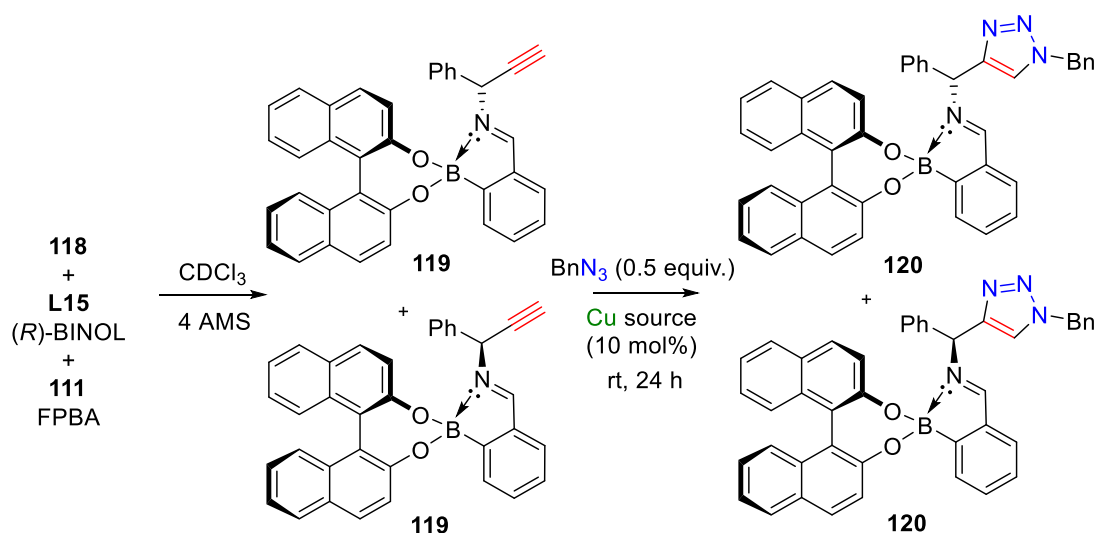
With the confirmation that the Bull-James three-component assembly was working as desired as a dual-function chiral auxiliary and *in situ ee* determination methodology, the selectivity factor for the resolution of alkyne **118** needed calculating. Due to agreement across multiple chromatographic methods with the levels of enantioenrichment calculated from ^1H NMR spectroscopic analysis, the values for selectivity could be calculated directly from the ^1H NMR integrations. In selected cases, benzoylation and chiral HPLC of the recovered materials **118** and **121** was carried out to confirm that the NMR spectroscopically determined *ee* value was an accurate representation of the true *ee*. The recovered protected material was found to be a complex mixture of components and therefore identity of the components could only be surmised from the relative retention times.

Knowing that *in situ* ^1H NMR spectroscopic analysis of assemblies **119** and **120** was an accurate measure of enantioenrichment of the kinetic resolution process, optimisation was then targeted. Unfamiliar with the ability of different copper sources to affect a CuAAC in chloroform-*d* (a solvent rarely used for CuAAC) a series of test reactions were carried out.

Phenylacetylene **48** and benzyl azide **8a** were allowed to react in a 1:1 ratio in chloroform-*d* at room temperature with 5 mol% copper source. After 24 hours, the reaction mixtures were analysed by ¹H NMR spectroscopy. It was found that a range of copper salts was amenable to reaction in chloroform (CuCl, CuBr and CuI). No turnover was observed with the classic Sharpless and Fokin catalyst system of CuSO₄·5H₂O and sodium ascorbate.

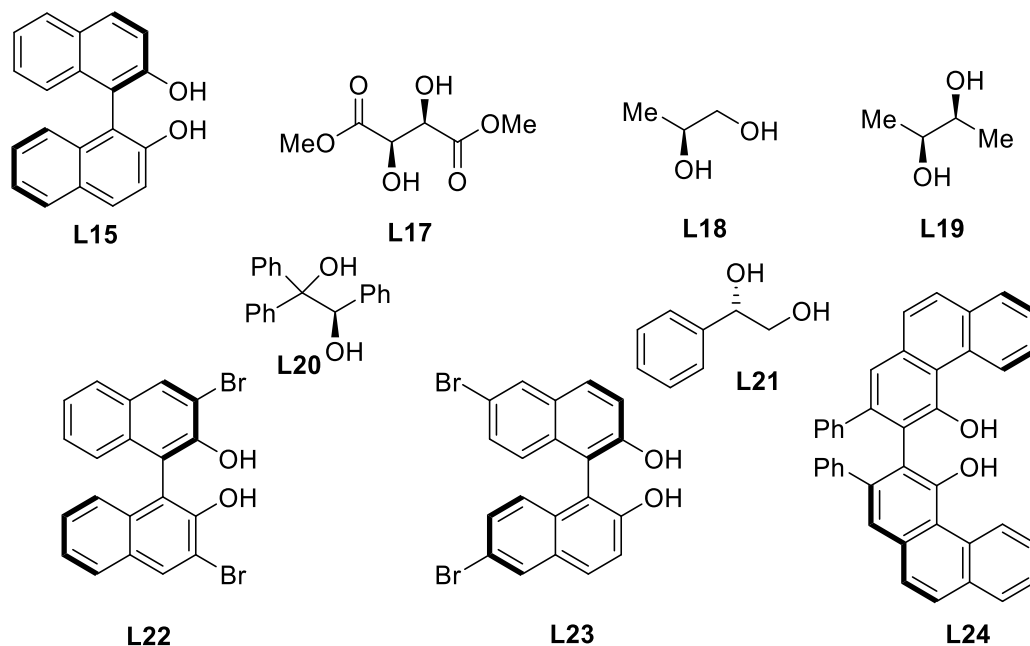
With the knowledge that a CuAAC reaction could proceed in chloroform-*d*, a series of copper sources was tested in the three-component assembly system. A range of copper(II), (I) and (0) sources were tested. A trend was observed in the copper halides: it was found that CuCl > CuBr > CuI in terms of selectivity (*s* = 4.1, 3.7, 2.4). However, the trend was reversed in terms of reaction conversion (Table 11, Entries 1, 2 and 3). Copper(I) triflate gave fair conversion and selectivity along with Cu(MeCN)₄·BF₄, [Cu(MeCN)₄]·PF₆, and copper(II) triflate (Table 11 Entries 5, 6, 7 and 10). Surprisingly, catalytic turnover was observed when copper turnings were employed, this was the only copper(0) source to give any reaction, giving good conversion (36%) and selectivity (*s* = 3.3) (Table 11, Entry 15). A range of other copper sources tested gave no turnover (Table 11, Entries 4, 9, 11-14).

Table 11 Copper source screening in the kinetic resolution of **118**



Entry	Copper Source	Conv. (%) ^a	<i>ee</i> 118 (%) ^b	<i>ee</i> 121 (%) ^b	<i>s</i> ^c
1	CuCl	30	23	39	4.1
2	CuBr	34	25	48	3.7
3	CuI	39	21	13	2.4
4	CuOAc	0	5	-	-
5	Cu(OTf)·0.5 Toluene	31	18	31	2.8
6	Cu(MeCN) ₄ ·BF ₄	54	25	15	1.9
7	[Cu(MeCN) ₄]PF ₆	50	36	16	3.0
8	Cu(OAc) ₂	11	6	19	3.1
9	CuSO ₄	0	0	-	-
10	Cu(OTf) ₂	22	10	28	2.3
11	Cu(NO ₃) ₂ ·3H ₂ O	0	0	-	-
12	Copper(II) acetylacetonate	0	0	-	-
13	Copper(II) carbonate basic	0	0	-	-
14	Cu powder	0	0	-	-
15	Cu turnings	36	25	23	3.3

^a Conversion was determined by integration of ¹H NMR spectra. ^b *Ee* was determined by integration of ¹H NMR spectra, selected examples checked by chiral HPLC. ^c $s = \ln[(1-c)(1-ee)]/\ln[(1-c)(1+ee)]$. All screening reactions were carried out once with the exception of entry 1 which was carried out in triplicate, best result shown.

Table 12 Screening of diols in the kinetic resolution of **118**

Entry	Diol	Conv. (%) ^a	<i>ee</i> of 118 (%) ^b	<i>ee</i> of 121 (%) ^b	<i>s</i> ^c
1	L15	30	23	39	4.1
2	L17	25	15	5	3.0
3	L18	40	3	2	1.1
4	L19	3	-	-	-
5	L20	40	29	19	3.3
6	L21	0	-	-	-
7	L22	NA	-	-	-
8	L23	NA	-	-	-
9	L24	NA	-	-	-

^a Conversion was determined by integration of ¹H NMR spectra. ^b *Ee* was determined by integration of ¹H NMR spectra, selected examples checked by chiral HPLC. ^c $s = \ln[(1-c)(1-ee)]/\ln[(1-c)(1+ee)]$. All screening reactions were carried out once with the exception of entry 1 which was carried out in triplicate, best result shown.

Next the screening of chiral diols was carried out. These screening reactions proceeded using 10 mol% CuCl in chloroform-*d* at room temperature with 0.5 equivalents of benzyl azide **8a** for 24 hours. Dimethyl-L-tartrate **L17** was found to give reasonable conversion (25%) and selectivity ($s = 3.0$) whilst **L18** gave good reaction conversion but with extremely poor selectivity (Table 12, Entries 2 and 3). **L19** gave very poor conversion (3%) and thus the

levels of enantioenrichment were not recorded (Table 12, Entry 4). **L20** is relatively bulky and gave both good conversion and selectivity whilst **L21** appeared to show no turnover (Table 12, Entries 5 and 6). As BINOL **L15** had thus far shown itself to be the superior ligand architecture of those tried, a series of substituted and extended BINOL type ligands was tested. The increased molecular weights of **L22**, **L23** and **L24**, however, led to solubility problems. These ligands were not soluble at the concentrations required to measure the *ee* via ^1H NMR spectroscopy. Therefore, of those diols investigated BINOL **L15** was deemed optimal in terms of selectivity ($s = 4.1$) whilst giving acceptable conversion.

Finally, solvent was considered. In previous kinetic resolution methodology development, solvent had proven critical in obtaining good selectivity (Section 2.1). Therefore, the reaction was carried out in a series of deuterated solvents (DMSO- d_6 , DMF- d_7 , acetonitrile- d_3 and toluene- d_8). Unfortunately, all of these solvents led to broad resonances which could not be successfully integrated.

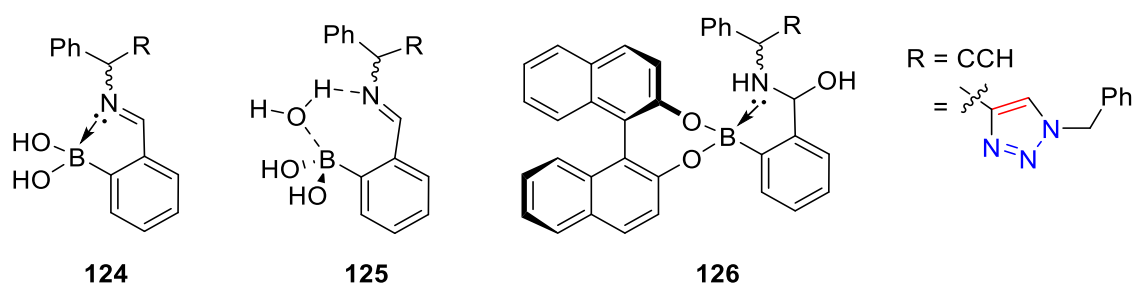


Figure 20 Possible boron-containing by-products present in the assembly mixture

This led to the observation that the exclusion of adventitious water in the assembly mixture was crucial in obtaining good quality data. Water can interact with the boronic acid moiety (in FPBA **111**) in two ways (Figure 20). The first is simple competition with the BINOL to give complex **124**. Water can successfully outcompete a diol for boronic acid binding, leading to the imine forming without BINOL binding. Secondly, due to the adjacent imine moiety, the

water can insert itself between the nitrogen lone pair and the boronic acid to form the adduct **125**. This type of nitrogen to boron interaction is known as solvent insertion.^[95] The water can also interact with the imine moiety, since it has the potential to act as a nucleophile and thus form a hemiaminal **126**. As seen in Figure 19, there are several other minor imine-containing components in addition to **119** and **120**. These were attributed to a mixture of species in which water has acted in these manners in both alkyne **119** and triazole **120** assemblies. To minimise formation of these water-promoted unwanted by-products, all components were dried under high vacuum and the chloroform-*d* was dried over 4 AMS. This level of drying was sufficient to minimise unwanted species to a level where they were very minor impurities within the ¹H NMR spectrum of the assembly mixture.

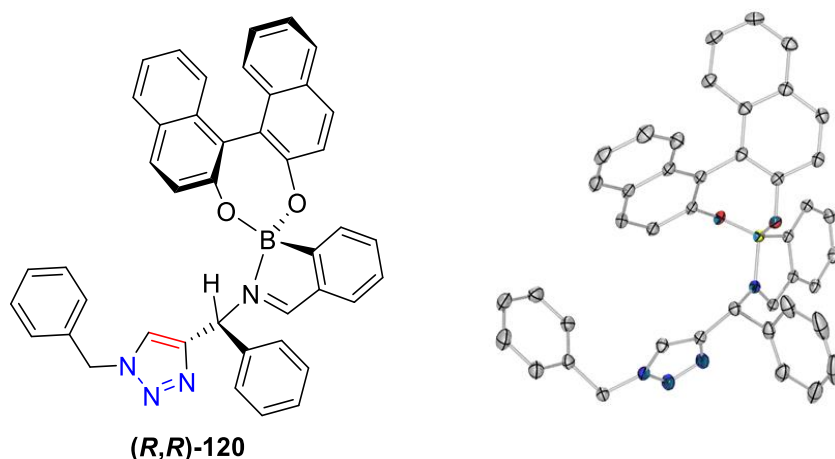


Figure 21 Crystal structure of triazole assembly **120**. Determined to be a single diastereoisomer (*R,R*) though comparison to the fixed chirality of the binaphthyl unit. Displacement ellipsoids are scaled to the 50% probability level

Fortuitously, during the solvent screening, an unpredicted observation was made. Upon assembly formation in acetonitrile-*d*₃ with triazole amine **121**, a precipitate appeared. Upon closer inspection by ¹H NMR spectroscopy, it was observed that this precipitate was a single diastereomer of the assembly **120**. Filtration of the solid, followed by dissolution of the solid

material and slow evaporation in a mixture of acetonitrile and chloroform led to crystals suitable for single-crystal XRD.

From the single-crystal X-ray structure, the absolute configuration at the triazole stereogenic centre in **120** was determined given the known chirality (*R*) of the BINOL (Figure 21). This gave the chirality of the crystalline species as (*R,R*), and from this it was possible to identify the chirality of the four major imine assembly peaks in the ¹H NMR spectrum (Figure 19). It was also possible to determine that the chirality of the amine **118** recovered at the end of the resolution was (*S*).

3.2.1 Summary

The assembly kinetic resolution project successfully demonstrated that the Bull-James assembly, in addition to its previous application as a chiral shift reagent, can also engender asymmetry in kinetic resolution processes.^[96] The imine functionality formed within the assembly circumvented the reactivity problems observed with the primary amine **118** when exposed to the conditions used in the KR of quaternary oxindoles (chapter 2). This system creates a dual sensing and catalysis regime which is advantageous for both high-throughput *ee* screening and asymmetric synthesis. Even though the maximum selectivity for the assembly system was measured to be only $s = 4.1$, the operational advantages and the fact that this methodology successfully kinetically resolves previously problematic alkynes does give this study an advantage over other KR methods.

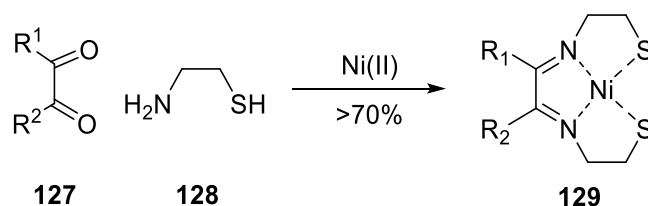
This work was subsequently published as a joint paper between the University of Birmingham and the University of Texas at Austin. The experimental work was carried out by the author of this thesis along with Dr Brette Chapin (UT Austin) and Dr Wenlei Zhai (UoB). The primary investigators were Dr John Fossey (UoB) and Professor Eric Anslyn (UT Austin) along with academic input from Dr Benjamin Buckley (LU). The crystal structure was solved

by Dr Vincent Lynch (UT Austin). The published communication can be seen in *Organic and Biomolecular Chemistry*.^[97]

3.3 Three-Component Boronic Acid Assemblies in Water and Potential Application in Dynamic Combinatorial Chemistry

Combinatorial chemistry is the study of synthetic methodologies which can be used to form large numbers of compounds in a single process. Therefore, combinatorial chemistry allows for the quick and facile building of molecular libraries, ideal for probing chemical space in arenas such as biological screening.^[98]

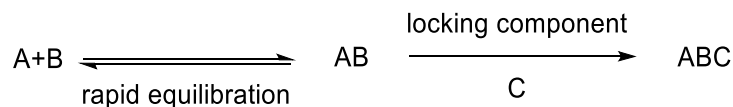
In small-molecule synthesis terms, dynamic combinatorial chemistry uses building blocks which can react with one another in a reversible manner. Mixing these equilibrating building blocks leads to a range of products under thermodynamic control. Utilising supramolecular interactions, certain products can be favoured through strategies such as templating. For example, by the introduction of a metal templating strategy Busch *et al.* used nickel ions to template for macrocyclic structures **129** (Scheme 37).^[99] This pioneering templating work would be built upon by Sanders and co-workers when they came to define the term “dynamic combinatorial chemistry”.^[100]



Scheme 37 Metal templating in dynamic combinatorial chemistry developed by Busch *et al.*^[99]

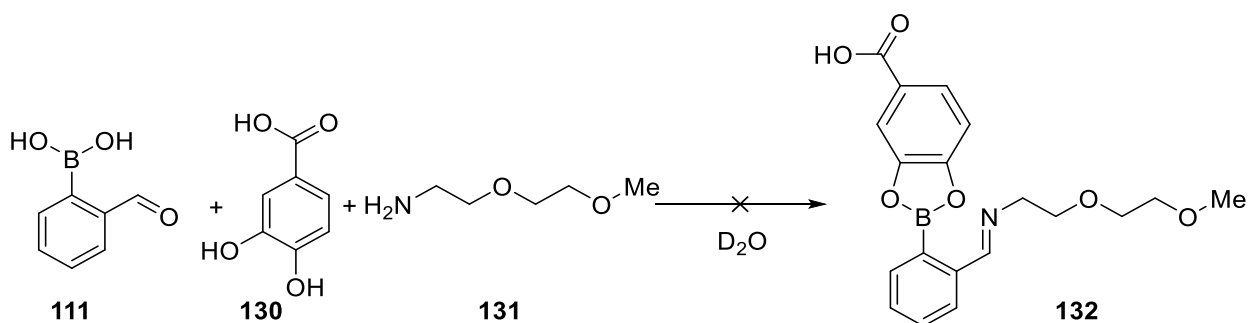
One of the challenges of dynamic combinatorial chemistry is that, due to all the components being in equilibrium, it is difficult to isolate products from the fluxional reaction mixture. One

way in which this can be overcome is to add a component to a rapidly equilibrating mixture which locks the whole system irreversibly (Scheme 38).



Scheme 38 Hypothesis behind this work

It was hypothesised that it might be possible for diol exchange to be significantly perturbed in three-component boronic acid assemblies in water as a solvent. It was postulated that a mixture of a boronic acid with a 2-formyl group along with a diol and amine would create a reversible three-component assembly. Then upon addition of a hydroxylamine, the diol would become locked and unable to exchange. Previous literature has demonstrated that hydroxylamines can use their oxygen atoms to coordinate to boron, forming a tetrahedral boronate ester, which from previous observations appears to be an irreversible process.^[93f]

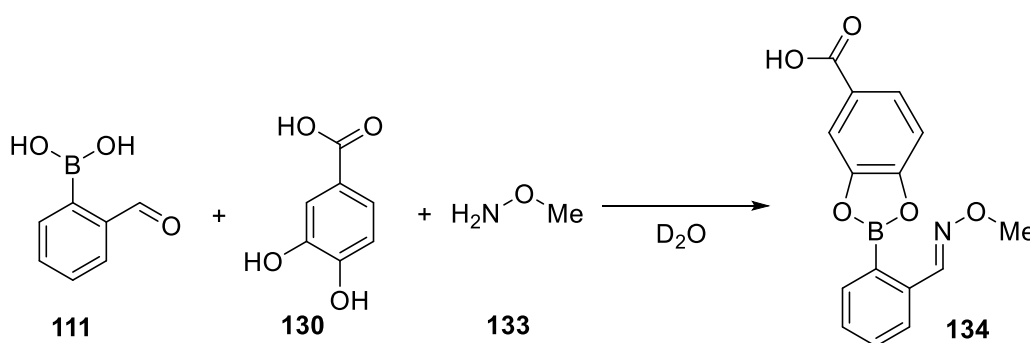


Scheme 39 Attempted assembly formation with 2-(2-methoxyethoxy)ethanamine

To test the theory that three-component assemblies can successfully form in aqueous environments, water-soluble components were required. To this end, FPBA **111**, 3,4-dihydroxybenzoic acid **130** and 2-(2-methoxyethoxy)ethanamine **131** were targeted as the three components (Scheme 39). Upon mixing the components in a 1:1:1 ratio in D_2O , it was clearly observed by 1H NMR spectroscopy that assembly formation was not occurring.

Overlaying the ^1H HMR spectra of the individual starting components, it was clear that the mixture did not include any of the desired assembly, only a mixture of starting materials.

As 2-(2-methoxyethoxy)ethanamine **131** appeared not to be nucleophilic enough in D_2O to successfully form an imine or that the equilibrium lay too far towards the starting materials, it was decided that increasing the nucleophilicity of the amine could lead to assembly formation. It is worth noting that it is hypothesised that amine and diol binding in three-component systems are cooperative, and thus without forming the imine the diol is less likely to successfully bind.^[101] With this in mind the next amine trialled was methoxyamine **133** (Scheme 40). Due to the alpha effect, methoxyamine is a more potent nucleophile than a standard primary amine and thus it was postulated that even in D_2O it would still be able to form an oxime.



Scheme 40 Assembly formation using methoxyamine in D_2O

Upon mixing the three components **111**, **130** and **133** in a 1:1:1 ratio in D_2O , clear oxime resonances were observed (Figure 22). Overlaying the ^1H NMR spectra of the starting materials showed that they had been fully transformed into the three-component assembly **134**.

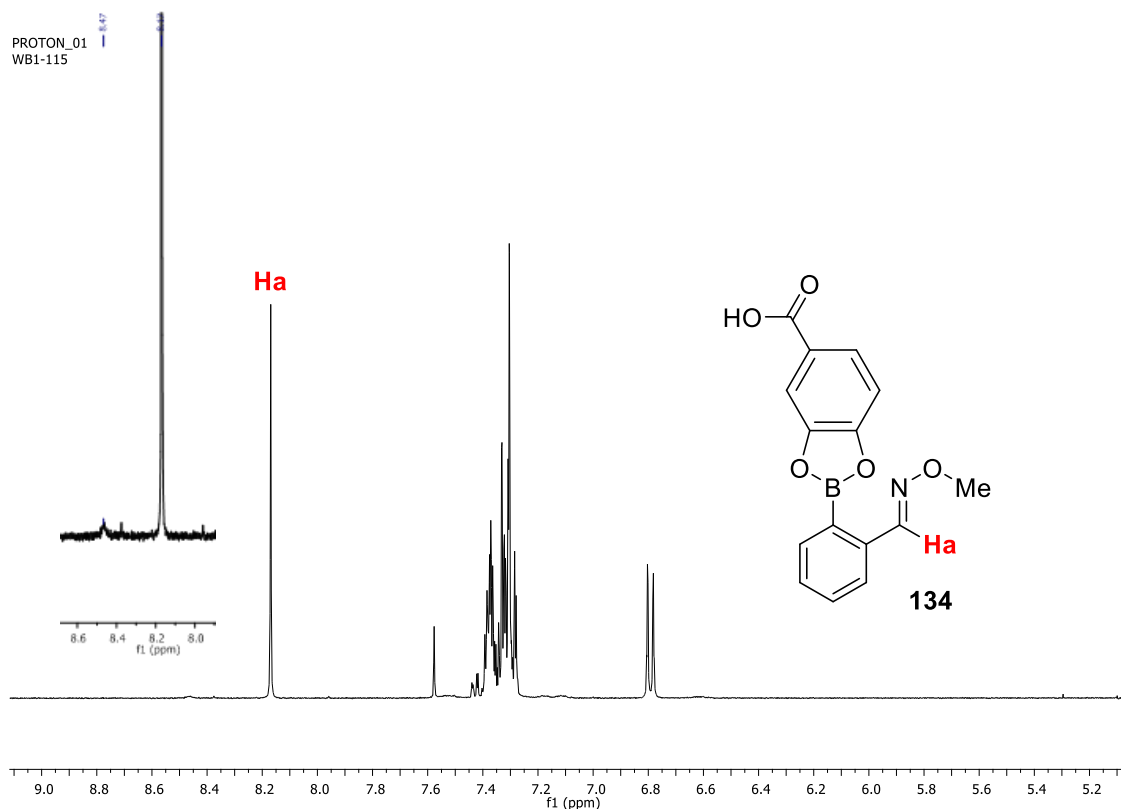


Figure 22 ^1H NMR spectrum of assembly **134**

Looking more closely at the ^1H NMR spectrum of the assembly **134**, it was noted that there were two oxime resonances: a major one at 8.17 ppm and a minor one at 8.47 ppm (Figure 22). These were attributed to the *E* and *Z* isomers of the condensed oxime. The major one was tentatively assigned as *E* due to sterics. This would be backed up by observations made in ^{11}B NMR titrations detailed below.

-To probe this system (**134**) in more detail, several ^{11}B - and ^1H NMR titrations were carried out on the assembly. By varying the concentrations of the components, the degree of tetrahedral and trigonal boron within the assembly system could be observed.^[101]

In the first titration shown below (Figure 23), the concentration of the amine **133** is increased with no diol present. In the ^1H NMR titration it was observed that as the concentration of amine **133** was increased, the characteristic aldehyde resonance (9.80 ppm) from the FPBA

diminished whilst an imine resonance grew (8.17 ppm). As the concentration of the amine increased further, the imine resonance became broader.

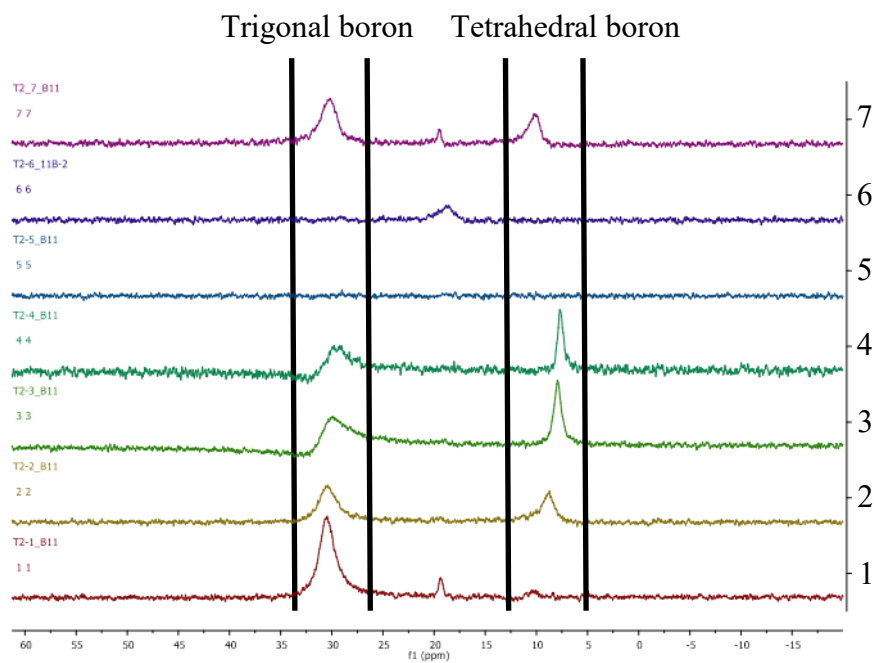
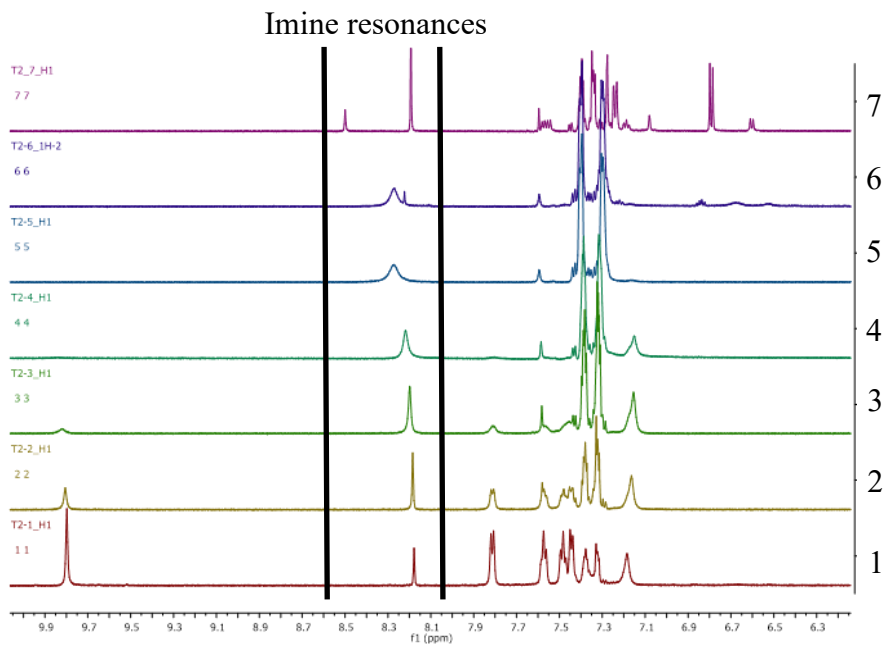


Figure 23 ¹H and ¹¹B NMR titration of methoxyamine **133** into 2-FPBA **111** with 3,4-dihydroxybenzoic acid **130** added at end. Spectra are numbered based upon the concentration of reagents given in Table 13.

Table 13 Titration of methoxyamine **133** into 2-FPBA **111** with 3,4-dihydroxybenzoic acid **130** added at end

Entry	[FPBA] / mM	[Diol] / mM	[Amine] / mM
1	10	0	2
2	10	0	4
3	10	0	6
4	10	0	8
5	10	0	10
6	10	0	12
7	10	10	12

The values shown in this table refer to the spectra shown in Figure 23.

The broadening of the imine resonance in the ^1H NMR titration (Figure 23) was attributed to the imine exchanging with free amine **133** in the solution. This hypothesis was supported by the observed ^{11}B NMR titration; it was seen as the concentration of imine increased the ratio of trigonal boron (30 ppm) decreased compared to tetrahedral boron (10 ppm), thus showing that amine was being successfully transformed to imine. Once one equivalent of amine was present in solution, rapid exchange on the NMR timescale was observed within the ^{11}B NMR spectra, with neither trigonal nor tetrahedral boron resonances present (Table 13 Entry 5, Figure 23 NMR spectrum 5). A mixture of all three components in a 1:1:1.2 (FPBA **111**/diol **130**/amine **133**) ratio was tested for comparison (i.e. to see if the addition of diol **130** altered the appearance of NMR resonances). In the ^1H NMR spectrum clear and sharp imine resonances were observed (Table 13 Entry 7, Figure 23 NMR spectrum 7), which lends evidence that the diol is successfully binding. This is due to the rate of exchange between imine and amine in solution being significantly perturbed by the presence of the diol this is due to the diol-amine-boronic acid (3 component) assembly being more stable than the amine-boronic acid (2 component) assembly. In addition, the ^{11}B NMR spectra showed a subtle shift

between spectra 1 and 7 in both resonances observed, giving further evidence of diol binding. The subtle shift indicates that the ratio of different trigonal and tetrahedral boron-containing species is changing across the titration.

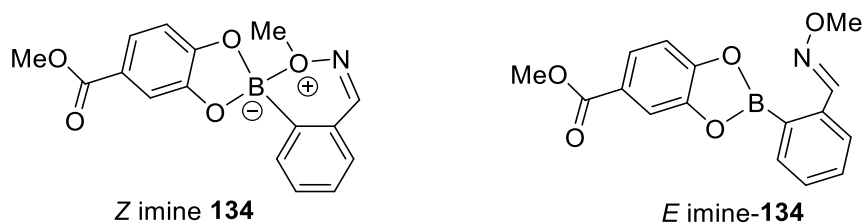


Figure 24. Possible O-B interactions in three-component boronic acid assembly **134**

As can be seen in the ^{11}B NMR titration (Figure 23), the resonance for trigonal boron dominates (30 ppm), which can be attributed to the *E* isomer of the imine being the major isomer in solution. The *E* isomer cannot position itself in a way for the oxygen to interact successfully with the boron centre (Figure 24). As this interaction cannot take place, the trigonal boron dominates (Figure 23). This also supports the hypothesis that the *E* imine resonance observed in the ^1H NMR spectrum of the assembly dominates compared to *Z*.^[93f]

The next titration that was carried out involved increasing the concentration of amine **133** with a constant concentration of diol **130** (Figure 25, Table 14). It was observed that the imine signal grew in as the aldehyde diminished, as was expected. Additionally, the ratio of trigonal to tetrahedral boron increased again with amine concentration. These findings support the hypothesis that successful three-component binding was occurring in D_2O .

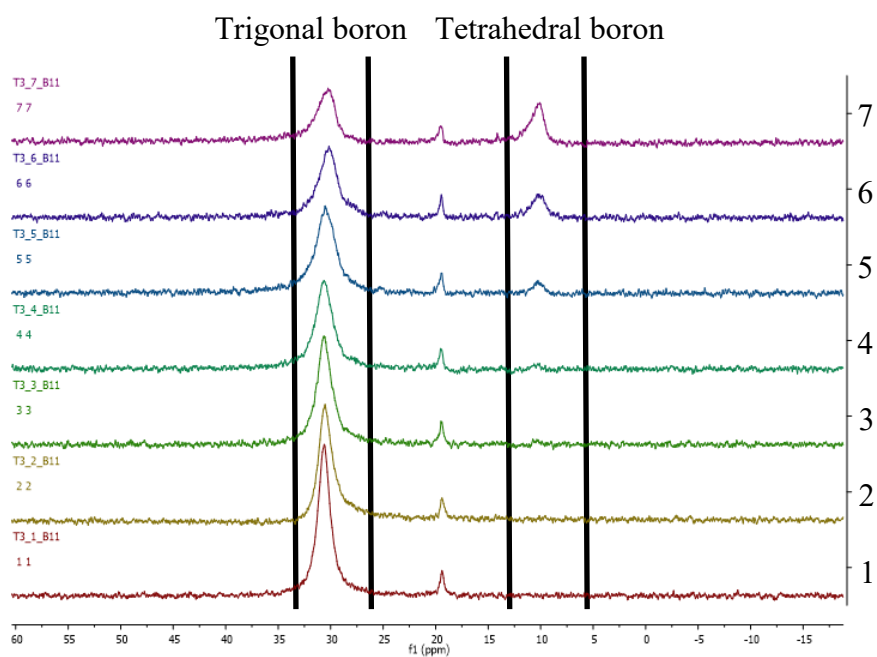
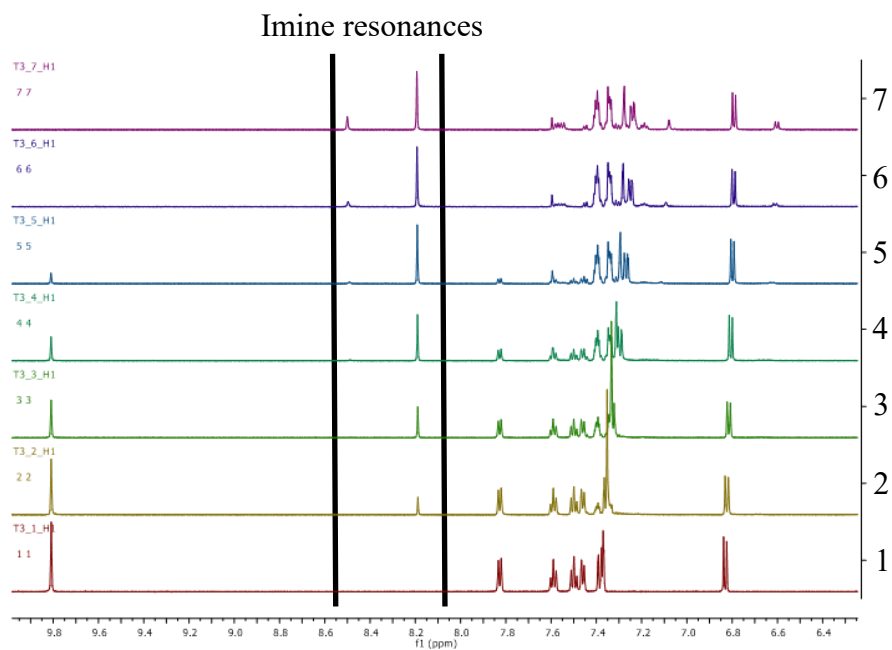


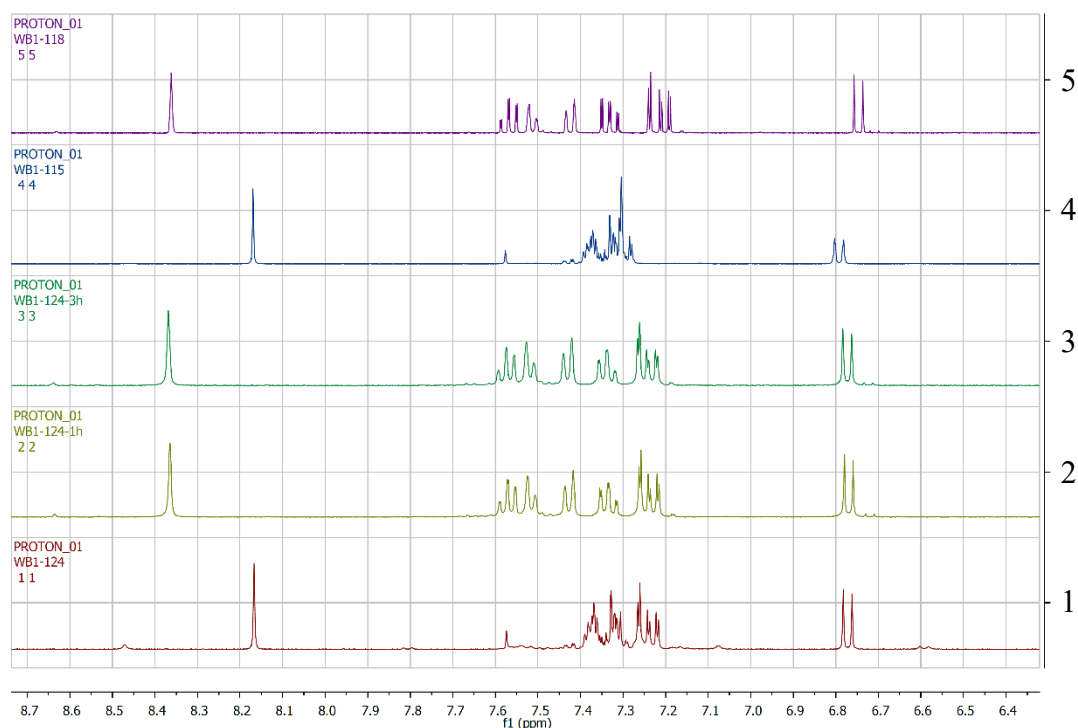
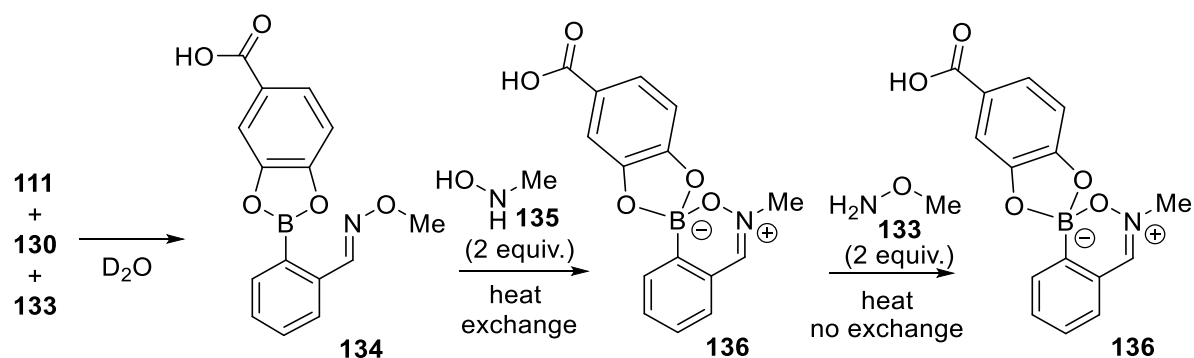
Figure 25 ^1H and ^{11}B NMR titration of methoxyamine **133** into 2-FPBA **111** and 3,4-dihydroxybenzoic acid **130**. Spectra are numbered based upon the concentration of reagents given in Table 14.

Table 14 Titration of methoxyamine **133** into 2-FPBA **111** and 3,4-dihydroxybenzoic acid **130**

Entry	[FPBA]	[Diol]	[Amine]
1	10	10	0
2	10	10	2
3	10	10	4
4	10	10	6
5	10	10	8
6	10	10	10
7	10	10	12

The values shown in this table refer to the spectra shown in Figure 25.

Following these titrations, the ability of a hydroxylamine to prevent exchange was probed (Figure 26). To do this, components **111**, **130** and **133** were mixed together in D₂O in a 1:1:1 ratio and an NMR spectrum was obtained (Figure 25, NMR spectrum 1) . To the assembly mixture was added 2 equivalents of hydroxylamine **135** and the assembly was heated to 40 °C for 1 hour to facilitate exchange (Figure 26, NMR spectra 2). From ¹H NMR spectroscopic analysis, it was observed that full exchange to the hydroxylamine assembly **136** had occurred. To prove that exchange to the hydroxylamine assembly was an irreversible process, a further 2 equivalents of methoxyamine **133** were added to the assembly mixture which was subsequently heated to 40 °C for another hour. Upon ¹H NMR spectroscopic analysis, it was observed that the assembly remained unchanged and the hydroxylamine had not been exchanged (Figure 26, NMR spectrum 3). This proved that the assembly had been essentially locked from further exchange upon hydroxylamine addition. This experiment was also carried out at room temperature with the same outcome. However, exchange to the hydroxylamine assembly **136** took significantly longer at 2 hours before full exchange was observed.



NMR Legend 1) Methoxyamine assembly before hydroxylamine addition. 2) Methoxyamine assembly with hydroxylamine (2 equiv.) heated. 3) Methoxyamine assembly with hydroxylamine and a further 2 equiv. of methoxyamine added heated (40 °C, 1 h). 4) Reference methoxyamine assembly. 5) Reference hydroxylamine assembly

Figure 26 Exchange experiment of three-component assembly with a hydroxylamine

The exchange experiment supported the hypothesis that a reversible three-component boronic acid assembly could be locked irreversibly with a hydroxylamine. The titrations carried out earlier in this section give evidence towards boronic acid-diol binding successfully occurring in the presence of methoxyamine in D_2O . This shows that the assembly is amenable to water/ D_2O , a solvent which can compete for diol binding.

3.3.1 Summary

This project demonstrated that the Bull-James three-component boronic acid assembly concept can be carried out in D₂O and thus aqueous environments when the correct components are selected.^[102] The coordination environment of the boron centre was probed via ¹¹B NMR titrations and it was found that trigonal boron dominates in D₂O. Evidence of amine-imine exchange and diol binding was seen in ¹H NMR titrations. Subsequent experiments utilising hydroxylamines showed that exchange within the system could be stopped, thus potentially irreversibly locking a diol and boronic acid together from a previously fluxional mixture. Further work on these systems is being carried out within the Anslyn group and it is hoped that these studies will prove applicable to dynamic combinatorial chemistry. Experimental work in this section was carried out by the author of this thesis and the primary investigator was Professor Eric Anslyn (UT Austin).

3.4 *The Bull-James Assembly Application in Pedagogy*

The determination of *ee* is a common task for the synthetic organic chemist, therefore chirality and the methods for determining *ee* are important concepts to teach undergraduate chemistry students. Even though students are taught these important topics, in many cases there is little to no hands-on *ee* determination carried out by undergraduate students. Classical methodologies to determine *ee* (chiral HPLC/chiral GC) require expert knowledge during method development and require a large monetary outlay to acquire for a teaching institution.

Proton NMR spectrometers are common at most universities where undergraduate chemistry students are taught. It was conceived that the Bull-James three-component boronic acid assembly may allow for undergraduates to experience hands-on *ee* determination whilst using

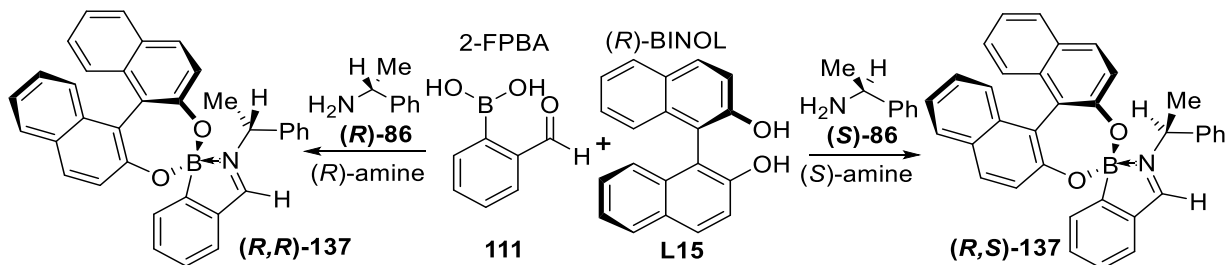
a supramolecular system, which is still part of much current research. The Bull-James assembly has been utilised for the *ee* determination of both chiral amines and diols (Section 3.1).^[93a, 93c] The assembly methodology is operationally straightforward to carry out and thus was deemed suitable for second-year undergraduate students. Undergraduates are commonly aware of other NMR spectroscopic *ee* determination methods through diastereomer formation, such as Mosher's acid, and it was hoped that through the application of the Bull-James assembly, students would reinforce their knowledge of this area along with other concepts such as carbonyl chemistry and supramolecular interactions.

In addition, the use of NMR spectroscopy as a manner of *ee* determination would allow students to process raw NMR data. This again is a standard task for a research chemist, but undergraduates do not normally have the opportunity to process and interpret raw digital NMR data. This experiment would allow students to become familiar with common NMR processing software and was another consideration in the design of the experiment and supporting materials.

3.4.1 Experimental Design

The Bull-James assembly uses the formation of diastereoisomers to infer the *ee* of a chiral analyte (Scheme 41). A chiral amine of known or unknown *ee* can be mixed with FPBA **111** and an enantiopure diol component **L15**. Upon, three-component binding, two diastereoisomers of assembly **137** are formed with a *dr* equivalent to the *ee* of the starting chiral analyte. Proton NMR spectroscopy of the diastereomeric mixture shows individual resonances for both assembly diastereoisomers, through the integration of one diastereomer to the other the *dr* and thus the *ee* of the original amine can be determined. This holds true if

there is full conversion to the assembly **137** from the starting materials and that no kinetic resolution of the analyte up on assembly formation is observed.



Scheme 41 Bull-James three-component assembly in the analysis of α -methylbenzylamine

In order to design an effective undergraduate experiment, the three components used in the assembly needed to be selected. This experiment was wished to be as universally applicable as possible and thus the cost of the components was of paramount importance. It was decided that the *ee* of the amine component should be the one to be measured. This led to the decision to choose 2-FPBA **111**, (*R*)-BINOL **L15** and α -methylbenzylamine **86** as the three components. This amine (**86**) is the cheapest commercially available chiral amine which could be found. Due to the modular nature of the assembly, it is worth noting that an institution could easily modify the experiment to include any chiral amine they possessed.

By mixing together different volumes of (*R*)- and (*S*)- α -methylbenzylamine **86**, a wide range of scalemic mixtures could be easily prepared. The original Bull-James protocol reports a ratio of 1:1:1.1 (FPBA **111**/amine **86**/(*R*)-BINOL **L15**), thus leaving the diol in excess. This leads to a problem in the presence of excess BINOL, as the exchangeable hydroxyl BINOL resonance can broaden out and interfere with one of the potentially integratable *ee*-determining resonances (*CH* quartet, α -methylbenzylamine assembly **137**) when the chloroform-*d* is not completely dry (Figure 27).

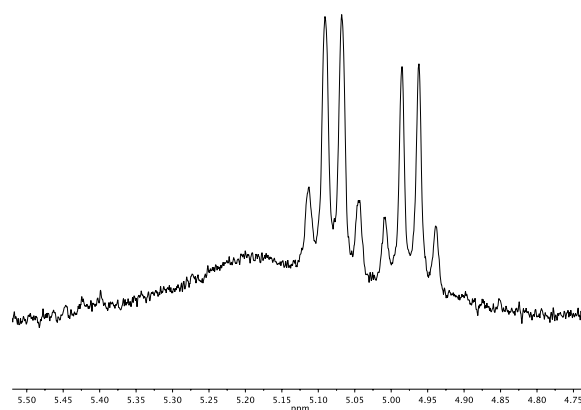
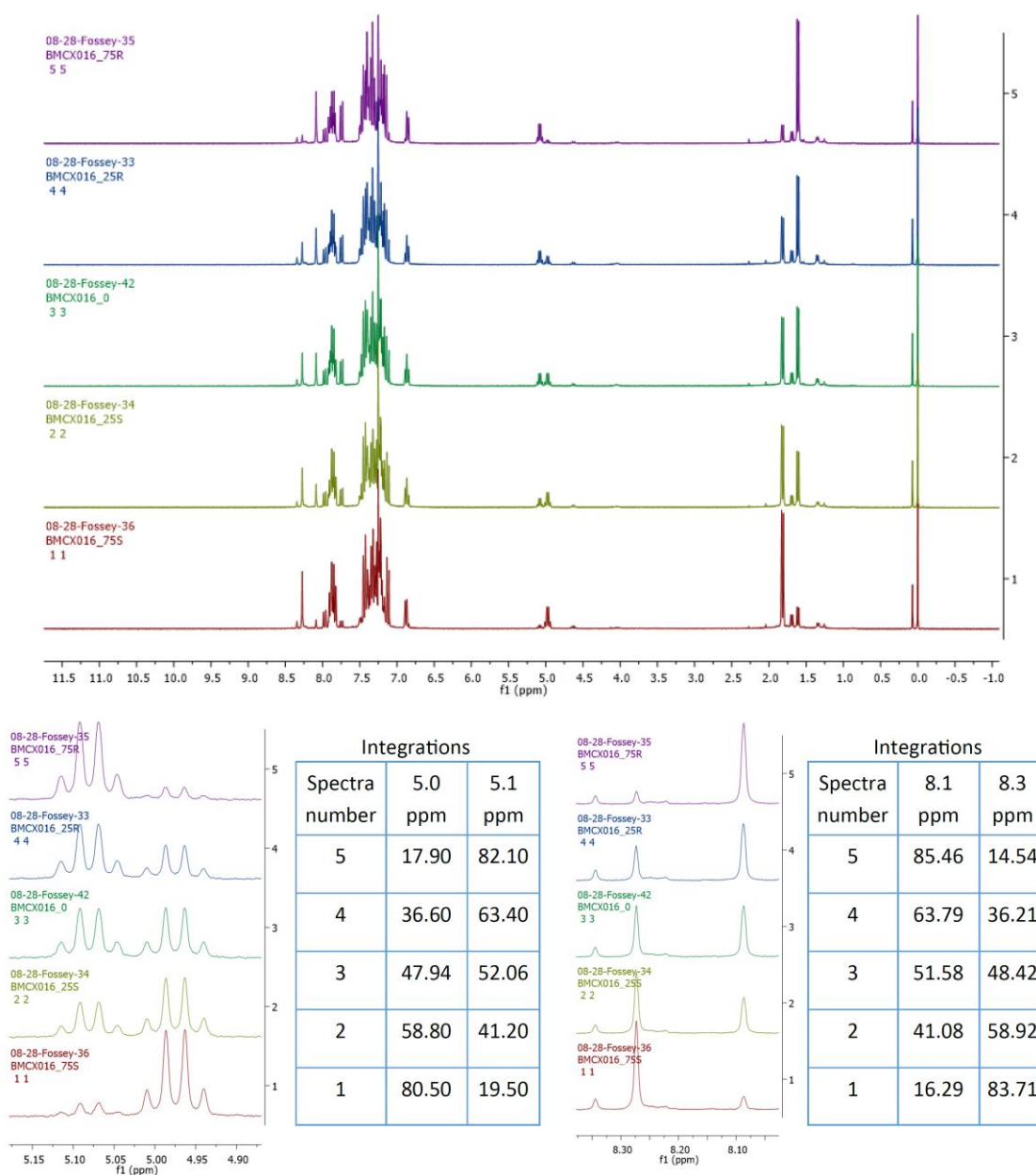


Figure 27 Interference of exchangeable BINOL protons with *CH* quartets in the ^1H NMR spectrum of α -methylbenzylamine-based three-component assembly **137**

In order to combat the excess diol problem, the ratio of assembly components was modified to 1:1.2:1 (2-FPBA **111**/amine **86**/*R*-BINOL **L15**) thus putting the amine in excess and preventing unbound BINOL being present in the assembly mixture. It was also important to check that no kinetic resolution of the amine was occurring upon assembly formation, so the number of equivalents of amine **86** was increased to 1.2, 1.5 and 2.0. In all cases, the ratio of the assembly *CH* quartets remained constant, showing that one enantiomer of amine was not being preferentially bound. The excess amine led to an additional set of resonances present in the ^1H NMR spectrum of the assembly mixture, but these were at chemical shifts sufficiently different from the resonances used for *ee* determination so as not to present a problem for analysis.

With three-component assembly methodology, adventitious water is of concern, as discussed in Section 3.2. It was found that the minimisation of water-bound by-products could be achieved through simple drying of the solvent over 4 AMS.



NMR Legend 1) Three component assembly **137** formed from 75% *ee* (*R*)-**86**. 2) Three component assembly **137** formed from 25% *ee* (*R*)-**86**. 3) Three component assembly **137** formed from racemic **86**. 4) Three component assembly **137** formed from 25% *ee* (*S*)-**86**. 5) Three component assembly **137** formed from 75% *ee* (*S*)-**86**.

Figure 28 Overlaid ¹H NMR assembly spectra containing various *ees* of α -methylbenzylamine, integratable imine resonances (8.1 ppm and 8.3 ppm) and methine resonances (5.0 ppm and 5.1 ppm) expanded. Spectra were recorded at 300 MHz.

Upon assembly formation with racemic α -methylbenzylamine **86** with 4 AMS in the solvent, it was noticed that the ratio of ¹H NMR resonances corresponding to the two diastereoisomers of assembly **137** was not accurate, giving a value of 1:0.79 [(*R*):(*S*)] rather than the desired

1:1 [(*R*):(*S*)]. It was hypothesised that this could be due to interference from other species within the NMR spectrum. Therefore, to obtain good accuracy, a calibration curve was required, and thus the students would need to construct their own curves before they could determine the *ee* of unknown samples.

Table 15 Comparison of true, measured and calibrated *ee* values for Bull-James three-component assembly at various known *ees*

Entry	True <i>ee</i> 86 (%)	Imine Resonances		Methine Resonances	
		Measured <i>ee</i> (%) ^a	Calibrated <i>ee</i> (%)	Measured <i>ee</i> (%) ^a	Calibrated <i>ee</i> (%)
1	89.3	87.0	86.3	77.0	88.6
2	-10.7	-3.6	-8.2	-4.8	-9.6
3	-50.0	-44.9	-51.3	-39.0	-50.7

^a *Ee* inferred from the integration of the assembly **135** ¹H NMR spectra where measured *dr* = inferred *ee*

It was decided that two calibration curves should be constructed: one for the methine protons of the assembly **137** and one for the imine protons (Figure 28). This increased the accuracy of the *ee* determination (which could be as far as 11% away from the true *ee* value as seen in Table 15). Values were within 1.1% of the true value for the imine signals and within 3.0% for the methine resonances. As a bonus, construction of calibration curves would also allow students to compare and judge which set of resonances they believed to be more accurate.

With knowledge of how to accurately carry out an *ee* determination with the limitations of an undergraduate laboratory, an effective laboratory practical procedure could be written. Students were instructed to work in groups of five to make the completion of the experiment feasible within the allotted laboratory time (2 h). Each group would be required to construct two calibration curves, each consisting of 5 points from α -methylbenzylamine assemblies **137** with known *ee* starting amine **86**. Students would need to make their own amine solutions using automatic pipettes and a “host” solution of FPBA **111** and (*R*)-BINOL **L15**. Finally, the

students would be required to prepare five assemblies with amine of unknown *ee*, which would be prepared by a laboratory technician. The students would then submit the samples which would be run by an NMR technician.

In a subsequent computer-based session, the students would process their raw NMR data which would require them to learn how to use NMR processing software. To make this easier, a series of demonstrational videos was recorded detailing the basics of using two well-known processing programs (MestrelNova and Topspin). Once their data was successfully processed, they could use their integration values to construct calibration curves and then calculate the *ees* of their five unknown amine samples. The published experimental procedure can be found in Appendix 3 Section 9.1.

3.4.2 Assessment and Feedback

A proforma (see Appendix 3 Section 9.2) was designed for the *ee* determination experiment, which the students were required to complete as part of assessment. This proforma was designed to not only judge students on the accuracy of their *ee* determinations, but also on their ability to think critically about their data. Students are often unable to stand back and critically assess the quality of their data, and are commonly hesitant to call their own data poor due to their fear of losing marks. The ability to assess data quality and know what needs to be repeated is a crucial skill within research, and it was hoped that students may be able to build these skills through this practical experiment.

From the answers given, however, it was found that in many cases students were still unable to question the quality of the data and values obtained. In some cases, students reported *ee* values in excess of 120% with no discussion or even acknowledgement of the fact that this is not possible. Students also found it difficult to deal with hypothetical questions; for example,

students were asked to come up with potential sources of error in the experiment, and many found it difficult to propose any factors other than human errors.

Despite these problems with answering the proforma questions, overall the second-year students could determine their unknown *ee* amine samples within $\pm 10\%$ of the true values. They were able to successfully construct and use their calibration curves, and in addition, the accuracy of the values obtained showed that the laboratory procedure worked well.

3.4.3 Summary

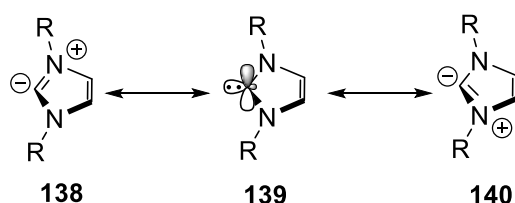
In conclusion, a new undergraduate laboratory procedure which utilises the Bull-James assembly for *ee* determination was successfully designed and implemented.^[103] The experiment was run with a cohort of 113 second-year chemistry undergraduate students at the University of Birmingham. The experiment has now been integrated into the laboratory courses at the university and will be run for the second time this year (2017). Student feedback from the experiment was overall positive with many finding the laboratory instructions clear and easy to follow.

The experiment and supporting materials for this experiment were developed by the author of this thesis along with Dr Brette Chapin (UT Austin), Daniel Payne (UoB), Dr Glenn Lees (UoB), Dr Cécile Le Duff (UoB), Dr Charles Manville (UoB), Dr Kimberley Roper (UoB), Stephanie Lim (UT Austin) and Jennifer Lloyd (UoB). The primary investigator and designer of the experiment was Dr John Fossey (UoB) with academic input from Dr Steven Bull (UB), Professor Tony James (UB) and Professor Eric Anslyn (UT Austin). This experiment was published in the *Journal of Chemical Education*,^[104] and it is hoped that other institutions may incorporate it into their undergraduate teaching programme.

4 Atropisomeric Triazoles and Triazoliums Designed for Use as Chiral *N*-Heterocyclic Carbenes

4.1 Synthesis of Novel Atropisomeric Triazolium Salts

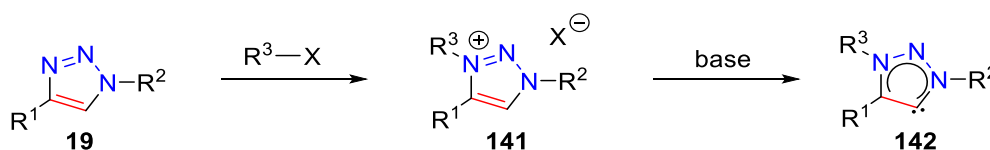
N-Heterocyclic carbenes (NHCs) take advantage of an easily deprotonated carbon atom in a position flanked by heteroatoms. Removal of the proton attached to this carbon leads to a carbene which is stabilised through orbital overlap (Scheme 42). Standard carbenes, by their nature, are electron-poor and are very short-lived. NHCs, in contrast, can be considered electron-rich and form long-lived stable species. NHCs can be used for a variety of applications; for example, they are used as ligands for transition metals or as organocatalysts.^[105] Binding with a metal creates an extremely robust complex, as the NHC is easily able to donate its unshared valence electrons to the metal centre, leading to an extremely strong C-M bond. NHCs can also act as π -acceptor ligands through back bonding increasing the stability of metal-NHC complexes. These metal complexes can then be employed in a variety of metal-mediated reactions.^[106] In addition, chiral NHCs can be employed as asymmetric ligands.^[106b, 107]



Scheme 42 Carbene stabilisation within *N*-heterocyclic carbenes

Triazolium salts are easily accessible NHC precursors.^[108] Using the CuAAC, vast libraries of ligand architectures can be synthesised rapidly.^[109] This is a great advantage, as the introduction of more sterically bulky or electronically different groups can be extremely challenging in other ligand syntheses.^[70b, 110] In the case of 1,2,3-triazolium salts,

derivatisation of the alkyne and azide building blocks is relatively trivial to carry out, and thus a wide range of chemical space can be probed during ligand screening. Triazolium salts also give three points of diversification: the azide (Scheme 43, R²), the alkyne (Scheme 43, R¹) and the alkylating agent (Scheme 43, R³) can all be modified, and therefore it is possible to fine-tune the sterics and electronics of the ligand.



Scheme 43 Alkylation and subsequent deprotonation of a 1,2,3-triazole to form a 1,2,3-triazolylidene

It has been shown that 1,2,3-triazolium salts are readily deprotonated to form 1,2,3-triazolylidenes which are *N*-heterocyclic carbenes (Scheme 43).^[111] The pK_a of N³-arylated and N³-alkylated 1,2,3-triazolium species range between 20-24 (depending on the substituents) and have been deprotonated by bases such as KO^tBu (pK_a = 22) or KN(SiMe₃)₂ (pK_a = 26).^[111] These have been used in a range of applications; like conventional NHCs, triazolylidenes have found uses in both metal-mediated catalysis and organocatalysis.^[111-112] Therefore, it was hypothesised that chiral 1,2,3-triazolium salts could be interesting pre-catalysts for asymmetric catalytic applications. In order to form said chiral triazolium salts, atropisomerism was targeted as a manner to introduce chirality. Atropisomerism takes advantage of restricting the rotation around a single bond to create a chiral environment. Atropisomerism is the basis for chiral ligands such as BINOL and BINAP.^[113] Restricted rotation in heterocyclic based systems has already been studied and utilised in a range of applications. The barriers to rotation of atropisomeric DMAP catalysts have been calculated by Spivey *et al.*^[114] A series of 3-naphthyl substituted pyridine catalysts were synthesised (143-146) and it was found that further substitution on the naphthyl moiety was vital in order

to increase the barrier to rotation (Figure 29). It was noted that across all the various systems tested tri-*ortho* substituted bi-aryl systems were significantly more stable towards rotation than di-*ortho* substituted variants.

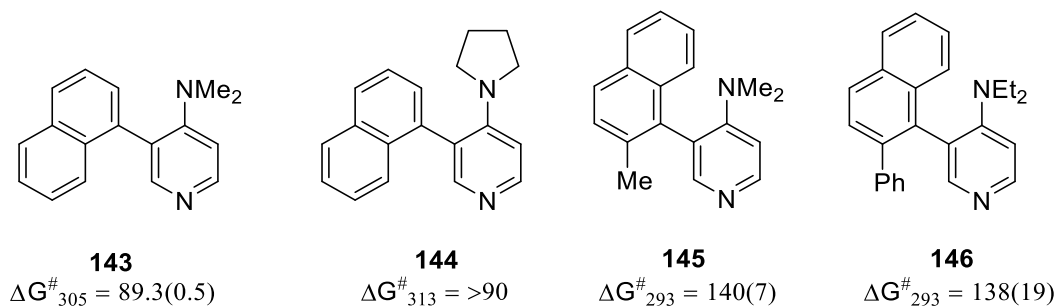
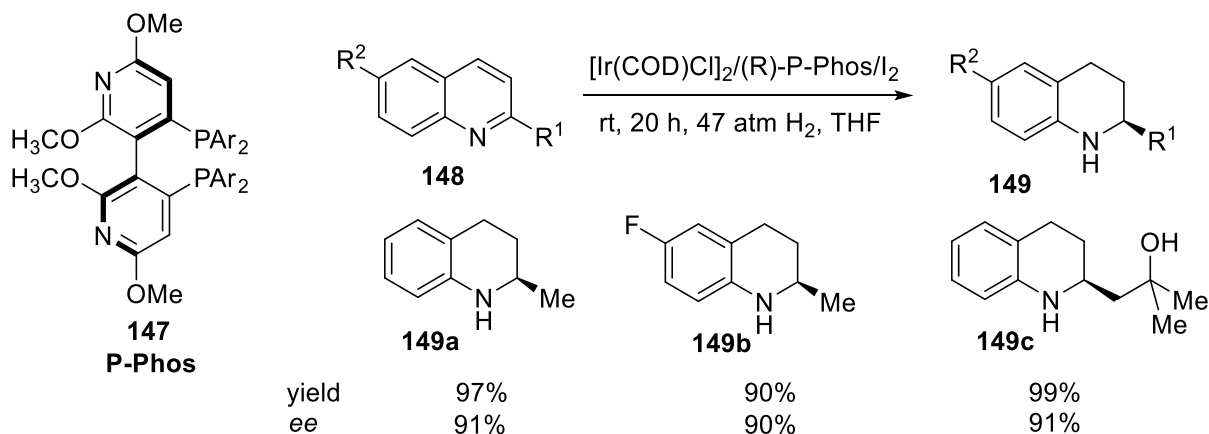


Figure 29 Experimentally determined barrier to rotation (ΔG^\ddagger (kJ/mol)) of a series of axially chiral DMAP catalysts, Spivey *et al.*^[114]

Atropisomerically stable bi-pyridyl species have been utilised in asymmetric metal based catalysis. P-Phos **147**, a commercially available ligand, has been developed for asymmetric hydrogenations by Chan and co-workers.^[115] This ligand uses restricted rotation around a C-C bond between two pyridine units to create a chiral environment. A P-Phos, iridium based catalysis system was employed for the asymmetric hydrogenation of quinolines **148**, garnering the hydrogenated products **149a-c** in up to 91% *ee*.^[116] The tetra-*ortho* substituted design of P-Phos **147** makes it stable toward rotation even at elevated temperature, at 90 °C the ligand has shown high levels of enantioselectivity in asymmetric hydrogenations.^[115]



Scheme 44 Asymmetric hydrogenation of quinolines utilising P-Phos as a chiral ligand, Chan and co-workers.^[116]

N-Arylation of pyrrole derivatives is another route which has been successfully employed to install atropisomerism in heterocyclic systems (Figure 30). Faigl *et al.* demonstrated that a tri-*ortho* substituted pyrrole based system **150** showed atropisomerism with a barrier to rotation of 32.9 kcal/mol.^[117] This value would give the system a half-life of racemisation at 298 K of 516 years.

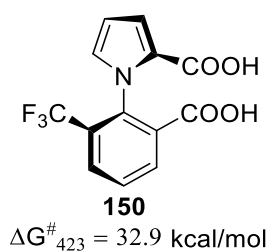
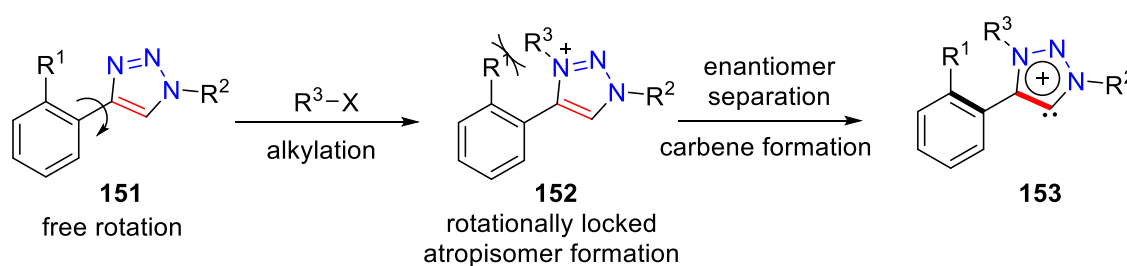


Figure 30 Atropisomeric *N*-arylated pyrrole derivative developed by Faigl *et al.*^[117]

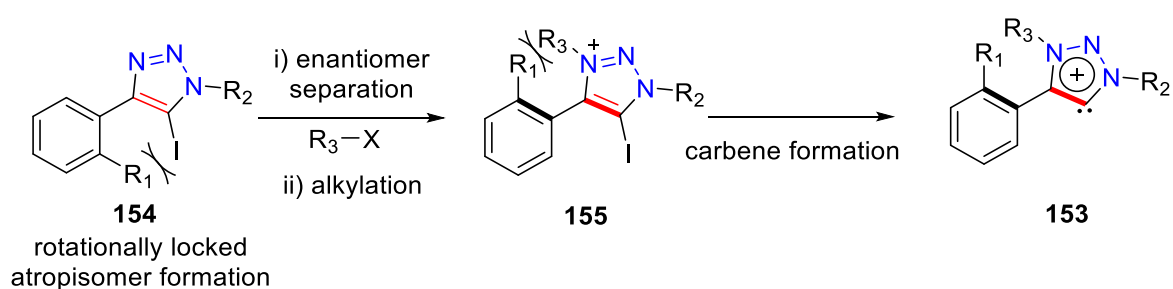
To restrict the rotation in a triazolonic system, two separate approaches were taken. Firstly, using an *ortho*-substituted aromatic alkyne, it was hoped that upon alkylation of the triazole the two R groups (R^1 and R^3 in Scheme 45) would no longer be able to pass one another, thus creating atropisomerism. It was envisaged that a single enantiomer of the chiral triazolium salt would be obtainable through either preparative chiral HPLC or through an asymmetric CuAAC reaction.



Scheme 45 Formation of atropisomeric triazolium species through alkylation

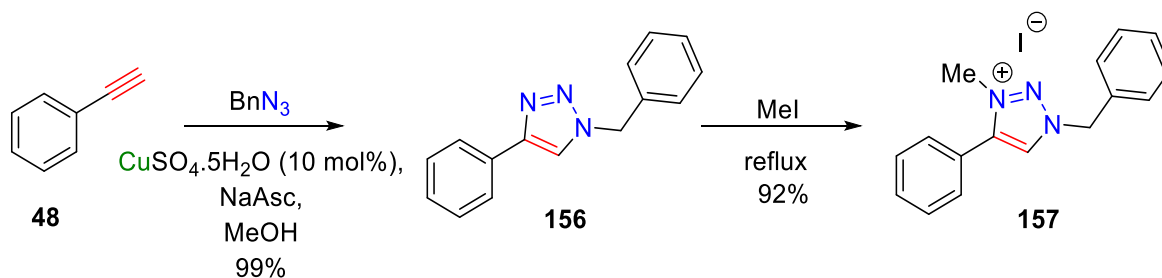
The second planned approach was to use 5-iodotriazoles. When utilising an *ortho*-substituted aromatic alkyne, it was hoped that the iodine atom and R^1 group (Scheme 46) would not be

able to pass one another, thus introducing atropisomerism. The introduction of a di-*ortho*-substituted alkyne may improve atropisomeric stability at room and elevated temperatures, these were also planned to be studied. Then enantiomer separation could be carried out *via* chiral preparative HPLC, or a single enantiomer could be synthesised by an asymmetric CuAAC. Following this, alkylation of the triazole would lead to the desired carbene precursor. It would therefore be important that atropisomerism was stable at the temperature needed for alkylation to occur. These two approaches gave flexibility to at which stage alkylation would occur. From other studies within the Fossey group, the HPLC separation of quaternary nitrogen-containing species has proven to be troublesome,^[118] thus the ability to isolate a single enantiomer of either a triazole or triazolium was deemed advantageous.



Scheme 46 Formation of atropisomeric triazolium species through iodotriazole synthesis

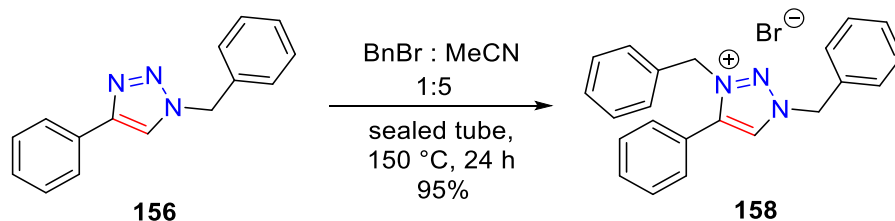
To begin with, a literature triazolium salt **157**^[112d] was targeted in order to get familiar with their synthesis. Phenylacetylene **48** was treated with benzyl azide *via* a CuAAC to form triazole **156** in 99% yield. In a sealed vial, the triazole was then alkylated with neat methyl iodide to form the triazolium species **157** in 92% yield (Scheme 47). The necessity for refluxing conditions for alkylation would therefore mean the atropisomers would have to be stable at high temperatures. These conditions were therefore less than ideal for the proposed synthetic route.



Scheme 47 CuAAC followed by alkylation to form triazolium salt **157**

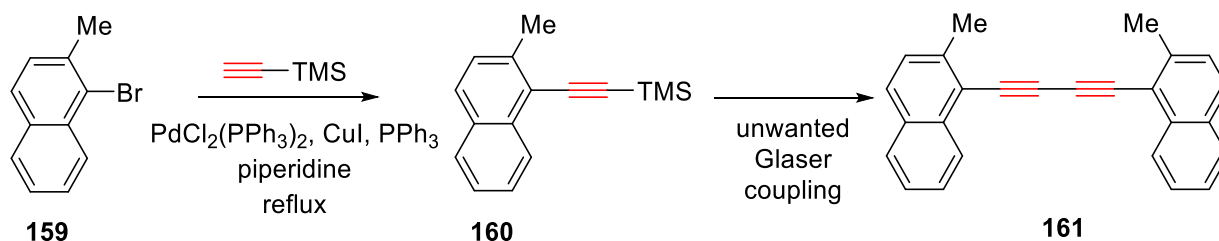
Benzyl bromide was another alkylating agent which was targeted for use in the synthesis of the novel triazolium salts. Benzyl bromide is a cheap alkylating agent and is much less toxic than methyl iodide, this in combination with the steric and electronic difference made it an interesting material for use in triazolium salt formation. In addition, the extra benzylic protons introduced by benzyl bromide would give a better chance to observe potential diastereotopic protons by ^1H NMR spectroscopy upon atropisomer formation. This would give a straightforward method to see if rotation was being restricted within the system.

A similar strategy to that shown in Scheme 47 was originally taken. Neat benzyl bromide was added to triazole **156** and the mixture was heated to $150\text{ }^\circ\text{C}$ in a sealed vial. This, however, led to the recovery of the starting material **156**. It was hypothesised that for successful alkylation to occur, the $\text{S}_{\text{N}}2$ transition state (through which the reaction is thought to proceed through) needed stabilising. Therefore, a mixture of benzyl bromide and acetonitrile were used in a 1:5 ratio, with the acetonitrile's polar, aprotic characteristics to stabilise the transition state. The triazole **156**, along with the mixture of benzyl bromide and solvent, were heated at $150\text{ }^\circ\text{C}$ in a sealed tube for 1 day. Following flash column chromatography, the desired benzylated triazolium salt **158** was successfully isolated in 95% yield (Scheme 48).



Scheme 48 Alkylation of triazole **156** with benzyl bromide

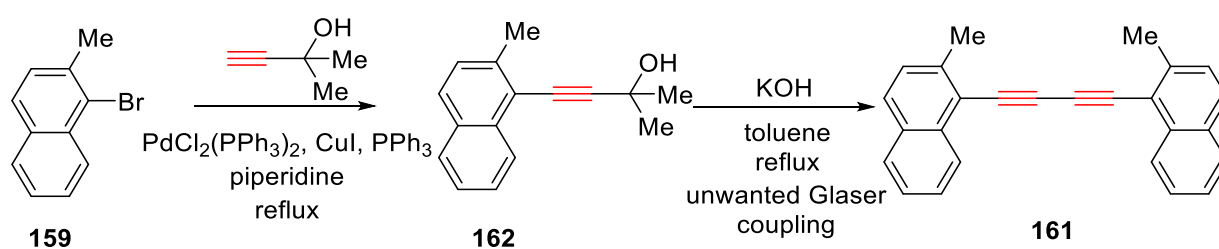
As both strategies outlined to form atropisomers (Scheme 45 and Scheme 46) require *ortho*-substituted aromatic alkynes, Sonogashira cross-coupling was targeted as a manner to introduce this functionality from an *ortho*-substituted aryl bromide. Commercially available naphthyl bromide **159** was chosen, since the methyl group in the *ortho* position would give the steric bulk adjacent to the alkyne, whilst the naphthyl motif would give greater steric bulk than a phenyl ring.



Scheme 49 Sonogashira cross-coupling of bromide **159** and formation of unwanted Glaser coupled product **161**

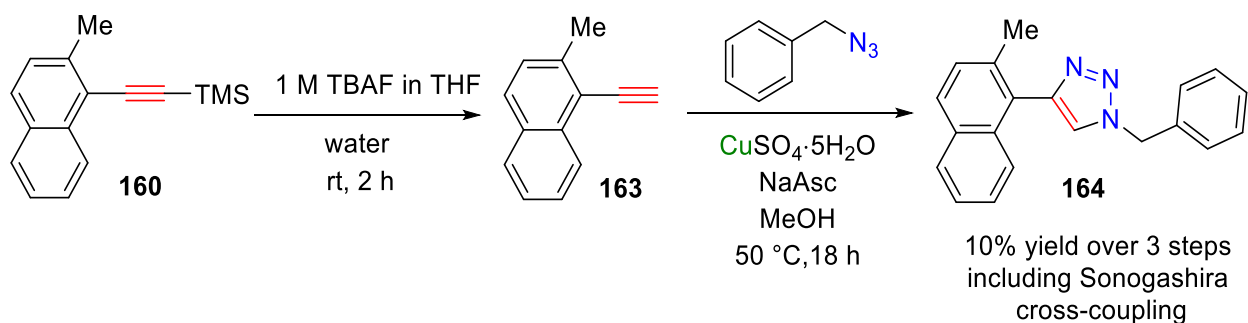
When the cross-coupling reaction of **159** with TMS acetylene was carried out in either triethylamine (TEA) or diisopropylethylamine (DIPEA), no desired product was observed and starting bromide **159** was recovered. A breakthrough was made when the coupling was carried out in piperidine; multiple methyl resonances were observed in the ^1H NMR spectrum of the crude reaction mixture. It is hypothesised that the amine bases may act as ligands towards the palladium and impact the mechanism of reaction, and this may be why piperidine is a superior solvent for this reaction.^[119] The Sonogashira coupling led to a mixture of three products. The first two were inseparable by flash column chromatography and were assigned

as the desired TMS-protected alkyne **160** and recovered starting material **159** (Scheme 49). The third product was a highly crystalline solid, and the Glaser-coupled product **161** was identified using mass spectrometry (Scheme 49). This highlighted the problem that the TMS was being cleaved during the reaction, leading to Glaser coupling. This has been noticed in the literature previously.^[120] Crisp and Jiang reported that the free alkyne **163** will homocouple slowly at room temperature even without copper present. They recommended using 2-methyl-3-butyn-2-ol as a coupling partner to minimise unwanted deprotection compared with a TMS-protected alkyne.^[120] Unfortunately, upon attempting deprotection to the terminal alkyne, the only recoverable product was the same Glaser-coupled product **161** as seen in the previous reactions (Scheme 50).



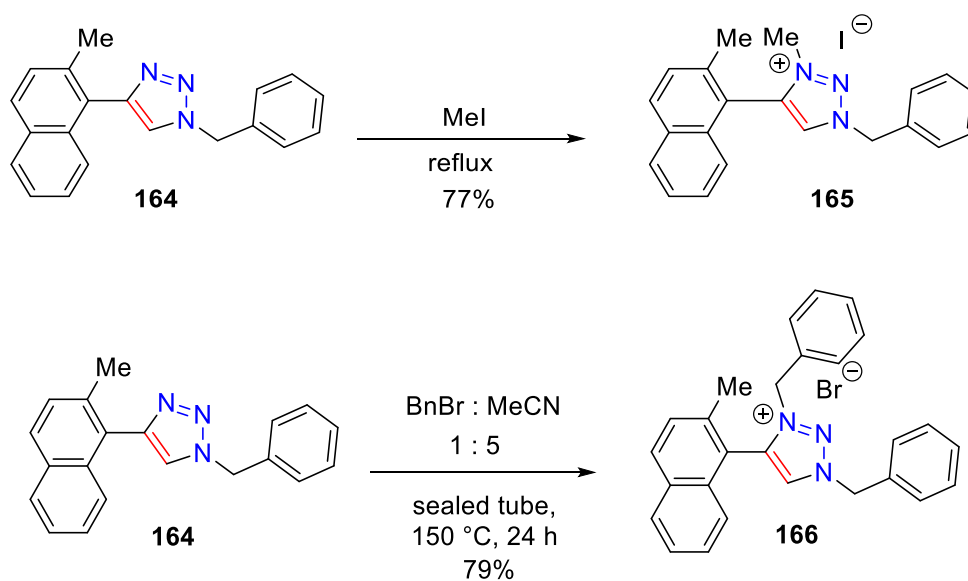
Scheme 50 Attempted Sonogashira cross-coupling leading to unwanted Glaser coupled product

Even though the material obtained from the Sonogashira reaction (piperidine and TMS acetylene, Scheme 49) was a mixture of starting aryl bromide and the desired alkyne, it was decided to continue with deprotection and a CuAAC with benzyl azide. It was hoped that the triazole product **164** would be sufficiently different in polarity to allow easy separation from bromide **159**. This was indeed the case, and the synthetic route yielded the desired triazole **164** in 10% overall yield over 3 steps (Scheme 51). This was a disappointing yield, but the route gave enough material for further elaboration towards the target triazolium salts.



Scheme 51 Synthesis of triazole **164**

Alkylation of triazole **164** with both methyl iodide and benzyl bromide was attempted using previously developed conditions. Methylation and benzylation occurred smoothly to garner triazolium salts **165** (77% yield) and **166** (79% yield), respectively (Scheme 52).



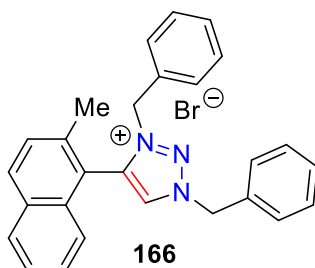
Scheme 52 Methylation and benzylation of triazole **164**

Upon inspection of the ^1H NMR spectra of compounds **165** and **166** in chloroform-*d*, it was noticed that the benzylic protons in both compounds were diastereotopic. This was encouraging, as it showed that rotation around the single bond between the triazole ring and naphthyl moiety was being restricted upon alkylation. To measure how stable this locked conformation was, chiral HPLC separation of enantiomers was originally targeted. It was

hoped that an enantioenriched sample of **165** or **166** could be obtained, and that this could then be heated and subjected to chiral HPLC analysis to see if any racemisation had occurred. Unfortunately, chiral separation conditions of the triazolium salts proved to be extremely challenging; normal and reverse phase, Phenomenex Cellulose 1 and 3, along with Chirapak OD and AD columns all proved ineffective at enantiomer separation. HPLC additives (e.g. TFA or TEA) were not tried because it was expected that this would lead to the switching of the triazolium counterion during separation.

Due to the failure to obtain HPLC separation conditions, variable temperature (VT) ^1H NMR was used to probe the stability of the formed atropisomers. The compounds **165** and **166** were dissolved in $\text{DMSO-}d_6$ and the benzylic position of the methyl-substituted compound **165** coalesced into a singlet at room temperature. This showed that the atropisomer was not configurationally stable in $\text{DMSO-}d_6$. Tetrachloroethane- d_2 (TCE) was then tried, but coalescence of the diastereotopic signals was observed. Thus, compound **165** was not suitable for VT ^1H NMR analysis. The benzyl-substituted compound **166** clearly showed diastereotopic splitting patterns at 5.30 ppm, and these signals did not coalesce even at 100 °C (Figure 31). This proved that rotation within this system was highly restricted and showed that this architecture was configurationally stable even at high temperature, which is a crucial facet of successful atropisomeric chiral ligands.

With a atropisomeric species successfully formed, it was hoped that this knowledge could be used to make other restricted-rotation triazolium salts, which could possibly be separated by chiral preparative HPLC. It was decided to investigate installing biphenyl moieties on each side of the triazole due to their steric demands. In addition, biphenyl moieties can be easily modified to incorporate a range of substituents due to their possible synthesis *via* Suzuki cross-coupling.



Diastereotopic CH₂

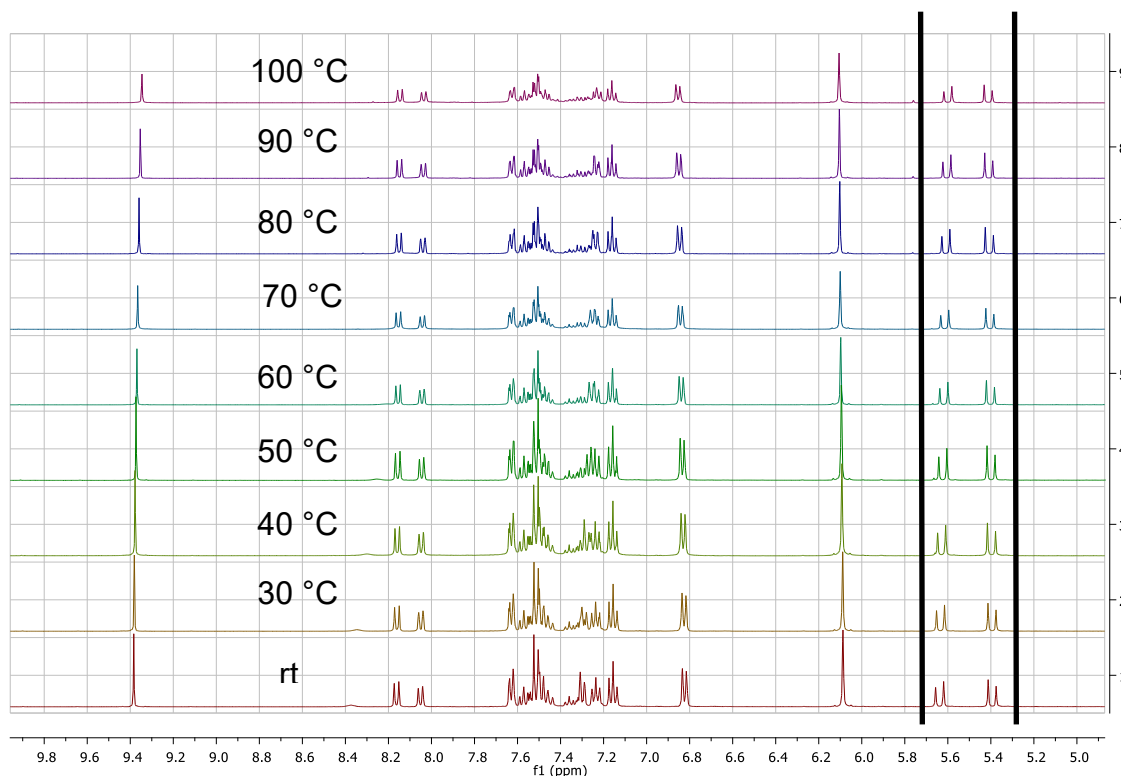
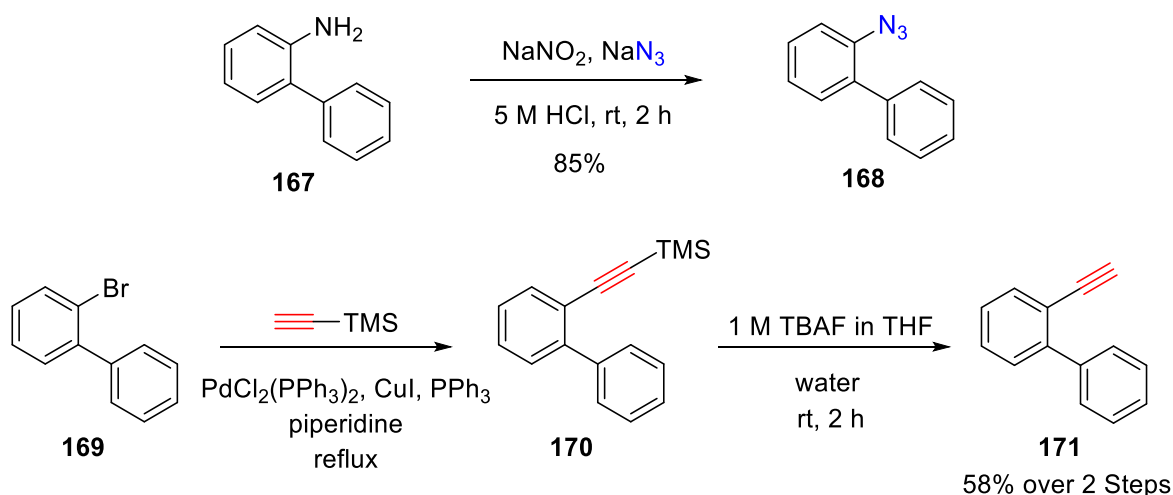


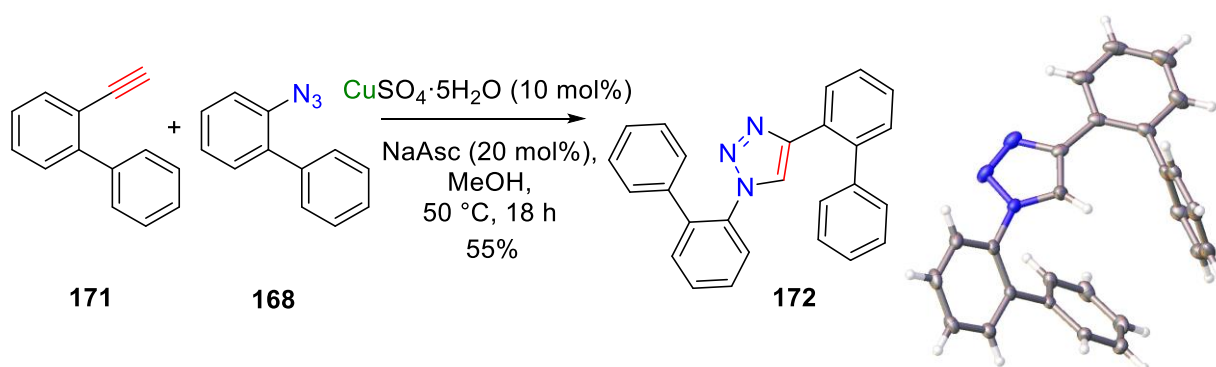
Figure 31 Diastereotopic resonances within the ¹H NMR spectrum of triazolium **166**, VT NMR spectroscopic study to 100 °C shows no coalescence in the resonance centred at 5.5 ppm

Azide **168** was prepared from the corresponding amine **167** in 85% yield, and alkyne **170** was synthesised successfully through a Sonogashira cross-coupling in 58% yield over two steps (Scheme 53). It was noted that Glaser coupling products were not observed in this reaction.

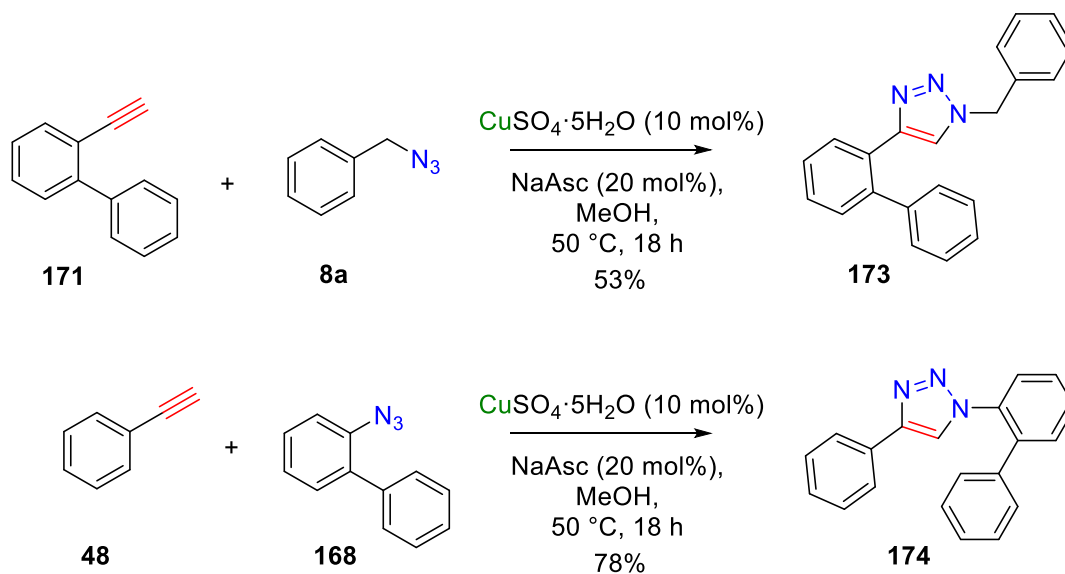


Scheme 53 Synthesis of azide **168** (top), synthesis of alkyne **171** (bottom)

A CuAAC reaction successfully joined azide **168** with alkyne **171** in 55% yield to garner triazole **172** (Scheme 54). This material was successfully crystallised by evaporation from acetonitrile and its structure obtained by single-crystal XRD.



Scheme 54 Synthesis of triazole **172** with corresponding crystal structure. Ellipsoids are drawn at the 50% probability level. To fully explore what steric requirements were needed for atropisomer formation, it was decided that synthesising the related triazoles **173** and **174** was of value. The two biphenyl components **171** and **168** were treated with benzyl azide and phenylacetylene, respectively, to generate the related compounds **173** (53% yield) and **174** (78% yield) (Scheme 55).



Scheme 55 CuAAC reactions to form triazoles **173** and **174**

With triazoles **172**, **173** and **174** in hand, further elaboration of the triazole scaffold was attempted through the use of alkylating agents. Benzylation and methylation occurred smoothly across all three triazoles forming six novel triazolium salts **175-180** in yields ranging between 33% and 93% (Figure 32).

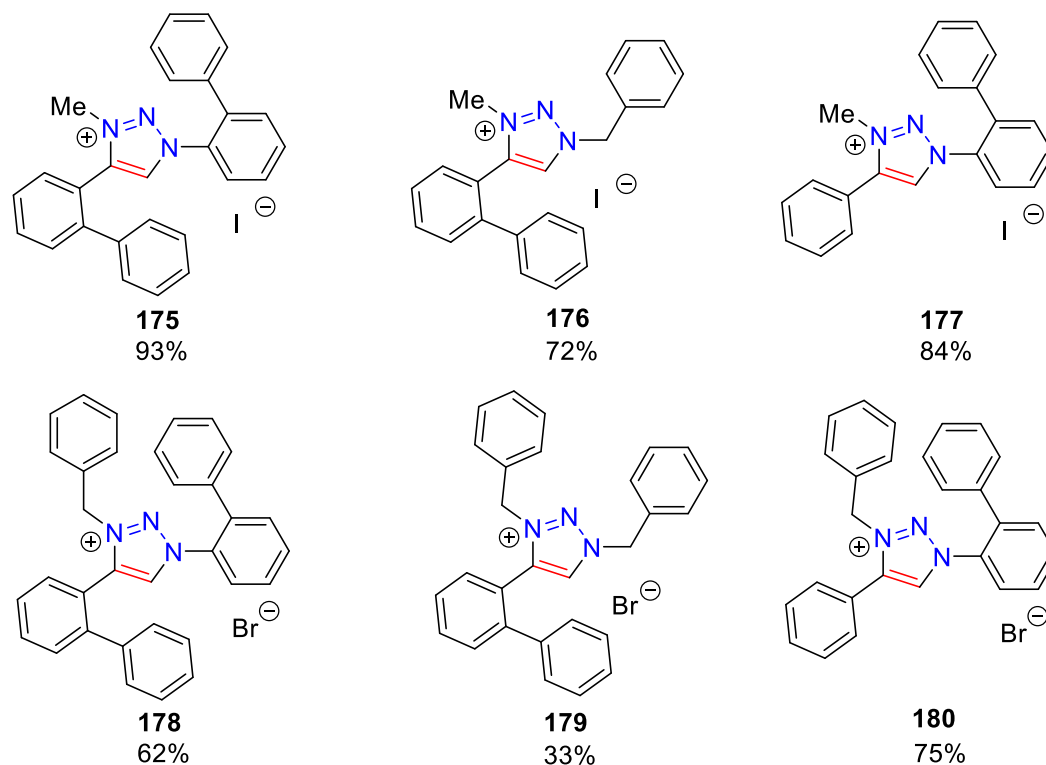


Figure 32 Synthesised novel triazolium species

Proton NMR spectroscopic analysis of compounds **175-180** (Figure 32) showed no evidence of diastereotopic methylene protons. From this it was concluded that none of these compounds were atropisomeric, which can be rationalised by the fact that a methyl group is sterically less demanding than a benzyl group. This, however, does not explain why the benzyl-substituted compounds **178**, **179** and **180** showed no atropisomerism. It was argued that due to the rotational flexibility in biphenyl moieties there was not enough rigid steric bulk around alkylated triazole to induce an overall locked conformation. Intriguingly, compound **178** was found to be a colourless crystalline solid, whilst the other compounds across the series **175-180**, even after drying under high vacuum, were very viscous brown oils, possibly due to quaternary nitrogen salts' classical hygroscopic properties.^[121] Compound **178**, however, was found to be very stable – even after leaving open to air for a week it remained as a crystalline solid.

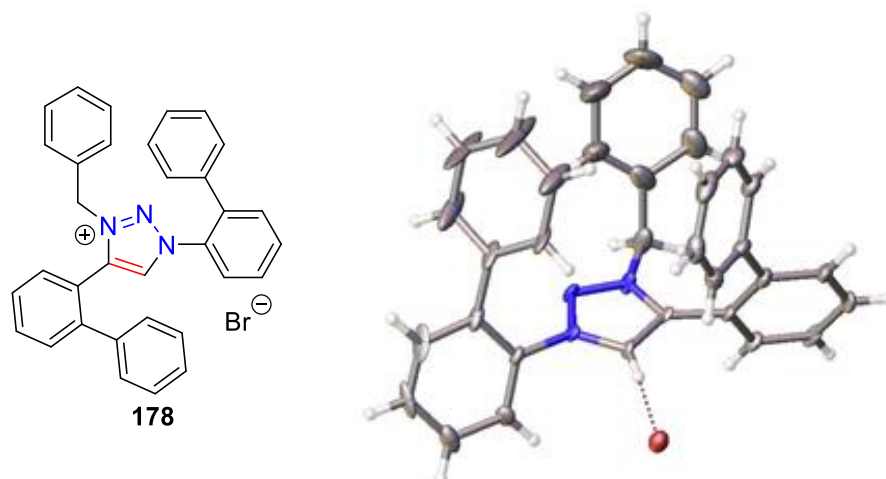
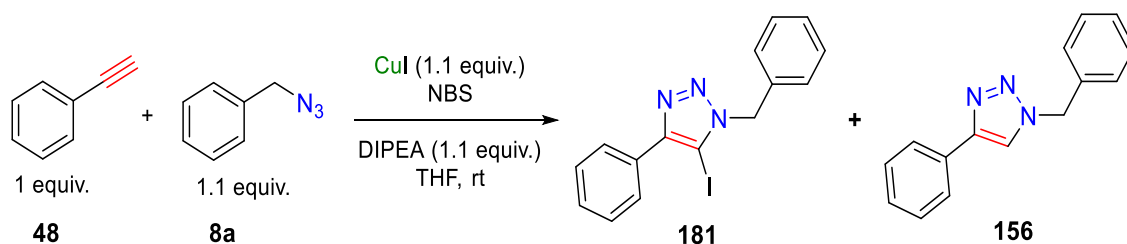


Figure 33 Crystal structure of triazolium **178**. Ellipsoids are drawn at the 50% probability level.

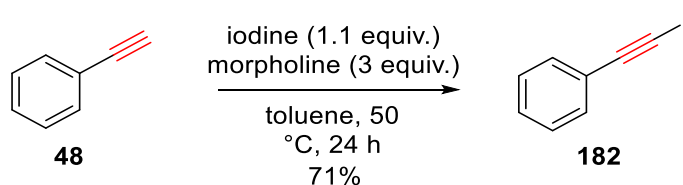
The crystalline behaviour of **178** allowed for single-crystal XRD analysis and a crystal structure was successfully obtained (Figure 33). This bench stability is a rare characteristic in these systems, as there appears to be no literature precedents for crystal structure determination of *N*-benzylated 1,2,3-triazolium salts. It is hoped that this crystallinity could make future application of these materials more operationally simple to carry out, because non-hygroscopic crystalline materials are easier to handle in open bench situations than hygroscopic ones.

With none of the triazoles **175-180** displaying any atropisomerism, it was decided to move on to the other strategy of using iodo substituents to restrict rotation and it was hoped that the iodo substituent could be introduced during the CuAAC reaction. There was literature precedent for this,^[122] where the addition of NBS, copper(I) iodide and DIPEA to the CuAAC reaction could deliver iodo-substituted triazoles. Unfortunately, when the reaction was attempted, a mixture of 5-iodotriazole **181** and prototriazole **156** were observed (Scheme 56). Increasing the number of equivalents of NBS from 1.2 to 1.3 to 1.5 to 2.4 showed no improvement, still garnering a mixture of compounds **181** and **156**.



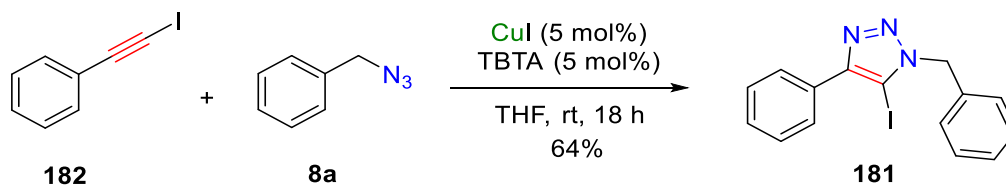
Scheme 56 Attempted formation of an iodotriazole during cycloaddition

With the failure of installing the iodo substituent during the cycloaddition step, it was decided that preforming iodoalkynes could be a way to successfully form 5-iodotriazoles. In order to test this hypothesis, literature iodoalkyne **182**^[123] was synthesised in 71% yield from phenylacetylene **48** (Scheme 57).



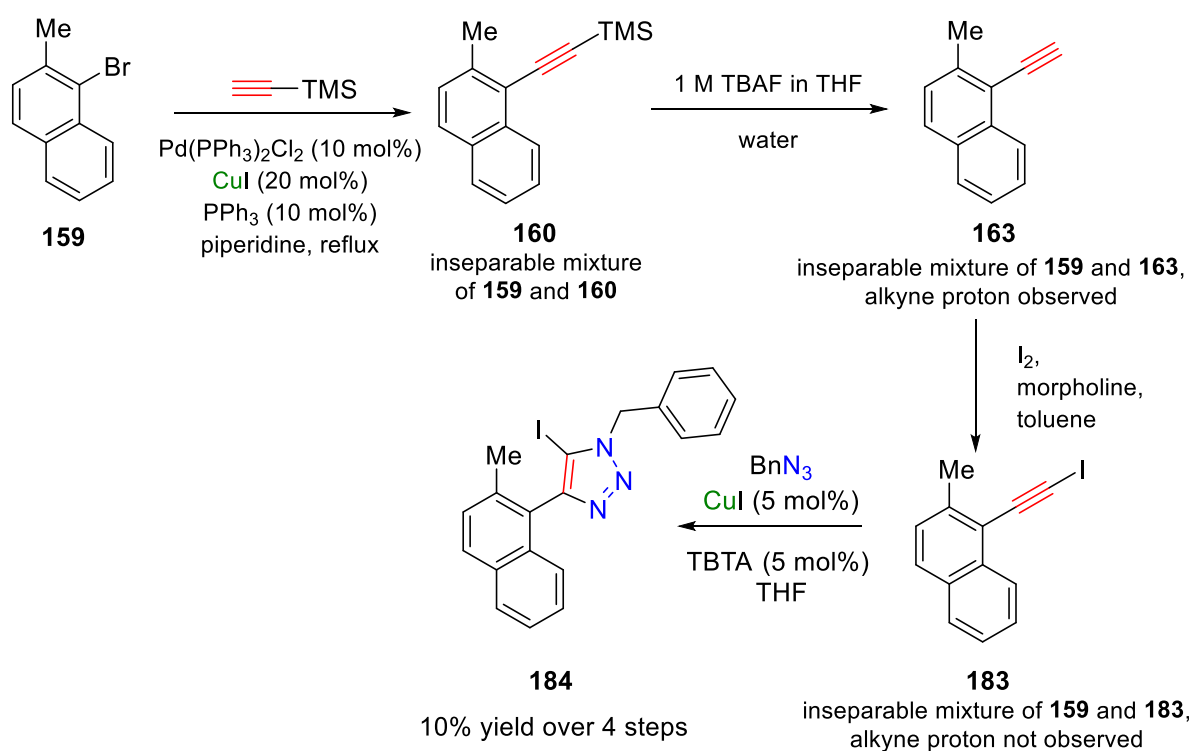
Scheme 57 Synthesis of iodoalkyne **182**

The iodoalkyne **182** was then treated with benzyl azide to form 5-iodotriazole **181** in 64% yield (Scheme 58). With this methodology successfully demonstrated, the 5-iodotriazole equivalent of prototriazole **166** was targeted. This motif had already been shown to have atropisomeric characteristics, and it was hoped that the iodo version would have a good chance of displaying the same properties.



Scheme 58 CuAAC reaction of iodoalkyne **182** to yield iodotriazole **181**

The previously synthesised alkyne **163** was converted to the iodoalkyne **183**, and subsequently reacted with benzyl azide to furnish the desired 5-iodotriazole **184** in 10% overall yield over 4 steps (Scheme 59). Due to similarities in polarity of products and starting materials in this synthetic route, it was decided to proceed to the triazole **184** before attempting purification. The success of each step could be monitored by the presence and absence of acetylenic resonances by ^1H NMR spectroscopic analysis of the crude reaction mixture following each reaction.



Scheme 59 Synthetic route to iodotriazole **184**

Following successful isolation of the desired 5-iodotriazole **184**, ^1H NMR spectroscopic analysis of the pure material showed evidence of the methylene protons being diastereotopic (Figure 34). This was a pleasing result, and it was hoped that the chiral HPLC separation of the atropisomers of the iodotriazole **184** would be easier than that for the previous triazolium salts, due to the lack of charge.

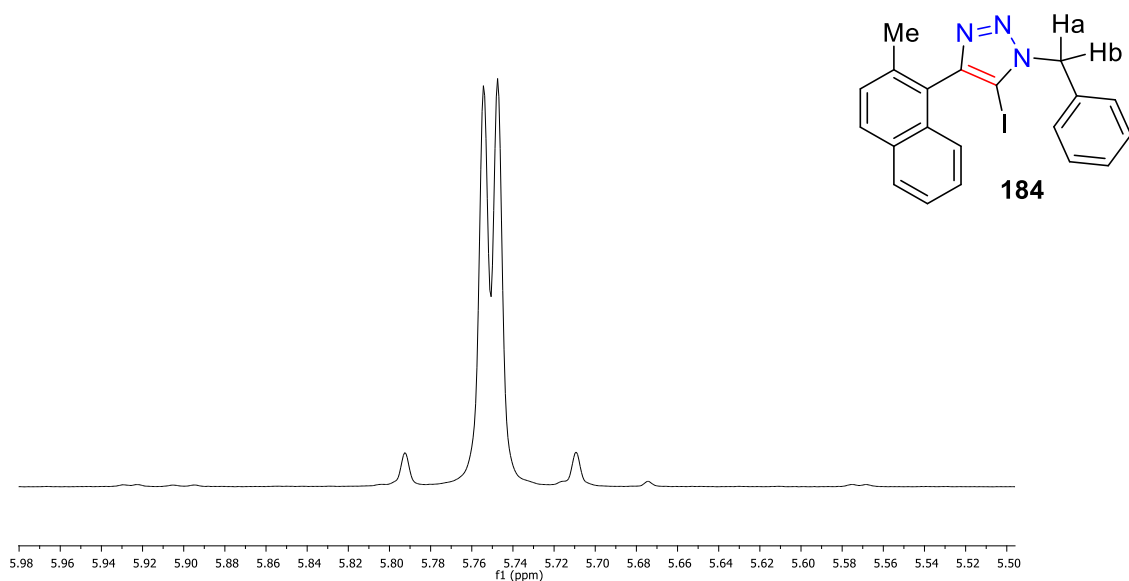


Figure 34 Selected section of ¹H NMR spectrum of iodotriazole **184** showing diastereotopic protons (Ha and Hb). Indeed, HPLC separation of the two atropisomers was found to be straightforward. The two atropisomers were found to be separable in a mixture of 20:80 water/acetonitrile (Figure 35). Close inspection of the baseline between the peaks in the trace showed that the UV signal did not return to zero, suggesting that the atropisomerism of this system was not fixed. This phenomenon has been observed by other researchers and has been attributed to slow rotation around a single bond, creating species with intermediate rotatory states between the two main species seen in the HPLC trace.^[124]

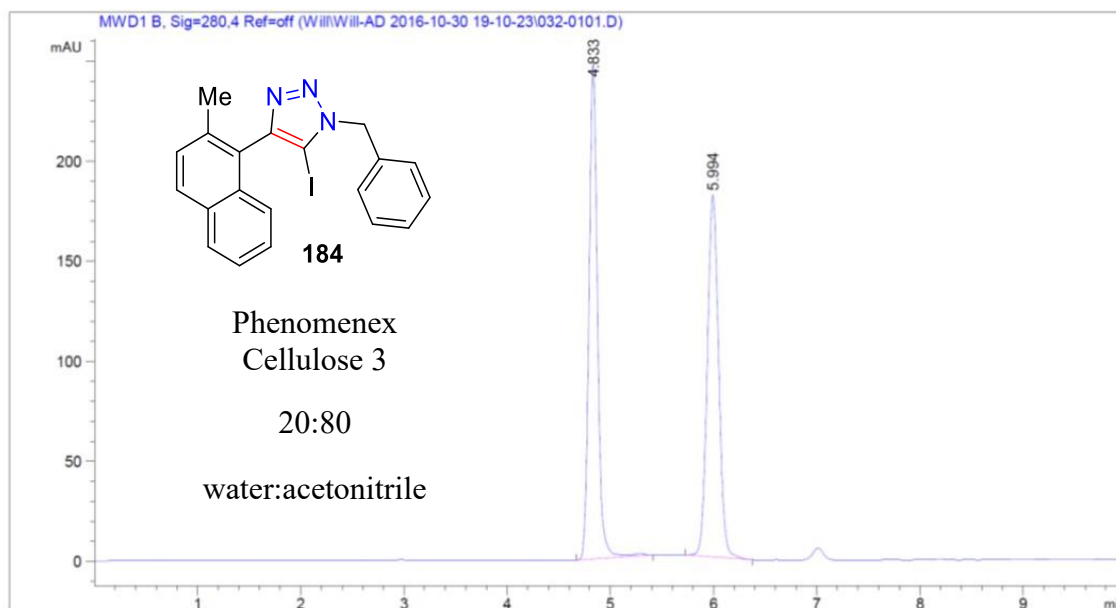


Figure 35 HPLC separation of iodotriazole **184**

In order to test how stable (or unstable) restricted rotation in **184** was, an enantioenriched sample was obtained by collection of the material following analytical chiral HPLC separation. This material was then resubjected to chiral HPLC separation every thirty minutes and the change in *ee* was monitored over time. It was found that **184** was not atropisomerically stable at room temperature. The material was determined to be 87% *ee* following its first injection after collection. However, slow erosion of enantiomeric excess was observed, and by the time 408 minutes had passed, the material had almost completely racemised (5% *ee*) (Figure 36). It should be noted that an enantioenriched sample of the second observed peak (5.9 min) was not collected and subjected to the same analysis. Due to this the identity of the two peaks as the two atropisomers can only be surmised and not confirmed; it is possible that the second peak is a degradation product of **184**.

Even though slow racemisation was not desired for the formation of stable chiral ligands, slowly rotating species have been successfully utilised as a way to control atropisomerism.^[124d] For example, Clayden and co-workers have demonstrated that dynamic

kinetic resolution of slowly rotating molecules can garner high *ee* atropisomeric materials.^[124d, 125]

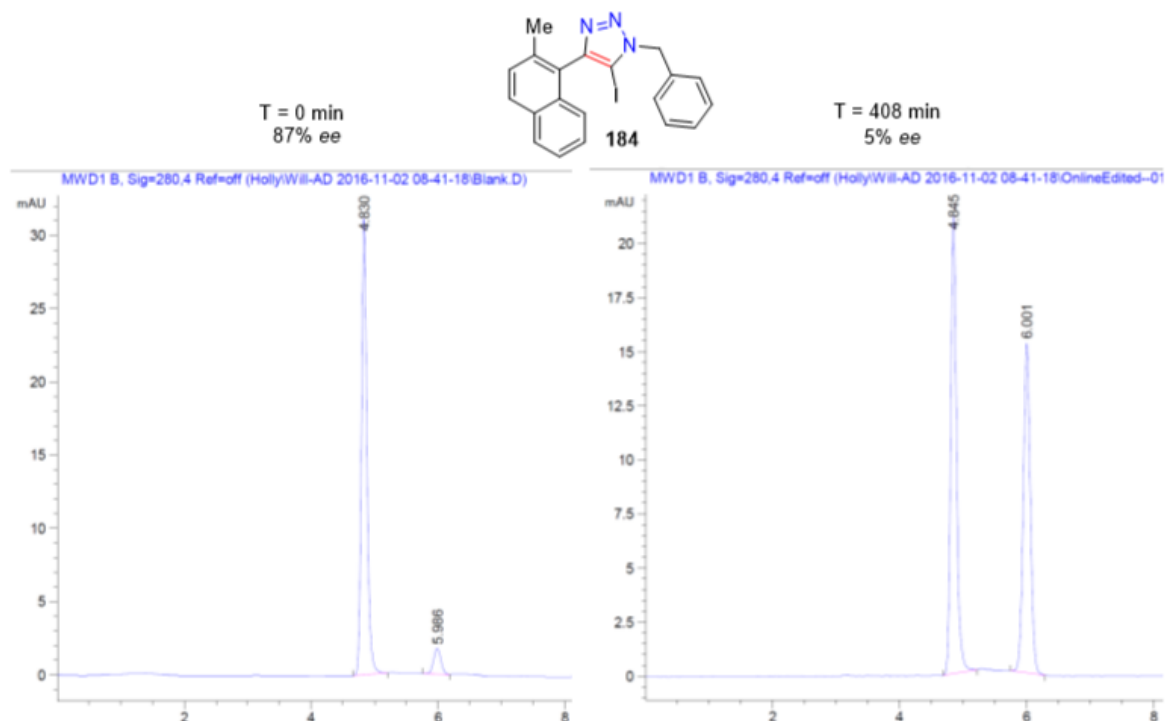


Figure 36 Erosion of *ee* over time monitored by chiral HPLC

Due to time constraints, it was decided that a possible straightforward method to retard the rotation in **184** was to change the pH of the HPLC solvent. It was hoped that by lowering the pH, the triazole would become protonated on nitrogen atom 3, and thus the barrier to rotation would increase. Running the same HPLC experiment as shown above (Figure 35) with 0.05% trifluoroacetic acid in the eluent, the rotation was marginally slower; calculation of loss of *ee* per hour showed that erosion of enantiomeric excess was 2% per hour slower in the presence of TFA.

4.1.1 Summary

Within this section, a series of novel triazoles and triazolium salts were successfully synthesised.^[126] Triazolium salt **166** was shown to be a highly stable atropisomeric species by

VT ^1H NMR spectroscopy, but unfortunately, chiral HPLC separation conditions could not be established for this compound, and thus it was not accessible as a single enantiomer. Bis(biphenyl) triazolium **178** was observed to be a bench-stable crystalline material and was successfully subjected to single crystal XRD analysis. 5-Iodotriazole **184** was synthesised and shown to not have configurational stability at room temperature, confirmed by HPLC separation and analysis. Due to time constraints within the laboratory, the species in this section were not successfully applied to catalytic reactions, but the knowledge of the ligand designs are currently informing further work within the group on the synthesis and application of atropisomeric triazolium species.

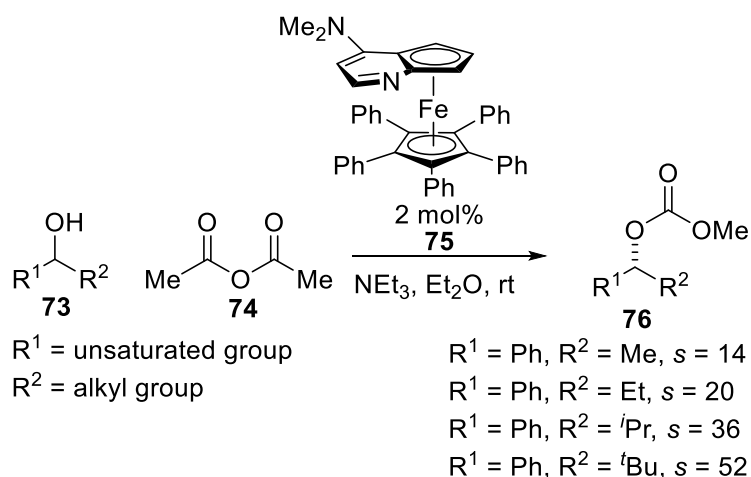
The experimental work in this section was carried out by the author of this thesis. The primary investigators were Dr John Fossey (UoB) and Dr Benjamin Buckley (LU).

4.2 Chiral 4-Dimethylaminopyridine Derivatives Synthesised by CuAAC and Attempted Kinetic Resolution of Secondary Alcohols

Thus far, in this thesis, kinetic resolution methodologies have been developed to utilise the CuAAC reaction directly as a means of obtaining resolution of chiral materials. This section of work attempted to use a different approach, in which the CuAAC would be used as a manner to form a chiral catalyst for use within a kinetic resolution. Before the work in this section was carried out, another member of the Fossey group had been synthesising and testing chiral DMAP derivatives in kinetic resolutions of secondary alcohols. It was deemed a good opportunity for a collaborative project in which chiral triazoles could be appended to a DMAP core to form novel chiral catalysts.

Kinetic resolution of secondary alcohols is an established field, and many researchers have developed a myriad of chiral DMAP motifs to achieve various kinetic resolutions of different

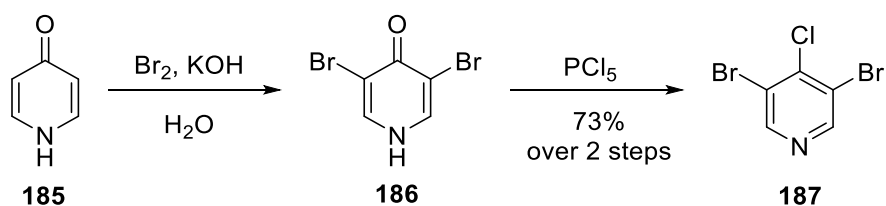
substrates.^[124b, 127] One well-known example of a chiral DMAP catalyst for KR of secondary alcohols was developed by Fu and co-workers.^[46-47, 50, 127a] Utilising planar chirality, Fu was able to demonstrate highly selective kinetic resolution of secondary alcohols through acylation (Scheme 60).



Scheme 60 Kinetic resolution of secondary alcohols, Fu and co-workers^[47]

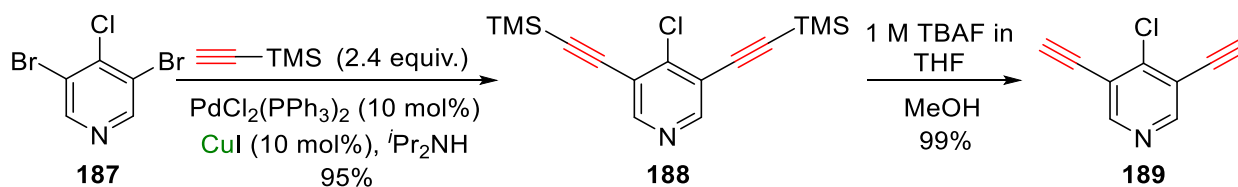
Chiral secondary alcohols are important building blocks in organic synthesis and have been used in the synthesis of active pharmaceuticals^[128] and natural products.^[129] Therefore, accessing chiral secondary alcohols in their enantiopure forms is an important area of research within asymmetric catalysis.

Using chiral azides as CuAAC partners to a bis(alkyne)-appended pyridine core, it was hoped that a chiral C_2 -symmetric bis(triazole) system could be obtained following a relatively straightforward synthetic approach. To achieve this, a 3,4,5-substituted pyridine was required as a core which could be further elaborated through CuAAC. Reaction of 4-pyridone **185** with bromine and subsequent substitution of the ketone **186** with PCl_5 led to the formation of the tri-substituted pyridine **187** in 73% overall yield (Scheme 61).



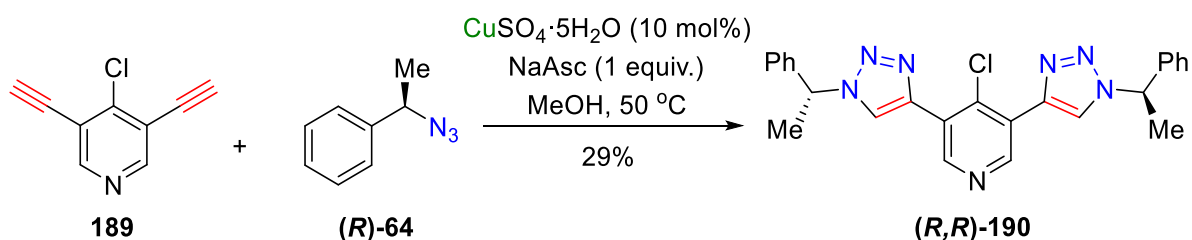
Scheme 61 Synthesis of trisubstituted pyridine core **187**

Sonogashira cross-coupling of pyridine **187** with TMS acetylene led to the formation of the bis(TMS)-protected alkyne **188** in 95% yield. It was found that this could be smoothly deprotected using tetrabutyl ammonium fluoride (TBAF) in THF (1 M) with methanol as a co-solvent to give bis(alkyne) **189** in 99% yield (Scheme 62).



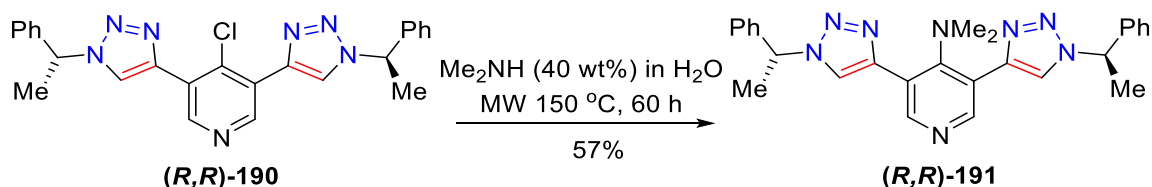
Scheme 62 Sonogashira cross coupling to afford bis(alkyne) **189**

With dialkyne **189** successfully synthesised, CuAAC with an enantiopure chiral azide could be attempted. Previously synthesised chiral azide (**R**)-**64** was chosen and allowed to react with bis(alkyne) **189** to furnish bis(triazole) **190** as a single diastereoisomer in 29% yield (Scheme 63).



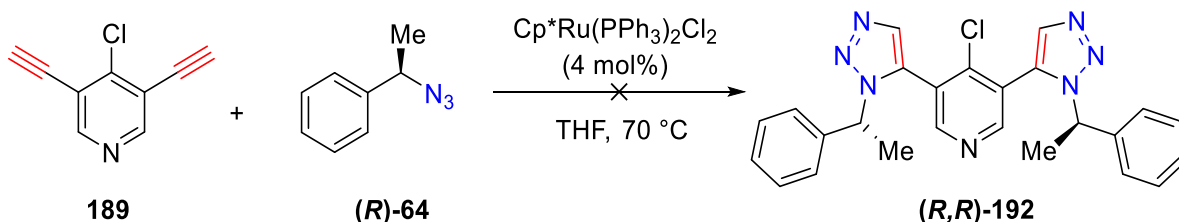
Scheme 63 Double CuAAC reaction to form DMAP precursor **190**

Finally, to create a DMAP catalyst, the dimethylamino substituent needed to be introduced. To achieve this, a microwave-promoted S_NAr reaction of chloride **190** with dimethylamine in water was used. This reaction provided the C_2 -symmetric DMAP catalyst **191** in 57% yield. To achieve this yield, 60 hours in the microwave reactor was required, which was attributed to the large steric hindrance of the two triazoles flanking the chloride.



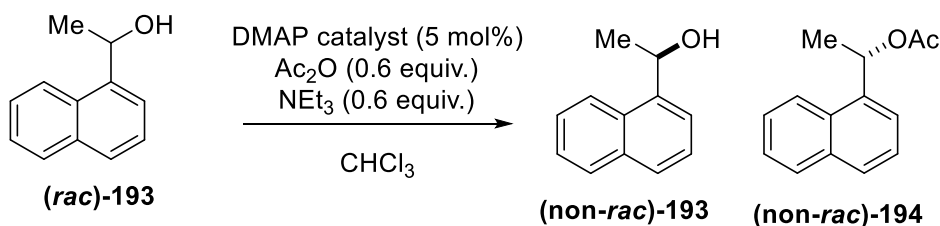
Scheme 64 Microwave-assisted S_NAr reaction to yield chiral DMAP catalyst **191**

It should also be noted that the synthesis of 1,5-bis(triazole) DMAP catalyst **192** was also attempted using the reported literature ruthenium catalyst under the reported reaction conditions^[130] but led to no product (Scheme 65). Even after 72 h, TLC analysis showed no conversion to triazolic product **192**. The synthesis of bis(triazole) **192** was therefore suspended and catalysis was attempted with 1,4-bis(triazole) **191**.



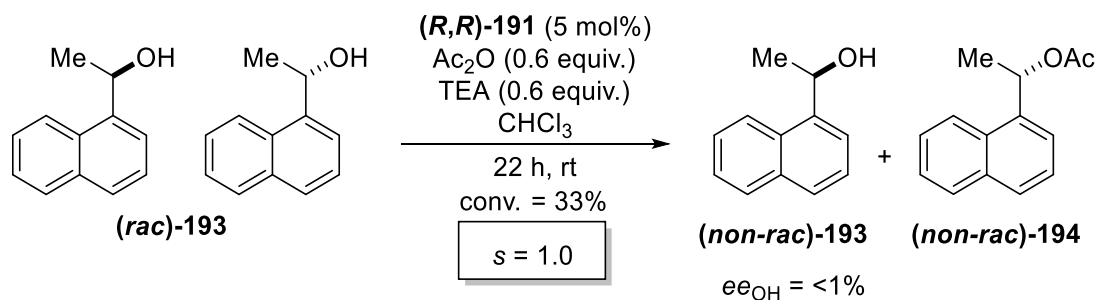
Scheme 65 Attempted synthesis of 1,5-bis(triazole) chiral DMAP catalyst **192**

In order to test the efficiency of catalyst **191**, the kinetic resolution of 1-(1-naphthyl)ethanol was chosen as a test reaction (Scheme 66). Monitoring of the resolution could be carried out in real time using chiral GC methodology. It was possible to measure the remaining amounts of each enantiomer of alcohol along with formation of ester **194**.

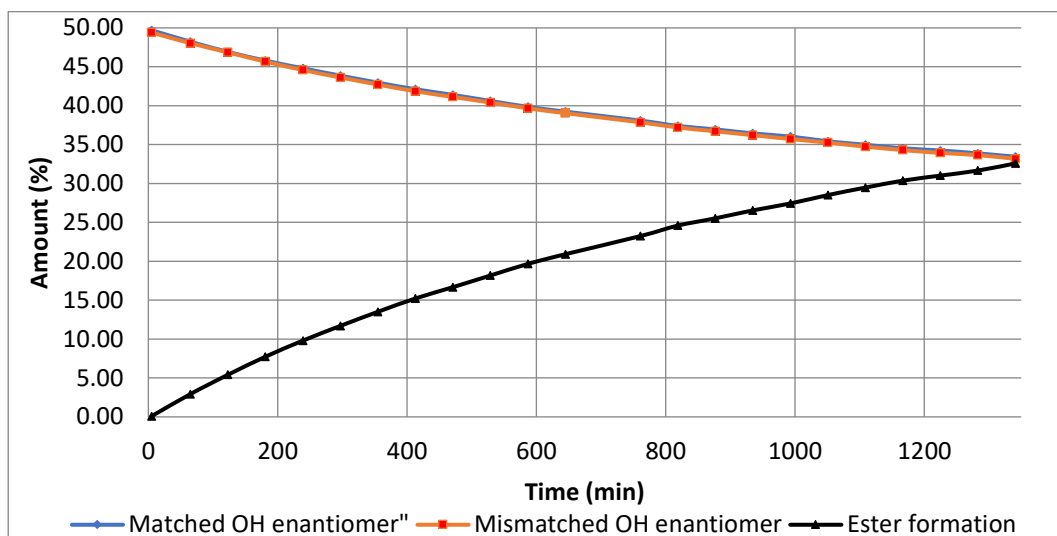


Scheme 66 Catalytic test reaction, enantioselective acylation of 1-(1-naphthyl)ethanol

It became apparent from the GC measurements that no kinetic resolution was occurring with catalyst **191** (Scheme 67). Both enantiomers of naphthylethanol were reacting at the same rate. Overall, the reaction was measured to reach 33% conversion with the average selectivity over 20 timepoints (181 min -1341 min) of $s = 1.03 \pm 0.01$ (Graph 1). Compound **191** was acting as a catalyst as the background reaction over the same time period gave a conversion of less than 2%.



Scheme 67 Acylation of 1-(1-naphthyl)ethanol under asymmetric conditions using chiral DMAP catalyst **(R,R)-191**



Graph 1 Real time monitoring by chiral GC of the kinetic resolution of 1-(1-naphthyl)ethanol using chiral DMAP catalyst (*R,R*)-**191**. Matched refers to the fastest reacting enantiomer of **193** whilst mismatched refers to the slowest reacting enantiomer of **193**.

The kinetic resolution data was disappointing; however, examining three-dimensional representations^[131] of the catalyst, it was maybe not surprising that chiral relay did not occur (Figure 37). The pyridine nitrogen atom is the one which takes part directly in DMAP-catalysed reactions. Therefore, for the efficient transfer of chiral information, the ligand's chirality needs to be placed proximal to the pyridine nitrogen atom, which is not the case for catalyst **191**.

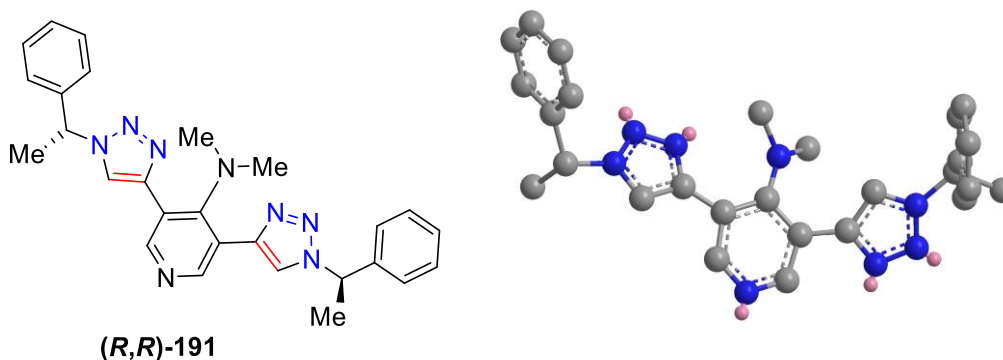


Figure 37 3D Representation of one possible conformation of chiral DMAP catalyst (*R,R*)-**191**

It was hoped that the 1,5-bis(triazole) **192** might increase steric bulk around the pyridine nitrogen. However, as discussed above, the synthesis of that catalyst was not successfully

completed. There are other possible strategies which could be employed to improve the selectivity of a CuAAC-constructed DMAP catalyst. For instance, moving the triazole moieties from the 3,5 positions to the 2,6 positions would place the stereogenic centres closer to the catalytic nitrogen centre. Increasing the steric bulk, such as by replacing the methyl substituents with isopropyl moieties, around the stereogenic centres could also improve selectivity.

4.2.1 Summary

In this section, a novel triazole-based chiral DMAP catalyst **(R,R)-191** was successfully synthesised and tested in the kinetic resolution of 1-(1-naphthyl)ethanol.^[132] Unfortunately, no kinetic resolution was observed and a selectivity factor of $s = 1.03 \pm 0.01$ was measured. The use of CuAAC reactions to quickly and efficiently construct chiral DMAP catalysts is still of interest within the Fossey group, and hopefully the observations within this section may lead to more efficient catalyst design.

The experimental work in this section was carried out jointly between the author of this thesis and Daniel Payne (UoB). The primary investigator was Dr John Fossey (UoB).

5 Studies Toward Asymmetric 5,5'-Bis(triazole) Formation and The Use of Ruthenium-Based Olefin Metathesis Catalysts in the Synthesis of 1,5-Triazoles

5.1 Studies Toward Asymmetric 5,5'-Bis(triazole) Formation

In 2007, Burgess and co-workers reported a modification to the CuAAC reaction to produce 5,5'-bis(triazoles).^[133] They found that through the addition of potassium carbonate as a base to a CuAAC, afforded bis(triazoles) in high yields with minimal amounts of prototriazole (a triazole with a proton in the 5 position) present. Recently (since the work in this chapter was carried out), Brassard *et al.* have reported an efficient protocol for the synthesis of bis(triazoles) using $\text{Cu}(\text{OAc})_2 \cdot \text{H}_2\text{O}$ in air.^[134]

Burgess reported that the of a 5,5-bis(triazole) formed from phenyl acetylene and benzyl azide displayed atropisomerism. Rotation around the central single bond between the two triazole moieties is extremely hindered (Figure 38). This was confirmed through the observation of an AB-quartet for the diastereotopic protons in the benzyl group in the ^1H NMR spectrum of the bis(triazole). Burgess further showed that this rotation was restricted by carrying out variable temperature ^1H NMR studies. Even at 115 °C in DMSO, the spectrum showed no coalescence in the AB quartet, demonstrating that this atropisomerism was locked at this temperature.

^[134]^[134]Atropisomerism is interesting because various chiral ligands use this form of chirality in their designs. Ligands such as BINAP, BINOL and phosphoramidites all take advantage of restricted rotation. Therefore, bis(triazoles) may find utility as structural motifs within new classes of chiral ligands. One way in which atropisomers could be synthesised as single enantiomers is through the formation of a racemic mixture followed by enantiomer separation using preparative HPLC with a chiral stationary phase.. This is not the most elegant approach;

it would be preferable to form a single atropisomer during synthesis, which would negate the need for HPLC separation.

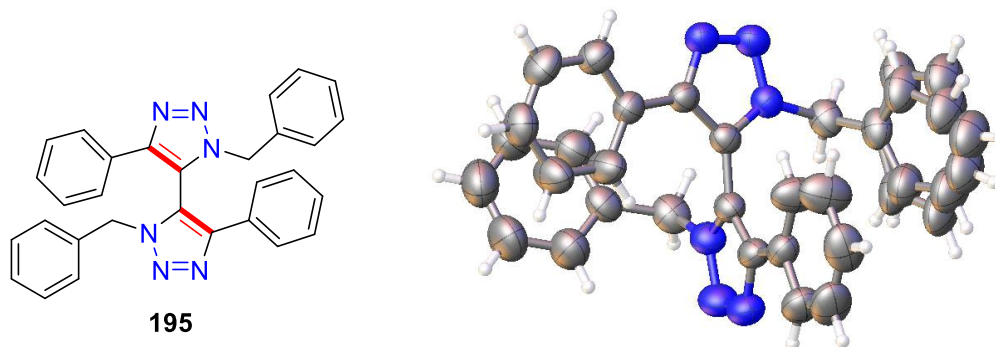
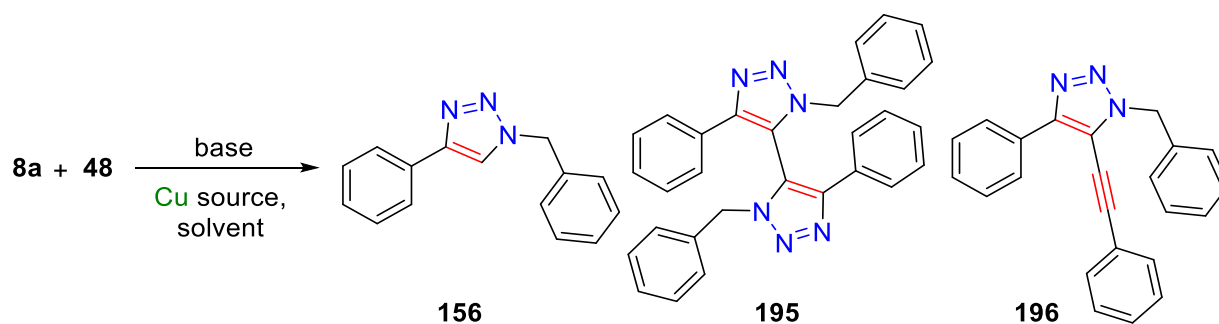


Figure 38 Crystal structure of 5,5'-bis(triazole) reported by Gonzalez *et al.*^[135] Ellipsoids are shown at the 50% probability level.

It was hypothesised that using chiral CuAAC methodology developed within Section 2.1, a single atropisomer could be obtained in a bis(triazole) synthesis. To do this, pure samples of bis(triazole) would be needed, and then chiral HPLC separation of the two atropisomers would be required. After this, a series of reactions using chiral ligands for copper would need to be carried out, and the resulting levels of enantioenrichment (if any) quantified.

To begin with, reproduction of the literature reaction reported by Burgess and co-workers was carried out. Following their methodology 32% of the crude product mixture (measured *via* integration of the benzylic protons in the ¹H NMR spectrum of the crude reaction mixture) appeared to be bis(triazole) **195**, whilst the major product was the undesired mono(triazole) species **156** (Table 16, entry 1). This result was in line with that of Burgess, who reported an isolated yield of 37% of bis(triazole) **195** in the same reaction with the same conditions. However, considering that 63% of the reaction mixture contained unwanted products this distribution was considered unsatisfactory.

The reaction conditions were screened to optimise the reaction in favour of the bis(triazole) species **195**. Firstly, the conditions reported by Burgess were probed. The reaction was carried out at 0 °C and 60 °C, and both reactions showed almost complete conversion to the undesired mono(triazole) **156** species, giving 92% and 93% respectively (Table 16 entries 2 and 3). Next, the concentration of base was probed. Increasing from 2 M Na₂CO₃ solution to 4 M increased the percentage of bis(triazole) **195** observed by ¹H NMR spectroscopy to 40% (Table 16, entry 4). When the base was changed to K₂CO₃, only 17% of the desired bis(triazole) **156** was obtained (Table 16, entry 5). Through discussion with the Zhu group, it was decided to try their developed conditions which would be published after this work was completed.^[134] This involved switching the copper source for Cu(OAc)₂·H₂O, using K₂CO₃ in its solid form as a base, and performing the reaction in methanol. These conditions led to a jump in the selectivity for the desired species, giving 45% bis(triazole) **195** (Table 16, entry 6). Upon reducing the quantity of base in the reaction to 1 equivalent (from 2), the proportion of bis(triazole) **195** increased further to 54% (Table 16, entry 7). Reducing the copper loading from 5 mol% to 1 mol% had a detrimental effect on the selectivity of the reaction, returning 64% unwanted mono(triazole) **156** and 27% of the unwanted alkyne coupling product **196** (Table 16, entry 8). Doubling the number of equivalents of benzyl azide in the reaction mixture led to the best observed product distribution, giving 64% of the desired bis(triazole) **195** species (Table 16, entry 9). Finally, addition of the base as a solution instead of a solid powder was trialled, but it was found that this did not affect the selectivity of the reaction; both the solid base and the base in solution gave 54% bis(triazole) **195** (Table 16, entries 7 and 10).



Entry	Base	Conc. of Base	Cu Source	Cu Loading	Azide equiv.	Solvent	Temp (°C)	% 156 ^a	% 195 _a	% 196 _a
1	Na ₂ CO ₃	2 M	CuSO ₄ /Cu Powder	1 equiv.	1	MeCN/Water	rt	60	32	8
2	Na ₂ CO ₃	2 M	CuSO ₄ /Cu Powder	1 equiv.	1	MeCN/Water	0	92	8	<1
3	Na ₂ CO ₃	2 M	CuSO ₄ /Cu Powder	1 equiv.	1	MeCN/Water	60	93	7	<1
4	Na ₂ CO ₃	4 M	CuSO ₄ /Cu Powder	1 equiv.	1	MeCN/Water	rt	51	40	9
5	K ₂ CO ₃	2 M	CuSO ₄ /Cu Powder	1 equiv.	1	MeCN/Water	rt	78	17	5
6	K ₂ CO ₃	2 equiv.	Cu(OAc) ₂ ·H ₂ O	5 mol%	1	MeOH	rt	28	45	27
7	K ₂ CO ₃	1 equiv.	Cu(OAc) ₂ ·H ₂ O	5 mol%	1	MeOH	rt	28	54	18
8	K ₂ CO ₃	1 equiv.	Cu(OAc) ₂ ·H ₂ O	1 mol%	1	MeOH	rt	64	9	27
9	K₂CO₃	1 equiv.	Cu(OAc)₂·H₂O	5 mol%	2	MeOH	rt	17	64	19
10	K ₂ CO ₃	2 M	Cu(OAc) ₂ ·H ₂ O	5 mol%	1	MeOH	rt	26	54	20

^a Ratio **156/195/196** determined by integration of benzylic resonances with the ¹H NMR spectra of the crude reaction mixture. All screening reactions were carried out once.

Table 16 Screening of various conditions in the synthesis of 5,5'-bis(triazoles)

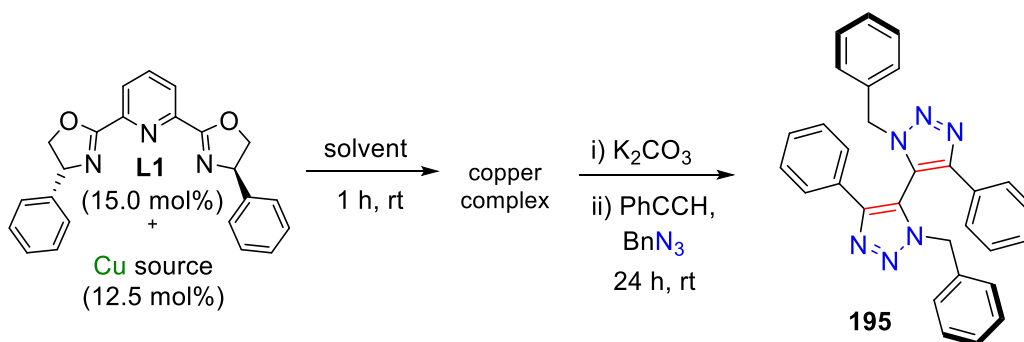
With optimised reaction conditions in hand for bis(triazole) synthesis, the purification of the bis(triazole) **195** was developed. It was found that the polarity of the mono(triazole) **156** and bis(triazole) **195** were very similar. This led to multiple failed attempts to carry out silica flash column chromatography. Both DCM/methanol and hexane/ethyl acetate, in both isocratic and gradient mixtures, were found to be ineffective in separating the triazole species. Therefore, reverse-phase C18 purification was targeted, and it was found that using automated reverse-phase chromatography, the mono and bis(triazolic) species could be separated. Following separation, the material was recrystallised from ethyl acetate and hexane to yield an analytically pure sample of bis(triazole) **195**.

Even though Burgess had reported that bis(triazole) **195** was stable towards rotation, no chiral HPLC separation conditions for the atropisomers had been reported for the compound. To test the hypothesis that one atropisomer could be favoured in an asymmetric click variant, chiral HPLC separation of the racemic bis(triazole) species **195** was needed. Taking the pure bis(triazole) **195** recovered after C18 purification, chiral HPLC conditions were screened. It was found that the two atropisomers could be successfully resolved using a Phenomenex Cellulose 1 stationary phase with 50:50 water/acetonitrile as the mobile phase. Pleasingly, it was found that the mono(triazole) **156** had a characteristically different retention time to that of the two peaks of the bis(triazole) **195**. This meant that screening could be carried out without the need for prior C18 separation of the mono and bis species.

Once the chiral HPLC separation conditions were in place, the asymmetric variant of the reaction could be attempted. It was decided that using conditions which had been found to achieve kinetic resolution of **94** (Section 2.1) and conditions which had given the best bis(triazole) ratio of those screened (Table 16) in combination with a (*R,R*)-PhPyBox ligand

L1 would give the best chance of seeing some level of enantioenrichment in addition to observing at least some bis(triazole) **195** (Table 17).

Table 17 Formation of 5,5'-bis(triazoles) under asymmetric conditions



Entry	Copper Source	Solvent	^a Ee 192 (%)
1	CuCl	MeOH	4
2	Cu(OAc) ₂ ·H ₂ O	MeOH	4
3	CuCl	Acetone	0
4	Cu(OAc) ₂ ·H ₂ O	Acetone	0
5	CuCl	2,5-Hexanedione	10
6	Control (isolated pure bis(triazole))		4

^aDetermined by chiral HPLC analysis of the reaction mixture following aqueous work up. Material identity determined by relative retention times compared with pure samples of bis(triazole) **195** and mono(triazole) **156**. All screening reactions were carried out once.

Chiral HPLC analysis of pure bis(triazole) **195** synthesised from conditions detailed in Table 16, entry 7, showed a small level of enantioenrichment (4% *ee*, Table 17, entry 6). When an asymmetric variant using methanol as a solvent was tested, enantioenrichments of 4% *ee* were determined (Table 17, entries 1 and 2), consistent with the control material. When the reaction was carried out in acetone, 0% *ee* was observed (Table 17, entries 3 and 4). Finally, when the reaction was carried out in 2,5-hexanedione (the best solvent for the KR of **94**) an enantioenrichment of 10% *ee* was observed (Table 17, entry 5).

From direct comparison of HPLC integrations of the bis(triazole) **195** and mono(triazole) **156**, it was observed that the reactions carried out in methanol contained a higher proportion of bis(triazole) compared to the mono(triazole). 2,5-Hexanedione gave the greatest enantioselectivity, but by the integration area of the bis(triazole) peaks compared to the mono(triazole) peak, it was shown that the dione gave an inferior ratio of mono to bis species compared with methanol or acetone.

The levels of enantioenrichment obtained in the formation of 5,5'-bis(triazole) **195** using PhPyBox-mediated conditions was disappointing. With only 10% *ee* afforded using the best previously developed condition for the KR of quaternary oxindole **94**. At this point, it was decided that this avenue of research should not be pursued further.

5.1.1 Summary

This section attempted to apply the reaction conditions developed for the KR of oxindole **94** to the asymmetric synthesis of 5,5'-bis(triazoles).^[136] Unfortunately, the levels of enantioenrichment obtained were low, with 10% *ee* in the best case.

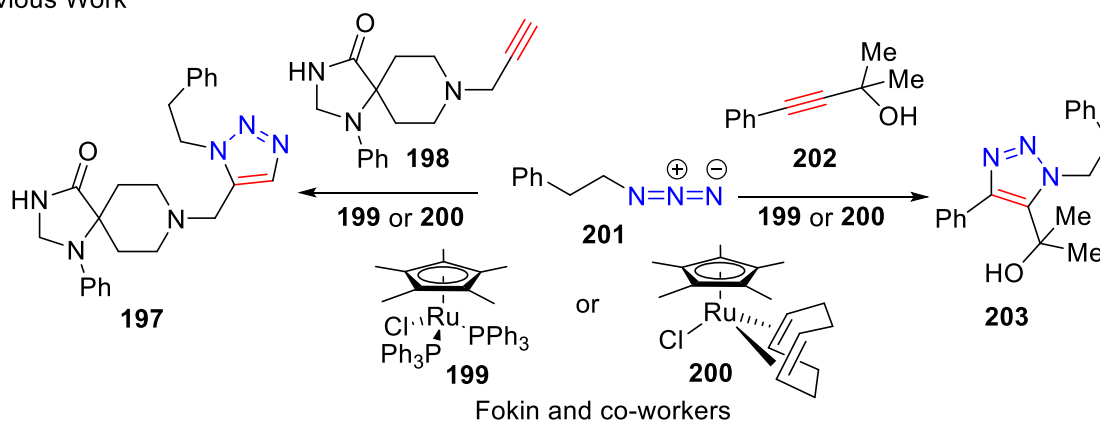
Experimental work in this section was carried out by the author of this thesis. The primary investigators were Dr John Fossey (UoB) and Dr Benjamin Buckley (LU).

5.2 *The Use of Ruthenium-Based Olefin Metathesis Catalysts in the Synthesis of 1,5-Triazoles*

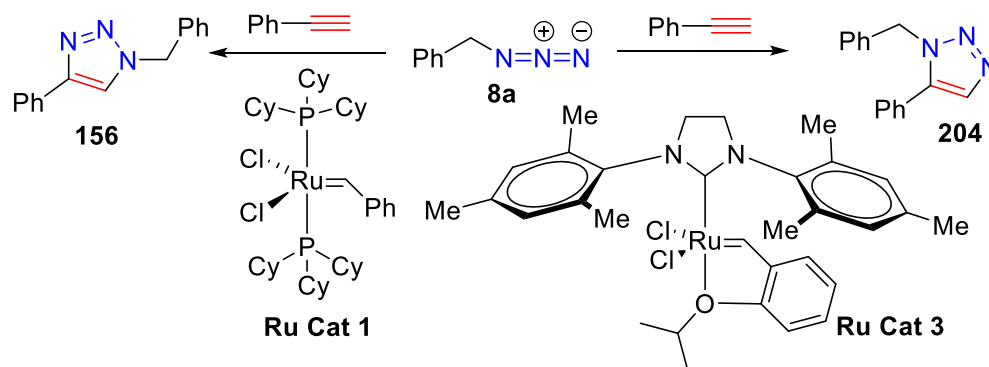
Ruthenium-based olefin metathesis catalysts based upon Grubbs' architectures^[137] have become a widely-utilised system for processes such as cross metathesis (CM),^[138] ring-opening metathesis (ROM),^[139] ring-closing metathesis (RCM)^[140] and ring-closing ene-yne metathesis (RCEYM).^[141] These catalysts have also been shown to have practical application

in other non-metathesis-based reactions. Cycloaddition reactions are one such class in which Grubbs-type ruthenium alkylidene catalysts have been applied. For example, [3 + 2] cycloaddition processes such as the intramolecular cycloaddition of alk-5-ynylidene-cyclopropanes by Mascarenas *et al.* have been successfully carried out using a Grubbs first-generation ruthenium carbene-based catalyst.^[142]

Previous Work



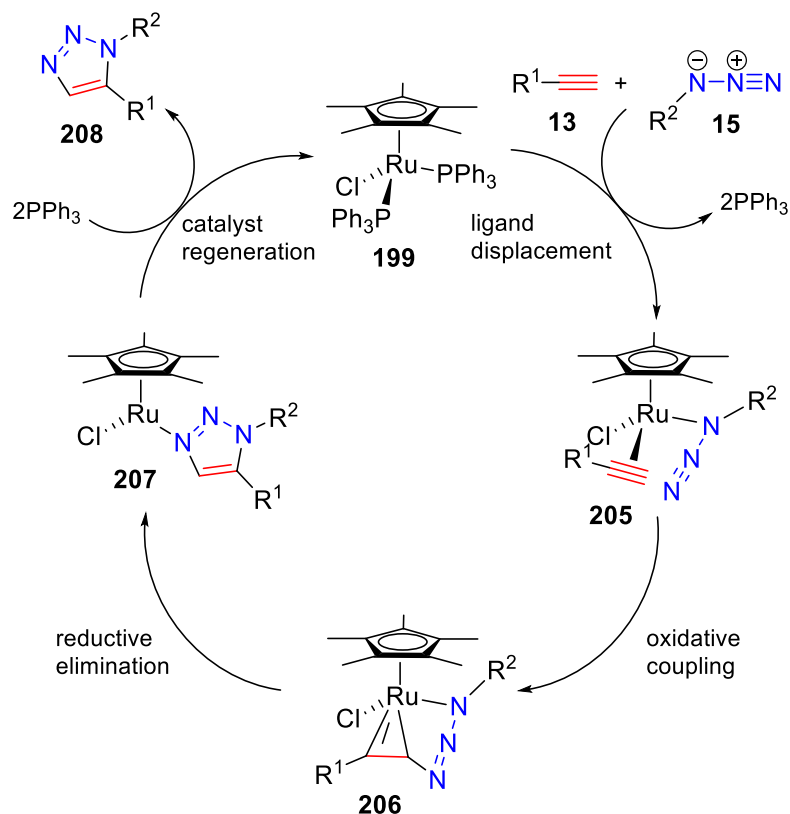
This Work



Scheme 68 Ruthenium-catalysed azide-alkyne cycloaddition reported by Fokin and co-workers (top).^[130] Work carried out here on the synthesis of triazoles utilising ruthenium alkylidene-based olefin metathesis catalysts (bottom).

Triazoles are a species which have been successfully synthesised *via* ruthenium-catalysed azide-alkyne cycloadditions (RuAACs). In 2008, Fokin and co-workers reported the selective synthesis of 1,5-disubstituted 1,2,3-triazoles utilising $\text{Cp}^*\text{RuCl}(\text{PPh}_3)_2$ **199** and $\text{Cp}^*\text{RuCl}(\text{COD})$ **200** catalysts (Scheme 68, Top). This reaction was shown to deliver 1,5-disubstituted triazoles in good to excellent yield on a range of terminal and internal alkynes.

This methodology has been used by many researchers to deliver triazoles for applications such as formation of nucleoside analogues,^[143] synthesis of heterocyclic libraries^[144] and creation of novel ligand architectures.^[145]

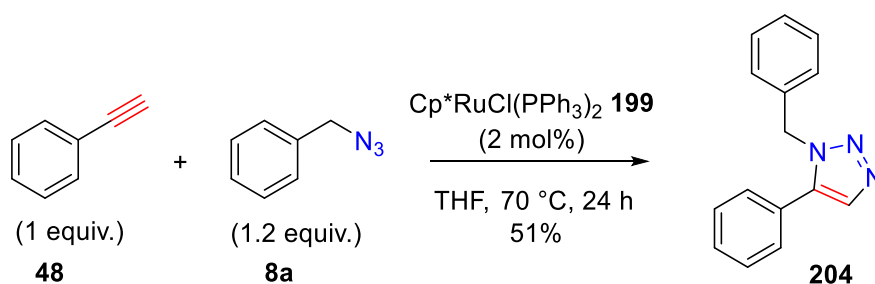


Scheme 69 Proposed catalytic cycle of the RuAAC reaction, Fokin and co-workers^[130]

The RuAAC is amenable to internal and terminal alkynes; this is in sharp contrast to its copper-catalysed equivalent, in which only terminal alkynes are applicable. Therefore, the RuAAC is postulated to proceed through different catalytic intermediates than the copper-mediated reaction does. In 2008, Fokin and co-workers proposed a catalytic cycle for this reaction (Scheme 69).^[130] To account for the reaction's ability to tolerate internal alkynes, they hypothesised that the ruthenium centre must first intercept the alkyne in a π -coordinating fashion **205**. Ruthenium is known to do this during the cyclotrimerisation of alkynes.^[146] In this case, however, before the trimerisation process can occur, the ruthenium is intercepted by

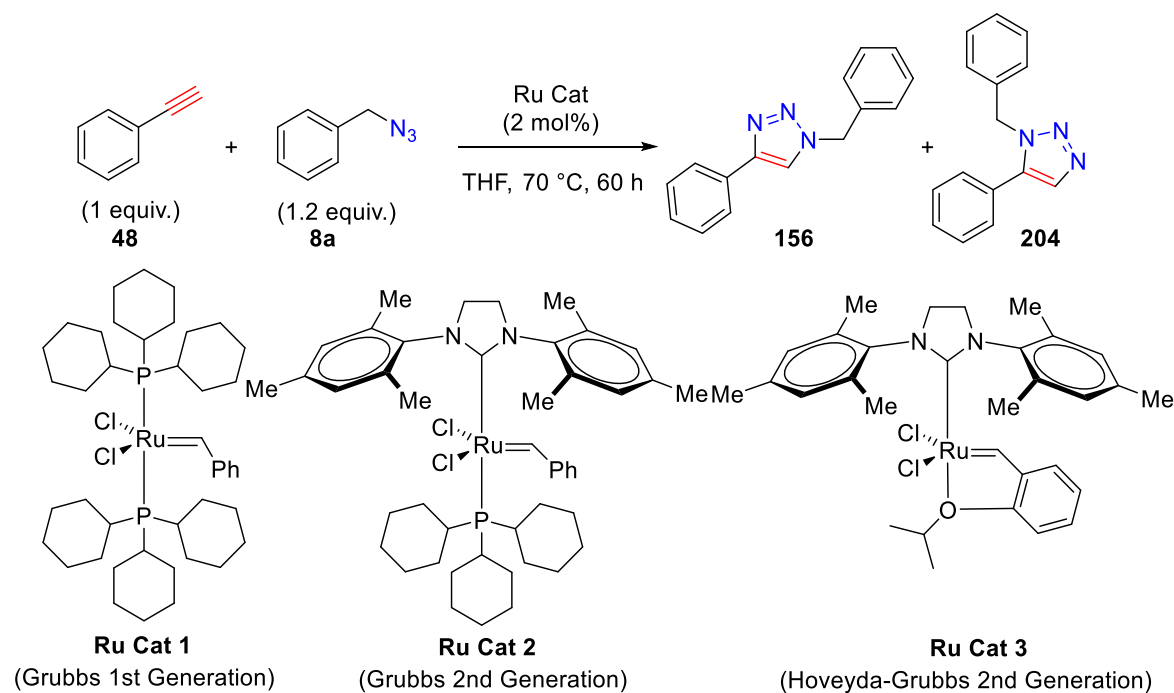
an azide, which displaces another ligand. The azide and alkyne can then undergo oxidative coupling to form ruthenacycle **206**. The formation of this ruthenacycle is the step in which the regioselectivity of the reaction occurs. The new C-N bond is formed between the less electronegative (and in addition, the less sterically demanding) carbon of the alkyne and the distal nitrogen of the azide to form complex **207**. From this position the ruthenacycle undergoes reductive elimination to form the 1,5-triazole, which is then subsequently replaced by a ligand in solution, giving the desired triazolic product **208** and regenerating the catalyst.

During Fokin and co-workers' reaction screening, a range of ruthenium catalysts were tested.^[130] However, Grubbs-type olefin metathesis catalysts were not trialled. Due to olefin metathesis being a well-established field, the ruthenium catalysts used are often commercially available and there are many different catalyst architectures to choose from. Looking at the availability of ruthenium sources in the laboratory, it was decided to test whether olefin metathesis catalysts could give catalytic turnover in a RuAAC reaction, and if different ligand structures could influence the ratio of 1,4- to 1,5-triazole formed.



Scheme 70 Repetition of literature reaction to yield triazole **204**

The literature reaction reported by Fokin and co-workers was repeated (Scheme 70). The $\text{Cp}^*\text{RuCl}(\text{PPh}_3)_2$ catalyst **199** gave solely the 1,5-disubstituted 1,2,3-triazole **204** in 51% isolated yield.

Table 18 Screening of olefin metathesis catalysts in a RuAAC reaction

Entry	Catalyst	156 : 204 ^a	Conv. (%) ^b
1	Ru Cat 1	67:33	6
2	Ru Cat 2	79:21	12
3	Ru Cat 3	20:80	53
4	None	54:46	2

^a Determined by relative integration of benzylic resonances of the two triazolic products within the ¹H NMR spectrum of the crude reaction mixture. ^b Determined by relative integration of the combined product benzylic resonances to the remaining benzyl azide benzylic resonance within the ¹H NMR spectrum of the crude reaction mixture. All screening reactions were carried out once.

The ¹H NMR spectra of 1,5-substituted triazole **204** and 1,4-substituted triazole **156** were characteristically different (chemical shift of the benzylic protons within the ¹H NMR spectra of the 1,4- and 1,5- triazoles are observed at 5.58 ppm and 5.55 ppm, respectively). Therefore, during catalyst screening, ¹H NMR integration of the two benzylic positions within the spectrum of the crude reaction mixture would give the product distribution. Whilst integration of combined products with the remaining benzylic resonance corresponding to benzyl azide at 4.18 ppm would give the reaction conversion.

The preliminary results detailed in Table 18 were encouraging. **Ru Cat 1** and **2** both favoured formation of the 1,4-triazole **156** in ratios of 67:33 and 79:21, respectively (Table 18, entries 1 and 2), whilst **Ru Cat 3** favoured 1,5-triazole **204** by 20:80 (Table 18, entry 3). The regioisomeric selectivity of all the olefin metathesis catalysts screened was significantly different from the thermally-promoted reaction, which gave a ratio of 54:46 **156:204** (Table 18, entry 4).

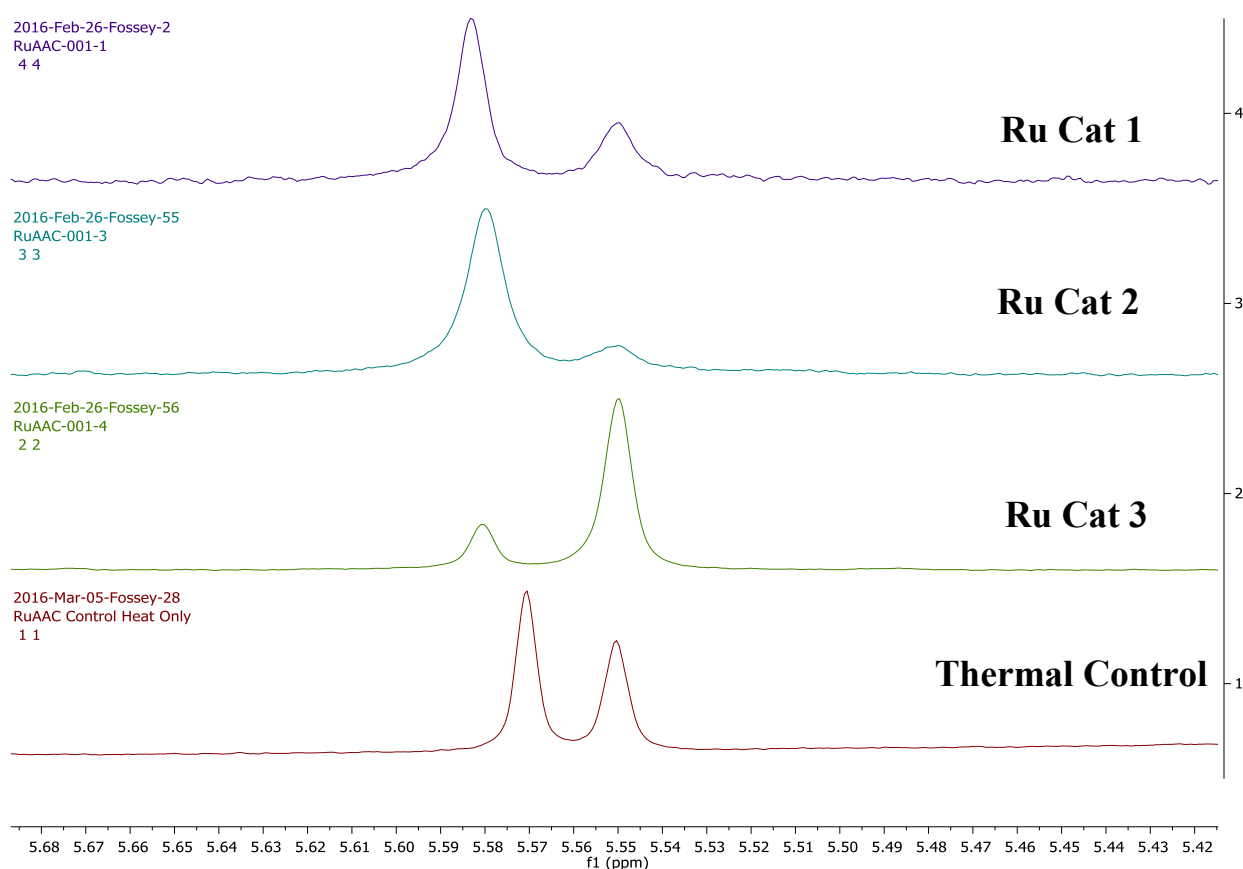
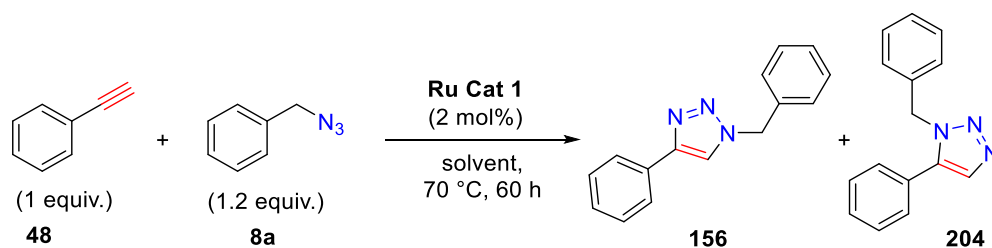


Figure 39 ¹H NMR stacked spectra showing benzylic resonances of compounds **156** and **204**. Resonance at 5.50 ppm is attributed to compound **204** whilst the resonance at 5.57 ppm is attributed to compound **156**.

As shown in Figure 39, the difference observed in the benzylic regions of the ¹H NMR spectra of the crude screening reaction mixtures was stark. It had been shown that Grubbs-type olefin metathesis catalysts could have an impact on the regiochemical selectivity of a RuAAC reaction.

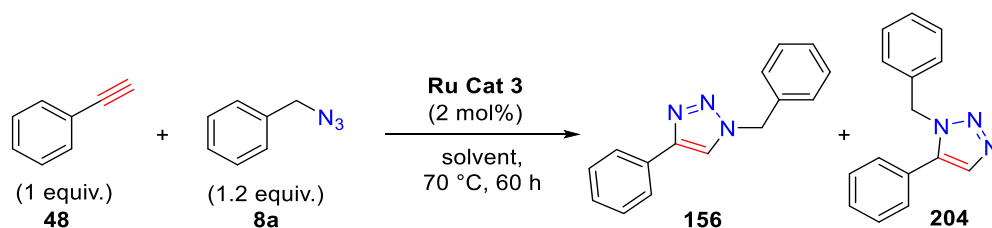
Table 19 Solvent screening of **Ru Cat 1** in a RuAAC reaction

Entry	Solvent	156:204 ^a	Conv. (%) ^b
1	THF	67:33	6
2	Acetonitrile	100:0	79
3	Methanol	100:0	26
4	DMSO	88:12	9
5	EtOAc	92:8	26

^a Determined by relative integration of benzylic resonances of the two triazolic products within the ¹H NMR spectrum of the crude reaction mixture. ^b Determined by relative integration of the combined product benzylic resonances to the remaining benzyl azide benzylic resonance within the ¹H NMR spectrum of the crude reaction mixture. All screening reactions were carried out once.

It was hoped that the regioselectivity, as well as the conversion, could be improved by reaction condition screening. Due to the amounts of the various catalysts available within the laboratory combined with the fact that **Ru Cat 1** and **2** had both shown broadly the same regioselectivity, it was decided that **Ru Cat 1** and **Ru Cat 3** should be the focus of optimisation. Solvent screening was carried out using **Ru Cat 1**, and it was observed that solvent had a marked effect on both regioselectivity and conversion.

In all the solvents tested, the reaction favoured the 1,4-regioisomer **156**. Acetonitrile and methanol gave solely **156** (Table 19, Entries 2 and 3), and DMSO and EtOAc both highly favoured 1,4-triazole **156**, giving selectivities of 88:12 and 92:8, respectively (Table 19, Entries 4 and 5). Acetonitrile was seen to give the best reaction conversion of 79%, based upon ¹H NMR integration values.

Table 20 Solvent screening of Ru Cat 3 in a RuAAC reaction

Entry	Solvent	156:204 ^a	Conv. (%) ^b
1	THF	20:80	53
2	Acetonitrile ^c	26:74	12
3	Acetonitrile ^d	15:85	17
4	Acetonitrile ^e	36:64	12
5	Methanol ^d	91:9	17
6	DCE	65:35	8

^a Determined by relative integration of benzylic resonances of the two triazolic products within the ¹H NMR spectrum of the crude reaction mixture. ^b Determined by relative integration of the combined product benzylic resonances to the remaining benzyl azide benzylic resonance within the ¹H NMR spectrum of the crude reaction mixture. ^c Dried over 4 AMS. ^d Taken from a solvent purification system to remove water. ^e Taken direct from Winchester without drying. All screening reactions were carried out once.

Solvent screening was also carried out using Hoveyda-Grubbs 2nd generation (**Ru Cat 3**) catalyst. Focusing on acetonitrile, it was found that the level of water present in the solvent could have a dramatic impact on the ratio of products. Acetonitrile with no prior drying was found to give the worst regioselectivity at 36:64 **156:204** (Table 20, entry 4) whilst acetonitrile dried with molecular sieves or from a solvent purification system gave ratios of 26:74 and 15:85, respectively (Table 20, entries 2 and 3). Surprisingly, it was found that when methanol or DCE were used as solvents, the regioselectivity of the reaction was reversed. Ratios of 91:9 and 65:35 (1,4:1,5) were noted (Table 20, entries 5 and 6). Overall THF showed the best conversion of those screened (Table 20, entry 1).

Taking the reaction which had given the best conversion (Table 19, Entry 2), isolation of the 1,5-disubstituted triazole **204** was attempted. Upon chromatographic separation, compound

204 was successfully isolated, but only 5 mg of product was obtained, giving an isolated yield of 4%. The isolated yield was not improved over multiple repeats. Looking closer at the ^1H NMR spectra of the crude reaction mixtures, it was noted that the integration across the aromatic region was not consistent with the integration of the benzylic region. In addition, there was a singlet at a chemical shift consistent with an aldehyde being present (10.0 ppm), which led to the hypothesis that one or more by-products were being formed. It was also postulated that these by-products could be volatile species, leading to such poor overall mass recovery.

The aldehyde-containing by-product was identified as benzaldehyde **115**. Previous researchers in the area have found that ruthenium catalysts mixed with benzyl azides can lead to a myriad of products. For example, Severin and co-workers showed that ruthenium complexes in anhydrous solvents in the presence of benzylic azides can form mixtures of hydrobenzamides **209**, imines **210** and nitriles **211** (Figure 40).^[147]

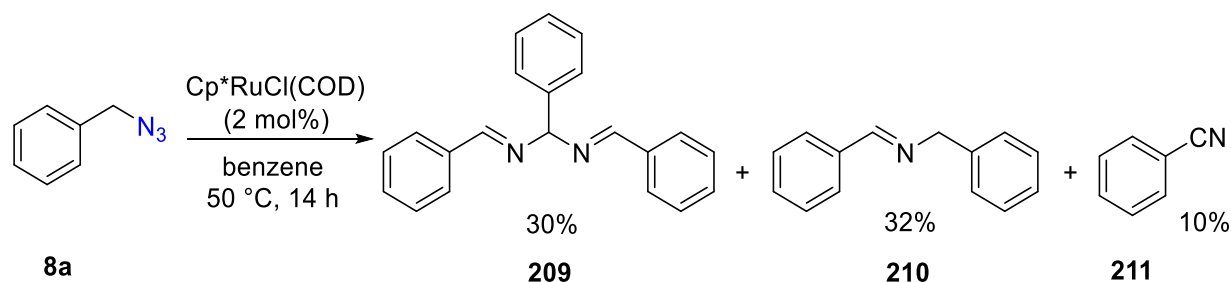


Figure 40 Reactivity of benzyl azides with ruthenium catalysts, Severin and co-workers^[147]

Severin's study also showed that aldehydes could be formed if non-anhydrous solvents were employed (Figure 41).^[147] This study helped explain the complex aromatic regions which were being observed with the RuAAC reaction, as well as the fact that benzaldehyde was being formed as a by-product.

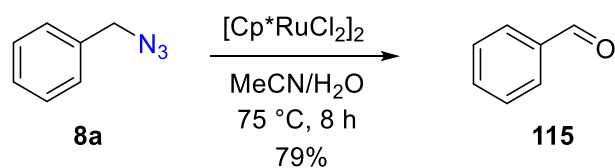


Figure 41 Reactivity of benzyl azide with ruthenium complexes in the presence of water, Severin and co-workers^[147]

At this point, it was decided that due to the limited time available within the laboratory this project would not be pursued further.

One final intriguing observation was made: Fokin had reported that $\text{Cp}^*\text{RuCl}(\text{PPh}_3)_2$ could efficiently convert internal alkynes into 1,4,5-trisubstituted triazoles. When **Ru Cat 3** was employed in the reaction of diphenyl acetylene with benzyl azide, no turnover was observed and the alkyne starting material was recovered (Figure 42).

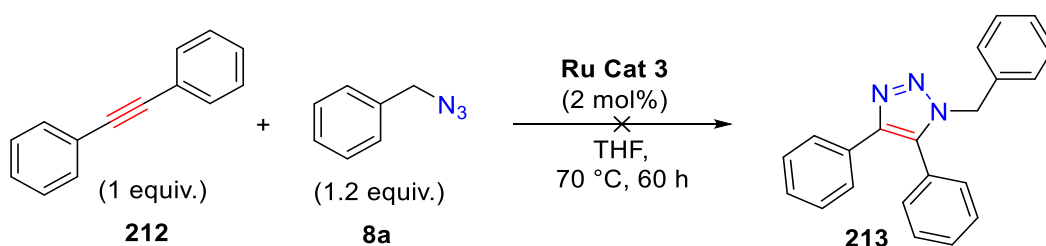


Figure 42 Attempted reaction of an internal alkyne with benzyl azide

This implies that the metathesis catalyst-mediated reaction does not follow the same catalytic intermediates as the catalyst developed by Fokin. If internal alkynes do not lead to any catalytic turnover, then there are two possibilities. One possibility is that upon interception of an alkyne or azide by the ruthenium centre, an unreactive intermediate is formed. The ruthenium alkyne complex formed must then collapse, and the alkyne is recovered after workup. Alternatively, the ruthenium catalyst could be incapable of successfully intercepting the internal alkyne, and thus no reaction proceeds. Ruthenium olefin metathesis catalysts have previously been shown to be able to interact successfully with internal alkynes,^[148] so it is more likely that unreactive intermediates are being formed.

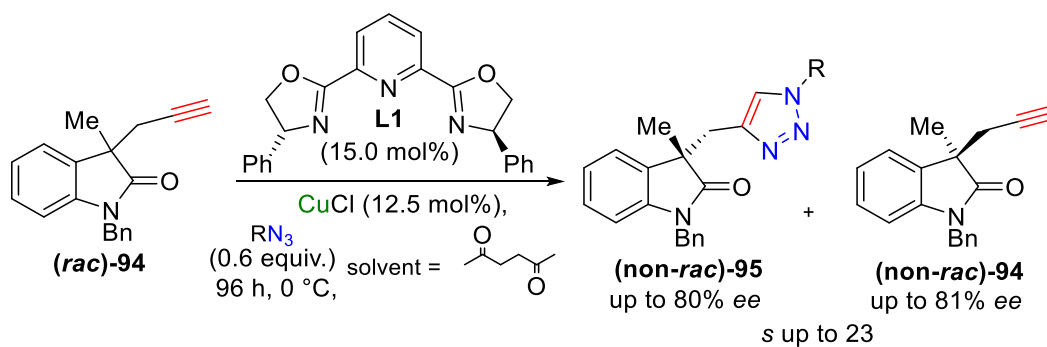
5.2.1 Summary

This section detailed preliminary studies into the use of ruthenium-based olefin metathesis catalysts in RuAAC reactions.^[149] It was demonstrated that different ruthenium complexes could give different ratios of 1,4- and 1,5-triazoles. Solvents have a wide-ranging effect on the regioselectivity and conversion of the reaction. Eventually it was found that benzylic azides could lead to a wide range of by-products and that ¹H NMR integration was not an accurate representation of reaction conversion. Internal alkynes did not react. Perturbing the formation of by-products was found to be difficult, and due to time constraints, the project was not progressed further. It is hoped that these preliminary results can be built upon, and that an efficient RuAAC reaction utilising olefin metathesis catalysts will be developed.

Experimental work in this section was carried out jointly between the author of this thesis and Daniel Payne (UoB). The primary investigator was Dr John Fossey (UoB).

6 Conclusion and Future Work

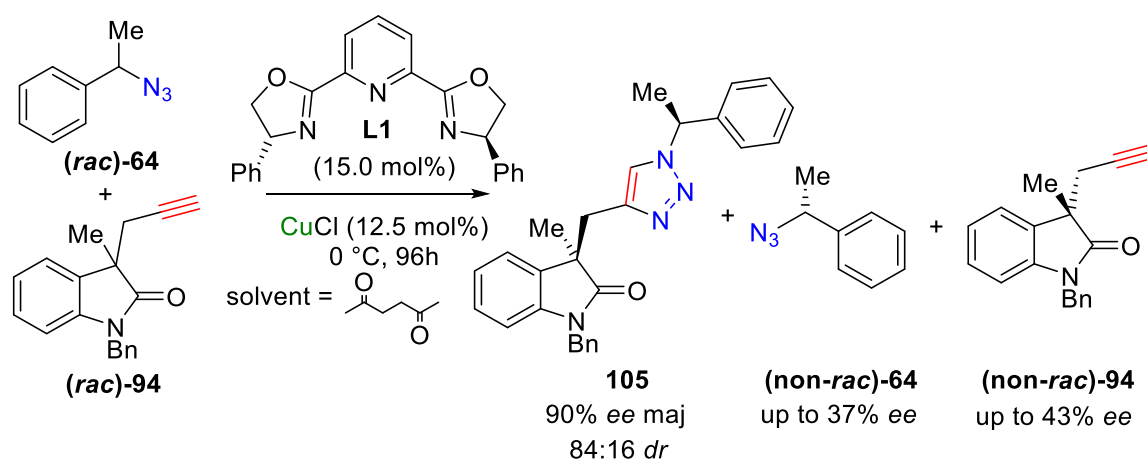
The CuAAC reaction has been successfully employed in a variety of ways throughout this thesis. The first examples of kinetic resolution of alkynes were demonstrated utilising CuAAC reactions. The selectivity of the resolution of a quaternary oxindole was shown to be high, with $s = 22.1 \pm 0.5$ measured (Scheme 71). A range of benzylic azides was shown to be applicable within the resolution. Chiral HPLC showed that a quaternary oxindole alkyne in excess of 80% *ee* was recoverable and triazoles of up to 80% *ee* were obtainable. Further exploration of the substrate scope would be interesting to carry out. For instance, it is unclear why oxindole frameworks are so effective in asymmetric CuAAC chemistry.^[33] Utilising the same reaction conditions using γ -lactam equivalents would probe the need for the fused aromatic structure. Additionally, investigating indole derivatives towards KR would show whether the carbonyl moiety plays any significant role in selectivity.



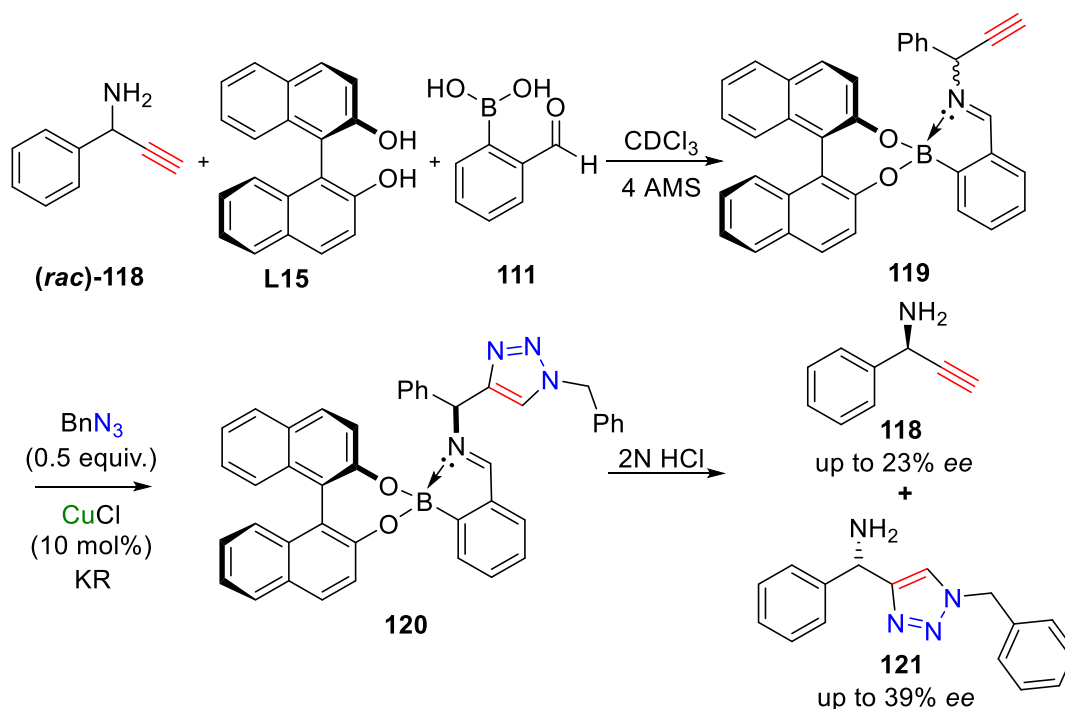
Scheme 71 Kinetic resolution of quaternary oxindole **94**

Utilising the same reaction conditions as in the KR of quaternary oxindole alkyne **94**, a novel kinetic resolution process was developed. It was shown that the developed KR conditions were applicable to both alkynes and azides, allowing both chiral components to be resolved in a single process (Scheme 72). The reaction was found to give highly enantioenriched triazole diastereoisomers with 90% *ee* measured for the major diastereoisomer. The recovered alkyne

and azide were found to have more modest enantioenrichments of up to 43% *ee* and 37% *ee*, respectively. This reaction is unique to other types of kinetic resolution, as two chiral components can be resolved at the same time, giving it advantages over classical KR. The scope of this reaction is, at present, unknown due to the fact this project was designed as a proof of principle; two previously reported substrates were chosen to give the best chance of some enantioenrichment being observed. Probing the scope in both the azide and the alkyne substrates would be interesting to carry out. In addition, this first example of simultaneous kinetic resolution utilised the CuAAC, but other reactions could use the principle to create a myriad of enantioenriched diastereoisomers and efficiently allow access to a wide range of enantioenriched and enantiopure chiral building blocks.



Scheme 72 Simultaneous kinetic resolution of alkyne **92** and azide **62**



Scheme 73 Kinetic resolution of primary amine alkynes using the Bull-James assembly

The final kinetic resolution reported within this thesis detailed the successful resolution of a primary amine alkyne (Scheme 73). Primary amine **118** was found to be incompatible with the conditions developed for the oxindole alkyne **94**. Applying the Bull-James three-component boronic acid-based assembly technique as a way of perturbing the reactivity of the primary amine allowed the development of a novel dual chiral auxiliary and chiral shift reagent. Selectivity was moderate at $s = 4.1$, and the best recovered alkyne ee was 23%. However, the ability to directly measure the ee of both the remaining alkyne and the formed triazole by ^1H NMR spectroscopy gives this methodology an operational simplicity compared with chiral HPLC method development. Again, the scope of this resolution needs exploration into other primary amine alkynes, and in addition, diol alkynes could also be employed using this procedure. This reaction also utilised the CuAAC, but again, it is easy to envisage that the principle behind this resolution could be applied to a multitude of asymmetric transformations. In fact, this methodology may prove useful in other transformations which are incompatible with primary amine substrates.

Throughout all of the developed kinetic resolution methodology, the base mechanistic understanding of selectivity has not been established. More work is required here to probe how asymmetry is engendered in these reactions. As seen in the debate over the catalytic cycle of the non-asymmetric CuAAC reaction, the nature of catalysis is still not clear. The complex nature of copper acetylides and their clusters mean that modelling of catalytic transition states is a difficult job. In this thesis, there have not been any proposed transition states; this is due to a base lack of knowledge of the mechanistic pathways these reactions can take. Thus far, the examples of asymmetric “click” chemistry which have been reported here and within the literature do not appear to have many features in common. Ligands which work well for certain substrates are ineffective for others, solvents and reaction protocols can have drastic effects on the overall reaction outcome, and little is known about why any of this is the case. The work of people such as Panera in combination with NLE studies have given some insight into PyBox-copper dimer complexes,^[38, 41, 72] but whether these structures are present in solution and which species is responsible for asymmetric induction is not clear. Deeper, more fundamental mechanistic questions need to be asked of asymmetric CuAAC reactions to make them universal to a wide range of substrates. Further knowledge of how the asymmetry is induced during the CuAAC could lead to the directed synthesis of bespoke new ligand structures. Hopefully, with more fundamental studies, the asymmetric CuAAC can be more widely applicable and utilised in line with other common metal-mediated asymmetric methodologies.

Other work in this thesis detailed the synthesis of novel triazolium salts. This probed the steric requirements around a triazole ring to induce atropisomerism. Several atropisomeric salts were formed, in the case where prototriazoles were used, VT NMR spectroscopic studies proved that atropisomeric stability of **166** was good^[111] even at elevated temperature. This

salt, however, was found to be inseparable *via* chiral HPLC methods. Iodotriazoles were then targeted, and the enantiomeric separation of this atropisomeric species was found to be straightforward by chiral HPLC. However, the iodotriazole **182** was found not to be atropisomerically stable at room temperature. It was found that over time an enantioenriched sample would racemise at room temperature. Other salts were also synthesised, but none were found to display atropisomerism. Interestingly, one (**178**) was found to be a bench-stable crystalline solid, a rarity for triazolium salts. Due to time constraints, these triazolium species were not tested successfully within an asymmetric catalytic reaction. There are two avenues to explore in this regard: metal-catalysed transformations (e.g. palladium cross coupling^[111] or olefin metathesis^[150]) and organocatalysis (e.g. benzoin condensation^[151] or Stetter reaction^[152]). Both forms of catalysis have been shown to be applicable to chiral triazolium salts, and both would be good tests for these novel carbene precursors. In addition, there are possibilities to circumvent the need for separation of enantiomers. For example, forming the triazole core through an asymmetric CuAAC reaction or alkylation with a chiral alkylating agent.

Finally, two smaller projects were outlined, both reporting preliminary results. Asymmetric formation of 5,5'-bis(triazoles) was found to be difficult to achieve with the greatest enantioenrichment obtained being only 10% *ee*. In addition to selectivities being poor, the product ratios were difficult to control, with mono(triazoles) observed as the major products under many (even literature) reaction conditions. The synthesis of single atropisomers of 5,5'-bis(triazoles) is of interest to researchers wishing to build new chiral ligands. However, the conditions applied here were not successful at garnering high *ee* materials.

Grubbs-type olefin metathesis catalysts were shown to have some influence on the ratios of 1,4- to 1,5-disubstituted 1,2,3-triazoles within a RuAAC reaction. Even though it was shown

that different olefin metathesis catalysts could influence the regiochemical outcome of triazole formation, the isolated yields were extremely poor. It appears as if ruthenium catalysts can form multiple by-products when they interact with benzyl azide (such as volatile aldehydes). Future work in this area would be to try to perturb the formation of these by-products to increase the isolated yields to synthetically useful levels. Looking further, the ability to carry out cycloaddition processes and metathesis processes simultaneously would be a particularly interesting line to pursue.

7 Appendix 1 Experimental

7.1 General

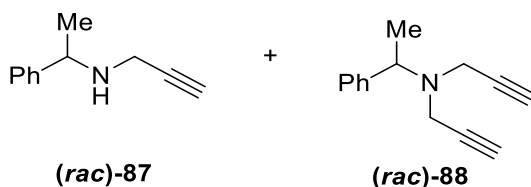
Reagents were used as purchased from suppliers without further purification; in cases where anhydrous solvents were required these were dried using a solvent purification system (SPS) which is monitored by Karl-Fisher titrations for water levels (THF 20-40 ppm H₂O, DCM 4.0-8.0 ppm H₂O, MeCN 0.5-3.0 ppm H₂O). 2-Formylphenylboronic acid was recrystallised from chloroform before use. ¹H NMR spectra were recorded at 300, 400 and 600 MHz using Bruker AVIII 300 NMR (UoB), Bruker AVIII 400 NMR (UoB), Varian DirectDrive 400 NMR (UT Austin) and Varian DirectDrive 600 NMR (UT Austin) spectrometers. ¹³C NMR experiments were carried out on a Bruker AVIII 400 NMR (UoB) and Varian DirectDrive 400 NMR (UT Austin) spectrometers recorded at 101 MHz; in cases where it was required 2D NMR techniques were used to confirm compound identity. ¹⁹F NMR spectra were recorded at 282 MHz using a Bruker AVIII 300 NMR spectrometer (UoB). ¹¹B NMR spectra were recorded at 192 MHz on a Varian Direct Drive 600 NMR spectrometer (UT Austin). All coupling constants are reported in Hertz (Hz). ¹H NMR chemical shifts are reported in ppm relative to TMS (δ 0.00) (UoB) or chloroform (δ 7.26) (UT Austin) and ¹³C NMR chemical shifts relative to chloroform (δ 77.36). Where diastereoisomers are reported the diastereomer ratio is given from the corresponding ¹H NMR spectrum and the total number of protons reported is equal to a single diastereomer of said compound. Reactions carried out at low temperatures were cooled using a Lab Plant Cryoprobe or dry ice / acetone bath on a case by case basis. Melting points were carried out in triplicate and an average of the values taken and reported as a range using a Stuart SMP10 (UoB) melting point apparatus. IR spectra were recorded on a PerkinElmer 100FT-IR spectrometer (UoB) at room temperature using ATR.

Optical rotations were recorded on a polar 2001 Automatic Polarimeter (UoB). Measurements of each sample were recorded three times and used as an average. HPLC analysis was carried out using Agilent 1260 Infinity (UoB and UT Austin) and Shimadzu LC2010 (UoB) HPLC systems. Traces were recorded at eight UV wavelengths 210, 214, 230, 250, 254, 260, 273 and 280 nm. Enantiomeric excess calculations were carried out using the supplied traces recorded at 254 nm. GC analysis was carried out on a Varian 430-GC (UoB) using a Chirasil-Dex CB chiral column using a UV detector. Column chromatography was carried out using a Combiflash Rf 200i (UoB) and column traces were recorded at two UV wavelengths (254 nm and 280 nm).

7.2 Experimental for Chapter 2

7.2.1 Synthesis

Synthesis of *N*-(1-phenylethyl)prop-2-yn-1-amine (**87**)



A mixture of (*rac*)- α -methylbenzylamine (0.91 g, 0.97 mL, 7.50 mmol), propargyl bromide (1.06 g, 0.79 mL, 7.40 mmol) and potassium carbonate (1.26 g, 9.12 mmol) in acetonitrile (15 mL) was stirred at rt for 3 h. The resulting mixture was filtered through celite and concentrated under reduced pressure. The resulting residue was purified by flash column chromatography hexane/EtOAc 20:1 to give compound **87** and compound **88** as yellow oils in 63% (0.74 g) and 9% (0.13 g) yields, respectively.

Characterisation data were in agreement with the reported literature values.^[153] Compound **87**

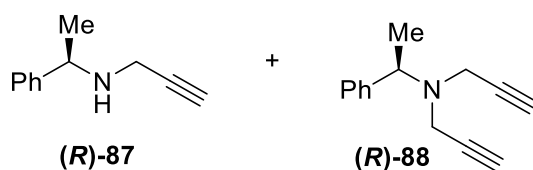
¹H NMR (300 MHz, CDCl₃) δ 7.36 – 7.21 (m, 5H, Ar-*H*), 4.00 (q, *J* = 6.6, 1H, *CH*), 3.24

(ABX, $\Delta\delta_{AB} = 0.19$, $J = 17.1$, 2.4, 2H, CH_2), 2.20 (app t, $J = 2.4$, 1H CCH), 1.50 (br s, 1H, NH), 1.35 (d, $J = 6.6$, 3H, CH_3); ^{13}C NMR (101 MHz, $CDCl_3$) δ 144.5, 128.5, 127.2, 126.9, 82.3, 71.3, 56.4, 35.9, 24.0; MS ESI⁺ m/z 160.1 ($[M+H]^+$, 9%), 118.1 (74), 105.1 (100); IR ν_{max} (ATR)/ cm^{-1} 3292, 3028, 2964; GC (CP-Chirasil-Dex CB), FID, $t(R) = 22.4$ min, $t(S) = 22.6$ min.

Characterisation data were in agreement with the reported literature values.²⁰¹ Compound **88** 1H NMR (300 MHz, $CDCl_3$) δ 7.87 – 6.80 (m, 5H, Ar-H), 3.64 (q, $J = 6.6$, 1H, CH), 3.49 (d, $J = 2.4$, 4H, CH_2), 2.22 (app t, $J = 2.3$, 2H, CCH), 1.38 (d, $J = 6.6$, 3H, CH_3); ^{13}C NMR (101 MHz, $CDCl_3$) δ 144.31, 128.62, 127.34, 79.21, 72.86, 60.78, 39.83, 21.64; MS ESI⁺ m/z 198.1 ($[M+H]^+$, 17%), 118.1 (58, $[M-(CH_2CCH)_2]^+$), 105.1 (100, $[M-C_8H_6N]^+$).

Only eight of the expected nine carbon environments were observed for compound **88** literature also only reports eight carbon environments.²⁰¹ Due to this agreement with literature values the identity of **88** was confirmed.

Synthesis of (*R*)-*N*-(1-phenylethyl)prop-2-yn-1-amine ((*R*)-**87**)



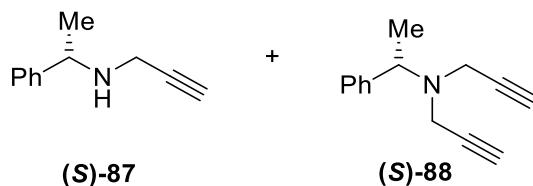
A mixture of (*R*)-(+)- α -methylbenzylamine (1.82 g, 1.94 mL, 15.0 mmol), propargyl bromide (2.12 g, 1.58 mL, 14.8 mmol) and potassium carbonate (2.04 g, 14.8 mmol) in acetonitrile (15 mL) was stirred at rt for 3 h. The resulting mixture was filtered through celite and concentrated under reduced pressure. The resulting residue was purified by flash column chromatography hexane/EtOAc 20:1 to give compound (*R*)-**87** and compound (*R*)-**88** as yellow oils in 56% (1.30 g) and 3% (0.08 g) yields, respectively.

(R)-87 ^1H NMR (300 MHz, CDCl_3) δ 7.33 – 7.21 (m, 5H Ar-*H*), 3.99 (q, $J = 6.6$, 1H, CH), 3.22 (ABX, $\Delta\delta_{\text{AB}} = 0.19$, $J = 17.1$, 2.4, 2H, CH_2), 2.19 (app t, $J = 2.4$, 1H, CCH), 1.33 (d, $J = 6.6$, 3H, CH_3); ^{13}C NMR (101 MHz, CDCl_3) δ 144.52, 128.55, 127.24, 126.94, 82.38, 71.40, 56.34, 35.92, 24.03; IR ν_{max} (ATR)/ cm^{-1} 3293, 3028, 2964; MS ESI $^+$ m/z 355.2 (100%), 317.2 (46), 160.1 (15, $[\text{M}+\text{H}]^+$), 118.1 (86), 105.1 (59); HRMS ESI $^+$ Calculated for $\text{C}_{11}\text{H}_{14}\text{N}^+$ = 160.1121 Found = 160.1126; $[\alpha]_{\text{D}}^{290} = -128.8^\circ$ ($c = 1$, CH_2Cl_2); GC (CP-Chirasil-Dex CB), FID, $t = 22.4$ min.

(R)-88 ^1H NMR (300 MHz, CDCl_3) δ 7.41 – 7.29 (m, 5H, Ar-*H*), 3.69 (q, $J = 6.6$, 1H, CH), 3.54 (d, $J = 2.4$, 4H, CH_2), 2.27 (t, $J = 2.3$, 2H, CCH), 1.43 (d, $J = 6.6$, 3H, CH_3); ^{13}C NMR (101 MHz, CDCl_3) δ 144.36, 128.65, 127.36, 79.24, 72.95, 60.80, 39.87, 21.70; MS ESI $^+$ m/z 198.1 ($[\text{M}+\text{H}]^+$, 13%), 118.1 (43), 105.1 (100); HRMS ESI $^+$ Calculated for $\text{C}_{14}\text{H}_{16}\text{N}^+$ = 198.1283 Found = 198.1282.

Eight of an expected nine carbon environments were observed for **(R)-88** this was consistent with observations made for compound **88**.

Synthesis of (*S*)-*N*-(1-phenylethyl)prop-2-yn-1-amine ((*S*)-**87**)



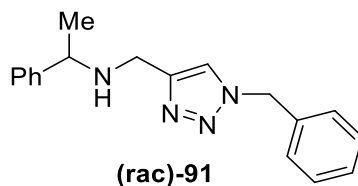
A mixture of (*S*)-(-)- α -methylbenzylamine (1.82 g, 1.94 mL, 15.0 mmol), propargyl bromide (2.12 g, 1.58 mL, 14.8 mmol) and potassium carbonate (2.04 g, 14.8 mmol) in acetonitrile (15 mL) was stirred at rt for 3 h. The resulting mixture was filtered through celite and concentrated under reduced pressure. The resulting residue was purified by flash column chromatography hexane/EtOAc 20:1 to give compound (*S*)-**87** and compound (*S*)-**88** as yellow oils in 67% (1.57 g) and 11% (0.32 g) yields, respectively.

(S)-87 ^1H NMR (300 MHz, CDCl_3) δ 7.35 – 7.19 (m, 5H, Ar-*H*), 3.99 (q, $J = 6.6$, 1H, *CH*), 3.22 (ABX, $\Delta\delta_{\text{AB}} = 0.19$, $J = 17.1$, 2.4, 2H, CH_2), 2.19 (app t, $J = 2.4$, 1H, *CCH*), 1.50 (s, 1H, *NH*), 1.33 (d, $J = 6.6$, 3H, CH_3); ^{13}C NMR (101 MHz, CDCl_3) δ 144.52, 128.55, 127.24, 126.94, 82.38, 71.40, 56.34, 35.92, 24.03; IR ν_{max} (ATR)/ cm^{-1} 3293, 3028, 2964; $[\alpha]^{290}_{\text{D}} = +148.8^\circ$ ($c = 1$, CH_2Cl_2); MS ESI^+ m/z 160.1 ($[\text{M}+\text{H}]^+$, 10%), 118.1 (100), 105.1 (100); HRMS ESI^+ Calculated for $\text{C}_{11}\text{H}_{14}\text{N}^+$ = 160.1121 Found = 160.1125; GC (CP-Chirasil-Dex CB), FID, $t = 22.6$ min.

(S)-88 ^1H NMR (300 MHz, CDCl_3) δ 7.39 – 7.27 (m, 5H, Ar-*H*), 3.67 (q, $J = 6.6$, 1H, *CH*), 3.53 (d, $J = 2.4$, 4H, CH_2), 2.25 (app t, $J = 2.3$, 2H, *CCH*), 1.41 (d, $J = 6.6$, 3H, CH_3). ^{13}C NMR (100 MHz, CDCl_3) δ 144.30, 128.61, 127.33, 79.20, 72.84, 60.78, 39.82, 21.63.

Eight of an expected nine carbon environments were observed for (*S*)-**88** this was consistent with observations made for compound **88**.

Synthesis of *N*-((1-benzyl-1*H*-1,2,3-triazol-4-yl)methyl)-1-phenylethanamine (**91**)

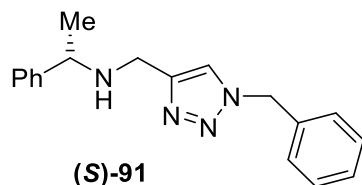


A solution of benzyl bromide (0.214 g, 1.26 mmol, 0.149 mL) and sodium azide (0.082 g, 1.26 mmol) in MeOH/H₂O 1:1 (10 mL) was stirred at rt for 24 h. To the solution, NaAsc (0.012 g, 0.63 mmol), copper(II) sulfate pentahydrate (0.002 g, 0.063 mmol) and alkyne **87** (0.10 g, 0.63 mmol) were added and the resulting mixture was stirred for 8 h. The reaction mixture was diluted with H₂O (20 mL), extracted with EtOAc (3 x 50 mL) and washed with brine (50 mL). The organic layers were combined, dried over MgSO₄ and concentrated under reduced pressure. The residue was taken up in EtOAc (5 mL) and passed through a silica plug using 100% EtOAc as eluent. The recovered organic layer was washed with aqueous ammonia solution 5% v/v (20 mL) to remove any remaining copper residues. The recovered aqueous layer was extracted with EtOAc (2 x 25 mL) and combined with the organic layer which had been washed with aqueous ammonia. The combined organic layers were dried over MgSO₄ and concentrated under reduced pressure to afford the triazole product **91** as a brown oil in 45% (0.083 g) yield.

¹H NMR (300 MHz, CDCl₃) δ 7.98 (s, 1H, Triazole-*H*), 7.60 – 7.56 (m, 2H, Ar-*H*), 7.40 – 7.25 (m, 8H, Ar-*H*), 5.51 (ABq, Δδ_{AB} = 0.04, *J* = 14.8, 2H, CH₂), 4.25 (q, *J* = 6.8, 1H, CH), 4.01 (ABq, Δδ_{AB} = 0.04, *J* = 14.1, 2H, CH₂), 1.72 (d, *J* = 6.8 Hz, 3H, CH₃); ¹³C NMR (101 MHz, CDCl₃) δ 139.96, 137.41, 134.36, 129.13, 129.10, 128.96, 128.78, 128.12, 125.46, 57.58, 54.27, 40.00, 20.82.

Thirteen of an expected fourteen carbon environments were observed for **91** two Ar carbon environments overlapped within the carbon spectra. Several different ^{13}C NMR experiments were carried out, in all, thirteen environments were observed.

Synthesis of (*S*)-*N*-((1-benzyl-1*H*-1,2,3-triazol-4-yl)methyl)-1-phenylethanamine ((*S*)-**91**)



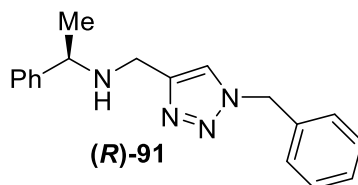
A solution of benzyl bromide (0.214 g, 1.26 mmol, 0.149 mL) and sodium azide (0.082 g, 1.26 mmol) in MeOH/H₂O 1:1 (10 mL) was stirred at reflux for 8 h. To the solution, NaAsc (0.012 g, 0.63 mmol), copper(II) sulfate pentahydrate (0.002 g, 0.063 mmol) and alkyne (**S**-**87**) (0.10 g, 0.63 mmol) were added and the resulting mixture was stirred for 8 h. The reaction mixture was diluted with H₂O (20 mL) extracted with EtOAc (3 x 50 mL) and washed with brine (50 mL). The organic layers were combined, dried over MgSO₄ and concentrated under reduced pressure. The residue was taken up in EtOAc (5 mL) and passed through a silica plug using 100% EtOAc as eluent. The recovered organic layer was washed with aqueous ammonia solution 5% v/v (20 mL) to remove any remaining copper residues. The recovered aqueous layer was extracted with EtOAc (2 x 25 mL) and combined with the organic layer which had been washed with aqueous ammonia. The combined organic layers were dried over MgSO₄ and concentrated under reduced pressure to afford the triazole product (**S**)-**91** as a brown oil in a 52% (0.095g) yield.

^1H NMR (400 MHz, CDCl₃) δ 7.53 – 7.11 (m, 11H, Ar-H/Triazole-H), 5.49 (s, 2H, CH₂), 3.82 (q, J = 6.6, 1H, CH), 3.72 (s, 2H, CH₂), 2.00 (br s, 1H, NH), 1.37 (d, J = 6.6, 3H, CH₃);

^{13}C NMR (101 Hz, CDCl₃) δ 147.21, 145.03, 134.72, 129.07, 128.70, 128.50, 128.10, 127.05,

126.72, 121.46, 57.86, 54.06, 42.68, 24.27; IR ν_{\max} (ATR)/ cm^{-1} 2972, 2924, 1493, 1451; MS ESI^+ m/z 315.2 ($[\text{M}+\text{Na}]^+$, 58%), 293.1 (100, $[\text{M}+\text{H}]^+$), 189.1 (38), 144.1 (78), 143.1 (42); HRMS ESI^+ $[\text{M}+\text{H}]$ Calculated for $\text{C}_{20}\text{H}_{21}\text{N}_4^+$ = 293.1761 Found = 293.1766.

Synthesis of (*R*)-*N*-((1-benzyl-1*H*-1,2,3-triazol-4-yl)methyl)-1-phenylethanamine (*R*)-91

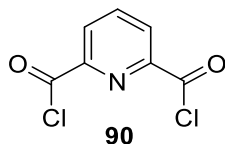


A solution of benzyl bromide (0.214 g, 1.26 mmol, 0.149 mL) and sodium azide (0.082 g, 1.26 mmol) in MeOH/ H_2O 1:1 (10 mL) was stirred at reflux for 8 h. To the solution, NaAsc (0.012 g, 0.63 mmol), copper(II) sulfate pentahydrate (0.002 g, 0.063 mmol) and alkyne (*R*)-87 (0.10 g, 0.63 mmol) were added and the resulting mixture was stirred for 8 h. The reaction mixture was diluted with H_2O (20 mL) extracted with EtOAc (3 x 50 mL) and washed with brine (50 mL). The organic layers were combined, dried over MgSO_4 and concentrated under reduced pressure. The residue was taken up in EtOAc (5 mL) and passed through a silica plug using 100% EtOAc as eluent. The recovered organic layer was washed with aqueous ammonia solution 5% v/v (20 mL) to remove any remaining copper residues. The recovered aqueous layer was extracted with EtOAc (2 x 25 mL) and combined with the organic layer which had been washed with aqueous ammonia. The combined organic layers were dried over MgSO_4 and concentrated under reduced pressure to afford the triazole product (*R*)-91 as a brown oil in a 85% (0.156 g) yield.

^1H NMR (300 MHz, CDCl_3) δ 7.53 – 7.11 (m, 11H, Ar/triazole), 5.49 (s, 2H, CH_2), 3.82 (q, J = 6.6, 1H, CH), 3.72 (s, 2H, CH_2), 2.00 (br s, 1H, NH), 1.37 (d, J = 6.6, 3H, CH_3); ^{13}C NMR (101 Hz, CDCl_3) δ 147.21, 145.03, 134.72, 129.07, 128.70, 128.50, 128.10, 127.05, 126.72,

121.46, 57.86, 54.06, 42.68, 24.27; IR ν_{\max} (ATR)/ cm^{-1} 2972, 2924, 1493, 1451; MS ESI⁺ m/z 315.2 ($[\text{M}+\text{Na}]^+$, 49%), 294.2 (56), 293.1 (100, $[\text{M}+\text{H}]^+$), 189.1 (46), 144.1 (81), 143.1 (49); HRMS ESI⁺ Calculated for $\text{C}_{20}\text{H}_{21}\text{N}_4^+$ = 293.1761 Found = 293.1766.

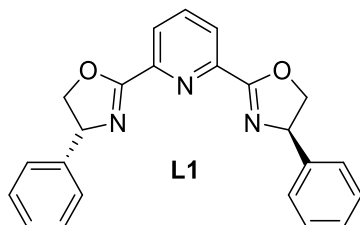
Synthesis of pyridine-2,6-dicarbonyl dichloride **90**



To a mixture of 2,6-pyridine dicarboxylic acid (1.67 g, 10.0 mmol) and catalytic DMF (0.05 mL) was added thionyl chloride (20 mL). The mixture was stirred at reflux for 2 h during which time a white suspension dissolved. The remaining thionyl chloride was removed under reduced pressure. Residual thionyl chloride was removed under reduced pressure by azeotropic distillation with toluene (5 mL) to give the desired acyl chloride **90** in quantitative yield.

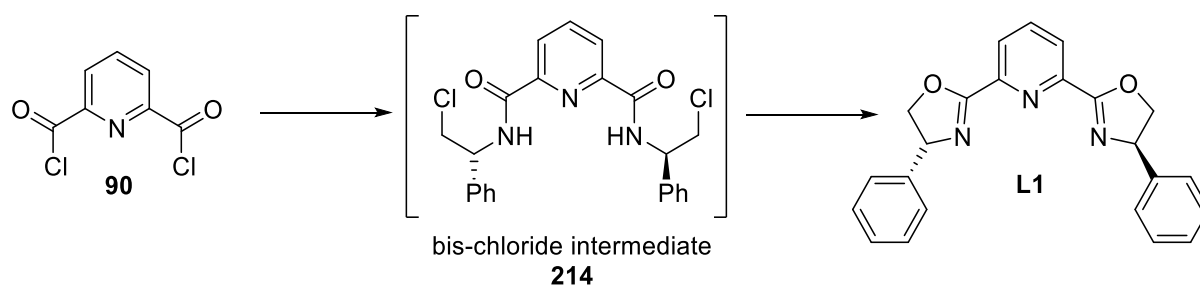
Characterisation data was in agreement with the reported literature values.^[154] ¹H NMR (300 MHz, CDCl_3) δ 8.38 (d, 2H, $J = 7.5$, Ar-*H*), 8.18 (t, 1H, $J = 7.8$, Ar-*H*); ¹³C NMR (100 MHz, CDCl_3) δ 129.0, 139.4, 149.3, 169.5; MP 55-60 °C. Literature value, MP 55-58 °C.^[154]

Synthesis of 2,6-bis((*R*)-4-phenyl-4,5-dihydrooxazol-2-yl)pyridine **L1**



To a solution of (*R*)-phenylglycinol (3.43 g, 25.0 mmol) and triethylamine (4.3 mL, 30.0 mmol) in dichloromethane (30 mL), cooled in an ice bath was added a solution of 2,6-

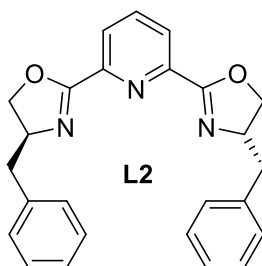
pyridine dicarbonyl dichloride (**90**, 2.04 g, 10.0 mmol) in dichloromethane (30 mL) over a 10 minute period. The reaction mixture was stirred for 24 h at room temperature. The mixture was cooled in an ice bath and thionyl chloride (20 mL) was added. The solution was heated at reflux for 2 h. The reaction mixture was concentrated under reduced pressure and the residual thionyl chloride was removed by azeotropic distillation with toluene (5 mL). The residue was taken up in dichloromethane (30 mL) and washed sequentially with saturated sodium hydrogen carbonate solution (15 mL), water (15 mL) and brine (15 mL), and then dried with MgSO₄. The solvent was removed under reduced pressure and the crude material was purified using automated flash column chromatography combiflash Rf (0-100% hexane/EtOAc gradient 15 min), to give bis-chloride intermediate **214** (7.64 g, 8.19 mmol).



To a solution of a small proportion of the recovered material (0.25 g, 0.57 mmol) in methanol (6 mL) was added potassium hydroxide solution (5% w/v, 6 mL). The solution was stirred at rt for 72 h and then concentrated under reduced pressure. The residue was taken up in dichloromethane (20 mL). The solution was washed sequentially with water (15 mL) and brine (15 mL), and then dried with MgSO₄. The solution was concentrated under reduced pressure to give 2,6-bis((*R*)-4-phenyl-4,5-dihydrooxazol-2-yl)pyridine **L1** as a white solid in a 73% (0.153 g) yield.

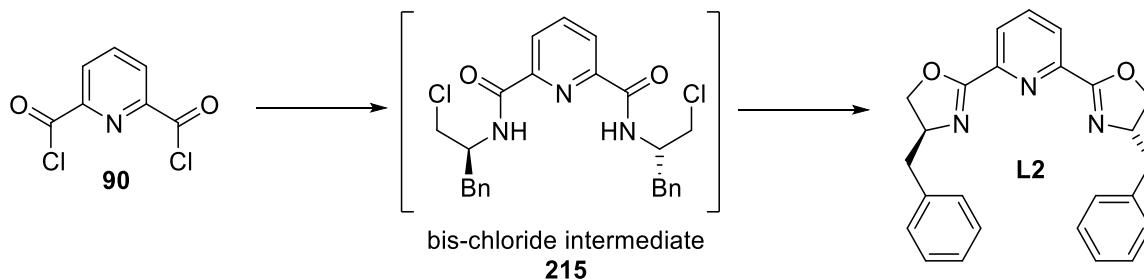
Characterisation data were in agreement with the reported literature values.^[69] ¹H NMR (300 MHz, CDCl₃) δ 8.36 (d, *J* = 7.9, 2H, Py-*H*), 7.94 (t, *J* = 7.9, 1H, Py-*H*), 7.43 – 7.30 (m, 10H, Ar-*H*), 5.48 (dd, *J* = 10.3, 8.7, 2H, CH₂), 4.95 (dd, *J* = 10.3, 8.7, 2H, CH₂), 4.44 (app t, *J* = 8.6, 2H, CH); ¹³C NMR (101 MHz, CDCl₃) δ 163.5, 146.76, 141.69, 137.46, 128.91, 127.84, 126.92, 126.34, 75.54, 70.37; MS ESI⁺ *m/z* 370.1 [M+H]⁺, 388.2 [M+H₂O+H]⁺; MP 168 – 170 °C; [α]²⁹⁰_D = 152.8° (c=1, CH₂Cl₂). Literature values, MP 170-172 °C, [α]²⁹⁹_D = 183.5° (c = 1, CH₂Cl₂).^[69]

Synthesis of 2,6-bis((*S*)-4-benzyl-4,5-dihydrooxazol-2-yl)pyridine L2



To a solution of (*S*)-phenylalaninol (2.04 g, 10.0 mmol) and triethylamine (4.3 mL, 30.0 mmol) in dichloromethane (30 mL), cooled in an ice bath, was added a solution of 2,6-pyridine dicarbonyl dichloride (0.82 g, 4.0 mmol) in dichloromethane (30 mL) over a 10-minute period. The reaction mixture was stirred for 24 h at room temperature. The mixture was cooled in an ice bath and thionyl chloride (20 mL) was added. The solution was heated at reflux for 2 h. The reaction mixture was concentrated under reduced pressure and the residual thionyl chloride was removed by azeotropic distillation with toluene. The resulting residue was taken up in dichloromethane and washed with saturated sodium hydrogen carbonate solution (15 mL), water (15 mL) and brine (15 mL), and then dried with MgSO₄. The solvent was removed under reduced pressure and the crude material was purified using automated

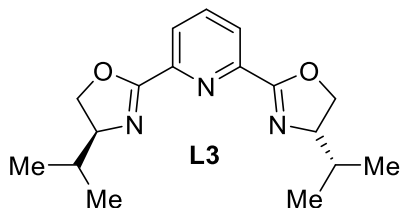
flash column chromatography combiflash Rf (0-100% hexane/EtOAc gradient 15 min) to give bis-chloride intermediate **215**.



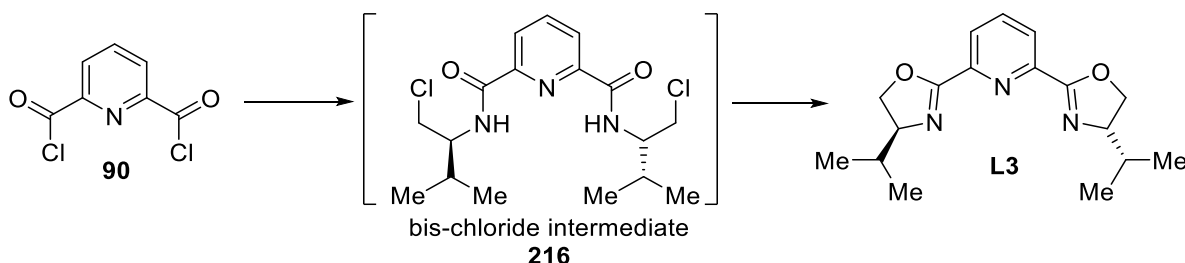
To a solution of the recovered material (1.80 g) in methanol (50 mL) was added potassium hydroxide (0.70 g, 12.5 mmol). The solution was stirred at reflux for 4 h and then concentrated under reduced pressure. The residue taken up in dichloromethane (20 mL). The solution was washed sequentially with water (15 mL) and brine (15 mL), and then dried with MgSO₄. The solution was concentrated under reduced pressure to give 2,6-bis((*S*)-4-benzyl-4,5-dihydrooxazol-2-yl)pyridine **L2** as a white solid in a 84% (1.34 g) yield.

Characterisation data were in agreement with the reported literature values^[154] ¹H NMR (300 MHz, CDCl₃) δ 8.24 (d, *J* = 7.8, 2H, Py-*H*), 7.95 – 7.89 (m, 1H, Py-*H*), 7.36 – 7.26 (m, 10H, Ar-*H*), 4.67 (tdd, *J* = 9.1, 7.6, 5.1, 2H, CH), 4.48 (app t, *J* = 9.0, 2H, CH₂), 4.28 (dd, *J* = 8.5, 7.7, 2H, CH₂), 3.29 (dd, *J* = 13.7, 5.1, 2H, BnCH₂), 2.76 (dd, *J* = 13.7, 9.0, 2H, BnCH₂); ¹³C NMR (101 MHz, CDCl₃) δ 162.82, 146.81, 137.72, 137.38, 129.23, 128.63, 126.63, 125.82, 72.61, 68.12, 41.70; MS ESI⁺ *m/z* 398.2 ([M+H]⁺, 100%), 283.1 (88), 208.6 (27), 117.1 (32); MP 153–154 °C; [α]²⁹⁰_D = -65.6° (c=1, CH₂Cl₂). Literature values, MP 155–156 °C; [α]²⁹⁸_D = -58.0° (c=0.1, CH₂Cl₂).^[154]

Synthesis of 2,6-bis((*S*)-4-isopropyl-4,5-dihydrooxazol-2-yl)pyridine **L3**



To a solution of (*S*)-valinol (1.13 g, 11.0 mmol) and triethylamine (4.3 mL, 30.0 mmol) in dichloromethane (30 mL), cooled in an ice bath was added a solution of 2,6-pyridine dicarbonyl dichloride (1.17 g, 5.74 mmol) in dichloromethane (30 mL) over a 10-minute period. The reaction mixture was stirred for 24 h at room temperature. The mixture was cooled in an ice bath and thionyl chloride (20 mL) was added. The solution was heated at reflux for 2 h. The reaction mixture was concentrated under reduced pressure and the residual thionyl chloride was removed by azeotropic distillation with toluene (5 mL). The resulting residue was taken up in dichloromethane and washed with saturated sodium hydrogen carbonate solution (15 mL), water (15 mL) and brine (15 mL), and then dried with MgSO₄. The solvent was removed under reduced pressure and the crude material was purified using automated flash column chromatography combiflash Rf (0-100% hexane/EtOAc gradient 15 min) to give bis-chloride intermediate **216**.



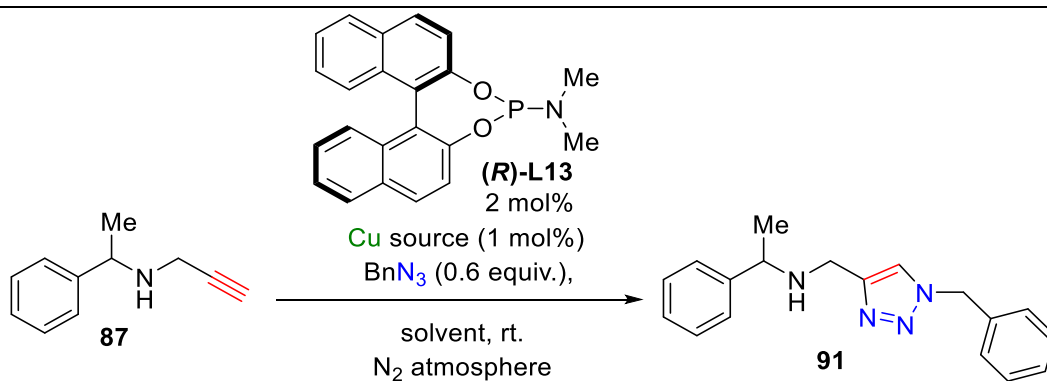
To a solution of the recovered material (1.06 g) in methanol (50 mL) was added potassium hydroxide (0.70 g, 12.5 mmol). The solution was stirred at reflux for 4 h and then

concentrated under reduced pressure. The residue taken up in dichloromethane (20 mL). The solution was washed with water (15 mL) and brine (15 mL), and then dried with MgSO₄. The solution was concentrated under reduced pressure to give 2,6-bis((*S*)-4-isopropyl-4,5-dihydrooxazol-2-yl)pyridine **L3** as a white solid in 56% (0.84 g) yield.

Characterisation data were in agreement with the reported literature values.^[69] ¹H NMR (300 MHz, CDCl₃) δ 8.15 (d, *J* = 7.8, 2H, Py-*H*), 7.79 (t, *J* = 7.8, 1H, Py-*H*), 4.46 (dd, *J* = 9.3, 8.3, 2H, *CH*), 4.28 – 3.94 (m, 4H, *CH*₂), 1.79 (m, 2H, *CH*), 0.97 (d, *J* = 6.7, 6H, *CH*₃), 0.86 (d, *J* = 6.8, 6H, *CH*₃); ¹³C NMR (100 MHz, CDCl₃) δ 162.12, 146.83, 137.10, 125.65, 72.83, 70.89, 32.77, 18.99, 18.26; MS ESI⁺ *m/z* 302.2 ([*M*+*H*]⁺, 100%); MP 150-152 °C; [*α*]²⁹⁰_D = -98.8° (*c*=1, CH₂Cl₂). Literature values, MP 152-153°C; [*α*]²⁹⁹_D = -117.0° (*c*=1, CH₂Cl₂).^[69]

7.2.2 Screening Tables for Kinetic Resolution of Compound 87

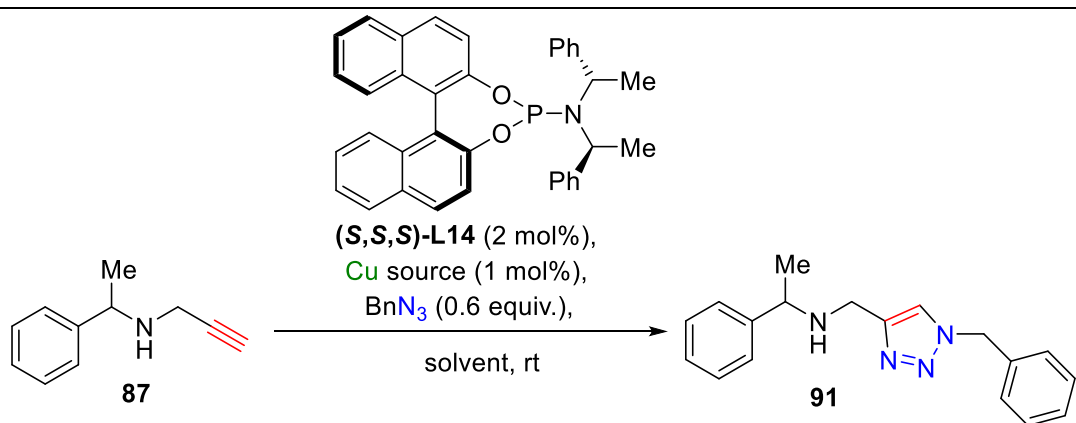
Table 21 Reaction screening of alkyne **87** with phosphoramidite ligand **L13**



Entry	Copper Source	Solvent	<i>ee</i> 87 , 70 h (%) ^a	<i>ee</i> 87 , 94 h (%) ^a
1	CuSO ₄	MeCN	2	0
2	CuSO ₄	THF	0	0
3	CuSO ₄	Toluene	0	0
4	CuSO ₄	Acetone	0	0
5	CuI	MeCN	0	0
6	CuI	THF	0	0
7	CuI	Toluene	2	4
8	CuI	Acetone	-	0
9	Cu(OTf) ₂	MeCN	0	0
10	Cu(OTf) ₂	THF	0	0
11	Cu(OTf) ₂	Toluene	0	0
12	Cu(OTf) ₂	Acetone	0	0
13 Control			0	

^a *Ee* determined by chiral GC. ^b Control sample of compound **87**.

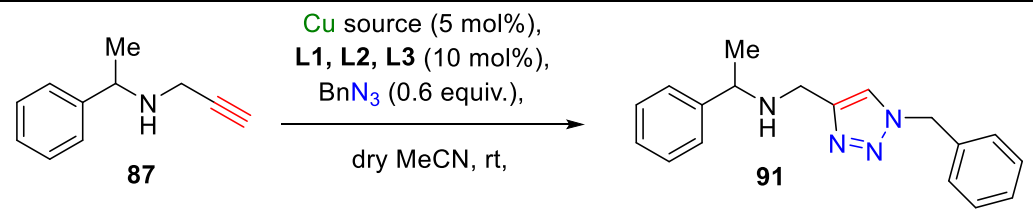
Table 22 Reaction screening of alkyne **87** with phosphoramidite ligand **L14**



Entry	Copper Source	Solvent	<i>ee</i> 87 , 70 h (%) ^a	<i>ee</i> 87 , 94 h (%) ^a
1	CuSO ₄	MeCN	0	0
2	CuSO ₄	THF	0	0
3	CuSO ₄	Toluene	0	2
4	CuSO ₄	Acetone	0	0
5	CuI	MeCN	0	0
6	CuI	THF	-	0
7	CuI	Toluene	-	-
8	CuI	Acetone	2	0
9	Cu(OTf) ₂	MeCN	0	0
10	Cu(OTf) ₂	THF	0	0
11	Cu(OTf) ₂	Toluene	-	-
12	Cu(OTf) ₂	Acetone	0	0
13 Control			0	

^a *Ee* determined by chiral GC; ^b Control sample of compound **87**.

Table 23 Reaction screening of alkyne **87** with PyBox ligands **L1**, **L2** and **L3**


Reaction scheme showing the conversion of alkyne **87** to product **91**. Reagents: Cu source (5 mol%), **L1**, **L2**, **L3** (10 mol%), BnN_3 (0.6 equiv.), dry MeCN, rt.

Entry	Copper Source	Solvent	Ligand	<i>ee</i> 87 , 70 h (%) ^a
1	CuSO ₄	MeCN	L1	0
2	CuI	MeCN	L1	0
3	CuSO ₄	MeCN	L2	0
4	CuI	MeCN	L2	0
5	CuSO ₄	MeCN	L3	0
6	CuI	MeCN	L3	0
7	Control ^b			0

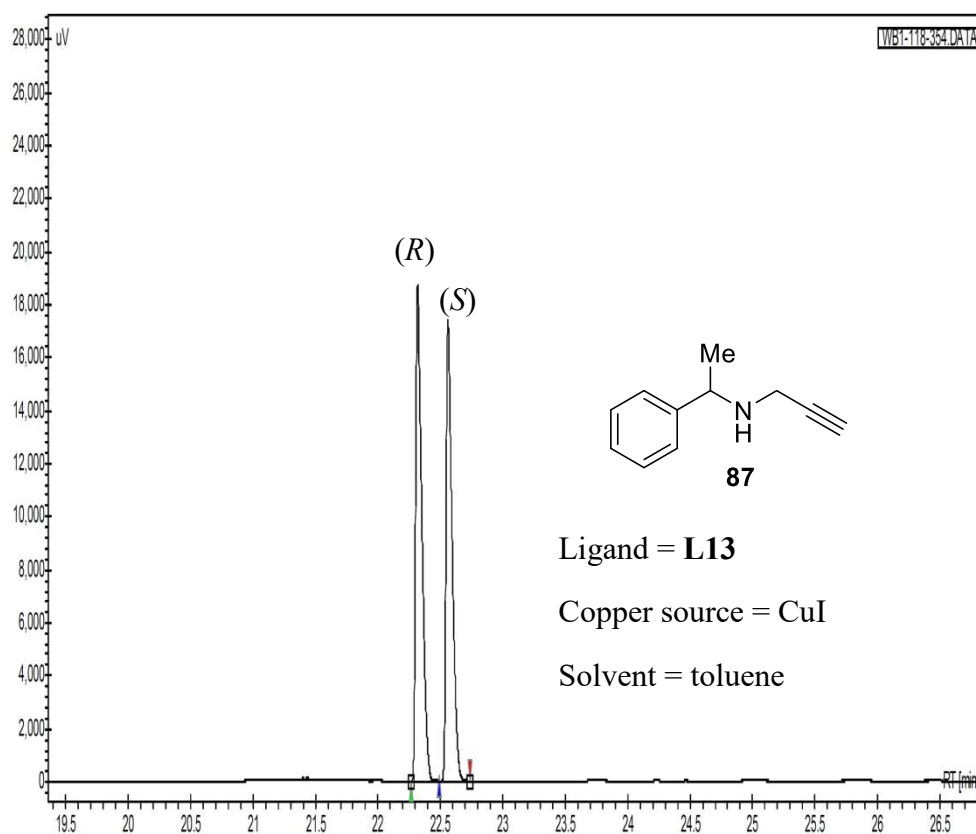
^a *Ee* determined by chiral GC; ^b Control sample of compound **87**.

7.2.3 Chromatography for Chapter 2

7.2.3.1 Chiral GC Trace of Compound 87

WB1-118-3

Vial- 55
Method- GB METHOD.METH
Acq time- 21/03/2014 16:13:37
Injection volume- 8.000 μ L
Sample name- N.A.



Peak results :

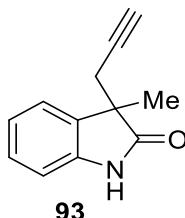
WB1-118-354.DATA [FID]

Index	Time [Min]	Area [uV.Min]	Area % [%]
1	22.32	1070.7	51.898
2	22.56	992.4	48.102

7.2.4 Experimental for the Kinetic Resolution of Quaternary Oxindoles (Section 2.1)

7.2.4.1 Synthesis

Synthesis of 3-methyl-3-(prop-2-yn-1-yl)indolin-2-one (**93**)

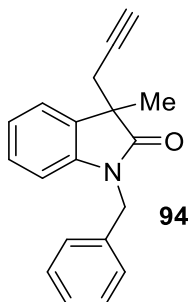


n-Butyl lithium in hexanes (1.5 M, 8.15 mmol, 5.09 mL) was transferred into a nitrogen-flushed flask, THF (40 mL) was added and the solution was cooled to $-78\text{ }^{\circ}\text{C}$. A solution of 3-methyl-2-oxindole (1.00 g, 6.79 mmol) in THF (10 mL) was added dropwise over a period of 5 minutes under stirring. The reaction mixture was stirred for 10 minutes before propargyl bromide (7.13 mmol, 0.76 mL) was added. The solution was allowed to warm to room temperature and stirred for 3 h. Methanol (20 mL) was added to decompose any remaining butyl lithium. The solution was concentrated under reduced pressure and the residual oil extracted with water (50 mL) and ethyl acetate (3 x 50 mL). The organic phase was dried over MgSO_4 and concentrated under reduced pressure. The oil was then purified using automated column chromatography combiflash Rf (0-25% hexane/EtOAc gradient 20 min) to yield 3-methyl-3-(prop-2-yn-1-yl)indolin-2-one **93** as a cream solid in 55% (0.69 g) yield.

^1H NMR (300 MHz, CDCl_3) δ 7.75 (s, 1H, NH), 7.42 (d, $J = 7.4$, 1H, Ar-H), 7.29 – 7.21 (m, 1H, Ar-H), 7.07 (app td, $J = 7.7$, 1.0, 1H, Ar-H), 6.91 (d, $J = 7.7$, 1H, Ar-H), 2.63 (ABX, $\Delta\delta_{\text{AB}} = 0.14$, $J = 16.6$, 2.7, 2H, CH_2), 1.98 (app t, $J = 2.7$, 1H, CCH), 1.48 (s, 3H, CH_3); ^{13}C NMR (101 MHz, CDCl_3) δ 182.08, 140.24, 133.47, 128.22, 123.53, 122.54, 109.97, 79.55, 70.85, 47.21, 27.58, 21.93; IR ν_{max} (ATR)/ cm^{-1} 3255, 2981, 2968, 2925, 1705, 1667, 1622,

1471, 1341, 1235, 1191; MS ESI⁺ m/z 208.1 ([M+Na]⁺, 3%), 186.1 (100, [M+H]⁺); HRMS ESI⁺ Calculated for C₁₂H₁₁NONa⁺ = 208.0733 Found = 208.0739; MP 112-114 °C.

Synthesis of 1-benzyl-3-methyl-3-(prop-2-yn-1-yl)indolin-2-one (**94**)



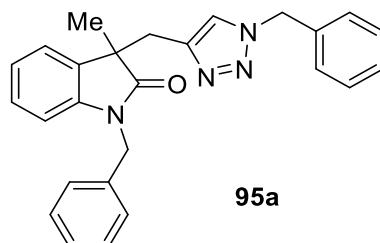
Sodium hydride (2.38 mmol, 0.082 g) was suspended in THF (10 mL). The reaction was cooled to 0 °C using an ice bath, at this temperature a solution of 3-methyl-3-(prop-2-yn-1-yl)indolin-2-one **93** (1.08 mmol, 0.20 g) in THF (10 mL) was added dropwise. When the formation of gas had ceased, benzyl bromide (1.08 mmol, 0.185 g, 0.129 mL) was added to the mixture. The reaction was allowed to warm to room temperature and left to stir for 2 h. Water (5 mL) was added to decompose any remaining sodium hydride and the solution was extracted with water (50 mL) and diethyl ether (3 x 50 mL). The combined organic phases were dried over MgSO₄ and concentrated under reduced pressure. This gave 1-benzyl-3-methyl-3-(prop-2-yn-1-yl)indolin-2-one **94** as a colourless crystalline solid this was then washed with hexane (50 mL) to remove any residual benzyl bromide. This gave the pure compound as a colourless crystalline solid in a 77% (0.23g) yield.

¹H NMR (300 MHz, CDCl₃) δ 7.43 (dd, $J = 7.4, 0.8$, 1H, Ar-*H*), 7.36 – 7.28 (m, 5H, Ar-*H*), 7.18 (app td, $J = 7.7, 1.3$, 1H, Ar-*H*), 7.05 (app td, $J = 7.7, 1.0$, 1H, Ar-*H*), 6.73 (d, $J = 7.8$ Hz, 1H, Ar-*H*), 4.96 (ABq, $\Delta\delta_{AB} = 0.16$, $J = 15.7$, 2H, CH₂), 2.72 (ABX, $\Delta\delta_{AB} = 0.14$, $J = 16.5$, 2H, CH₂), 1.92 (app t, $J = 2.6$, 1H, CCH), 1.51 (s, 3H, CH₃); ¹³C NMR (101 MHz,

CDCl₃) δ 179.46, 142.16, 135.84, 132.96, 128.70, 128.14, 127.59, 127.32, 123.21, 122.60, 109.12, 79.76, 70.77, 46.77, 43.76, 27.76, 22.36; IR ν_{\max} (ATR)/cm⁻¹ 3285, 2924, 1711, 1608, 1489, 1466, 1426, 1378, 1179; MS ESI⁺ m/z 298.1 ([M+Na]⁺, 20%), 276.1 (100, [M+H]⁺); HRMS ESI⁺ Calculated for C₁₉H₁₈NO⁺ = 276.1383 Found = 276.1378; MP 140-141°C; HPLC (Phenomenex Cellulose 3) acetonitrile/water 50:50, 1.0 mL/min, λ = 254 nm, t_{major} = 7.5 min, t_{minor} = 8.5 min; $[\alpha]_D^{293}$ t_{minor} = -41° (c = 1.0, CHCl₃).

Enantiopure material was recovered by preparative HPLC using Phenomenex Cellulose 1 acetonitrile/water 50:50 15 mL/min, λ = 254 nm. The enantiopure material was subjected to optical rotation analysis and from this it was calculated that the (-) enantiomer was eluting as the t_{minor} peak in the cellulose 3 analytical HPLC. Therefore, the recovered enantioenriched alkyne from the kinetic resolution should have a positive optical rotation. The (-) enantiomer was later assigned as (*R*) and (+) enantiomer was assigned as (*S*) from single crystal x-ray diffractometry.

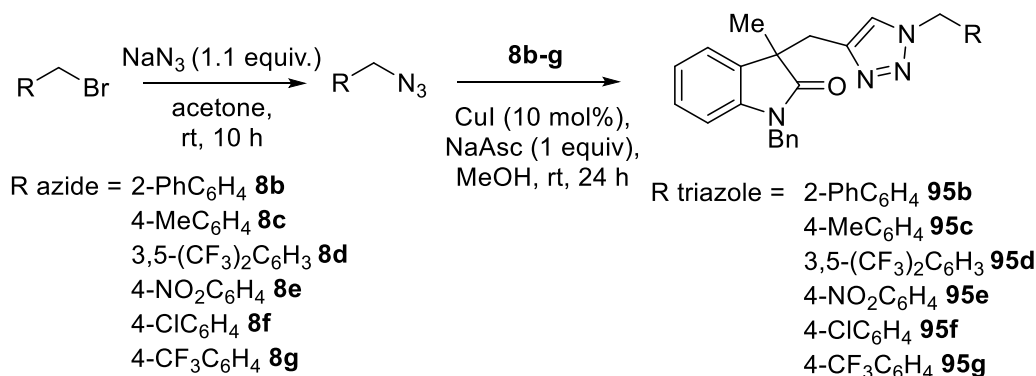
Synthesis of 1-benzyl-3-((1-benzyl-1*H*-1,2,3-triazol-4-yl)methyl)-3-methylindolin-2-one (95a)



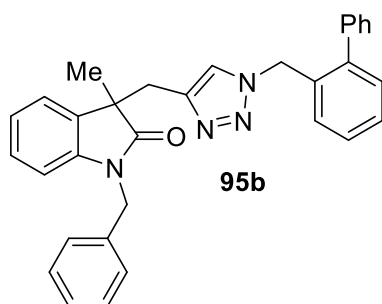
To a solution of **94** (0.24 mmol, 0.066 g) in methanol (10 mL) was added copper(I) iodide (0.0046 g, 0.024 mmol), sodium ascorbate (0.24 mmol, 0.048g) and finally benzyl azide (0.24 mmol, 0.032 g) this was allowed to stir overnight. The reaction was quenched with aqueous ammonia solution 5% v/v (10 mL) and extracted with diethyl ether (3 x 25 mL) then washed with water (100 mL). The remaining starting material and the triazolic product were isolated by automated flash column chromatography combiflash Rf (petroleum ether/diethyl ether 0-100% gradient over 15 min followed by EtOAc 100% for 5 min). This gave 1-benzyl-3-((1-benzyl-1*H*-1,2,3-triazol-4-yl)methyl)-3-methylindolin-2-one **95a** as a brown oil in a 71% (0.070 g) yield.

¹H NMR (300 MHz, CDCl₃) δ 7.35 – 6.93 (m, 13 H, Ar-*H*), 6.73 (s, 1H, Triazole *CH*), 6.57 (d, *J* = 7.6, 1H, Ar-*H*), 5.28 (s, 2H, CH₂), 4.70 (s, 2H, CH₂), 3.81 (ABq, Δδ_{AB} = 0.13, *J* = 14.3, 2H, CH₂) 1.54 (s, 3H, CH₃); ¹³C NMR (101 MHz, CDCl₃) δ 179.88, 143.35, 142.11, 135.94, 134.87, 132.91, 128.95, 128.71, 128.44, 127.85, 127.69, 127.52, 127.28, 123.25, 122.58, 121.84, 108.82, 53.71, 48.58, 43.48, 34.39, 23.46; IR ν_{max} (ATR)/cm⁻¹ 2924, 1708, 1611, 1489, 1468, 1454, 1355, 1176; HPLC (Phenomenex Cellulose 3) acetonitrile/water 40:60, 1.0 mL/min, λ = 254 nm, t_{major} = 11.2 min, t_{minor} = 12.7 min.

General procedure for synthesis of racemic oxindole triazoles *via in situ* azide formation

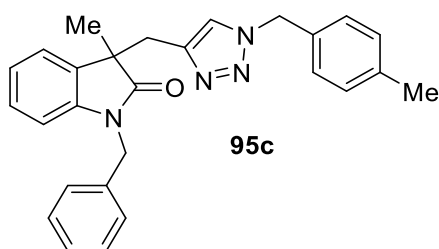


The alkyl bromide (0.12 mmol, 1.0 equiv.) was stirred at rt with sodium azide (0.13 mmol, 0.0085 g, 1.1 equiv.) in acetone (5 mL). After 10 h, the reaction was diluted with methanol (10 mL) and **94** (0.12 mmol, 0.033 g, 1.0 equiv.) added along with copper(I) iodide (2.3 mg, 0.012 mmol, 0.1 equiv, 10 mol%) and sodium ascorbate (0.12 mmol, 0.024 g, 1.0 equiv.). The reaction was stirred at rt for 24 h. The reaction was quenched with aqueous ammonia solution 5% v/v (10 mL) and extracted with ether (3 x 25 mL) dried over MgSO₄ and concentrated under reduced pressure. The triazolic product was isolated by automated flash column chromatography combiflash Rf (petroleum ether/diethyl ether 0-100% gradient 15 min followed by EtOAc 100%, 5 min).

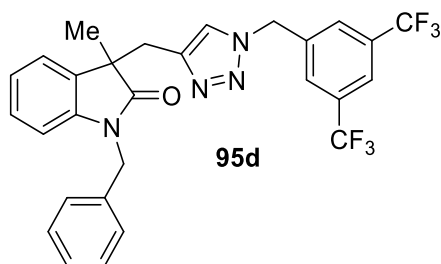


(95b) Brown oil (0.030 g, 52% yield); ¹H NMR (300 MHz, CDCl₃) δ 7.46 – 6.97 (m, 16H, Ar-*H*/Triazole *CH*), 6.75 (d, *J* = 7.6, 1H, Ar-*H*), 6.64 – 6.53 (m, 2H, Ar-*H*), 5.22 (s, 2H, CH₂), 4.68 (ABq, Δδ_{AB} = 0.06, *J* = 15.6, 2H, CH₂), 3.26 (ABq, Δδ_{AB} = 0.11, *J* = 14.3, 2H, CH₂),

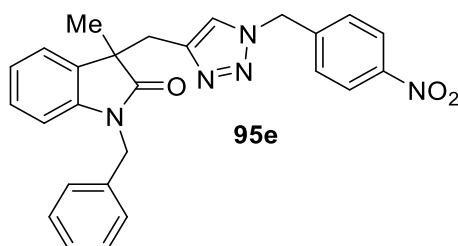
1.50 (s, 3H, CH_3); ^{13}C NMR (101 MHz, $CDCl_3$) δ 179.90, 143.04, 142.10, 141.68, 139.74, 135.89, 132.93, 132.27, 130.30, 128.99, 128.66, 128.54, 128.46, 128.30, 128.05, 127.85, 127.67, 127.49, 127.22, 123.31, 122.58, 121.95, 108.83, 51.35, 48.56, 43.48, 34.27, 23.57; IR ν_{max} (ATR)/ cm^{-1} 2925, 2854, 1707, 1611, 1488, 1467, 1453; MS ESI⁺ m/z 508.3 (28%), 507.2 (87, $[M+Na]^+$), 485.2 (100, $[M+H]^+$); HRMS ESI⁺ Calculated for $C_{32}H_{28}N_4ONa^+$ = 507.2155 Found = 507.2166.



(95c) Brown oil (0.038 g, 75% yield); 1H NMR (300 MHz, $CDCl_3$) δ 7.28 – 6.93 (m, 10H, Ar-*H*), 6.85 (d, J = 8.0, 2H, Ar-*H*), 6.70 (s, 1H, Triazole *CH*), 6.55 (d, J = 7.6, 1H, Ar-*H*), 5.21 (s, 2H, CH_2), 4.68 (s, 2H, CH_2), 3.26 (Abq, $\Delta\delta_{AB}$ = 0.12, J = 14.3, 2H, CH_2), 2.34 (s, 3H, CH_3), 1.51 (s, 3H, CH_3); ^{13}C NMR (101 MHz, $CDCl_3$) δ 179.89, 143.23, 142.11, 138.30, 135.95, 132.94, 131.84, 129.60, 128.70, 127.82, 127.77, 127.51, 127.23, 123.26, 122.57, 121.76, 108.83, 53.53, 48.57, 43.48, 34.39, 23.43, 21.16; IR ν_{max} (ATR)/ cm^{-1} 2925, 1707, 1611, 1489, 1467, 1453, 1379, 1354, 1175; MS ESI⁺ m/z 445.2 ($[M+Na]^+$, 85%), 423.2 (100, $[M+H]^+$); HRMS ESI⁺ Calculated for $C_{27}H_{26}N_4ONa^+$ = 445.1999 Found = 445.2006.



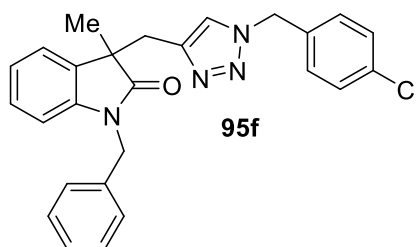
(95d) Brown oil (0.035g, 53% yield); ^1H NMR (300 MHz, CDCl_3) δ 7.83 (s, 1H, Ar-*H*), 7.46 (s, 2H, Ar-*H*), 7.31 – 6.93 (m, 9H, Ar-*H*), 6.74 (s, 1H, Triazole *CH*), 6.60 (d, $J = 7.5$, 1H, Ar-*H*), 5.32 (s, 2H, CH_2), 4.76 (Abq, $\Delta\delta_{\text{AB}} = 0.13$, $J = 15.5$, 1H, CH_2), 3.32 (Abq, $\Delta\delta_{\text{AB}} = 0.15$, $J = 14.4$, 2H, CH_2), 1.52 (s, 3H, CH_3); ^{13}C NMR (101 MHz, CDCl_3) δ 179.77, 143.92, 142.06, 137.28, 135.97, 132.81, 132.44 (q, $^2J_{\text{C-F}} = 33.7$), 128.68, 128.00, 127.88, 127.53, 127.43, 123.17, 122.84 (q, $^1J_{\text{C-F}} = 272.9$), 122.66, 122.00, 108.77, 52.51, 48.37, 43.51, 34.22, 23.62; ^{19}F NMR (282 MHz, CDCl_3) δ -62.83; IR ν_{max} (ATR)/ cm^{-1} 2928, 1706, 1612, 1489, 1468, 1454, 1382, 1354, 1277, 1173, 1132; MS ESI $^+$ m/z 568.2 (36%), 567.2 (100, $[\text{M}+\text{Na}]^+$), 545.2 (59, $[\text{M}+\text{H}]^+$); HRMS ESI $^+$ Calculated for $\text{C}_{28}\text{H}_{22}\text{N}_4\text{OF}_6\text{Na}^+$ = 567.1590 Found = 567.1593.



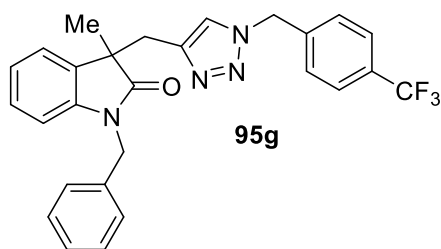
(95e) Colourless solid (0.035g, 64% yield); ^1H NMR (300 MHz, CDCl_3) δ 8.15 – 7.96 (m, 2H, Ar-*H*), 7.26 – 6.88 (m, 10H, Ar-*H*), 6.75 (s, 1H, Triazole *CH*), 6.65 (d, $J = 7.7$, 1H, Ar-*H*), 5.35 (ABq, $\Delta\delta_{\text{AB}} = 0.05$, $J = 15.7$, 2H, CH_2), 4.79 (Abq, $\Delta\delta_{\text{AB}} = 0.30$, $J = 15.5$, 2H, CH_2), 3.36 (Abq, $\Delta\delta_{\text{AB}} = 0.22$, $J = 14.4$, 2H, CH_2), 1.55 (s, 3H, CH_3); ^{13}C NMR (101 MHz, CDCl_3) δ 179.74, 143.90, 142.19, 141.85, 135.94, 132.90, 128.69, 127.96, 127.90, 127.55, 124.06, 123.22, 122.67, 122.15, 108.77, 52.60, 48.56, 43.70, 34.18, 23.81; IR ν_{max} (ATR)/ cm^{-1} 2925,

1707, 1611, 1521, 1489, 1467, 1453, 1379, 1346, 1176; MS ESI⁺ *m/z* 476.2 ([M+Na]⁺, 100%), 454.2 (43, [M+H]⁺); HRMS ESI⁺ Calculated for C₂₆H₂₃N₅O₃Na⁺ = 476.1693 Found = 476.1698.

Twenty of an expected twenty two carbon environments were observed for **95e** due to Ar carbon environments overlapping within the carbon spectra.

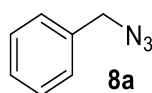
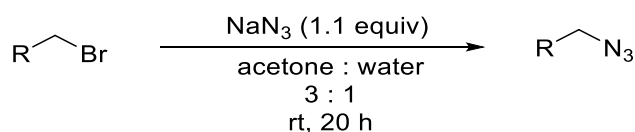


(**95f**) Brown oil (0.043 g, 82% yield); ¹H NMR (300 MHz, CDCl₃) δ 7.27 – 6.94 (m, 10H, Ar-H), 6.78 (t, *J* = 9.7 Hz, 2H, Ar-H), 6.65 (s, 1H, Triazole CH), 6.56 (d, *J* = 7.7, 1H, Ar-H), 5.27 – 5.12 (m, 2H, CH₂), 4.70 (Abq, Δδ_{AB} = 0.09, *J* = 15.6, 2H, CH₂), 3.29 (Abq, Δδ_{AB} = 0.18, *J* = 14.3, 2H, CH₂) 1.52 (s, 3H, CH₃); ¹³C NMR (101 MHz, CDCl₃) δ 179.80, 143.54, 142.13, 135.92, 134.41, 133.32, 132.89, 129.11, 128.97, 128.71, 127.86, 127.55, 127.37, 123.20, 122.60, 121.79, 108.81, 52.93, 48.57, 43.56, 34.34, 23.57; IR ν_{max} (ATR)/cm⁻¹ 2925, 1707, 1611, 1490, 1467, 1454, 1380, 1355, 1174; MS ESI⁺ *m/z* 467.2 (35%), 465.2 (100, [M+Na]⁺), 443.2 (85, [M+H]⁺); HRMS ESI⁺ Calculated for C₂₇H₂₃N₄O³⁵ClNa⁺ = 465.1453 Found = 465.1453.



(95g) Brown oil (0.036 g, 63% yield); ^1H NMR (300 MHz, CDCl_3) δ 7.49 (d, $J = 8.1$, 2H, Ar-*H*), 7.28 – 6.89 (m, 10H, Ar-*H*), 6.67 (s, 1H, Triazole *CH*), 6.57 (d, $J = 7.6$, 1H, Ar-*H*), 5.28 (ABq, $\Delta\delta_{\text{AB}} = 0.03$, $J = 15.5$, 2H, CH_2), 4.72 (Abq, $\Delta\delta_{\text{AB}} = 0.17$, $J = 15.5$, 2H, CH_2), 3.31 (Abq, $\Delta\delta_{\text{AB}} = 0.20$, $J = 14.3$, 2H, CH_2), 1.53 (s, 3H, CH_3); ^{13}C NMR (101 MHz, CDCl_3) δ 179.77, 143.68, 142.16, 138.75, 135.92, 132.88, 130.64 (q, $^2J_{\text{C-F}} = 32.5$) 130.47, 128.70, 127.88, 127.73, 127.56, 127.42, 125.87 (q, $^3J_{\text{C-F}} = 3.3$), 123.19, 122.60, 121.96, 108.77, 52.97, 48.56, 43.61, 34.28, 23.67; ^{19}F NMR (282 MHz, CDCl_3) δ -62.69; IR ν_{max} (ATR)/ cm^{-1} 2925, 1709, 1612, 1490, 1468, 1381, 1326, 1169, 1124; MS ESI $^+$ m/z 500.2 (35%), 499.2 (100, $[\text{M}+\text{Na}]^+$), 477.2 (55, $[\text{M}+\text{H}]^+$); HRMS ESI $^+$ Calculated for $\text{C}_{27}\text{H}_{23}\text{N}_4\text{OF}_3\text{Na}^+$ = 499.1716 Found = 499.1721.

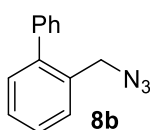
General procedure for synthesis and isolation of azides



Sodium azide (1.20 g, 18.5 mmol, 1.1 equiv.) was added to a mixture of acetone : water (3:1), to this benzyl bromide was added (2.88 g, 16.8 mmol, 2 mL, 1.0 equiv.) and the reaction mixture was stirred at rt for 20 h. Water (100 mL) was added and the reaction mixture was extracted with diethyl ether (3 x 25 mL). The combined organic extracts were combined,

dried over MgSO₄ and concentrated under reduced pressure to yield benzyl azide **8a** as a colourless oil in a 80% (1.79 g) yield.

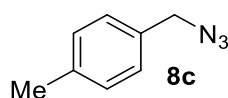
Characterisation data were in agreement with the reported literature values.^[155] ¹H NMR (300 MHz, CDCl₃) δ 7.35 – 7.18 (m, 5H, Ar-*H*), 4.18 (s, 2H, CH₂); ¹³C NMR (101 MHz, CDCl₃) δ 135.65, 128.98, 128.43, 128.38, 54.83; MS EI⁺ m/z 133.1 ([M]⁺, 53%), 104.0 (73, [M-N₂]⁺), 91.1 (100, [M-N₃]⁺), 77.0 (57, [M-CH₂N₃]⁺) 51.0 (33).



Prepared from 2-phenylbenzyl bromide (0.50 g, 2.39 mmol) and sodium azide (0.17 g, 2.63 mmol) according to the general procedure. Isolated as a yellow oil **8b** in a 85% (0.42 g) yield.

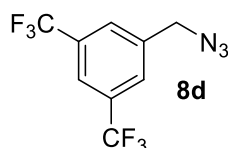
Characterisation data were in agreement with the reported literature values.^[156] ¹H NMR (300 MHz, CDCl₃) δ 7.44 – 7.25 (m, 9H, Ar-*H*), 4.24 (s, 2H, CH₂); ¹³C NMR (101 MHz, CDCl₃) δ 142.33, 140.37, 132.92, 130.56, 129.69, 129.31, 128.45, 127.91, 127.57, 52.68.

Ten of the expected eleven carbon signals were observed for **8b** this matches with the ten observed within the literature.^[156] Mass spectrometry was attempted to confirm compound identity but fragmentation occurred with several mass spectrometry techniques. The azide **8b** was successfully used to form triazole **95b**.



Prepared from 4-methylbenzyl bromide (0.5 g, 2.70 mmol) and sodium azide (0.19 g, 3.00 mmol) according to the general procedure. Isolated as a orange oil **8c** in a 64% (0.40 g) yield.

Characterisation data were in agreement with the reported literature values.^[157] ¹H NMR (300 MHz, CDCl₃) δ 7.21 – 7.13 (m, 4H, Ar-*H*), 4.25 (s, 2H, CH₂), 2.33 (s, 3H, CH₃); ¹³C NMR (101 MHz, CDCl₃) δ 138.18, 132.39, 129.56, 128.33, 54.65, 21.20; MS EI⁺ m/z 147.1 ([M]⁺, 32%), 105.1 (100, [M-N₃]⁺), 91.1 (36, [M-CH₂N₃]⁺).



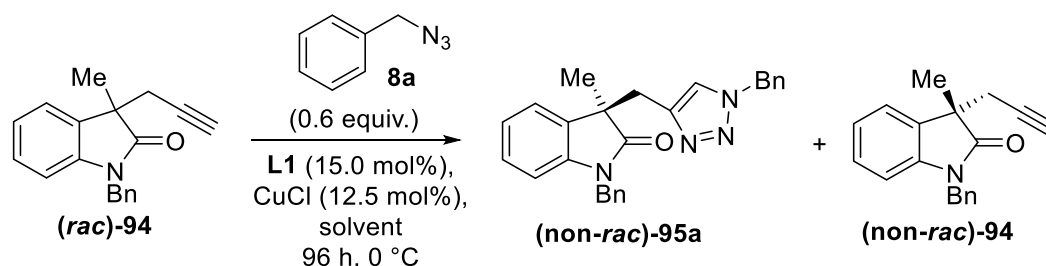
Prepared from 3,5-Bis(trifluoromethyl)benzyl bromide (0.20 g, 0.65 mmol) and sodium azide (0.05 g, 0.72 mmol) according to the general procedure. Isolated as a yellow oil **8d** in a 55% (0.096 g) yield.

Characterisation data were in agreement with the reported literature values.^[157] ¹H NMR (300 MHz, CDCl₃) δ 7.86 (s, 1H, Ar-*H*), 7.79 (s, 2H, Ar-*H*), 4.56 (s, 2H, CH₂); ¹³C NMR (101 MHz, CDCl₃) δ 138.20, 132.22 (q, ²J_{C-F} = 33.6 Hz), 127.84, 123.06 (q, ¹J_{C-F} = 272.7) 122.15, 53.54.

Mass spectrometry was attempted to confirm compound identity but fragmentation occurred with several mass spectrometry techniques. The azide **8c** was successfully used to form triazole **95c**.

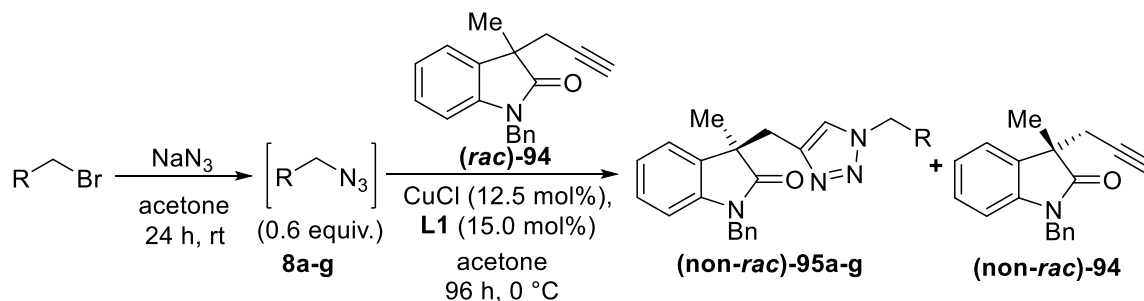
7.2.4.2 Catalysis

General procedure for oxindole kinetic resolution screening



To an oven-dried Radleys multi reactor tube, under an atmosphere of nitrogen, were added **L1** (0.0067 g, 0.018 mmol, 15.0 mol%) and CuCl (0.0015 g, 0.015 mmol, 12.5 mol%) followed by 2,5-hexanedione (1 mL). After the solution was stirred at rt for 1 h, compound **94** (0.033 g, 0.12 mmol, 1.0 equiv) dissolved in 2,5-hexanedione (1 mL) was added. The reaction mixture was stirred for a further 15 min at rt and then cooled to 0 °C for another 15 min. Benzyl azide (0.0095 g, 0.07 mmol, 0.6 equiv) was then added. The resulting mixture was maintained at 0 °C for 96 h with stirring. The reaction was quenched with aqueous ammonia solution 5% v/v (10 mL) and extracted with diethyl ether (2 x 25mL), dried over MgSO₄ and concentrated under reduced pressure. A ¹H NMR spectrum of the crude reaction mixture was taken to determine conversion. The remaining starting material and the triazolic product were then isolated by automated flash column chromatography combiflash Rf (petroleum ether/diethyl ether 0-100% gradient 15 min followed by 100% EtOAc, 5 min) and enantiomeric excess determined by HPLC with a chiral stationary phase.

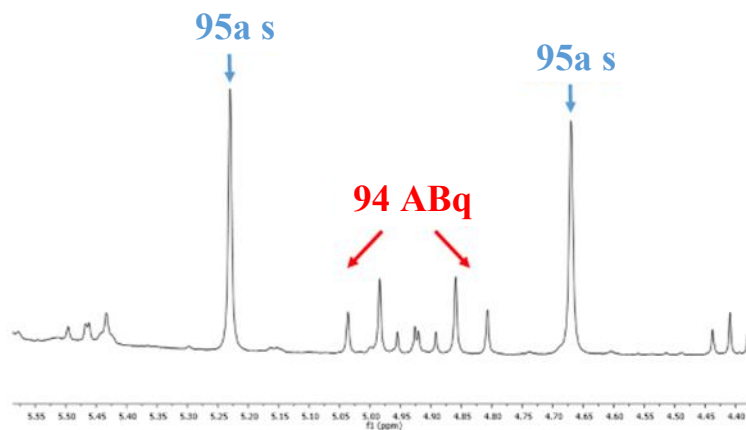
Representative procedure for oxindole kinetic resolution screening using *in situ* azide formation



4-Nitrobenzyl bromide (0.015 g, 0.07 mmol, 0.6 equiv) was stirred at rt with sodium azide (0.0052 g, 0.08 mmol, 1.1 equiv) in acetone (5 mL) for 10 h. In a separate reaction vessel, a solution of **L1** (0.0067 g, 0.018 mmol, 15.0 mol%) and CuCl (0.0015 g, 0.015 mmol, 12.5 mol%) in acetone (1mL) was stirred for 1 h at rt. To this a solution of **94** (0.033 g, 0.12 mmol, 1.0 equiv) in acetone (1 mL) was added. The reaction was cooled to 0°C and stirred for 30 minutes. The azide formation solution was then transferred by syringe and the combined solution was maintained at 0°C for 96 h. The reaction was quenched with aqueous ammonia 5% v/v (10 mL) and extracted with diethyl ether (2 x 25 mL). The combined organic layers were combined, dried over MgSO₄ and concentrated under reduced pressure. The remaining starting material and the triazolic product were isolated by automated flash column chromatography, combiflash Rf (petroleum ether/diethyl ether 0-100% gradient 15 min followed by 100% EtOAc 5 min) and enantiomeric excess determined by HPLC with a chiral stationary phase.

Representative determination of conversion *via* ^1H NMR Spectroscopy

Conversion of alkyne **94** to triazole **95a** was determined by direct comparison of the integrations of a series of peaks in the ^1H NMR spectrum of the resolution reaction mixture. Due to the high boiling point of 2,5-hexanedione it was only possible to remove this *via* column chromatography therefore HPLC was not an appropriate manner for conversion analysis. The signals in the benzylic region were used as this was a clear area away from any interference from remaining solvent. The ABq centred at 4.96 ppm of compound **94** (Bn CH₂) was directly compared with the two singlets at 5.28 ppm (Bn CH₂) and 4.70 ppm (Bn CH₂) of compound **95a**. A representative example is shown in Figure 43. When the azide was varied the analogous signals in the triazolic product were used.



$$\text{Integration per proton in } \mathbf{94} = \frac{1.00 + 0.95}{2} = 0.98$$

$$\text{Integration per proton in } \mathbf{95a} = \frac{1.90 + 1.84}{2} = 0.94$$

$$\% \text{ Conversion} = \frac{0.94}{0.94 + 0.98} \times 100 = 49\%$$

Figure 43 Determination of conversion from oxindole **94** to triazole **95a**

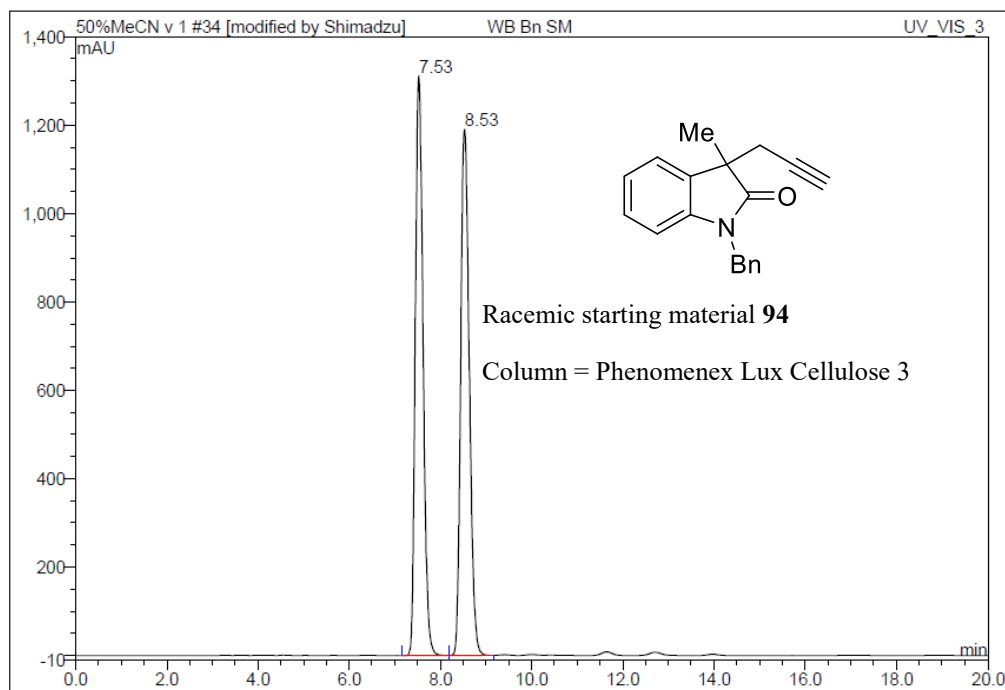
7.2.5 Kinetic Resolution of Quaternary Oxindoles Chromatography

7.2.5.1 Chiral HPLC Trace of Racemic Compound 94

Operator: Shimadzu Timebase: LC_System1 Sequence: 50% MeCN v 1

Page 1-1
18/2/2015 3:48 PM

34 WB Bn SM			
Cell-3 50% MeCN 50% water, 1ml/min			
Sample Name:	WB Bn SM	Injection Volume:	10.0
Vial Number:	1_2	Channel:	UV_VIS_3
Sample Type:	unknown	Wavelength:	n.a.
Control Program:	50% MeCN v 1	Bandwidth:	n.a.
Quantif. Method:	50% MeCN v 1	Dilution Factor:	1.0000
Recording Time:	28/8/2014 13:32	Sample Weight:	1.0000
Run Time (min):	20.01	Sample Amount:	1.0000



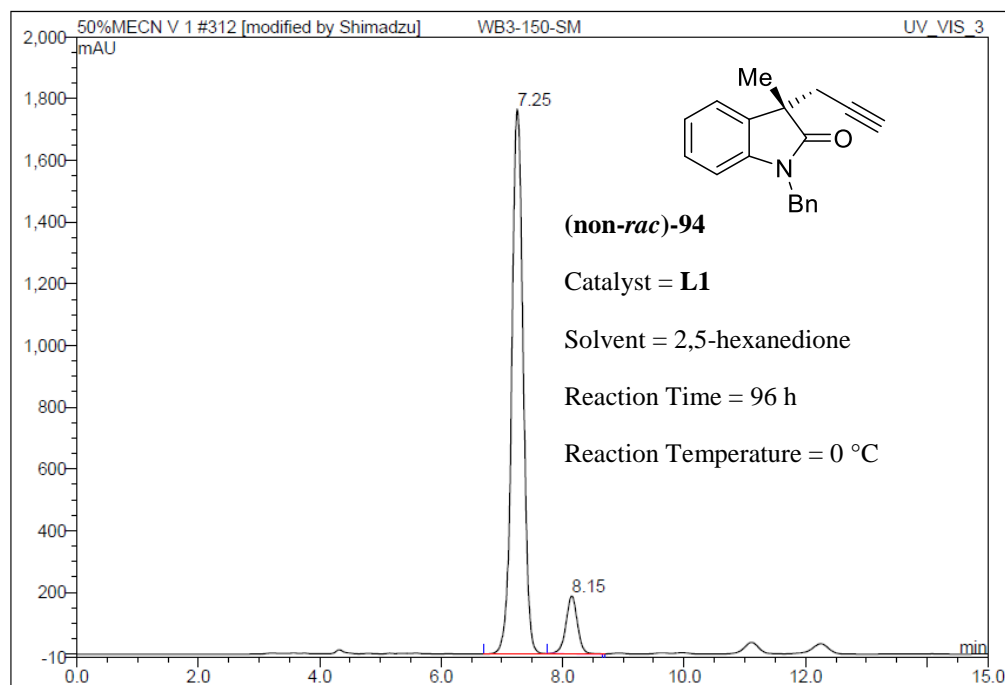
No.	Ret.Time min	Peak Name	Height mAU	Area mAU*min	Rel.Area %	Amount	Type
1	7.53	n.a.	1311.427	259.060	49.82	n.a.	BM
2	8.53	n.a.	1189.898	260.893	50.18	n.a.	MB
Total:			2501.325	519.952	100.00	0.000	

7.2.5.2 Chiral HPLC Trace of Enantioenriched Compound 94

Operator: Shimadzu Timebase: LC_System1 Sequence: 50%MECN V 1

Page 1-1
5/5/2015 4:16 PM

312 WB3-150-SM			
50% MeCN 50% Water Cell-3, 1mL/min			
Sample Name:	WB3-150-SM	Injection Volume:	10.0
Vial Number:	1_6	Channel:	UV_VIS_3
Sample Type:	unknown	Wavelength:	n.a.
Control Program:	50% MeCN v 1	Bandwidth:	n.a.
Quantif. Method:	50% MeCN v 1	Dilution Factor:	1.0000
Recording Time:	21/3/2015 19:35	Sample Weight:	1.0000
Run Time (min):	30.01	Sample Amount:	1.0000



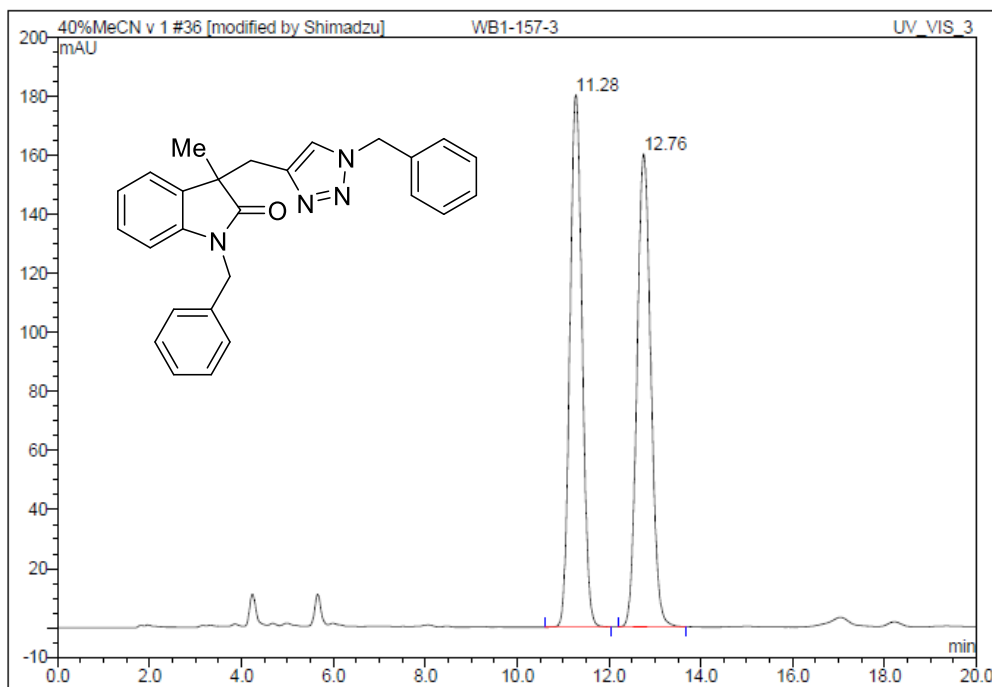
No.	Ret.Time min	Peak Name	Height mAU	Area mAU*min	Rel.Area %	Amount	Type
1	7.25	n.a.	1765.969	383.333	90.40	n.a.	BMB
2	8.15	n.a.	186.806	40.689	9.60	n.a.	Rd
Total:			1952.775	424.023	100.00	0.000	

7.2.5.3 Chiral HPLC Trace of Racemic Compound 95a

Operator:Shimadzu Timebase:LC_System1 Sequence:40%MeCN v 1

Page 1-1
5/5/2015 4:04 PM

36 WB1-157-3			
Cell-3 40% MeCN 60% water, 1ml/min			
Sample Name:	WB1-157-3	Injection Volume:	10.0
Vial Number:	1_5	Channel:	UV_VIS_3
Sample Type:	unknown	Wavelength:	n.a.
Control Program:	40% MeCN v 1	Bandwidth:	n.a.
Quantif. Method:	40% MeCN v 1	Dilution Factor:	1.0000
Recording Time:	28/8/2014 15:00	Sample Weight:	1.0000
Run Time (min):	27.18	Sample Amount:	1.0000



No.	Ret.Time min	Peak Name	Height mAU	Area mAU*min	Rel.Area %	Amount	Type
1	11.28	n.a.	180.202	55.610	49.83	n.a.	BMB
2	12.76	n.a.	160.133	55.988	50.17	n.a.	BMB
Total:			340.335	111.598	100.00	0.000	

7.2.5.4 Chiral HPLC Trace of Enantioenriched Compound 95a

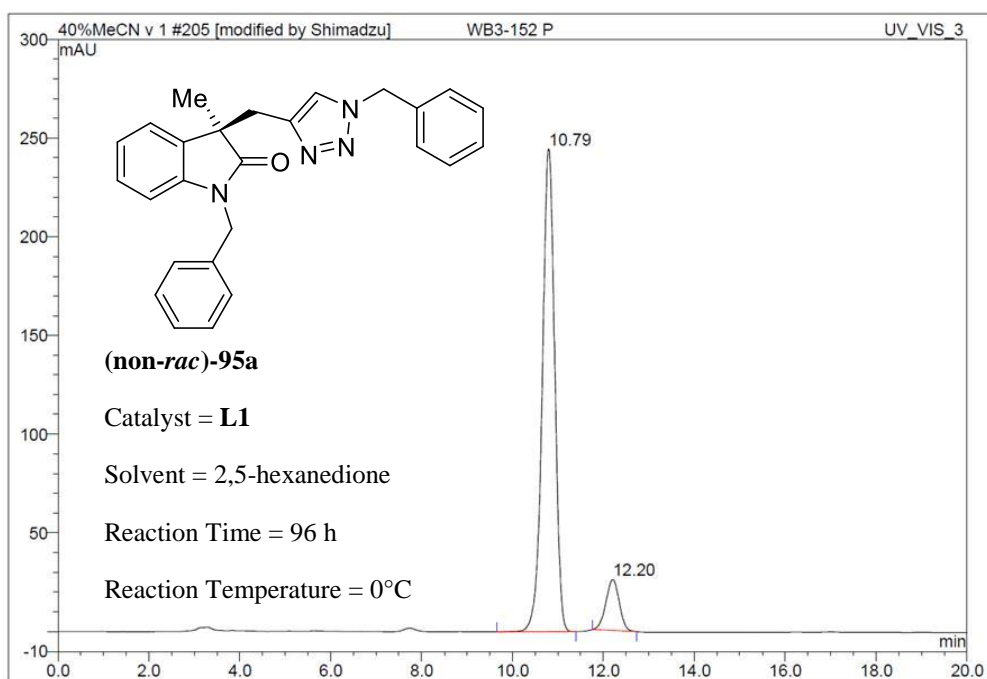
Operator: Shimadzu Timebase: LC_System1 Sequence: 40% MeCN v 1

Page 1-1
5/5/2015 4:11 PM

205 WB3-152 P

40% MeCN 60% water Cell-3, 1ml/min

Sample Name:	WB3-152 P	Injection Volume:	10.0
Vial Number:	1_9	Channel:	UV_VIS_3
Sample Type:	unknown	Wavelength:	n.a.
Control Program:	40% MeCN v 1	Bandwidth:	n.a.
Quantif. Method:	40% MeCN v 1	Dilution Factor:	1.0000
Recording Time:	31/3/2015 15:12	Sample Weight:	1.0000
Run Time (min):	30.01	Sample Amount:	1.0000

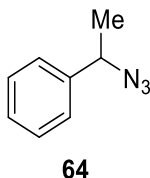


No.	Ret.Time min	Peak Name	Height mAU	Area mAU*min	Rel.Area %	Amount	Type
1	10.79	n.a.	244.634	77.375	89.78	n.a.	BMB
2	12.20	n.a.	25.753	8.810	10.22	n.a.	BMB*
Total:			270.387	86.184	100.00	0.000	

7.2.6 Simultaneous Kinetic Resolution of Azides and Alkynes

7.2.6.1 Synthesis

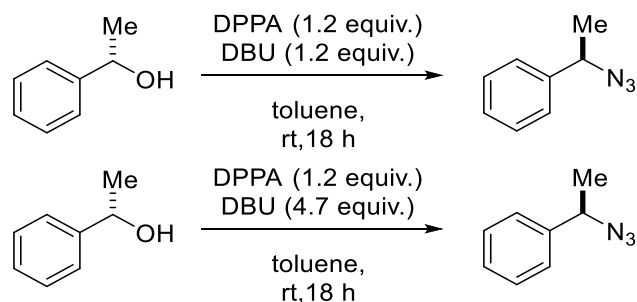
Synthesis of (1-Azidoethyl)benzene (**64**)



To a solution of sodium azide (105 mg, 1.61 mmol) in DMSO (6 mL) was added (1-bromoethyl)benzene (200 μ L, 271 mg, 1.47 mmol). The reaction mixture was stirred at rt for 2 h. To this mixture was added water (10 mL) and the mixture was extracted with ether (3 x 10 mL). The organic extracts were combined, washed sequentially with water (2 x 10 mL) and brine (10 mL) and then dried over MgSO_4 , filtered and concentrated under reduced pressure to give (1-azidoethyl)benzene **64** as a pale yellow oil, in 40% (84 mg) yield.

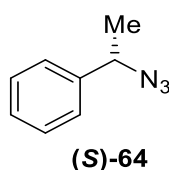
Characterisation data were in agreement with reported literature values.^[158] ^1H NMR (300 MHz, CDCl_3) δ 7.40 –7.25 (m, 5H, Ar-H), 4.60 (q, J = 6.8, 1H, CH), 1.52 (d, J = 6.8, 3H, CH_3); ^{13}C NMR (101 MHz, CDCl_3) δ 140.90, 128.80, 128.15, 126.41, 61.12, 21.59; IR ν_{max} (ATR)/ cm^{-1} 3032, 2979, 2090, 1244; MS AP^+ m/z 120.1 ($[\text{M}-\text{N}_2+\text{H}]^+$, 100%); GC (CP-Chirasil-Dex CB), FID, t_{minor} = 28.1 min, t_{major} = 28.4 min.

General Procedure for the Synthesis of Enantiopure Azides



Under an atmosphere of nitrogen, the corresponding alcohol (2.54 mmol, 1.0 equiv.) was dissolved in anhydrous toluene (4 mL) to this was added diphenylphosphoryl azide (DPPA) (633 μ L, 810 mg, 2.94 mmol, 1.2 equiv.). The mixture was cooled to 0 °C for 5 min and DBU (440 μ L, 448 mg, 2.94 mmol, 1.2 equiv.) added. The reaction mixture was allowed to warm to room temperature and stirred for 18 h. The reaction was subsequently quenched with water (10 mL) and aq. HCl 5% v/v (10 mL) and extracted with EtOAc (2 x 10 mL). The organic phases were combined and dried over MgSO₄ and concentrated under reduced pressure, the crude residue was purified by flash column chromatography (20:1 hexane /EtOAc).

(S)-(1-Azidoethyl)benzene ((S)-64)

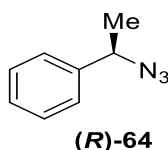


Prepared from (*R*)-phenylethanol according to the general procedure. Product was a colourless oil (**(S)-64**) formed in a 35% yield (131 mg).

Characterisation data were in agreement with reported literature values.^[79] ¹H NMR (300 MHz, CDCl₃) δ 7.50 – 6.97 (m, 5H, Ar-H), 4.57 (q, *J* = 6.8, 1H, CH), 1.49 (d, *J* = 6.8, 3H, CH₃); ¹³C NMR (101 MHz, CDCl₃) δ 140.90, 128.80, 128.14, 126.41, 61.12, 21.80; MS ESI⁺

m/z 147.1, 105.1, 77.0 147.1 ($[M]^+$, 22%), 106.1 (25, $[M-N_3+H]^+$), 105.7 (38), 105.1 (100, $[M-N_3]^+$), 104.0 (41), 103.0 (31), 79.1 (36), 77.0 (71, $[M-C_2H_4N_3]^+$), 51.0 (35); $[\alpha]^{293}_D = -100.8^\circ$ ($c=1$, CH_2Cl_2); GC (CP-Chirasil-Dex CB), FID, $t = 28.1$ min. Literature value, $[\alpha]^{298}_D = -115.1^\circ$ ($c=1$, hexane).^[79]

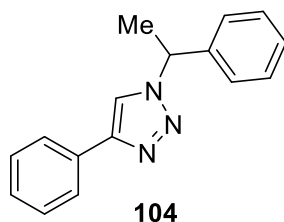
(R)-(1-Azidoethyl)benzene ((R)-64)



Prepared from (*S*)-phenylethanol according to the general procedure. Product was a colourless oil **(R)-64** formed in a 40% yield (150 mg).

1H NMR (300 MHz, $CDCl_3$) δ 7.30 – 6.94 (m, 5H, Ar-*H*), 4.46 (q, $J = 6.8$, 1H, *CH*), 1.38 (d, $J = 6.8$, 3H, *CH*₃); ^{13}C NMR (101 MHz, $CDCl_3$) δ 140.90, 128.80, 128.16, 126.41, 61.12, 21.58; MS ESI⁺ m/z 147.1 ($[M]^+$, 16%), 105.1 (100, $[M-N_3]^+$), 104.1 (27), 79.1 (24), 77.0 (62, $[M-C_2H_4N_3]^+$), 51.0 (25); $[\alpha]^{293}_D = 105.2^\circ$ ($c=1$, CH_2Cl_2); GC (CP-Chirasil-Dex CB), FID, $t = 28.4$ min.

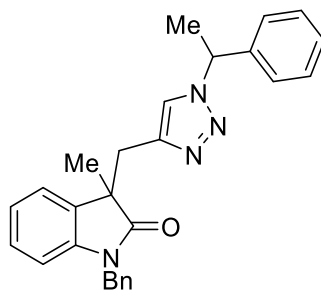
Synthesis of Racemic 4-phenyl-1-(1-phenylethyl)-1*H*-1,2,3-triazole (**104**)



Phenylacetylene (20 mg, 0.20 mmol), (1-azidoethyl)benzene **64** (30 mg, 0.20 mmol) and sodium ascorbate (39 mg, 0.20 mmol) were added to a solution of $\text{CuSO}_4 \cdot 5\text{H}_2\text{O}$ (5.0 mg, 0.020 mmol) in MeOH (4 mL). The reaction mixture was stirred for 24 h at rt. The reaction mixture was quenched with aq. ammonia solution 5% v/v (5 mL) and extracted with EtOAc (2 x 10 mL). The combined organic extracts were dried over MgSO_4 and concentrated under reduced pressure to yield 4-phenyl-1-(1-phenylethyl)-1*H*-1,2,3-triazole **104** as a cream solid in a 26% yield (13 mg).

Characterisation data were consistent with reported literature values.^[159] ^1H NMR (300 MHz, CDCl_3) δ 7.82 – 7.76 (m, 2H, Ar-*H*), 7.64 (s, 1H, CH), 7.45 – 7.26 (m, 8H, Ar-*H*), 5.86 (q, $J = 7.1$, 1H, CH), 2.02 (d, $J = 7.1$, 3H, CH_3); ^{13}C NMR (101 MHz, CDCl_3) δ 147.80, 139.92, 130.67, 129.07, 128.79, 128.58, 128.10, 126.55, 125.69, 118.40, 60.29, 21.32; IR ν_{max} (ATR)/ cm^{-1} 3090, 2991; MS ESI⁺ m/z 272.1, 250.1 272.1 ($[\text{M}+\text{Na}]^+$, 100%), 250.1 (7, $[\text{M}+\text{H}]^+$), 146.1 (20, $[\text{M}-\text{C}_6\text{H}_5\text{CHCH}_3+\text{H}]^+$); HPLC (Phenomenex Cellulose 1) acetonitrile/water 60:40, 1.0 mL/min, $\lambda = 210$ nm, $t_{\text{minor}} = 8.4$ min, $t_{\text{major}} = 9.1$ min.

Synthesis of 1-benzyl-3-methyl-3-((1-(1-phenylethyl)-1*H*-1,2,3-triazol-4-yl)methyl)indolin-2-one (**105**)



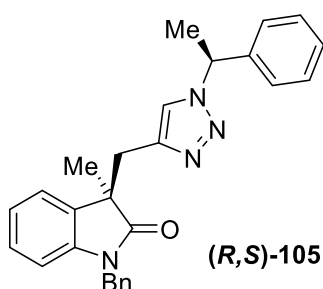
105

To a solution of 1-benzyl-3-methyl-3-(prop-2-yn-1-yl)indolin-2-one **94** (100 mg, 0.36 mmol) in acetone (5 mL) was added copper(I) chloride (1.8 mg, 0.018 mmol), TBTA (9.6 mg, 0.018 mmol) and (1-azidoethyl)benzene **64** (60 mg, 0.40 mmol,) in acetone (1 mL). The mixture was heated to reflux and stirred for 96 h. The reaction mixture was then quenched with aq. ammonia 5% v/v (5 mL) and extracted with EtOAc (3 x 10 mL). The combined organic extracts were washed with water (10 mL), dried over MgSO₄ and concentrated under reduced pressure. The crude residue was purified by automated flash column chromatography combiflash Rf (0-100% hexane/EtOAc gradient, 12 min) to yield the triazole **105** as a colourless oil in a 42% yield (65 mg). Reported as a mixture of diastereoisomers (*dr* = 50:50).

¹H NMR (400 MHz, CDCl₃) δ 7.32-7.19 (m, 6H, Ar-*H*), 7.15-7.02 (m, 4H, Ar-*H*), 7.00-6.88 (m, 3H, Ar-*H*), 6.72 (s, 0.5H, CH), 6.68 (s, 0.5H, CH), 6.56-6.48 (m, 1H, Ar-*H*), 5.62-5.54 (m, 1H, CH), 4.76-4.55 (m, 2H, CH₂), 3.38-3.16 (m, 2H, CH₂), 1.79 (d, *J* = 7.1, 1.5H, CH₃), 1.69 (d, *J* = 7.1, 1.5H, CH₃), 1.52 (s, 1.5H, CH₃), 1.51 (s, 1.5H, CH₃); ¹³C NMR (101 MHz, CDCl₃) δ 179.93, 142.97, 142.88, 142.17, 140.24, 140.19, 135.97, 135.86, 132.97, 128.86, 128.71, 128.20, 128.16, 127.80, 127.51, 127.48, 127.29, 127.19, 126.20, 126.17, 123.30, 123.22, 122.52, 122.45, 120.80, 120.39, 108.85, 108.77, 59.78, 59.56, 48.57, 48.54, 43.51,

34.49, 34.45, 23.32, 21.17, 20.81; IR ν_{\max} (ATR)/ cm^{-1} 3032, 2968, 2925, 1705, 1610; MS ESI⁺ m/z , 446.2 ($[\text{M}+\text{Na}+\text{H}]^+$, 22%), 445.2 (100, $[\text{M}+\text{Na}]^+$), 423.2 (9, $[\text{M}+\text{H}]^+$); HRMS ESI⁺ Calculated for $\text{C}_{27}\text{H}_{26}\text{N}_4\text{ONa}^+$ = 445.1999 Found 445.2007; HPLC (Cellulose 3) acetonitrile/water 30:70, 1.0 mL/min, λ = 210 nm, 45 min, 55 min, 59 min, 67 min.

Synthesis of (*R*)-1-benzyl-3-methyl-3-((1-((*S*)-1-phenylethyl)-1*H*-1,2,3-triazol-4-yl)methyl)indolin-2-one (*R,S*)-105

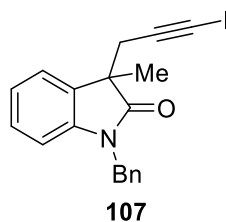


To a solution of (*R*)-1-benzyl-3-methyl-3-(prop-2-yn-1-yl)indolin-2-one (***R***-94 (30 mg, 0.11 mmol) in methanol (5 mL) was added (*S*)-(1-azidoethyl)benzene (***S***-64 (16 mg, 0.11 mmol), $\text{CuSO}_4 \cdot 5\text{H}_2\text{O}$ (3 mg, 0.011 mmol) and NaAsc (5 mg, 0.022 mmol). The reaction was stirred at 50 °C for 24 h. The reaction was quenched with the addition of aq. ammonia solution 5% v/v (5 mL), the reaction mixture was then extracted with EtOAc (2 x 10 mL). The combined organic fractions were dried over MgSO_4 and concentrated under reduced pressure. The crude residue was purified by automated flash column chromatography combiflash Rf (0-100% hexane/EtOAc gradient, 15 min). This yielded (*R*)-1-benzyl-3-methyl-3-((1-((*S*)-1-phenylethyl)-1*H*-1,2,3-triazol-4-yl)methyl)indolin-2-one (***R,S***-105 as a yellow oil in a 62% yield (29 mg).

¹H NMR (400 MHz, CDCl_3) δ 7.29 – 7.18 (m, 6H, Ar-*H*), 7.14 – 7.07 (m, 3H, Ar-*H*), 7.04 (td, J = 7.7, 1.3, 1H, Ar-*H*), 6.97 – 6.89 (m, 3H, Ar-*H*), 6.72 (s, 1H, Triazole CH), 6.50 (d, J =

7.7, 1H, Ar-*H*), 5.57 (q, $J = 7.1$, 1H, *CH*), 4.65 (ABq, $\Delta\delta_{AB} = 0.14$, $J = 15.6$, 2H, *CH*₂), 3.27 (ABq, $\Delta\delta_{AB} = 0.14$, $J = 14.3$, 2H, *CH*₂), 1.79 (d, $J = 7.1$, 3H, *CH*₃), 1.51 (s, 3H, *CH*₃); ¹³C NMR (101 MHz, CDCl₃) δ 179.92, 142.88, 142.16, 140.25, 135.91, 132.98, 128.85, 128.70, 128.15, 127.79, 127.48, 127.19, 126.16, 123.22, 122.44, 120.80, 108.84, 59.78, 48.53, 43.50, 34.45, 23.32, 21.16; MS AP⁺ m/z 424.2 (53%), 424.2 (100, [M+H]⁺), 424.2 (28), 319.2 (29 [M-C₆H₅CHCH₂]); HRMS AP⁺ Calculated for C₂₇H₂₆N₄O⁺ = 423.2179 Found 423.2187; IR ν_{\max} (ATR)/cm⁻¹ 2925, 2855, 1707, 1489, 1467, 1356, 1174, 855, 741, 698; HPLC (Phenomenex Cellulose 3) acetonitrile/water 30:70, 1.0 mL/min, $\lambda = 250$ nm, $t = 49$ min.

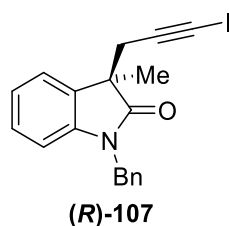
Synthesis of 1-benzyl-3-(3-iodoprop-2-yn-1-yl)-3-methylindolin-2-one (**107**)



Iodine (51 mg, 0.20 mmol) was dissolved in toluene (5 mL) and morpholine (261 mg, 3.0 mmol) was added. The mixture was stirred at room temperature for 30 min. After that, racemic 1-benzyl-3-methyl-3-(prop-2-yn-1-yl)indolin-2-one **94** (50 mg, 0.18 mmol) was added, and the mixture was stirred at 50 °C for 72 h. Water (5 mL) was then added and the mixture was extracted with ethyl acetate (2 x 5 mL). The combined organic layers were dried over MgSO₄. The solvent was removed under reduced pressure. The crude material was then purified by automated column chromatography combiflash (Rf: 0-100% hexane/EtOAc gradient, 20 min). This gave 1-benzyl-3-(3-iodoprop-2-yn-1-yl)-3-methylindolin-2-one **107** as a pale yellow solid in a 92% yield (66 mg).

^1H NMR (400 MHz, CDCl_3) δ 7.39 – 7.22 (m, 6H, Ar-*H*), 7.17 (app td, $J = 7.7, 1.3$, 1H, Ar-*H*), 7.05 (app td, $J = 7.5, 1.1$, 1H, Ar-*H*), 6.71 (d, $J = 7.7$, 1H, Ar-*H*), 4.92 (ABq, $\Delta\delta_{\text{AB}} = 0.24$, $J = 15.8$, 2H, CH_2), 2.85 (ABq, $\Delta\delta_{\text{AB}} = 0.16$, $J = 16.6$, 2H, CH_2), 1.49 (s, 3H, CH_3); ^{13}C NMR (101 MHz, CDCl_3) δ 179.24, 142.07, 135.74, 132.77, 128.90, 128.19, 127.51, 127.15, 123.22, 122.68, 109.19, 90.04, 47.13, 43.80, 29.99, 22.37, -3.61; IR ν_{max} (ATR)/ cm^{-1} 2964, 2924, 1714, 1610, 1490, 1455, 1359, 1321, 1182, 1154, 754; MS ESI $^+$ m/z 424.0 ($[\text{M}+\text{Na}]^+$, 100%); HRMS ESI $^+$ Calculated for $\text{C}_{19}\text{H}_{16}\text{NONa}^+$ = 424.0168 Found 424.0178; MP 140 – 143°C; HPLC (Phenomenex Cellulose 3) acetonitrile/water 50:50, 1.0 mL/min, $\lambda = 210$ nm, $t_{\text{S}} = 10.7$ min, $t_{\text{R}} = 14.4$ min

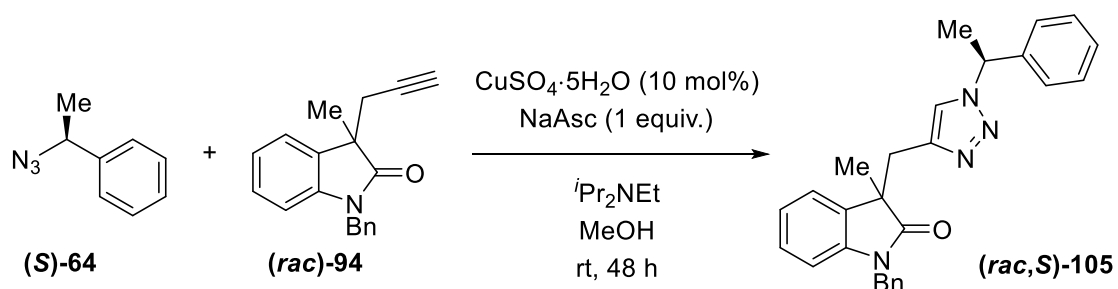
Synthesis of (*R*)-1-benzyl-3-(3-iodoprop-2-yn-1-yl)-3-methylindolin-2-one ((*R*)-107)



Iodine (51 mg, 0.20 mmol) was dissolved in toluene (2 mL) and morpholine (261271 mg, 3.0 mmol) was added. The mixture was stirred at room temperature for 30 min. A solution of (*R*)-1-benzyl-3-methyl-3-(prop-2-yn-1-yl)indolin-2-one (**(*R*)-94**) (50 mg, 0.18 mmol) in toluene (3 mL) was then added, and the mixture was stirred at 50 °C for 72 h. Water (5 mL) was then added and the reaction mixture extracted with EtOAc (2 x 5 mL). The combined organic layers were dried over MgSO_4 , and concentrated under reduced pressure. The crude material was purified by automated column chromatography combiflash Rf (0-100% hexane/EtOAc gradient, 20 min). This gave (*R*)-1-benzyl-3-(3-iodoprop-2-yn-1-yl)-3-methylindolin-2-one (**(*R*)-107**) as a pale yellow solid in a 74% yield (54 mg).

^1H NMR (400 MHz, CDCl_3) δ 7.38 – 7.22 (m, 6H, Ar-*H*), 7.17 (td, $J = 7.7, 1.3$, 1H, Ar-*H*), 7.05 (td, $J = 7.5, 1.0$, 1H, Ar-*H*), 6.71 (d, $J = 7.7$, 1H, Ar-*H*), 4.92 (ABq, $\Delta\delta_{\text{AB}} = 0.23$, $J = 15.7$, 2H, CH_2), 2.85 (ABq, $\Delta\delta_{\text{AB}} = 0.16$, $J = 16.6$, 2H, CH_2), 1.49 (s, 3H, CH_3); ^{13}C NMR (101 MHz, CDCl_3) δ 179.24, 142.07, 135.74, 132.77, 128.90, 128.19, 127.51, 127.15, 123.22, 122.68, 109.20, 90.04, 47.13, 43.80, 29.99, 22.37, -3.61; IR ν_{max} (ATR)/ cm^{-1} 2984, 2924, 1682, 1609, 1490, 1467, 1451, 1435, 1422, 1383, 1365, 1354, 1321, 1180, 1076, 732; MS ES^+ m/z 424.0 ($[\text{M}+\text{Na}]^+$, 100%); HRMS ESI^+ Calculated for $\text{C}_{19}\text{H}_{16}\text{NONaI}^+ = 424.0168$ Found 424.0168; MP 158 – 159°C; $[\alpha]_{\text{D}}^{293} = -42.4^\circ$ ($c=1$, CH_2Cl_2); HPLC (Phenomenex Cellulose 3) acetonitrile/water 50:50, 1.0 mL/min, $\lambda = 210$ nm, $t_{\text{R}} = 14.7$ min.

Synthesis of 1-benzyl-3-methyl-3-(1-((*S*)-1-phenylethyl)-1*H*-1,2,3-triazol-4-yl)indolin-2-one ((*rac,S*)-107)

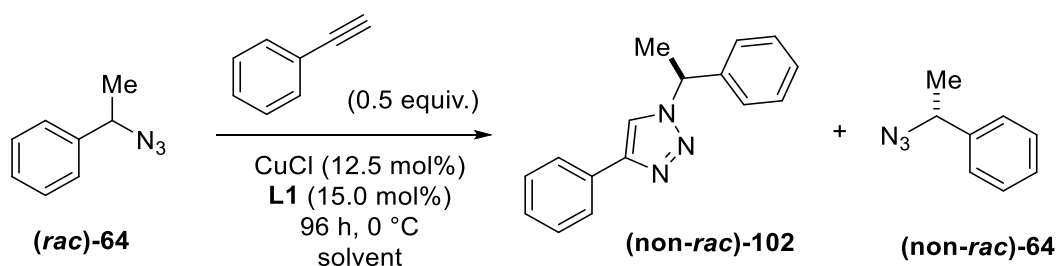


Compound **94** (85 mg, 0.31 mmol) and (**S**)-**64** (50 mg, 0.34 mmol) were dissolved in MeOH (5 mL). To this solution was added $\text{CuSO}_4 \cdot 5\text{H}_2\text{O}$ (7.7 mg, 0.031 mmol) and NaAsc (61 mg, 0.31 mmol) and the mixture stirred for 5 min at rt. *N,N*-diisopropylethylamine (100 μL , 7.4 mg, 5 mol%) was added and the mixture left to stir at rt for 48 h. The reaction mixture was quenched by the addition of aqueous ammonia solution 5% v/v (5 mL). The resulting solution was extracted with EtOAc (3 x 10 mL). The combined organic extracts were washed with water (10 mL), dried over MgSO_4 and concentrated under reduced pressure. The recovered material was purified by automated flash column chromatography combiflash Rf (0-100%

hexane/EtOAc gradient 12 min). This gave 1-benzyl-3-methyl-3-(1-((*S*)-1-phenylethyl)-1*H*-1,2,3-triazol-4-yl)indolin-2-one (***rac,S***-**105**) as a colourless oil in a 57% yield (72 mg). The ¹H NMR spectrum of the product was consistent with compound **105**. HPLC (Phenomenex Cellulose 3) acetonitrile/water 30:70, 1.0 mL/min, $\lambda = 210$ nm, 45 min, 67 min.

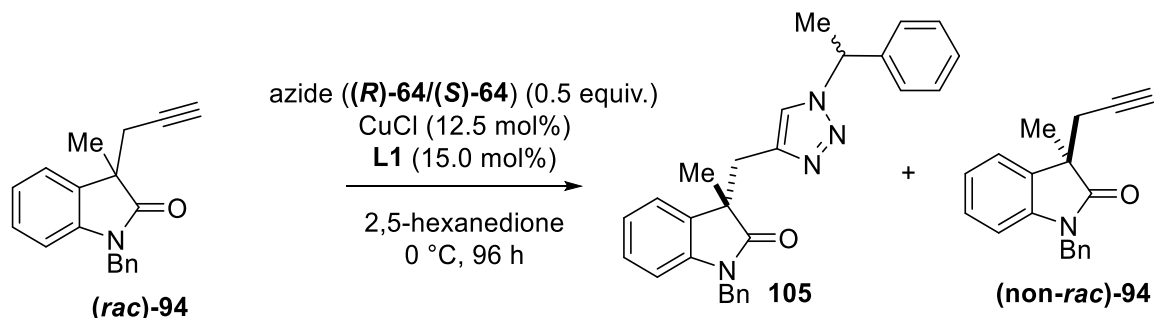
7.2.6.2 Catalysis

Representative Procedure for Kinetic Resolution of (1-Azidoethyl)benzene (**64**)



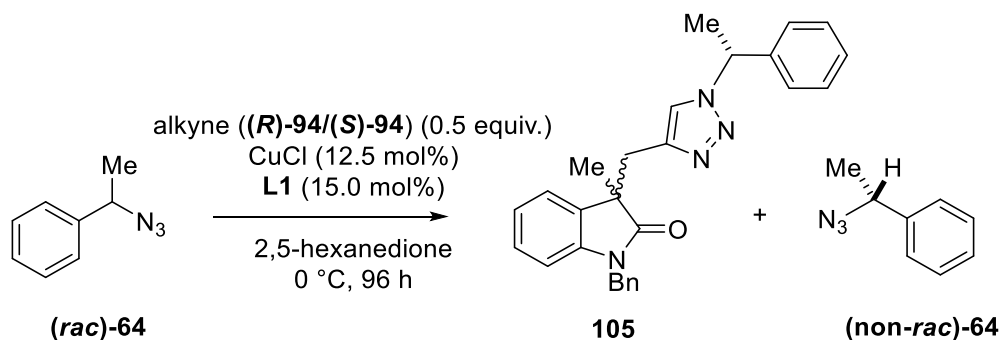
To an oven dried Radley's multi-reactor tube were added L1 (6.7 mg, 0.018 mmol, 15.0 mol%), CuCl (1.5 mg, 0.015 mmol, 12.5 mol%) and 2,5-hexanedione (1 mL). The mixture was stirred at rt for 1 h. To this solution was added phenylacetylene (6.2 mg, 0.06 mmol, 0.5 equiv.) in 2,5-hexanedione (0.5 mL) and the resulting mixture stirred for 15 min at rt before being cooled to 0 °C and stirred for a further 15 min. (1-Azidoethyl)benzene **64** (17.8 mg, 0.12 mmol, 1 equiv.) in 2,5-hexanedione (0.5 mL) was then added and the reaction mixture stirred for 96 h at 0 °C. The reaction mixture was then quenched with the addition of aq. ammonia solution 5% v/v (5 mL), then extracted with ether (2 x 10 mL). The combined organic extracts were dried over MgSO₄ and concentrated under reduced pressure. Conversion of the reaction was determined through ¹H NMR spectroscopy of the recovered crude material. Enantiomeric excess was determined by chiral GC. The remaining azide and triazolic product were isolated by automated flash column chromatography combiflash Rf (0-40% hexane/EtOAc, 15 min).

General Procedure for the Kinetic Resolution of **94** with Azide **64**



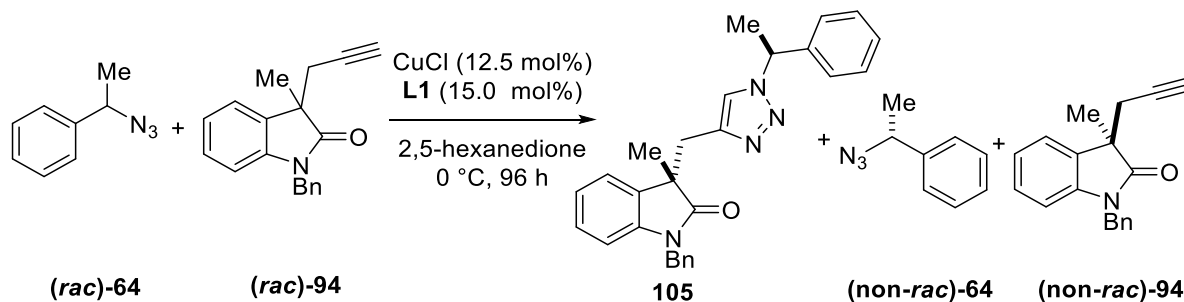
To an oven dried Radley's multi-reactor tube **L1** (6.7 mg, 0.018 mmol, 15.0 mol%) and **CuCl** (1.5 mg, 0.015 mmol, 12.5 mol%) followed by 2,5-hexanedione (1 mL) were added. After stirring at rt for 1 h, compound **94** (33.4 mg, 0.12 mmol, 1 equiv.) dissolved in 2,5-hexanedione (0.5 mL) was added. The reaction mixture was stirred for a further 15 min before being cooled to 0 °C for 15 min. Azide **(R)-64** (8.9 mg, 0.06 mmol, 1 equiv.) dissolved in 2,5-hexanedione was then added. The reaction mixture was stirred at 0 °C for 96 h. The reaction was then quenched by addition of aqueous ammonia 5% v/v (5 mL). The reaction mixture was then extracted with ethyl acetate (2 x 10 mL), dried over **MgSO₄** and concentrated under reduced pressure. Conversion was determined by integration of the ¹H NMR spectrum of the recovered material. The remaining starting material and the triazolic product were subsequently isolated by automated column chromatography combiflash Rf (0-100% hexane/EtOAc gradient 12 min). Enantiomeric excess and diastereomer ratio of **105** and enantiomeric excess of **94** were determined by HPLC using a chiral stationary phase.

General Procedure for the Kinetic Resolution of **62** with Alkyne **92**



To an oven dried Radley's multi-reactor tube was added **L1** (6.7 mg, 0.018 mmol, 15.0 mol%) and **CuCl** (1.5 mg, 0.015 mmol, 12.5 mol%) followed by 2,5-hexanedione (1 mL), the resulting solution to stirred at rt for 1 h. After this time compound **94** (16.7 mg, 0.06 mmol, 0.5 equiv.) dissolved in 2,5-hexanedione (0.5 mL) was added. The reaction mixture was stirred at rt for a further 15 min after which it was cooled to 0 °C in an ice bath and stirred for a further 15 min. After this azide **64** (17.8 mg, 0.12 mmol, 1 equiv.) dissolved in 2,5-hexanedione (0.5 mL) was added. The reaction mixture was stirred for 96 h at 0 °C before being quenched by the addition of aqueous ammonia 5% v/v (5 mL). The resulting solution was extracted with EtOAc (2 x 10 mL), the combined organic fractions were dried over **MgSO₄** and concentrated under reduced pressure. GC using a chiral stationary phase was carried out on the recovered material to measure the *ee* of the remaining azide **64**. The remaining crude material was purified by automated flash column chromatography combiflash Rf (0-100% hexane/EtOAc gradient, 12 min). The *dr* and *ee* of the triazolic product was then determined by HPLC using a chiral stationary phase.

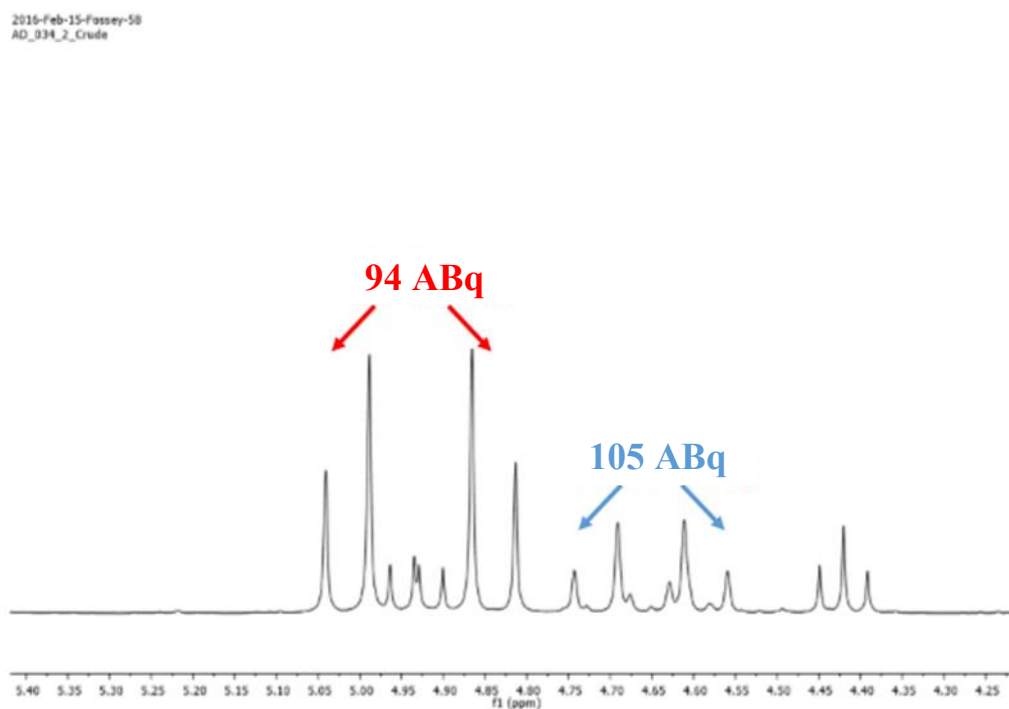
General Procedure for Simultaneous Kinetic Resolution of **94** and **64**



To an oven dried Radley's multi-reactor tube was added **L1** (6.7 mg, 0.018 mmol, 15.0 mol%) and CuCl (1.5 mg, 0.015 mmol, 12.5 mol%) followed by 2,5-hexanedione (1 mL), the resulting solution was stirred at rt for 1 h. After this time compound **94** (33.4 mg, 0.12 mmol, 1 equiv.) dissolved in 2,5-hexanedione (0.5 mL) was added. The reaction mixture was stirred at rt for a further 15 min after which it was cooled to 0 °C in an ice bath and stirred for a subsequent 15 min. After this azide **64** (17.8 mg, 0.12 mmol, 1 equiv.) dissolved in 2,5-hexanedione (0.5 mL) was added. The reaction mixture was stirred for 96 h at 0 °C before being quenched by the addition of aqueous ammonia 5% v/v (5 mL). The resulting solution was extracted with EtOAc (2 x 10 mL), the combined organic fractions were dried over MgSO₄ and concentrated under reduced pressure. GC using a chiral stationary phase was carried out on the recovered material to measure the *ee* of the remaining azide **64**. The remaining material was purified by automated flash column chromatography combiflash Rf (0-100% hexane/EtOAc gradient, 12 min). The *dr* and *ee* of the triazolic product and *ee* of the recovered alkyne **94** was then determined by HPLC using a chiral stationary phase.

Representative Determination of Conversion of Alkyne **94** to Triazole **103** via ^1H NMR Spectroscopy

Conversion of alkyne **94** to triazole **105** was determined by comparison of the integrations of signals in the crude ^1H NMR spectrum of the reaction mixture following work up after kinetic resolution. The ABq of compound **105** was compared with the ABq centred at 4.65 ppm of compound **94**.



$$\text{Integration per proton in } \mathbf{94} = 1.01$$

$$\text{Integration per proton in } \mathbf{105} = \frac{0.52 + 0.61}{2} = 0.57$$

$$\% \text{ Conversion} = \frac{0.57}{1.01 + 0.57} \times 100 = 36\%$$

Figure 44 Determination of conversion from oxindole **94** to triazole **105**

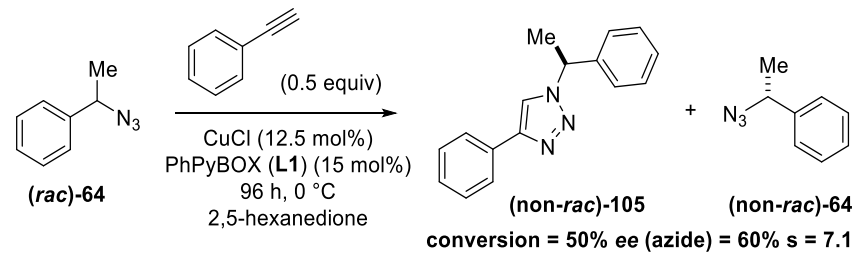
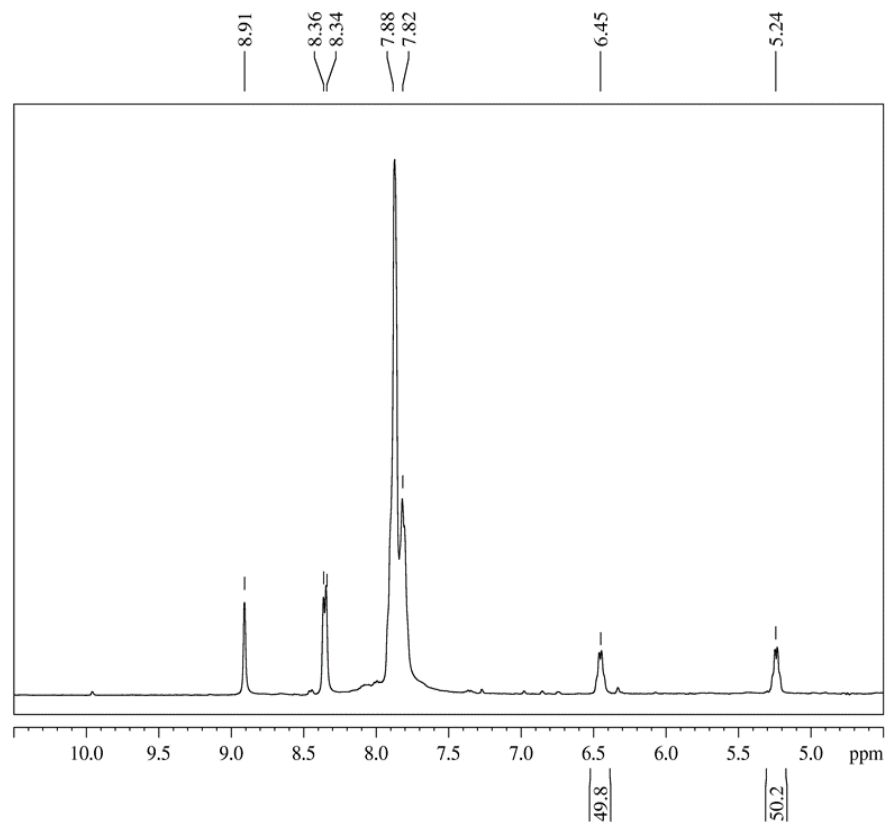
Unlocked ^1H NMR Study of the Kinetic Resolution of 64 in 2,5-Hexanedione

NMR experiments were run on a Bruker AVANCE spectrometer operating at 400 MHz for ^1H and equipped with a 5 mm Broadband (BBO) z-gradient probe.

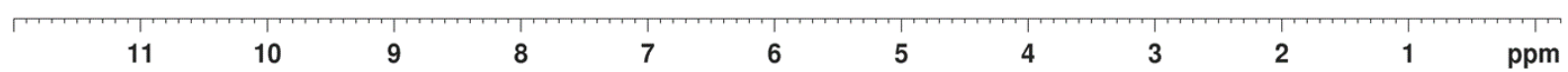
Samples in non-deuterated 2,5-hexanedione were run unlocked and shimmed directly on the solvent peaks. The ^1H spectral width was set to 16 ppm with 32000 data points. Measurements were acquired with 128 scans, a delay between scans of 10 s (to allow sufficient time for spin relaxation and therefore accurate integration), of 32000 data points and an acquisition time of 2.5 s.

The spectra were indirectly calibrated to the residual ^1H peak of deuterated chloroform at 7.26 ppm. Data were processed using an exponential multiplication window function with a line broadening of 2 Hz. The final spectral resolution was 0.19 Hz per point.

¹H NMR Spectrum Recorded Unlocked in 2,5-Hexanedione



2,5-hexanedione



¹H NMR Chemical Shifts (ppm)

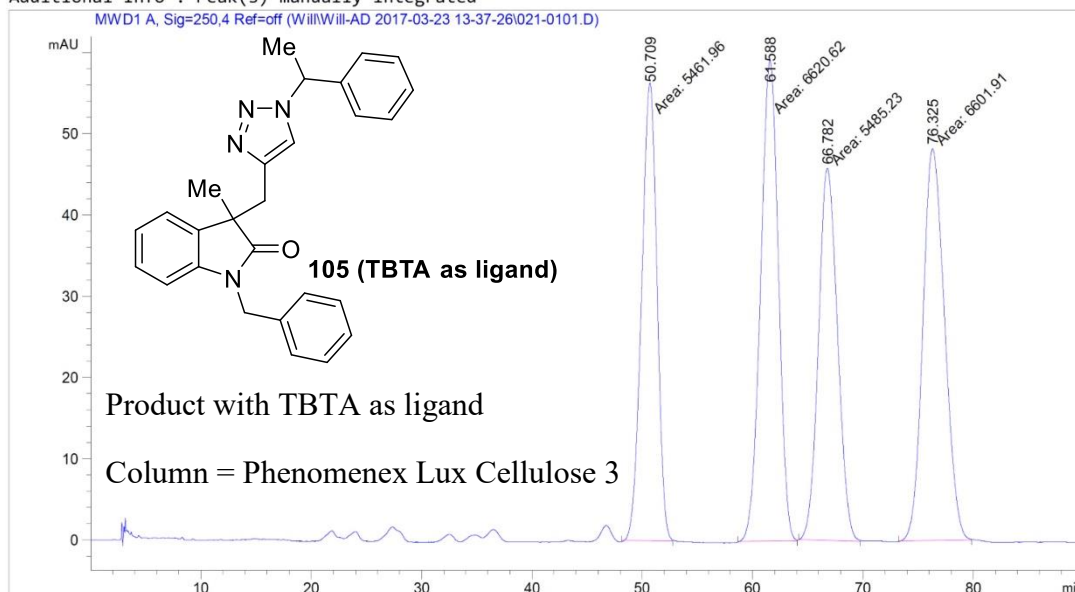
7.2.7 Simultaneous Kinetic Resolution Chromatography

7.2.7.1 Chiral HPLC Trace of Compound 105

Data File C:\Chem32\1\Data\Will\Will-AD 2017-03-23 13-37-26\021-0101.D

Sample Name: WB6-40 TBTA Reaction

```
=====
Acq. Operator   : SYSTEM                      Seq. Line :    1
Acq. Instrument : LC                        Location  :   21
Injection Date  : 3/23/2017 1:38:22 PM      Inj       :    1
                                           Inj Volume: 5.000 µl
Different Inj Volume from Sample Entry! Actual Inj Volume : 10.000 µl
Method         : C:\Chem32\1\Data\Will\Will-AD 2017-03-23 13-37-26\Oxindole5050.M (Sequence
                Method)
Last changed   : 3/23/2017 1:37:27 PM by SYSTEM
Additional Info : Peak(s) manually integrated
MWD1 A, Sig=250,4 Ref=off (Will\Will-AD 2017-03-23 13-37-26\021-0101.D)
```



Area Percent Report

```
Sorted By      : Signal
Multiplier     : 1.0000
Dilution      : 1.0000
Use Multiplier & Dilution Factor with ISTDs
```

Signal 1: MWD1 A, Sig=250,4 Ref=off

Peak #	RetTime [min]	Type	Width [min]	Area [mAU*s]	Height [mAU]	Area %
1	50.709	MM	1.6159	5461.96143	56.33541	22.5984
2	61.588	MM	1.8655	6620.61914	59.14888	27.3922
3	66.782	MM	1.9972	5485.23047	45.77386	22.6946
4	76.325	MM	2.2802	6601.91260	48.25550	27.3148

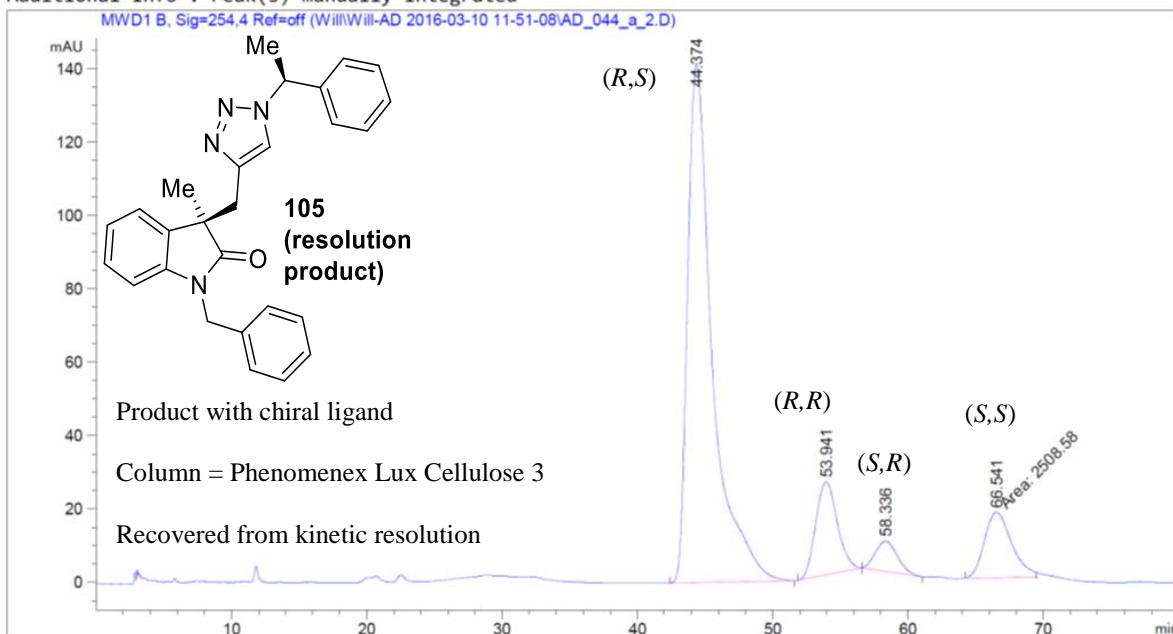
Totals : 2.41697e4 209.51366

7.2.7.2 Chiral HPLC Trace of Resolution Product 105

Data File C:\Chem32\1\Data\Will\Will-AD 2016-03-10 11-51-08\AD_044_a_2.D
 Sample Name: AD_044_a_2

```

=====
Acq. Operator   : SYSTEM                      Seq. Line :   14
Acq. Instrument : LC                        Location  :   17
Injection Date  : 3/11/2016 5:25:06 AM      Inj       :    1
                                           Inj Volume: 5.000 µl
Different Inj Volume from Sample Entry! Actual Inj Volume : 10.000 µl
Acq. Method    : C:\Chem32\1\Data\Holly\Will-AD 2016-03-10 11-51-08\Oxindole5050.M
Last changed   : 3/10/2016 11:51:08 AM by SYSTEM
Analysis Method : C:\Chem32\1\Data\Will\Will-AD 2016-03-10 11-51-08\Oxindole5050.M (Sequence
Method)
Last changed   : 3/10/2016 11:51:08 AM by SYSTEM
Additional Info : Peak(s) manually integrated
  
```



Area Percent Report

```

Sorted By      : Signal
Multiplier    : 1.0000
Dilution      : 1.0000
Use Multiplier & Dilution Factor with ISTDs
  
```

Signal 1: MWD1 B, Sig=254,4 Ref=off

Peak #	RetTime [min]	Type	Width [min]	Area [mAU*s]	Height [mAU]	Area %
1	44.374	BB	1.9074	1.78983e4	141.33484	74.0904
2	53.941	BB	1.4131	2818.38110	25.42906	11.6668
3	58.336	BB	1.3377	932.11700	8.27787	3.8585
4	66.541	MM	2.3322	2508.57983	17.92732	10.3843

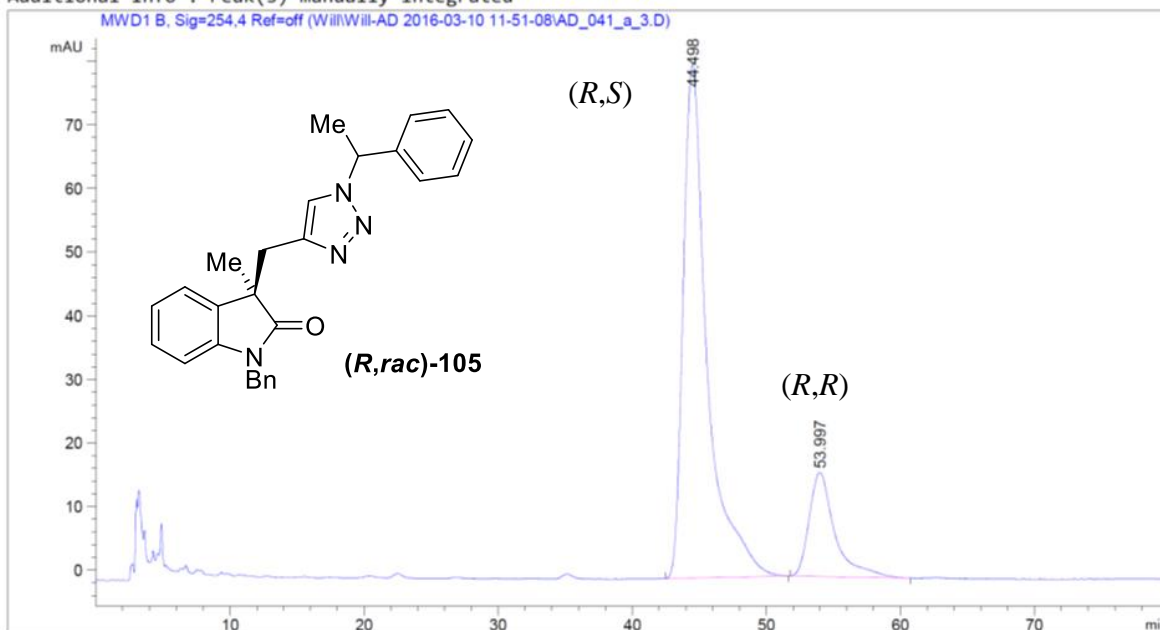
Totals : 2.41573e4 192.96909

7.2.7.3 Chiral HPLC Trace of Compound (*R,rac*)-105

Data File C:\Chem32\1\Data\Will\Will-AD 2016-03-10 11-51-08\AD_041_a_3.D
 Sample Name: AD_041_a_3

```

=====
Acq. Operator   : SYSTEM                      Seq. Line : 10
Acq. Instrument : LC                        Location  : 13
Injection Date  : 3/11/2016 12:01:08 AM      Inj       : 1
                                           Inj Volume: 5.000 µl
Different Inj Volume from Sample Entry! Actual Inj Volume : 10.000 µl
Acq. Method     : C:\Chem32\1\Data\Holly\Will-AD 2016-03-10 11-51-08\Oxindole5050.M
Last changed    : 3/10/2016 11:51:08 AM by SYSTEM
Analysis Method : C:\Chem32\1\Data\Will\Will-AD 2016-03-10 11-51-08\Oxindole5050.M (Sequence
Method)
Last changed    : 3/10/2016 11:51:08 AM by SYSTEM
Additional Info : Peak(s) manually integrated
  
```



Area Percent Report

```

=====
Sorted By      : Signal
Multiplier     : 1.0000
Dilution       : 1.0000
Use Multiplier & Dilution Factor with ISTDs
  
```

Signal 1: MWD1 B, Sig=254,4 Ref=off

Peak #	RetTime [min]	Type	Width [min]	Area [mAU*s]	Height [mAU]	Area %
1	44.498	BB	1.8134	1.00087e4	80.78741	82.1463
2	53.997	BB	1.5917	2175.29468	16.31323	17.8537

Totals : 1.21840e4 97.10063

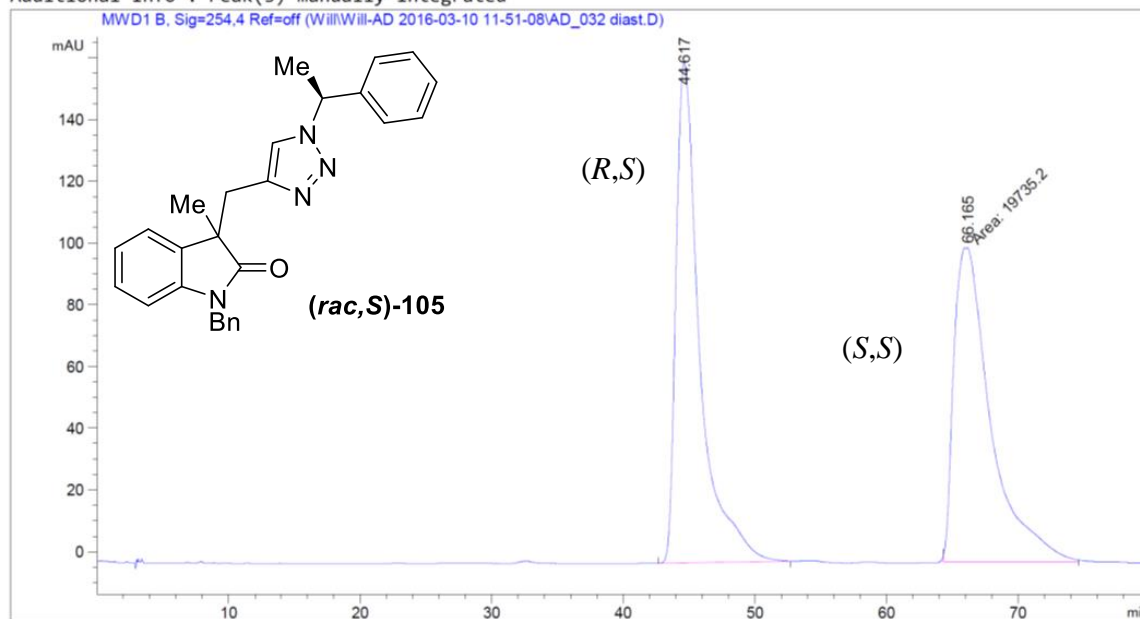
7.2.7.4 Chiral HPLC Trace of Compound (rac,S)-105

Data File C:\Chem32\1\Data\Will\Will-AD 2016-03-10 11-51-08\AD_032 diast.D

Sample Name: AD_032 diast

```

=====
Acq. Operator   : SYSTEM                      Seq. Line :    3
Acq. Instrument : LC                        Location  :    6
Injection Date  : 3/10/2016 2:34:06 PM      Inj       :    1
                                           Inj Volume: 5.000 µl
Different Inj Volume from Sample Entry! Actual Inj Volume : 10.000 µl
Acq. Method     : C:\Chem32\1\Data\Holly\Will-AD 2016-03-10 11-51-08\Oxindole5050.M
Last changed    : 3/10/2016 11:51:08 AM by SYSTEM
Analysis Method : C:\Chem32\1\Data\Will\Will-AD 2016-03-10 11-51-08\Oxindole5050.M (Sequence
Method)
Last changed    : 3/10/2016 11:51:08 AM by SYSTEM
Additional Info  : Peak(s) manually integrated
    
```



Area Percent Report

```

Sorted By      :      Signal
Multiplier     :      1.0000
Dilution       :      1.0000
Use Multiplier & Dilution Factor with ISTDs
    
```

Signal 1: MWD1 B, Sig=254,4 Ref=off

Peak #	RetTime [min]	Type	Width [min]	Area [mAU*s]	Height [mAU]	Area %
1	44.617	BB	1.8735	2.03228e4	162.23547	50.7334
2	66.165	MM	3.2339	1.97352e4	101.70866	49.2666

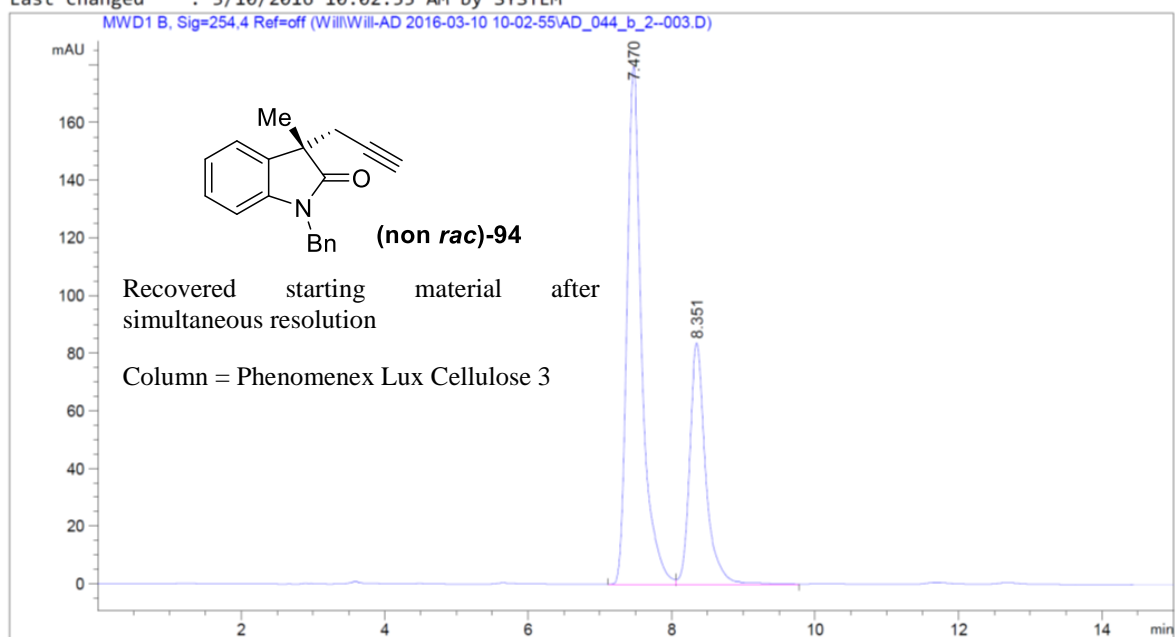
Totals : 4.00580e4 263.94413

7.2.7.5 Chiral HPLC Trace of 94 Following Simultaneous Kinetic Resolution

Data File C:\Chem32\1\Data\Will\Will-AD 2016-03-10 10-02-55\AD_044_b_2--003.D
 Sample Name: AD_044_b_2

```

=====
Acq. Operator   : SYSTEM                      Seq. Line :    3
Acq. Instrument : LC                        Location  :    3
Injection Date  : 3/10/2016 10:35:49 AM      Inj       :    1
                                           Inj Volume: 5.000 µl
Different Inj Volume from Sample Entry! Actual Inj Volume : 10.000 µl
Acq. Method    : C:\Chem32\1\Data\Holly\Will-AD 2016-03-10 10-02-55\Oxindole5050.M
Last changed   : 3/10/2016 10:02:55 AM by SYSTEM
Analysis Method: C:\Chem32\1\Data\Will\Will-AD 2016-03-10 10-02-55\Oxindole5050.M (Sequence
Method)
Last changed   : 3/10/2016 10:02:55 AM by SYSTEM
  
```



Area Percent Report

```

Sorted By      : Signal
Multiplier     : 1.0000
Dilution       : 1.0000
Use Multiplier & Dilution Factor with ISTDs
  
```

Signal 1: MWD1 B, Sig=254,4 Ref=off

Peak #	RetTime [min]	Type	Width [min]	Area [mAU*s]	Height [mAU]	Area %
1	7.470	BV	0.2153	2576.23193	179.67032	66.5780
2	8.351	VB	0.2302	1293.26392	83.74278	33.4220

Totals : 3869.49585 263.41310

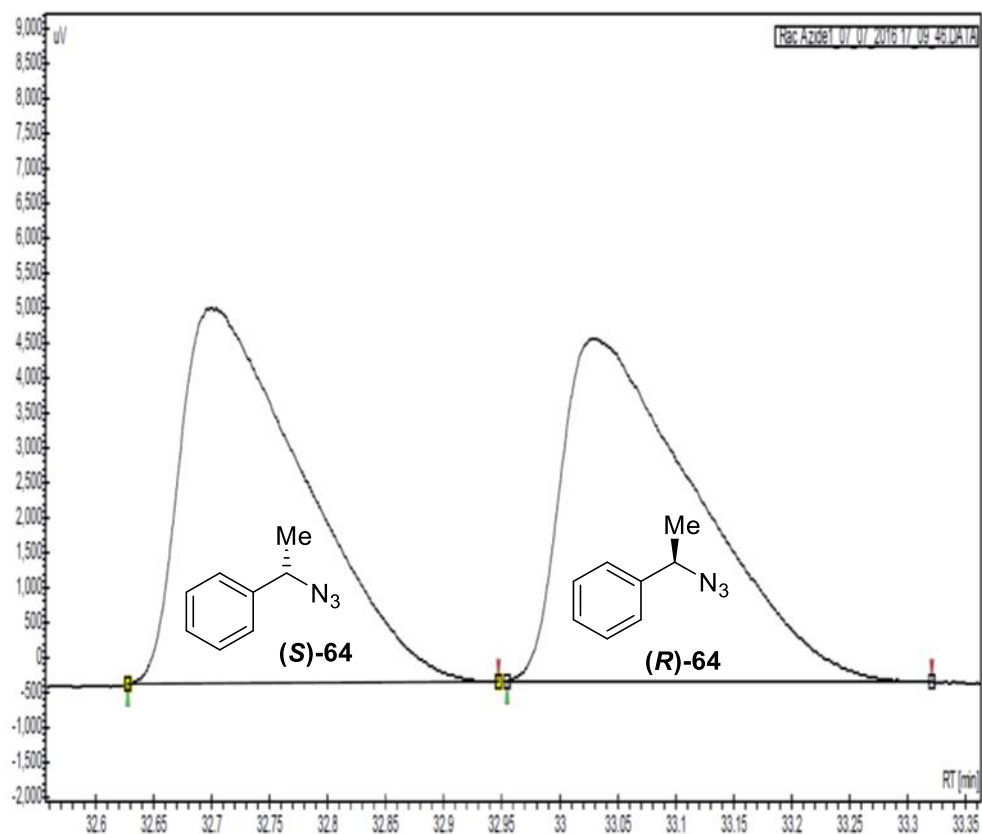
7.2.7.6 Chiral GC Trace of Compound 64

Rac Azide

Vial- 59
Method- AD_Azide Conversion.METH
Acq time- 07/07/2016 17:13:00
Injection volume- 5.000 µL
Sample name- N.A.



UNIVERSITY OF
BIRMINGHAM



Peak results :

Rac Azide1_07_07_2016_17_09_46.DATA [FID]

Index	Time [Min]	Area [uV.Min]	Area % [%]
1	32.70	667.7	50.010
2	33.03	667.5	49.990

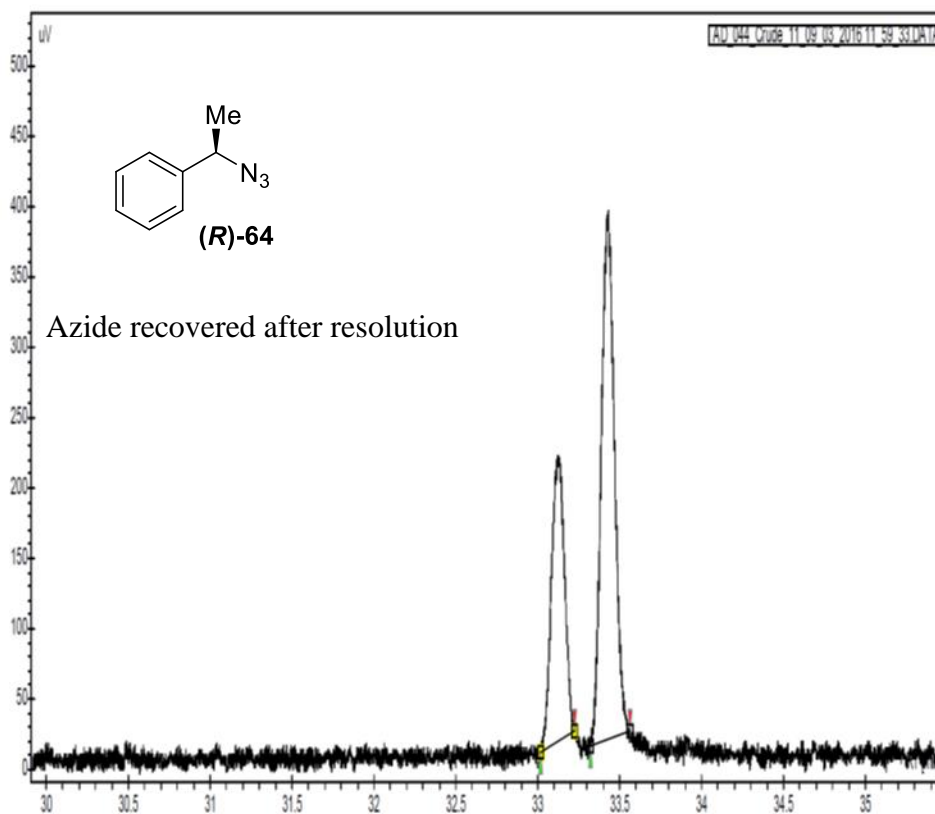
7.2.7.7 Chiral GC Trace of 64 Following Simultaneous Kinetic Resolution

AD_044_Crude_1

Vial- 1
Method- AD_Azide Conversion.METH
Acq time- 09/03/2016 12:02:51
Injection volume- 8.000 µL
Sample name- N.A.



UNIVERSITY OF
BIRMINGHAM



Peak results :

AD_044_Crude_11_09_03_2016_11_59_33.DATA [FID]

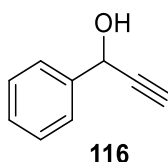
Index	Time [Min]	Area [uV.Min]	Area % [%]
1	33.13	18.7	34.945
2	33.43	34.7	65.055

7.3 Experimental Chapter 3

7.3.1 Experimental for the Kinetic Resolution of Primary Amine Alkynes

7.3.1.1 Synthesis

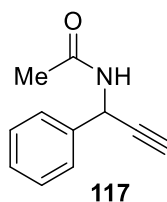
Synthesis of 1-phenylprop-2-yn-1-ol (**116**)



Under an atmosphere of nitrogen, a solution of benzaldehyde (1.0 mL, 10.0 mmol) in THF (10 mL) was stirred at -78 °C using a dry ice and acetone bath. To this solution ethynylmagnesium bromide (24 mL, 0.5 M in THF, 12.0 mmol) was added dropwise over a period of 10 min with stirring. This was then warmed slowly to room temperature and stirred for a further 3 h. The reaction mixture was then quenched with sat. NH_4Cl solution, and extracted with DCM (3 x 50 mL). The combined organic fractions were washed with water (100 mL), dried with MgSO_4 and concentrated under reduced pressure. The resulting brown oil was purified by automated flash column chromatography combiflash Rf (0-100% hexane/EtOAc gradient, 20 min) to yield 1-phenylprop-2-yn-1-ol **116** as a yellow oil in a 91% yield (1.20 g).

Characterisation data were in agreement with the reported literature values.^[160] ^1H NMR (400 MHz, CDCl_3) 7.58 – 7.51 (m, 2H, Ar-*H*), 7.41 – 7.31 (m, 3H, Ar-*H*), 5.45 (d, $J = 1.5$, 1H, *CH*), 2.66 (d, $J = 1.5$, 1H, *CCH*), 2.44 (br s, 1H, *OH*); ^{13}C NMR (101 MHz, CDCl_3) 140.05, 128.70, 128.58, 126.63, 83.52, 74.86, 64.43; IR ν_{max} (ATR)/ cm^{-1} 3431, 3289, 3066, 3032, 1453, 1019, 947.

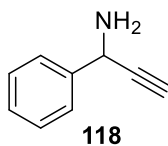
Synthesis of *N*-(1-phenylprop-2-yn-1-yl)acetamide (**117**)



To a mixture of 1-phenyl-2-propynyl-1-ol **116** (1.11 g, 8.40 mmol) and anhydrous sodium sulfate (1.20 g, 8.40 mmol) in acetonitrile (20 mL) at 0 °C was added a solution of 95% sulfuric acid (4.28 g, 42.0 mmol, 2.9 mL) in acetonitrile (10 mL). The mixture was warmed slowly to room temperature and stirred for 48 h. The solution was then concentrated under reduced pressure and the residue poured onto ice. This mixture was then extracted with EtOAc (3 x 50mL) and then DCM (50 mL). The combined organic fractions were dried with MgSO₄ and concentrated under reduced pressure. The crude mixture was subjected to automated flash column chromatography combiflash Rf (0-100% hexane/EtOAc gradient, 20 min) to yield *N*-(1-phenylprop-2-yn-1-yl)acetamide **117** as a cream coloured solid in a 59% yield (0.87 g).

Characterisation data were in agreement with the reported literature values.^[161] ¹H NMR (300 MHz, CDCl₃) δ 7.55 – 7.47 (m, 2H, Ar-*H*), 7.41 – 7.31 (m, 3H, Ar-*H*), 6.56 (br d, *J* = 7.8, 1H, NH), 6.01 (dd, *J* = 8.5, 2.4, 1H, CH), 2.50 (d, *J* = 2.5, 1H, CCH), 1.99 (s, 3H, CH₃); ¹³C NMR (101 MHz, CDCl₃) 168.79, 138.27, 128.78, 128.29, 127.05, 81.70, 72.99, 44.53, 23.18; IR ν_{\max} (ATR)/cm⁻¹ 3280, 3038, 1648, 1532, 1452, 1371, 1309, 1092; MS AP⁺ *m/z* 174.1 ([M+H]⁺, 23%), 132.1 (72), 116.1 (21, [M-CH₃CON]⁺), 115.1 (100, [M-CH₃CONH]⁺); HRMS AP⁺ Calculated for C₁₁H₁₂NO⁺ = 174.0913 Found = 174.0913; MP 89 – 90 °C. Literature value, MP 84-86 °C.^[162]

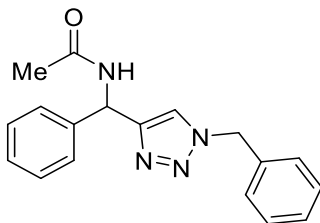
Synthesis of 1-phenylprop-2-yn-1-amine (**118**)



To a solution of *N*-(1-phenylprop-2-yn-1-yl)acetamide **117** (0.10 g, 0.76 mmol) in methanol (1 mL) was added 3.0 N aqueous HCl (20 mL) and the reaction mixture heated to 70 °C for 18 h. The resulting solution was extracted with EtOAc (50 mL). The aqueous phase was basified with aqueous 2.0 N NaOH_(aq) solution to pH ~ 10. This was then extracted with EtOAc (3 x 50mL), the organic layers were combined, dried with MgSO₄ and concentrated under reduced pressure to afford 1-phenylprop-2-yn-1-amine **118** as a yellow oil in a 35% yield (0.036 g). It was found that this compound will degrade if stored in its pure form, material was therefore stored as a solution in chloroform in the freezer.

Characterisation data were consistent with literature.^[163] ¹H NMR(300 MHz, CDCl₃) 7.58 – 7.50 (m, 2H, Ar-*H*), 7.40 – 7.29 (m, 3H, Ar-*H*), 4.78 (d, *J* = 1.9, 1H, *CH*), 2.49 (d, *J* = 1.9, 1H, *CCH*), 1.91 (br s, 2 H, NH₂); ¹³C NMR (101 MHz, CDCl₃) 141.59, 128.67, 127.82, 126.67, 86.01, 72.30, 47.31; IR ν_{max} (ATR)/cm⁻¹ 3666, 3288, 1492, 1451, 1275; MS AP⁺ *m/z* 261.1 (100%), 132.1 (23, [M+H]⁺), 115.1 (79, [M-NH₃]⁺); HRMS AP⁺ Calculated for C₉H₁₀N⁺ = 132.0913 Found = 132.0914.

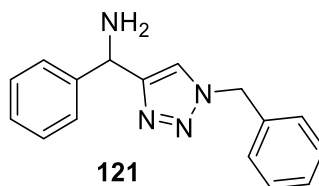
Synthesis of *N*-((1-benzyl-1*H*-1,2,3-triazol-4-yl)(phenyl)methyl)acetamide



To a solution of *N*-(1-phenylprop-2-yn-1-yl)acetamide **117** (0.050 g, 0.30 mmol) and benzyl azide (0.044 g, 0.33 mmol) in methanol (20 mL) was added sodium L ascorbate (0.059 g, 0.30 mmol) and copper(II) sulfate pentahydrate (0.008 g, 0.03 mmol). The mixture was stirred at 50 °C for 3 h. The reaction mixture was quenched with aqueous ammonia solution 5% v/v (10 mL). The solution was extracted with EtOAc (3 x 25 mL), the combined organic extracts were washed with water (100 mL), dried with MgSO₄ and concentrated under reduced pressure. This gave *N*-((1-benzyl-1*H*-1,2,3-triazol-4-yl)(phenyl)methyl)acetamide as a cream coloured solid in a 87% yield (0.081 g).

Characterisation data were consistent with the reported literature values.^[164] ¹H NMR (400 MHz, CDCl₃) 7.39 – 7.21 (m, 11 H, Ar-*H*/Triazole *CH*), 6.95 (br d, *J* = 7.7, 1H, *NH*), 6.27 (d, *J* = 7.9, 1H, *CH*), 5.47 (ABq, $\Delta\delta_{AB}$ = 0.06, *J* = 14.8, 2H, *CH*₂), 2.01 (s, 3H, *CH*₃); ¹³C NMR (101 MHz, CDCl₃) 169.26, 147.98, 140.88, 134.30, 129.17, 128.86, 128.71, 128.11, 127.73, 127.26, 121.53, 54.25, 49.56, 23.27; IR ν_{max} (ATR)/cm⁻¹ 1721, 1653, 1489, 1345, 1278, 1154; MS ESI⁺ *m/z* 329.1 ([*M*+*Na*]⁺, 100%); MP 155 – 156 °C.

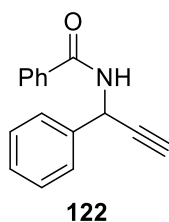
Synthesis of (1-benzyl-1*H*-1,2,3-triazol-4-yl)(phenyl)methanamine (**121**)



To a solution of *N*-((1-benzyl-1*H*-1,2,3-triazol-4-yl)(phenyl)methyl)acetamide (0.25 g, 3.24 mmol) in methanol (2 mL) was added 3.0 N aqueous HCl (20 mL). The mixture was heated to 70 °C for 18 h, after which the reaction mixture was extracted with EtOAc (50 mL), the aqueous phase basified to pH ~ 10 with 2.0 N aqueous NaOH and extracted with EtOAc (3 x 50 mL). The combined organic fractions were dried with MgSO₄ and concentrated under reduced pressure. This gave (1-benzyl-1*H*-1,2,3-triazol-4-yl)(phenyl)methanamine **121** as a cream coloured solid in a 56% yield (0.48 g).

¹H NMR (400 MHz, CDCl₃) 7.44 – 7.13 (m, 11H, Ar-*H*/Triazole *CH*), 5.45 (s, 2H, *CH*₂), 5.36 (s, 1H, *CH*); ¹³C NMR (101 MHz, CDCl₃) 152.76, 143.79, 134.64, 129.07, 128.66, 128.05, 127.50, 126.86, 120.73, 54.15, 52.54; IR ν_{max} (ATR)/cm⁻¹ 3366, 3122, 3064, 2925, 2853, 1494, 1454, 1216; MS ESI⁺ *m/z* 287.1 ([M+Na]⁺, 35%), 248.1 (28), 220.1 (100), 193.1 (96); HRMS ESI⁻ Calculated for C₁₆H₁₆N₄Na⁺ = 287.1278 Found = 287.1274.; MP 86 - 88°C.

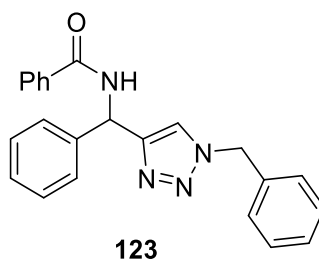
Synthesis of *N*-(1-phenylprop-2-yn-1-yl)benzamide (**122**)



To a solution of 1-phenylprop-2-yn-1-amine **118** (10 mg, 0.08 mmol) in DCM (10 mL) cooled in an ice bath was added benzoyl chloride (11 mg, 8.8 μ L, 0.08 mmol) and TEA (8.0 mg, 10 μ L, 0.08 mmol). The reaction was allowed to warm to room temperature and stirred for 2 h. The reaction was then quenched with water (10 mL) and extracted with EtOAc (3 x 25 mL) the organic fractions combined, dried over MgSO_4 and concentrated under reduced pressure. The crude mixture was purified by automated flash column chromatography combiflash Rf (0-100% hexane/EtOAc gradient, 20 min) to yield *N*-(1-phenylprop-2-yn-1-yl)benzamide **122** as a white solid in a 84% yield (15 mg).

^1H NMR (400 MHz, CDCl_3) 7.83 – 7.77 (m, 2H, Ar-*H*), 7.62 – 7.57 (m, 2H, Ar-*H*), 7.55 – 7.49 (m, 1H, Ar-*H*), 7.47 – 7.31 (m, 5H, Ar-*H*), 6.57 (br d, $J = 7.9$, 1H, NH), 6.25 (app dd, $J = 8.4, 2.4$, 1H, NCH), 2.55 (d, $J = 2.4$, 1H, CCH); ^{13}C NMR (101 MHz, CDCl_3) 166.20, 138.21, 133.67, 131.92, 128.85, 128.66, 128.36, 127.11, 81.64, 73.33, 44.99; IR ν_{max} (ATR)/ cm^{-1} 3291, 3034, 1639, 1522, 1488, 1331; MS AP^+ m/z 236.1 ($[\text{M}+\text{H}]^+$, 100%); HRMS AP^+ Calculated for $\text{C}_{16}\text{H}_{14}\text{NO}^+$ = 236.1070 Found = 236.1073; MP 131 – 132 $^\circ\text{C}$; HPLC (Chirapak IA) Hexane/IPA 80:20, 1.0 mL/min, $\lambda = 254$ nm, $t_{\text{major}} = 7.9$ min, $t_{\text{minor}} = 8.8$ min.

Synthesis of *N*-((1-benzyl-1*H*-1,2,3-triazol-4-yl)(phenyl)methyl)benzamide (**123**)

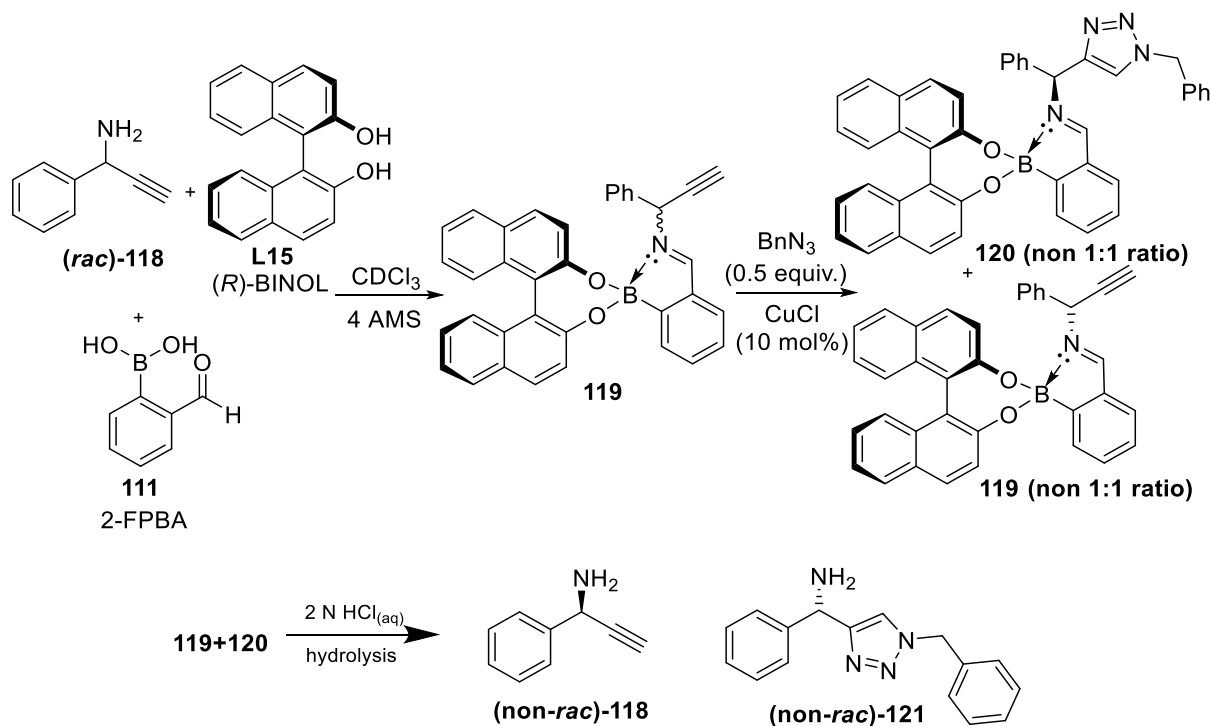


To a solution of (1-benzyl-1*H*-1,2,3-triazol-4-yl)(phenyl)methanamine **118** (0.079 g, 0.30 mmol) in DCM (10 mL) cooled in an ice bath was added benzoyl chloride (0.042 g, 35 μ L, 0.30 mmol) and TEA (0.030 g, 42 μ L, 0.30 mmol). The reaction was warmed to room temperature and stirred for 2 h. The reaction was then quenched with water (10 mL) and extracted with EtOAc (3 x 25 mL) the combined organic fractions were dried over MgSO₄ and concentrated under reduced pressure. The crude mixture was purified by automated flash column chromatography combiflash Rf (0-100% hexane/EtOAc gradient, 20 min) to yield the product **123** as a white solid in a 93% yield (0.102 g).

¹H NMR (400 MHz, CDCl₃) 7.83 (dd, *J* = 5.2, 3.3, 2H, Ar-*H*), 7.58 (d, *J* = 7.4, 1H, Ar-*H*), 7.52 – 7.21 (m, 13 H, Ar-*H*), 6.46 (d, *J* = 7.5, 1H, CH), 5.49 (ABq, $\Delta\delta_{AB}$ = 0.07, *J* = 14.8, 2 H, CH₂); ¹³C NMR (101 MHz, CDCl₃) 166.51, 147.97, 140.93, 134.29, 134.03, 131.68, 129.18, 128.87, 128.77, 128.55, 128.13, 127.79, 127.30, 127.18, 121.58, 54.30, 50.12; IR ν_{max} (ATR)/cm⁻¹ 3378, 3116, 1639, 1515, 1487, 1354; MS ESI⁺ *m/z* 391.2 ([M+Na]⁺, 100%); HRMS ESI⁺ Calculated for C₂₃H₂₀N₄ONa⁺ = 391.1540 Found = 391.1541; MP 207 – 209 °C; HPLC (Chirapak IA) Hexane/IPA 80:20, 1.0 mL/min, λ = 214 nm, *t*_{major} = 16.7 min, *t*_{minor} = 18.3 min.

7.3.1.2 Catalysis

Representative assembly based reaction



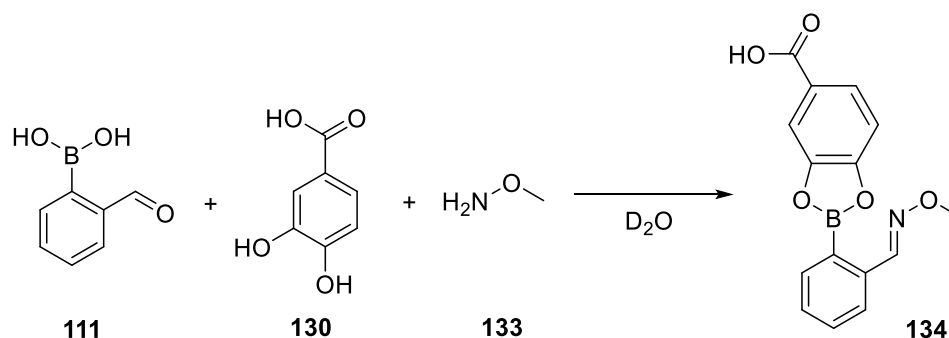
A mixture of FPBA **111** (5.7 mg, 0.038 mmol, 1.0 equiv.) and (*R*)-BINOL **L15** (10.9 mg, 0.038 mmol, 1.0 equiv.) were placed in a vial and dried under high vacuum for 2 hours. The mixture was then removed from high vacuum and a solution of amine **118** (5.0 mg, 0.038 mmol, 1.0 equiv.) in CDCl₃ (0.5 mL), dried over 4A MS, was added. A small number of 4A MS were added to the vial and the contents stirred at rt for 20 min. To this, 0.1 mL of benzyl azide stock solution (24 μ L per 1 mL, 0.5 equiv.) was added along with CuCl (0.19 mg, 0.0019 mmol, 5 mol%). The reaction mixture was stirred at rt for 24 h. After this time a ¹H NMR spectrum was taken of the reaction mixture to determine the conversion and enantiomeric excess of **118** and **121**. To recover the alkyne **118** and triazole **121**, after the reaction was completed 2.0 N HCl_(aq) solution (5 mL) was added to the NMR sample and the combined solution was stirred vigorously for 30 minutes. The mixture was then extracted with

EtOAc (25 mL) and water (25 mL). The aqueous phase was then basified to pH ~ 10 using 2.0 N NaOH_(aq) solution. The basified solution was then extracted with EtOAc (3 x 25 mL). The combined organic fractions were dried with MgSO₄ and concentrated under reduced pressure to give amine **118** and triazole **121** with minimal amounts of the other assembly components. The *ee* of selected examples was verified *via* either GC or HPLC using a chiral stationary phase. For HPLC determination, benzylation of the recovered mixture of components was carried out as detailed above.

7.3.2 Experimental for Boronic Acid Assemblies in Aqueous Environments

Procedure for ¹H/¹¹B NMR Titrations

¹H and ¹¹B NMR spectra were collected on a 600 MHz spectrometer with a sweep width of 56818 Hz, a 90 degree flip angle, and 2 second acquisition time using BF₃•OEt₂ as an external reference. Each spectrum was processed with 10 Hz line broadening, and a back linear prediction of the first 32 points was used to remove the ¹¹B background.



Stock solutions of 2-formylphenylboronic acid **111**, 3,4-dihydroxybenzoic acid **130** and methoxyamine hydrochloride with 1 equiv. Cs₂CO₃ were made to be 70 mM in D₂O. Then each (separate) quartz NMR tube was loaded according to the following tables. The samples

were stored overnight in a refrigerator and ^{11}B NMR spectra (as well as ^1H spectra, in order to support structural assignments) were obtained.

Titration of methoxyamine into 2-FPBA with 3,4-dihydroxybenzoic acid added at end

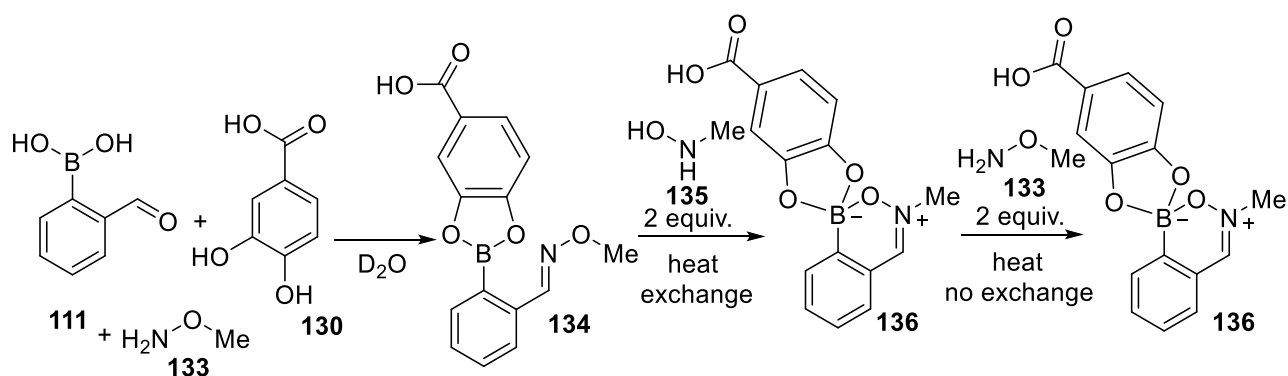
Entry	Vol FPBA / μL	Vol Diol / μL	Vol Amine / μL	Vol D_2O / μL	[FPBA] mM	[Diol] mM	[Amine] mM
1	100	0	20	580	10	0	2
2	100	0	40	560	10	0	4
3	100	0	60	540	10	0	6
4	100	0	80	520	10	0	8
5	100	0	100	500	10	0	10
6	100	0	120	480	10	0	12
7	100	100	120	380	10	10	12

Titration of methoxyamine into 2-FPBA and 3,4-dihydroxybenzoic acid

Entry	Vol FPBA / μL	Vol Diol / μL	Vol Amine / μL	Vol D_2O / μL	[FPBA] mM	[Diol] mM	[Amine] mM
1	100	100	0	500	10	10	0

2	100	100	20	480	10	10	2
3	100	100	40	460	10	10	4
4	100	100	60	440	10	10	6
5	100	100	80	420	10	10	8
6	100	100	100	400	10	10	10
7	100	100	120	380	10	10	12

Representative Procedure for Methoxyamine Assembly Exchange with Hydroxylamine



Stock solutions of 2-formylphenylboronic acid **111**, 3,4-dihydroxybenzoic acid **130** and methoxyamine hydrochloride with Cs_2CO_3 (1 equiv.) were made to be 70 mM in D_2O . The three stock solutions (100 μL) were combined and then made up with D_2O (400 μL) to a total volume of 700 μL in an NMR tube. The tube was left at rt for 30 min before a 1H NMR spectrum was taken to confirm assembly formation. To the NMR tube was added *N*-methylhydroxylamine hydrochloride (1.2 mg, 0.14 mmol, 2 equiv.) and Cs_2CO_3 (4.6 mg, 0.14 mmol, 2 equiv.) and the NMR tube was heated in a water bath (40 $^\circ C$) for 1 h. After this time

a ^1H NMR spectrum was taken and full exchange to the hydroxylamine amine assembly was noted. To this mixture was added methoxyamine hydrochloride (1.2 mg, 0.14 mmol, 2 equiv.) and Cs_2CO_3 (4.6 mg, 0.14 mmol, 2 equiv.) and the NMR tube heated in a water bath (40 °C) for 1 h. After this time a ^1H NMR spectrum was taken and no exchange was noted.

7.3.3 Chapter 3 Chromatography

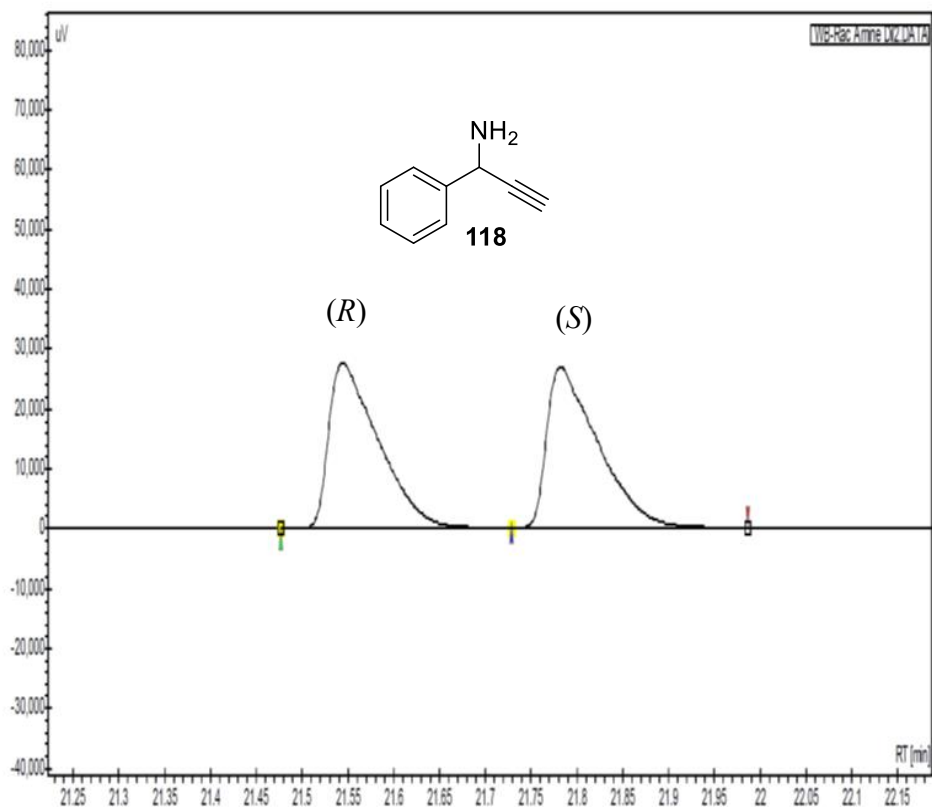
Gas Chromatography

GC analysis was run on a Varian 430-GC using a Varian WCOT fused silica 25M x 0.25 mm, Chirasil-DEX CB DF = 0.25 column. The injector was given a set point of 200 °C, split state was on with a split ratio of 500. The column stabilisation time was set at 0.50 min. The column oven program was set to an initial temperature of 50 °C, which was then ramped at 3.7 °C per min until 200 °C was reached, and the oven held at 200 °C for 10 minutes to give an overall run length of 50.54 min.

7.3.3.1 Chiral GC Trace of Racemic 118

Rac Amine

Vial- 3
 Method- GB METHOD.METH
 Acq time- 04/11/2015 10:58:36
 Injection volume- 5.000 µL
 Sampelname- N.A.



Peak results :

WB-Rac Amine Dil2.DATA [FID]

Index	Time [Min]	Area [uV.Min]	Area % [%]
1	21.55	1742.3	49.858
2	21.78	1752.2	50.142

Rac Amine

Vial- 3
 Method- GB METHOD.METH
 Acq time- 04/11/2015 10:58:36
 Injection volume- 5.000 µL
 Sampelname- N.A.

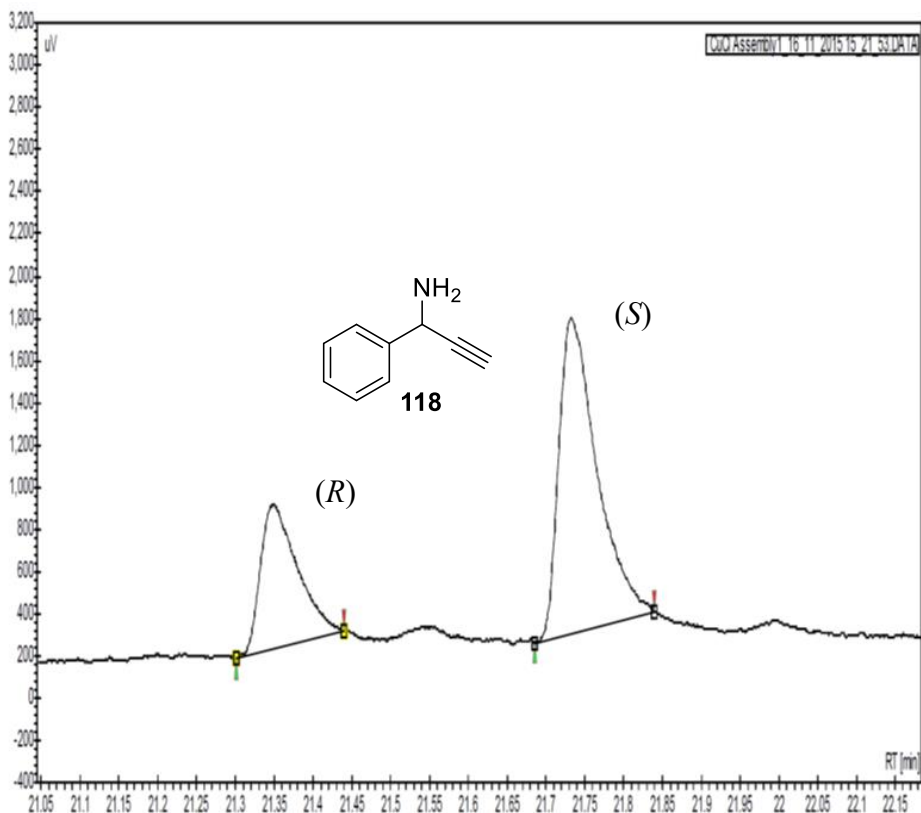


Index	Time [Min]	Area [uV.Min]	Area % [%]
Total		3494.5	100.000

7.3.3.2 Chiral GC Trace of 118 After Kinetic Resolution

CuCl Assembly

Vial- 15
 Method- GB METHOD.METH
 Acq time- 16/11/2015 15:30:42
 Injection volume- 8.000 µL
 Sampelname- N.A.



Peak results :

CuCl Assembly1 16 11 2015 15 21_53.DATA [FID]

Index	Time [Min]	Area [uV.Min]	Area % [%]
1	21.35	37.6	30.707
2	21.73	85.0	69.293

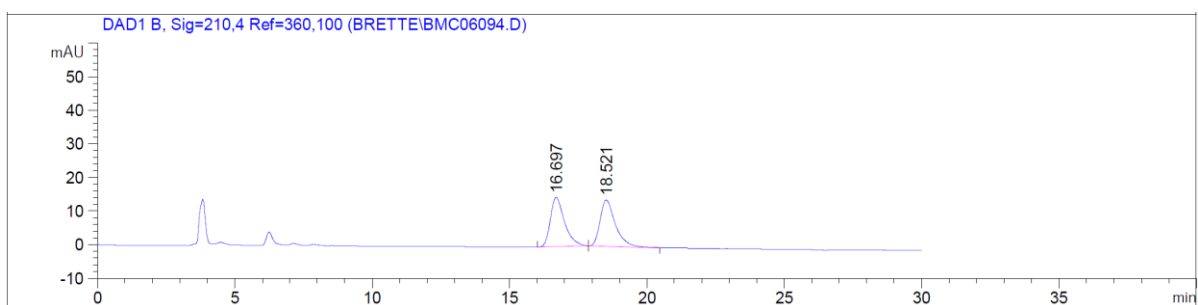
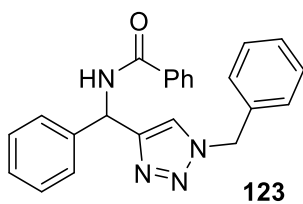
CuCl Assembly

Vial- 15
 Method- GB METHOD.METH
 Acq time- 16/11/2015 15:30:42
 Injection volume- 8.000 µL
 Sampelname- N.A.



Index	Time [Min]	Area [uV.Min]	Area % [%]
Total		122.6	100.000

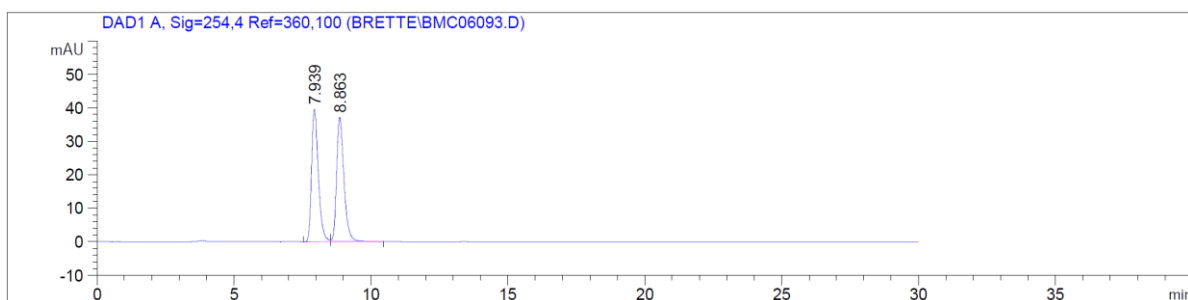
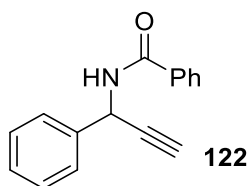
7.3.3.3 HPLC Trace of Racemic Compound 123



Signal 2: DAD1 B, Sig=210,4 Ref=360,100

Peak #	RetTime [min]	Type	Width [min]	Area [mAU*s]	Height [mAU]	Area %
1	16.697	BB	0.5409	525.99249	14.65044	49.7732
2	18.521	BB	0.5775	530.78601	13.77542	50.2268
Totals :				1056.77850	28.42586	

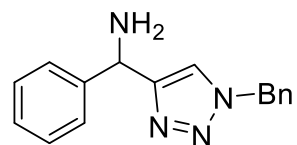
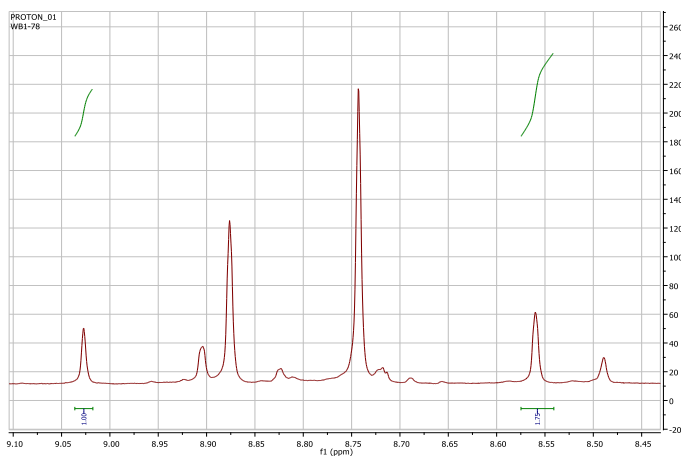
7.3.3.4 HPLC Trace of Racemic Compound 122



Signal 1: DAD1 A, Sig=254,4 Ref=360,100

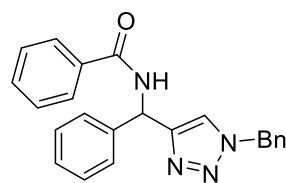
Peak #	RetTime [min]	Type	Width [min]	Area [mAU*s]	Height [mAU]	Area %
1	7.939	BV	0.2637	683.91754	39.56554	49.6011
2	8.863	VB	0.2838	694.91681	37.22253	50.3989
Totals :				1378.83435	76.78807	

7.3.3.5 Representative HPLC Trace and NMR Spectrum after Assembly Kinetic Resolution



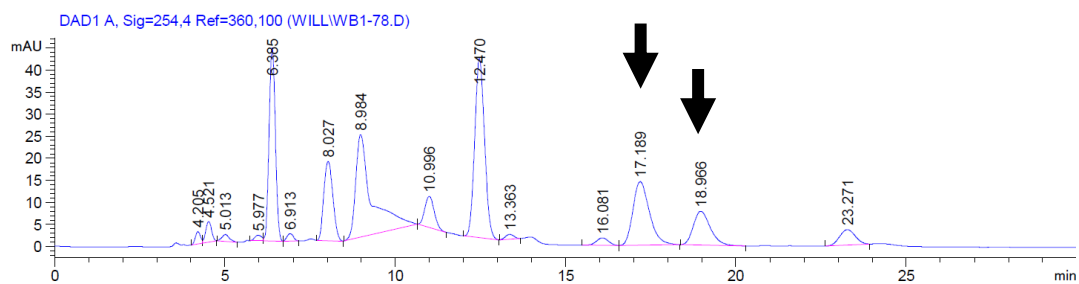
121

27% ee



123

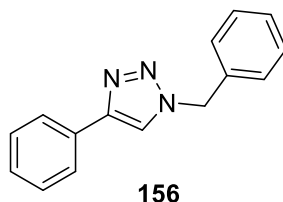
30% ee



7.4 Chapter 4 Experimental

7.4.1 Synthesis

Synthesis of 1-benzyl-4-phenyl-1H-1,2,3-triazole (**156**)

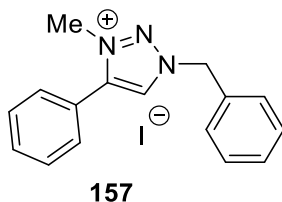


To a solution of phenyl acetylene (0.84 g, 8.3 mmol) and benzyl azide (1.0 g, 7.5 mmol) in MeOH (10 mL) was added NaAsc (1.50 g, 7.5 mmol,) and CuSO₄·5H₂O (0.19 g, 0.75 mmol). The reaction mixture was heated at 50 °C and stirred for 18 h. The reaction mixture was quenched by the addition of 5% v/v aq. ammonia solution (10 mL) and extracted with EtOAc (3 x 25 mL). The combined organic extracts were dried with MgSO₄ and concentrated under reduced pressure. The crude material was purified by automated flash column chromatography combiflash Rf (0-100% EtOAc/hexane gradient, 20 min) to yield 1-benzyl-4-phenyl-1H-1,2,3-triazole **156** as a white solid in a 99% yield (1.95 g).

Characterisation data were in agreement with reported literature values.^[165] ¹H NMR (300 MHz, CDCl₃) δ 7.84 – 7.75 (m, 2H, Ar-*H*), 7.66 (s, 1H, Triazole *CH*), 7.44 – 7.28 (m, 8H, Ar-*H*), 5.58 (s, 2H, CH₂); ¹³C NMR (101 MHz, CDCl₃) δ 148.28, 134.68, 130.54, 129.17, 128.81, 128.18, 128.08, 125.71, 119.46, 54.26; MS ESI⁺ *m/z* 258.1 ([M+Na]⁺, 43%), 236.1 (100, [M+H]⁺).

Only ten of the expected eleven carbon environments were observed for compound **156** literature also only reports ten carbon environments.^[165] Due to this agreement with literature values the identity of **156** was confirmed.

Synthesis of 1-benzyl-3-methyl-4-phenyl-1*H*-1,2,3-triazol-3-ium iodide (**157**)

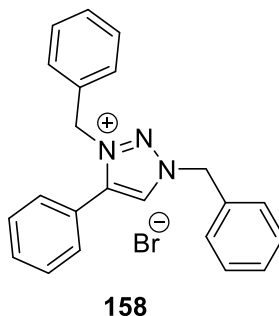


1-Benzyl-4-phenyl-1*H*-1,2,3-triazole **156** (240 mg, 1.02 mmol) was dissolved in methyl iodide (2 mL) in a sealed tube and heated at 80 °C for 24 h. After this time the reaction was concentrated under reduced pressure. No further purification was required yielding 1-benzyl-3-methyl-4-phenyl-1*H*-1,2,3-triazol-3-ium iodide **157** as a brown oil, in a 92% yield (354 mg).

Characterisation data were in agreement with reported literature values.^[112d] ¹H NMR (400 MHz, CDCl₃) δ 9.43 (s, 1H, Triazole *CH*), 7.74 – 7.68 (m, 4H, Ar-*H*), 7.60 – 7.50 (m, 3H, Ar-*H*), 7.45 – 7.39 (m, 3H, Ar-*H*), 6.05 (s, 2H, CH₂), 4.31 (s, 3H, CH₃); ¹³C NMR (101 MHz, CDCl₃) δ 143.08, 132.03, 131.23, 129.98, 129.74, 129.63, 129.44, 129.39, 121.68, 57.61, 39.29; MS ESI⁺ *m/z*, 251.1 ([M+H-I]⁺, 30%), 250.1 (100, [M-I]⁺); IR ν_{\max} (ATR)/cm⁻¹ 3041, 2924, 2850, 1611, 1492, 1456, 1310, 1155, 1078, 767, 745, 701.

Only eleven of the expected twelve carbon signals were observed for compound **157**. Literature values quote two signals at 129.9 ppm these signals were overlapping in the obtained spectrum.^[112d]

Synthesis of 1,3-dibenzyl-4-phenyl-1*H*-1,2,3-triazol-3-ium bromide (**158**)

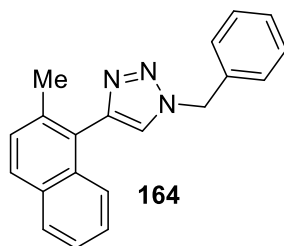


1-Benzyl-4-phenyl-1*H*-1,2,3-triazole **156** (100 mg, 0.43 mmol) was dissolved in acetonitrile (5 mL) and benzyl bromide (1 mL) in a sealed tube and heated at 150 °C for 24 h. After this time the reaction mixture was concentrated under reduced pressure. The crude material was subjected to automated flash column chromatography combiflash Rf (0-20% DCM/MeOH, 20 min) this yielded 1,3-dibenzyl-4-phenyl-1*H*-1,2,3-triazol-3-ium bromide **158** as a brown oil in a 95% yield (135 mg).

Characterisation data were in agreement with reported literature values.^[166] ¹H NMR (400 MHz, CDCl₃) δ 9.85 (s, 1H, Triazole CH), 7.78 – 7.71 (m, 2H, Ar-H), 7.58 – 7.44 (m, 5H, Ar-H), 7.42 – 7.37 (m, 3H, Ar-H), 7.35 – 7.27 (m, 3H, Ar-H), 7.12 – 6.99 (m, 2H, Ar-H), 6.20 (s, 2H, CH₂), 5.76 (s, 2H, CH₂); ¹³C NMR (101 MHz, CDCl₃) δ 142.85, 131.96, 131.85, 131.35, 130.15, 129.78, 129.72, 129.60, 129.33, 128.00, 121.75, 57.46, 55.51; MS ESI⁺ *m/z*, 327.2 ([M+H-Br]⁺, 31%), 326.2 (100, [M-Br]⁺); IR ν_{\max} (ATR)/cm⁻¹ 3039, 1610, 1495, 1456, 1341, 1156, 1059, 737, 698.

Only thirteen of the expected sixteen carbon signals were observed for compound **158**. Literature reports fourteen signals for compound **158**,^[166] two of these signals were overlapping in the obtained spectrum.

Synthesis of 1-benzyl-4-(2-methylnaphthalen-1-yl)-1*H*-1,2,3-triazole (**164**)

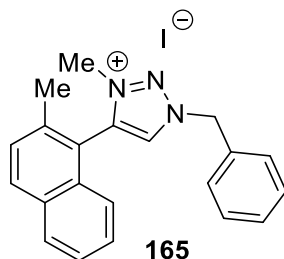


A solution of 1-bromo-2-methylnaphthalene **159** (1.20 g, 5.46 mmol) in piperidine (20 mL) was degassed by bubbling nitrogen for 20 min. To this solution was added Pd(PPh₃)₂Cl₂ (76 mg, 0.11 mmol), CuI (40 mg, 0.21 mmol) and PPh₃ (50 mg, 0.19 mmol) the solution was degassed for a further 20 min with bubbling nitrogen. Finally, trimethylsilylacetylene was added (0.7 g, 1.0 mL) and the reaction mixture heated at reflux for 18 h. The reaction mixture was then filtered through celite and extracted with water (50 mL) and EtOAc (3 x 25 mL), the combined organic fractions were dried over MgSO₄ and concentrated under reduced pressure. The crude material was subjected to automated flash column chromatography combiflash Rf (0-30% hexane/EtOAc, 20 min) this yielded an inseparable mixture of 1-bromo-2-methylnaphthalene and trimethyl((2-methylnaphthalen-1-yl)ethynyl)silane **160** which was carried forward. To the crude material was added a solution of TBAF in THF (1.0 M, 7 mL) and water (1 mL). The reaction mixture was stirred at room temperature for 2 h at which point it was concentrated under reduced pressure. The residue was taken up in EtOAc (25 mL) and washed with water (25 mL), the organic phase was dried over MgSO₄ and concentrated under reduced pressure. The crude material was subjected to automated flash column chromatography combiflash Rf (0-30% hexane/EtOAc, 20 min) this yielded an inseparable mixture of 1-bromo-2-methylnaphthalene and 1-ethynyl-2-methylnaphthalene **163** (0.30 g) which was carried forward. This mixture was added to a solution of benzyl azide (0.36 g, 2.7 mmol), in methanol (10 mL). To this solution was added CuSO₄·5H₂O (45 mg, 0.18 mmol)

and NaAsc (0.35 g, 1.8 mmol) and the reaction was stirred at 50 °C for 18 h. After this time the reaction mixture was quenched with 5% v/v aqueous ammonia solution and extracted with water (20 mL) and EtOAc (3 x 25 mL). The combined organic fractions were dried over MgSO₄ and concentrated under reduced pressure. The crude material was subjected to automated flash column chromatography combiflash Rf (0-100% hexane/EtOAc, 20 min) this yielded 1-benzyl-4-(2-methylnaphthalen-1-yl)-1*H*-1,2,3-triazole **164** as a brown crystalline solid in a 15% yield (242 mg).

¹H NMR (400 MHz, CDCl₃) δ 7.81 – 7.74 (m, 2H, Ar-*H*), 7.52 (d, *J* = 8.2, 1H, Ar-*H*), 7.50 (s, 1H, Triazole *CH*), 7.42 – 7.30 (m, 8H, Ar-*H*), 5.65 (s, 2H, CH₂), 2.29 (s, 3H, CH₃); ¹³C NMR (101 MHz, CDCl₃) δ 145.05, 135.74, 134.96, 133.36, 132.00, 129.20, 128.75, 128.73, 128.56, 127.93, 126.35, 125.31, 124.99, 123.61, 54.23, 20.89; MS ESI⁺ *m/z*, 322.2 ([M+Na]⁺, 21%), 300.2 (100, [M+H]⁺); HRMS ESI⁺ Calculated for C₂₀H₁₈N₃⁺ = 300.1495 Found = 300.1499; IR ν_{max} (ATR)/cm⁻¹ 3137, 3050, 2925, 1456, 1054, 813, 718; MP 115 – 117 °C.

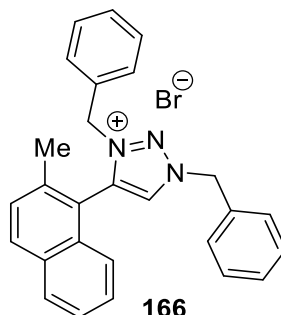
Synthesis of 1-benzyl-3-methyl-4-(2-methylnaphthalen-1-yl)-1*H*-1,2,3-triazol-3-ium iodide (165)



1-Benzyl-4-(2-methylnaphthalen-1-yl)-1*H*-1,2,3-triazole **164** (30 mg, 0.1 mmol) was dissolved in methyl iodide (2 mL) in a sealed tube and heated at 80 °C for 24 h. After this time the reaction was concentrated under reduced pressure. The crude material was subjected to automated flash column chromatography combiflash Rf (0-20% DCM/MeOH, 20 min) this yielded 1-benzyl-3-methyl-4-(2-methylnaphthalen-1-yl)-1*H*-1,2,3-triazol-3-ium iodide **165** as a brown oil in a 77% yield (34 mg).

¹H NMR (400 MHz, CDCl₃) δ 9.49 (s, 1H, Triazole CH), 7.98 (d, *J* = 8.5 Hz, 1H, Ar-*H*), 7.92 – 7.86 (m, 1H, Ar-*H*), 7.83 – 7.75 (m, 2H, Ar-*H*), 7.53 – 7.46 (m, 2H, Ar-*H*), 7.46 – 7.39 (m, 4H Ar-*H*), 7.26 – 7.19 (m, 1H, Ar-*H*), 6.31 (ABq, Δδ_{AB} = 0.04, *J* = 14.1, 2H, CH₂), 3.94 (s, 3H, CH₃), 2.34 (s, 3H, CH₃); ¹³C NMR (101 MHz, CDCl₃) δ 140.60, 138.57, 132.48, 131.76, 131.54, 131.47, 131.15, 129.98, 129.46, 128.80, 128.43, 126.47, 123.45, 116.17, 58.09, 38.40, 21.35; MS ESI⁺ *m/z*, 315.2 ([M-I+H]⁺, 28%), 314.2 (100, [M-I]⁺); HRMS ESI⁺ Calculated for C₂₁H₂₀N₃⁺ = 314.1652 Found = 314.1655; IR ν_{max} (ATR)/cm⁻¹ 2925, 2855, 1455, 1150, 821, 738, 705.

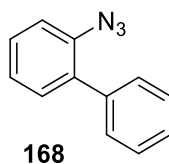
Synthesis of 1,3-dibenzyl-4-(2-methylnaphthalen-1-yl)-1*H*-1,2,3-triazol-3-ium bromide (166)



1-Benzyl-4-(2-methylnaphthalen-1-yl)-1*H*-1,2,3-triazole **164** (30 mg, 0.1 mmol) was added to a solution of acetonitrile (5 mL) and benzyl bromide (1 mL) in a sealed tube and heated at 150 °C for 24 h. After this time the reaction was concentrated under reduced pressure. The crude material was subjected to automated flash column chromatography combiflash Rf (0-20% DCM/MeOH, 20 min) this yielded 1,3-dibenzyl-4-(2-methylnaphthalen-1-yl)-1*H*-1,2,3-triazol-3-ium bromide **166** as a brown oil in a 79% yield (37 mg).

¹H NMR (400 MHz, CDCl₃) δ 10.14 (s, 1H, Triazole CH), 7.99 (d, *J* = 8.5 Hz, 1H, Ar-*H*), 7.91 (d, *J* = 7.9 Hz, 1H, Ar-*H*), 7.85 – 7.78 (m, 2H, Ar-*H*), 7.55 – 7.39 (m, 5H, Ar-*H*), 7.33 (d, *J* = 8.5 Hz, 1H, Ar-*H*), 7.25 (d, *J* = 7.5 Hz, 1H, Ar-*H*), 7.14 (t, *J* = 7.7 Hz, 2H, Ar-*H*), 6.98 (d, *J* = 8.3 Hz, 1H, Ar-*H*), 6.67 (d, *J* = 7.3 Hz, 2H, Ar-*H*), 6.47 (ABq, Δδ_{AB} = 0.14, *J* = 13.9, 2H, CH₂), 5.27 (ABq, Δδ_{AB} = 0.35, *J* = 14.3, 2H, CH₂), 1.89 (s, 3H, CH₃); ¹³C NMR (101 MHz, CDCl₃) δ 139.86, 139.04, 132.52, 132.42, 132.25, 131.69, 131.50, 130.09, 129.86, 129.80, 129.41, 129.11, 128.84, 128.66, 128.27, 126.39, 123.00, 116.42, 57.90, 55.72, 20.49; MS ESI⁺ *m/z*, 391.2 ([M+H-Br]⁺, 23%), 390.2 (100, [M-Br]⁺); HRMS ESI⁺ [M-Br]⁺ Calculated for C₂₇H₂₄N₃⁺ = 390.1965 Found = 380.1973; IR ν_{max} (ATR)/cm⁻¹ 3035, 2925, 1498, 1457, 1147, 821, 733.

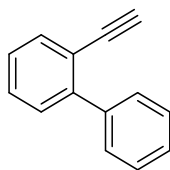
Synthesis of 2-azido-1,1'-biphenyl (**168**)



To a solution of [1,1'-biphenyl]-2-amine **167** (2.00 g, 11.9 mmol) in 5 M HCl_(aq) (11 mL) cooled in an ice bath was added NaNO₂ (0.98 g, 14.2 mmol) and the mixture stirred for 30 minutes. After this time sodium azide (1.49 g, 23.8 mmol) dissolved in water (5 mL) was added dropwise over a period of 5 min, the reaction mixture was then allowed to warm to room temperature and stirred for 2 h. The reaction was then diluted with the addition of water (30 mL) then extracted with diethylether (3 x 25 mL). The combined organic fractions were dried over magnesium sulfate and concentrated under reduced pressure. This yielded 2-azido-1,1'-biphenyl **168** as a brown oil in a 85% yield (1.97 g).

Characterisation data were in agreement with reported literature values.^[167] ¹H NMR (400 MHz, CDCl₃) δ 7.49 – 7.31 (m, 7H), 7.29 – 7.16 (m, 2H); ¹³C NMR (101 MHz, CDCl₃) δ 138.17, 137.15, 133.82, 131.26, 129.45, 128.70, 128.13, 127.54, 124.93, 118.78; GC MS ESI⁺ *m/z*, 168.1 ([M-N₂+H]⁺, 25%), 167.1 (100, [M-N₂]⁺), 166.1 (39, [M-HN₂]⁺), 140.1 (27), 139.1 (34), 63.0 (21).

Synthesis of 2-ethynyl-1,1'-biphenyl (**171**)

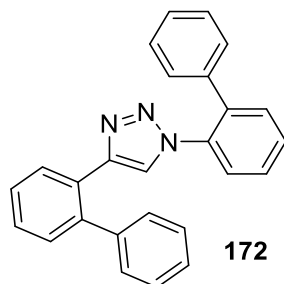


A solution of 2-bromo-1,1'-biphenyl **169** (1.2 g, 5.46 mmol) in piperidine (10 mL) was degassed for 20 minutes with bubbling nitrogen. After this Pd(PPh₃)₂Cl₂ (76 mg, 0.11 mmol), CuI (40 mg, 0.21 mmol) and PPh₃ (50 mg, 0.19 mmol) were added to the reaction mixture which was degassed for a further 20 minutes. Finally, trimethylsilylacetylene (0.7 g, 1.0 mL) was added and the reaction mixture heated to reflux for 18 h. The reaction mixture was then filtered through celite and extracted with water (50 mL) and EtOAc (3 x 25 mL), the combined organic fractions were dried over MgSO₄ and concentrated under reduced pressure. The crude material was subjected to automated flash column chromatography combiflash Rf (0-30% hexane/EtOAc, 20 min). The recovered material was taken forward for deprotection. To the crude material was added a solution of TBAF in THF (1.0 M, 7 mL) and water (1 mL). The reaction mixture was stirred at room temperature for 2 h at which point it was concentrated under reduced pressure. The residue was taken up in EtOAc (25 mL) and washed with water (25 mL), the organic phase was dried over MgSO₄ and concentrated under reduced pressure. The crude material was subjected to automated flash column chromatography combiflash Rf (0-30% hexane/EtOAc, 20 min) to yield 2-ethynyl-1,1'-biphenyl **171** as a brown oil in a 58% yield (0.56 g).

Characterisation data were in agreement with reported literature values.^[168] ¹H NMR (400 MHz, CDCl₃) δ 7.64 – 7.56 (m, 3H, Ar-*H*), 7.45 – 7.35 (m, 5H, Ar-*H*), 7.33 – 7.27 (m, 1H, Ar-*H*), 3.03 (s, 1H, CCH); ¹³C NMR (101 MHz, CDCl₃) δ 144.45, 140.28, 133.88, 129.60,

129.25, 128.97, 127.99, 127.55, 127.00, 120.47, 83.10, 80.15; GC MS ESI⁺ *m/z*, 178.1 ([M]⁺, 100%), 176.1 (32), 152.1 (32, [M-C₂H₂]⁺).

Synthesis of 1,4-di([1,1'-biphenyl]-2-yl)-1*H*-1,2,3-triazole (**172**)

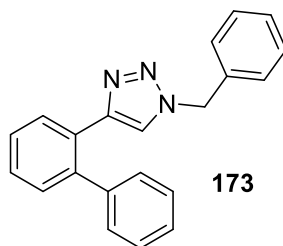


To a solution of 2-ethynyl-1,1'-biphenyl **171** (100 mg, 0.51 mmol) and 2-azido-1,1'-biphenyl **168** (99 mg, 0.51 mmol) in MeOH (5 mL) was added CuSO₄·5H₂O (13 mg, 0.051 mmol) and NaAsc (20 mg, 0.102 mmol). The reaction mixture was heated to 50 °C for 18 h. The reaction was then quenched with the addition of 5% v/v aq. ammonia solution (20 mL) and extracted with EtOAc (3 x 25 mL). The combined organic fractions were dried over MgSO₄ and concentrated under reduced pressure. The crude material was subjected to automated flash column chromatography combiflash Rf (0-100% hexane/EtOAc, 20 min). This gave 1,4-di([1,1'-biphenyl]-2-yl)-1*H*-1,2,3-triazole **172** as a white crystalline solid in a 55% yield (106 mg).

¹H NMR (400 MHz, CDCl₃) δ 8.25 (app dd, *J* = 7.9, 1.4, 1H, Ar-*H*), 7.55 – 7.47 (m, 1H, Ar-*H*), 7.47 – 7.40 (m, 4H, Ar-*H*), 7.35 (app td, *J* = 7.5, 1.4, 1H, Ar-*H*), 7.31 – 7.19 (m, 5H, Ar-*H*), 7.16 (app ddt, *J* = 8.4, 6.6, 1.5, 2H, Ar-*H*), 7.04 – 6.94 (m, 4H, Ar-*H*), 6.24 (s, 1H, Triazole *CH*); ¹³C NMR (101 MHz, CDCl₃) δ 145.92, 141.55, 140.15, 137.43, 137.20, 134.92, 131.15, 130.35, 129.92, 129.15, 128.85, 128.70, 128.64, 128.49, 128.46, 128.42, 128.33, 127.87, 127.78, 127.16, 126.82, 124.25; MS ESI⁺ *m/z*, 396.2 ([M+Na]⁺, 62%), 374.2

(100, $[M+H]^+$); HRMS ESI⁺ $[M+H]^+$ Calculated for $C_{26}H_{20}N_3^+$ = 374.1652 Found = 374.1659; IR ν_{max} (ATR)/ cm^{-1} 3058, 2925, 1487, 1476, 1230, 1035, 760, 700; MP 113 – 115 °C.

Synthesis of 4-([1,1'-biphenyl]-2-yl)-1-benzyl-1*H*-1,2,3-triazole (**173**)

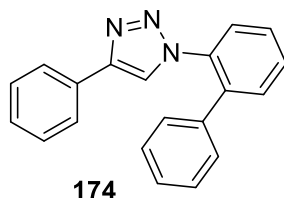


To a solution of 2-ethynyl-1,1'-biphenyl **171** (100 mg, 0.51 mmol, 1 equiv.) and benzyl azide (70 mg, 0.51 mmol) in MeOH (5 mL) was added $CuSO_4 \cdot 5H_2O$ (13 mg, 0.051 mmol) and NaAsc (20 mg, 0.102 mmol). The reaction mixture was heated at 50 °C for 18 h. The reaction was then quenched with the addition of 5% v/v aq. ammonia solution (20 mL) and extracted with EtOAc (3 x 25 mL). The combined organic fractions were dried over $MgSO_4$ and concentrated under reduced pressure. The crude material was subjected to automated flash column chromatography combiflash Rf (0-100% hexane/EtOAc, 20 min). This gave 4-([1,1'-biphenyl]-2-yl)-1-benzyl-1*H*-1,2,3-triazole **173** as a cream solid in a 53% yield (84 mg).

¹H NMR (400 MHz, $CDCl_3$) δ 8.11 (dd, $J = 7.8, 1.2$, 1H, Ar-*H*), 7.43 (app td, $J = 7.6, 1.5$, 1H, Ar-*H*), 7.36 (app td, $J = 7.5, 1.4$, 1H, Ar-*H*), 7.31 – 7.25 (m, 4H, Ar-*H*), 7.25 – 7.19 (m, 3H, Ar-*H*), 7.16 – 7.10 (m, 2H, Ar-*H*), 7.06 – 7.01 (m, 2H, Ar-*H*), 6.32 (s, 1H, Triazole *CH*), 5.30 (s, 2H, CH_2); ¹³C NMR (101 MHz, $CDCl_3$) δ 146.73, 141.59, 140.33, 134.65, 130.03, 129.25, 128.93, 128.67, 128.48, 128.32, 128.01, 127.83, 127.25, 122.42, 53.82; MS ESI⁺ m/z , 312.2 ($[M+H]^+$, 100%); HRMS ESI⁺ $[M+H]^+$ Calculated for $C_{21}H_{18}N_3^+$ = 312.1495 Found =

312.1497; IR ν_{\max} (ATR)/ cm^{-1} 3058, 3031, 2936, 1456, 1475, 1345, 1221, 1073, 1043, 972, 764, 720, 700; MP 163 – 165 °C.

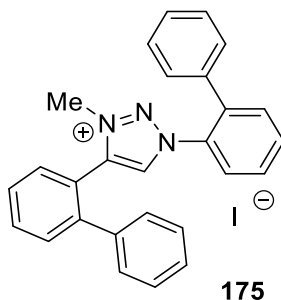
Synthesis of 1-([1,1'-biphenyl]-2-yl)-4-phenyl-1*H*-1,2,3-triazole (**174**)



To a solution of phenyl acetylene (54 mg, 0.51 mmol) and 2-azido-1,1'-biphenyl **168** (100 mg, 0.51 mmol) in MeOH (5 mL) was added $\text{CuSO}_4 \cdot 5\text{H}_2\text{O}$ (13 mg, 0.051 mmol) and NaAsc (20 mg, 0.102 mmol). The reaction mixture was heated at 50 °C for 18 h. The reaction was then quenched with the addition of 5% v/v aq. ammonia solution (20 mL) and extracted with EtOAc (3 x 25 mL). The combined organic fractions were dried over MgSO_4 and concentrated under reduced pressure. The crude material was subjected to automated flash column chromatography combiflash Rf (0-100% hexane/EtOAc, 20 min) to yield 1-([1,1'-biphenyl]-2-yl)-4-phenyl-1*H*-1,2,3-triazole **174** as a cream solid in a 78% yield (118 mg).

^1H NMR (400 MHz, CDCl_3) δ 7.71 – 7.63 (m, 3H, Ar-*H*), 7.60 – 7.50 (m, 3H, Ar-*H*), 7.38 (s, 1H, Triazole *CH*), 7.38 – 7.33 (m, 2H, Ar-*H*), 7.31 – 7.25 (m, 4H, Ar-*H*), 7.18 – 7.11 (m, 2H, Ar-*H*); ^{13}C NMR (101 MHz, CDCl_3) δ 147.44, 137.34, 137.00, 135.10, 131.17, 130.37, 129.91, 128.80, 128.76, 128.63, 128.53, 128.17, 128.07, 126.52, 125.77, 121.73; MS ESI⁺ m/z , 298.1 ($[\text{M}+\text{H}]^+$, 100%); HRMS ESI⁺ Calculated for $\text{C}_{20}\text{H}_{16}\text{N}_3^+$ = 298.1339 Found = 298.1341; IR ν_{\max} (ATR)/ cm^{-1} 3136, 3060, 1507, 1478, 1441, 1231, 1038, 1027, 759, 695; MP 168 – 170 °C.

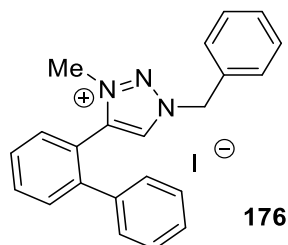
Synthesis of 1,4-di([1,1'-biphenyl]-2-yl)-3-methyl-1*H*-1,2,3-triazol-3-ium iodide (**175**)



1,4-Di([1,1'-biphenyl]-2-yl)-1*H*-1,2,3-triazole **172** (56 mg, 0.15 mmol) was dissolved in methyl iodide (2 mL) in a sealed tube and heated at 80 °C for 24 h. After this time the reaction was concentrated under reduced pressure. No further purification was required, this gave 1,4-di([1,1'-biphenyl]-2-yl)-3-methyl-1*H*-1,2,3-triazol-3-ium iodide **175** as a brown oil in a 93% yield (72 mg).

¹H NMR (400 MHz, CDCl₃) δ 8.39 (dd, *J* = 7.9, 1.4, 1H, Ar-*H*), 8.17 – 8.13 (m, 1H, Ar-*H*), 8.10 (s, 1H, Triazole *CH*), 7.73 – 7.60 (m, 3H, Ar-*H*), 7.56 – 7.48 (m, 3H, Ar-*H*), 7.49 – 7.42 (m, 3H, Ar-*H*), 7.42 – 7.35 (m, 3H, Ar-*H*), 7.25 – 7.19 (m, 2H, Ar-*H*), 7.03 – 6.96 (m, 2H, Ar-*H*), 3.62 (s, 3H, CH₃); ¹³C NMR (101 MHz, CDCl₃) δ 143.12, 141.67, 138.60, 136.93, 136.02, 133.93, 132.77, 132.56, 132.24, 131.40, 131.29, 130.53, 129.59, 129.26, 129.13, 128.86, 128.77, 128.74, 128.68, 128.42, 128.27, 119.62, 39.15; MS ESI⁺ *m/z*, 389.2 ([M+H-I]⁺ 25%), 388.2 (100, [M-I]⁺); HRMS ESI⁺ [M-I]⁺ Calculated for C₂₇H₂₂N₃⁺ = 388.1808 Found = 388.1812; IR ν_{max} (ATR)/cm⁻¹ 3033, 2827, 2857, 1601, 1479, 1438, 1269, 762, 704.

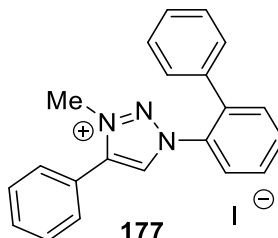
Synthesis of 1-([1,1'-biphenyl]-2-yl)-3-methyl-4-phenyl-1*H*-1,2,3-triazol-3-ium iodide (176)



4-([1,1'-Biphenyl]-2-yl)-1-benzyl-1*H*-1,2,3-triazole **173** (28 mg, 0.09 mmol) was dissolved in methyl iodide (2 mL) in a sealed tube and heated at 80 °C for 24 h. After this time the reaction was concentrated under reduced pressure. No further purification was required, this gave 1-([1,1'-biphenyl]-2-yl)-3-methyl-4-phenyl-1*H*-1,2,3-triazol-3-ium iodide **176** as a brown oil in a 72% yield (30 mg).

¹H NMR (400 MHz, CDCl₃) δ 9.30 (s, 1H, Triazole CH), 7.80 (dd, *J* = 7.7, 0.9, 1H, Ar-*H*), 7.69 (td, *J* = 7.7, 1.3, 1H, Ar-*H*), 7.60 – 7.50 (m, 4H, Ar-*H*), 7.45 – 7.39 (m, 3H, Ar-*H*), 7.34 – 7.26 (m, 3H, Ar-*H*), 7.14 – 7.07 (m, 2H, Ar-*H*), 6.09 (s, 2H, CH₂), 3.59 (s, 3H, CH₃); ¹³C NMR (101 MHz, CDCl₃) δ 142.74, 142.30, 138.27, 132.67, 132.22, 131.60, 130.88, 130.69, 129.85, 129.44, 129.28, 128.72, 128.66, 128.40, 127.79, 119.95, 57.63, 38.24; MS ESI⁺ *m/z*, 327.2 ([M+H-I]⁺ 21%), 326.2 (100, [M-I]⁺); HRMS ESI⁺ Calculated for C₂₂H₂₀N₃⁺ = 326.1652 Found = 326.1660; IR *v*_{max} (ATR)/cm⁻¹ 3030, 2926, 2855, 1730, 1441, 1477, 1312, 1155, 767, 732, 704.

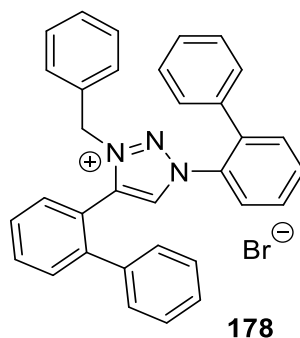
Synthesis of 1-([1,1'-biphenyl]-2-yl)-3-methyl-4-phenyl-1*H*-1,2,3-triazol-3-ium iodide (177)



1-([1,1'-Biphenyl]-2-yl)-4-phenyl-1*H*-1,2,3-triazole **174** (81 mg, 0.27 mmol) was dissolved in methyl iodide (2 mL) in a sealed tube and heated at 80 °C for 24 h. After this time the reaction was concentrated under reduced pressure. No further purification was required, this gave 1-([1,1'-biphenyl]-2-yl)-3-methyl-4-phenyl-1*H*-1,2,3-triazol-3-ium iodide **177** as a brown oil in a 84% yield (99 mg).

¹H NMR (400 MHz, CDCl₃) δ 8.38 (dd, *J* = 8.0, 1.2, 1H, Ar-*H*), 7.84 (s, 1H, Triazole *CH*), 7.73 (app td, *J* = 7.6, 1.3, 1H, Ar-*H*), 7.68 – 7.62 (m, 3H, Ar-*H*), 7.60 – 7.55 (m, 2H, Ar-*H*), 7.54 – 7.49 (m, 2H, Ar-*H*), 7.46 – 7.40 (m, 3H, Ar-*H*), 7.25 – 7.20 (m, 2H, Ar-*H*), 4.40 (s, 3H, CH₃); ¹³C NMR (101 MHz, CDCl₃) δ 143.36, 136.94, 135.74, 132.38, 132.02, 131.16, 130.14, 129.70, 129.58, 129.37, 128.93, 128.67, 127.96, 121.38, 39.96; MS ESI⁺ *m/z*, 313.2 ([M-I+H]⁺, 22%), 312.2 (100, [M-I]⁺); HRMS ESI⁺ Calculated for C₂₁H₁₈N₃⁺ = 312.1495 Found = 312.1502; IR ν_{max} (ATR)/cm⁻¹ 3047, 1480, 1441, 1040, 763, 698.

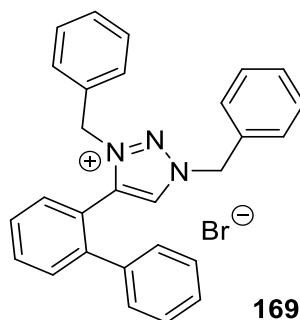
Synthesis of 1,4-di([1,1'-biphenyl]-2-yl)-3-benzyl-1*H*-1,2,3-triazol-3-ium bromide (**178**)



1,4-Di([1,1'-biphenyl]-2-yl)-1*H*-1,2,3-triazole **172** (30 mg,) was dissolved in acetonitrile (5 mL) and benzyl bromide (1 mL) in a sealed tube and heated at 150 °C for 24 h. After this time the reaction was concentrated under reduced pressure. The crude material was subjected to automated flash column chromatography combiflash Rf (0-20% DCM/MeOH, 20 min). This gave 1,4-di([1,1'-biphenyl]-2-yl)-3-benzyl-1*H*-1,2,3-triazol-3-ium bromide **178** as a colourless crystalline solid in a 62% yield (27 mg).

¹H NMR (400 MHz, CDCl₃) δ 8.57 (s, 1H, Triazole CH), 8.40 – 8.27 (m, 2H, Ar-H), 7.70 – 7.57 (m, 4H, Ar-H), 7.47 (dd, *J* = 7.5, 1.6, 1H, Ar-H), 7.44 – 7.36 (m, 2H, Ar-H), 7.34 – 7.28 (m, 4H, Ar-H), 7.25 – 7.14 (m, 4H, Ar-H), 7.01 (d, *J* = 7.0, 2H, Ar-H), 6.74 (d, *J* = 7.0, 2H, Ar-H), 6.55 (d, *J* = 7.0 Hz, 2H, Ar-H), 5.36 (s, 2H, CH₂); ¹³C NMR (101 MHz, CDCl₃) δ 142.13, 142.02, 138.64, 137.48, 136.38, 132.90, 132.82, 132.14, 132.03, 131.39, 130.46, 130.31, 129.55, 129.40, 129.00, 128.95, 128.92, 128.82, 128.73, 128.52, 128.21, 128.13, 128.04, 120.11, 55.75; MS ESI⁺ *m/z*, 465.2 ([M+H-Br]⁺, 37%), 464.1 (100, [M-Br]⁺); HRMS ESI⁺ Calculated for C₃₃H₂₆N₃⁺ = 464.2121 Found = 464.2129; IR ν_{max} (ATR)/cm⁻¹ 3029, 2926, 1602, 1482, 1456, 1438, 1268, 1180, 1021, 761, 701; MP 186 – 188 °C.

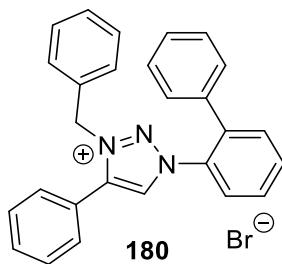
Synthesis of 4-([1,1'-biphenyl]-2-yl)-1,3-dibenzyl-1*H*-1,2,3-triazol-3-ium bromide (**179**)



4-([1,1'-Biphenyl]-2-yl)-1-benzyl-1*H*-1,2,3-triazole **173** (50 mg, 0.16 mmol) was dissolved in acetonitrile (5 mL) and benzyl bromide (1 mL) in a sealed tube and heated at 150 °C for 24 h. After this time the reaction was concentrated under reduced pressure. The crude material was subjected to automated flash column chromatography combiflash Rf (0-20% DCM/MeOH, 20 min) this gave 4-([1,1'-biphenyl]-2-yl)-1,3-dibenzyl-1*H*-1,2,3-triazol-3-ium bromide **179** as a brown oil in a 33% yield (25 mg).

¹H NMR (400 MHz, CDCl₃) δ 9.81 (s, 1H, Triazole CH), 7.69 – 7.62 (m, 1H, Ar-H), 7.58 – 7.43 (m, 5H, Ar-H), 7.41 – 7.34 (m, 3H, Ar-H), 7.32 – 7.15 (m, 6H, Ar-H), 6.96 – 6.88 (m, 2H, Ar-H), 6.81 – 6.70 (m, 2H, Ar-H), 6.19 (s, 2H, CH₂), 5.12 (s, 2H, CH₂); ¹³C NMR (101 MHz, CDCl₃) δ 142.34, 141.87, 138.03, 132.49, 132.32, 131.78, 131.56, 130.65, 130.46, 129.71, 129.56, 129.22, 129.18, 129.01, 128.68, 128.46, 128.39, 128.30, 120.18, 57.25, 55.28 MS ESI⁺ m/z, 403.2 ([M-Br+H]⁺, 29%), 402.2 (100, [M-Br]⁺); HRMS ESI Calculated for C₂₈H₂₄N₃⁺ = 402.1965 Found = 402.1970; IR ν_{max} (ATR)/cm⁻¹ 3060, 2923, 2851, 1497, 1475, 1456, 1346, 1222, 1074, 1044, 765, 722, 702.

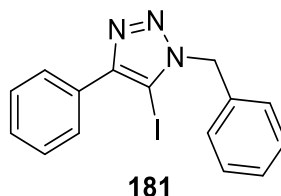
Synthesis of 1,3-dibenzyl-4-phenyl-1*H*-1,2,3-triazol-3-ium bromide (**180**)



1-([1,1'-Biphenyl]-2-yl)-4-phenyl-1*H*-1,2,3-triazole **174** (48 mg, 0.16 mmol) was dissolved in acetonitrile (5 mL) and benzyl bromide (1 mL) in a sealed tube and heated at 150 °C for 24 h. After this time the reaction was concentrated under reduced pressure. The crude material was subjected to automated flash column chromatography combiflash Rf (0-20% DCM/MeOH, 20 min) this gave 1,3-dibenzyl-4-phenyl-1*H*-1,2,3-triazol-3-ium bromide **180** as a brown oil in a 75% yield (58 mg).

¹H NMR (400 MHz, CDCl₃) δ 8.59 (s, 1H, Triazole *CH*), 8.45 (dd, *J* = 7.8, 1.0, 1H, Ar-*H*), 7.73 (app td, *J* = 7.5, 1.2, 1H, Ar-*H*), 7.67 (app td, *J* = 7.7, 1.5, 1H, Ar-*H*), 7.64 – 7.60 (m, 2H, Ar-*H*), 7.59 – 7.52 (m, 2H, Ar-*H*), 7.48 (m, 2H, Ar-*H*), 7.41 – 7.25 (m, 6H, Ar-*H*), 7.16 (m, 2H, Ar-*H*), 6.87 (m, 2H, Ar-*H*), 5.77 (s, 2H, CH₂); ¹³C NMR (101 MHz, CDCl₃) δ 143.13, 137.66, 136.16, 133.03, 132.38, 131.92, 131.76, 131.06, 130.86, 130.28, 129.64, 129.44, 129.36, 129.24, 129.01, 128.57, 128.51, 127.98, 127.91, 121.57, 55.77; MS ESI⁺ *m/z*, 389.2 ([M+H-Br]⁺, 27%), 388.2 (100, [M-Br]⁺); HRMS ESI⁺ Calculated for C₂₇H₂₂N₃⁺ = 388.1808, Found = 388.1817; IR *v*_{max} (ATR)/cm⁻¹ 3028, 1611, 1483, 1455, 1439, 1182, 1020.

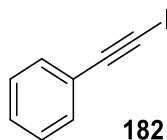
Synthesis of 1-benzyl-5-iodo-4-phenyl-1*H*-1,2,3-triazole (**181**)



Copper(I) iodide (2 mg, 0.011 mmol) and TBTA (6 mg, 0.011 mmol) were stirred together in THF (2 mL) for 30 minutes. To this solution was added (iodoethyl)benzene **182** (50 mg, 0.22 mmol) and benzyl azide (29 mg, 0.22 mmol) diluted in THF (0.5 mL) in one portion. The reaction mixture was stirred at rt for 18 h. The reaction was quenched with the addition of 5% v/v aq. ammonia solution (5 mL) and extracted with EtOAc (3 x 25 mL). The combined organic fractions were dried over MgSO₄ and concentrated under reduced pressure. The crude material was subjected to automated flash column chromatography combiflash Rf (0-100% hexane/EtOAc, 20 min). This gave 1-benzyl-5-iodo-4-phenyl-1*H*-1,2,3-triazole **181** as a white solid in a 64% yield (50 mg).

Characterisation data were in agreement with reported literature values.^[169] ¹H NMR (400 MHz, CDCl₃) δ 7.99 – 7.89 (m, 2H, Ar-*H*), 7.51 – 7.43 (m, 2H, Ar-*H*), 7.42 – 7.28 (m, 6H, Ar-*H*), 5.68 (s, 2H, CH₂); ¹³C NMR (101 MHz, CDCl₃) δ 150.21, 134.34, 130.21, 128.91, 128.59, 128.52, 128.48, 127.80, 127.44, 76.37, 54.40; MS ESI⁺ m/z, 384.0 ([M+Na]⁺, 51%), 362.0 (100, [M+H]⁺).

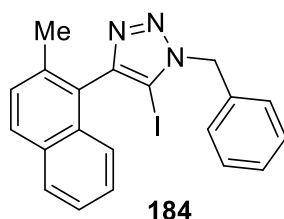
Synthesis of (iodoethynyl)benzene (**182**)



Iodine (1.4 g, 5.39 mmol) and morpholine (1.3 g, 14.7 mmol) were stirred together in toluene (10 mL) for 30 min at room temperature. Phenyl acetylene (0.5 g, 4.90 mmol) was then added and the suspension stirred at 50 °C for 24 h. The reaction mixture was quenched by the addition of water (25 mL) and extracted with EtOAc (3 x 25 mL). The combined organic extracts were dried over MgSO₄ and concentrated under reduced pressure. The crude material was subjected to automated flash column chromatography combiflash Rf (0-20% hexane/EtOAc, 20 min). This gave (iodoethynyl)benzene **182** as brown oil in a 71% yield (0.80 g).

Characterisation data were in agreement with reported literature values.^[170] ¹H NMR (400 MHz, CDCl₃) δ 7.46 – 7.37 (m, 2H, Ar-*H*), 7.33 – 7.25 (m, 3H, Ar-*H*); ¹³C NMR (101 MHz, CDCl₃) δ 132.38, 128.85, 128.29, 123.42, 94.22, 6.45; MS ESI⁺ *m/z*, 229.1 ([M+H]⁺, 15%) 228.1 (100, [M]⁺).

Synthesis of 1-benzyl-5-iodo-4-(2-methylnaphthalen-1-yl)-1*H*-1,2,3-triazole (**184**)



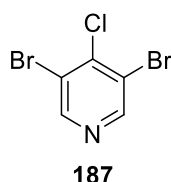
A solution of 1-bromo-2-methylnaphthalene **159** (1.20 g, 5.46 mmol) in piperidine (20 mL) was degassed by bubbling with nitrogen for 20 min. To this solution was added Pd(PPh₃)₂Cl₂

(76 mg, 0.11 mmol), CuI (40 mg, 0.21 mmol) and PPh₃ (50 mg, 0.19 mmol) the solution was degassed for a further 20 min with bubbling nitrogen. Finally, trimethylsilylacetylene was added (0.7 g, 1.0 mL) and the reaction mixture heated at reflux for 18 h. The reaction mixture was then filtered through celite and extracted with water (50 mL) and EtOAc (3 x 25 mL), the combined organic fractions were dried over MgSO₄ and concentrated under reduced pressure. The crude material was subjected to automated flash column chromatography combiflash Rf (0-30% hexane/EtOAc, 20 min) this gave an inseparable mixture of 1-bromo-2-methylnaphthalene and trimethyl((2-methylnaphthalen-1-yl)ethynyl)silane **160** which was carried forward. To the material was added a solution of TBAF in THF (1.0 M, 7 mL) and water (1 mL). The reaction mixture was stirred at room temperature for 2 hours at which point it was concentrated under reduced pressure. The residue was taken up in EtOAc (25 mL) and washed with water (25 mL). The organic phase was dried over MgSO₄ and concentrated under reduced pressure. The material was subjected to automated flash column chromatography combiflash Rf (0-30% hexane/EtOAc, 20 min) this gave an inseparable mixture of 1-bromo-2-methylnaphthalene and 1-ethynyl-2-methylnaphthalene which was carried forward. To a solution of iodine (0.62 g, 3.70 mmol) in toluene (10 mL) was added morpholine (1.04 g, 1.03 mL, 4.10 mmol) dropwise over a period of 5 min and allowed to stir at rt for 30 min. To this solution was added the mixture of 1-bromo-2-methylnaphthalene and 1-ethynyl-2-methylnaphthalene **163** and the reaction mixture was heated for 18 h at 50 °C. The reaction was quenched by addition of water (50 mL) and extracted with EtOAc (3 x 25 mL) the combined organic fractions were dried over MgSO₄ and concentrated under reduced pressure. This material was subjected to ¹H NMR spectroscopic analysis and the alkynyl proton resonance was no longer observed. This material was used in the next step without further purification. This material was added a solution of benzyl azide (0.24 g, 1.83 mmol) in

THF (10 mL). To this solution was added copper(I) iodide (17 mg, 0.09 mmol) and TBTA (47 mg, 0.09 mmol) and the reaction stirred at rt for 24 h. After this time the reaction was quenched with the addition of 5% v/v aqueous ammonia solution and extracted with water (20 mL) and EtOAc (3 x 25 mL). The combined organic fractions were dried over MgSO₄ and concentrated under reduced pressure. The crude material was subjected to automated flash column chromatography combiflash Rf (0-100% hexane/EtOAc, 20 min) this gave 1-benzyl-5-iodo-4-(2-methylnaphthalen-1-yl)-1*H*-1,2,3-triazole **184** as a yellow crystalline solid in a 10% yield (237 mg).

¹H NMR (400 MHz, CDCl₃) δ 7.85 (t, *J* = 7.3 Hz, 2H, Ar-*H*), 7.48 – 7.30 (m, 8H, Ar-*H*/Triazole *CH*), 7.25 (d, *J* = 8.3 Hz, 1H, Ar-*H*), 5.75 (ABq, Δδ_{AB} = 0.02, *J* = 15.8, 2H, CH₂), 2.25 (s, 3H, CH₃); ¹³C NMR (101 MHz, CDCl₃) δ 150.79, 136.46, 134.57, 133.04, 131.94, 129.34, 129.01, 128.53, 128.39, 127.99, 127.64, 126.50, 125.69, 125.15, 125.09, 54.59, 20.50; MS ESI⁺ *m/z*, 448.0 ([M+Na]⁺, 32%), 427.1 (21), 426.1 (100, [M+H]⁺); HRMS ESI⁺ Calculated for C₂₀H₁₆N₃I⁺ = 426.0462 Found = 426.0473; IR ν_{max} (ATR)/cm⁻¹ 3034, 2918, 2854, 1443, 1211, 1080, 966, 814, 724; MP 176 – 178 °C; HPLC (Phenomenex Cellulose 3) Acetonitrile/Water 80:20, 1.0 mL/min, λ = 250 nm, t₁ = 4.9 min, t₂ = 6.2 min.

Synthesis of 3,5-Dibromo-4-chloropyridine (**187**)

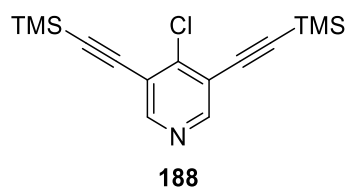


A solution of bromine (19 mL, 0.370 mol) was added dropwise over a period of 30 min to 4-pyridone (17.5 g, 0.185 mol) and KOH (20.5 g, 0.370 mmol) in water (350 mL). This was stirred for 30 minutes and the reaction mixture filtered to give 3,5-dibromopyridine which

was taken forward without further purification. Phosphorous pentachloride and 3,5-dibromopyridine **186** were then heated together for 3 h at 150 °C, the reaction was then cooled to 0 °C and quenched with water (100 mL). The reaction mixture was filtered and the recovered solid was recrystallised from ethanol to yield 3,5-dibromo-4-chloropyridine **187** as a yellow solid in a 73% yield (36.6 g).

Characterisation data were in agreement with reported literature values.^[171] ¹H NMR (300 MHz, CDCl₃) δ 8.54 (s, 2H, Py-*H*); ¹³C NMR (101 MHz, CDCl₃) δ 150.9, 144.0, 121.9; MS EI⁺ m/z, 274.9 ([M]⁺, 20%), 272.9 (75, [M]⁺), 270.9 (100, [M]⁺), 268.9 (53, [M]⁺), 191.9 (34, [M-Br]⁺), 189.9 (26, [M-Br]⁺); MP 100 - 102 °C. Literature value, MP 95-97 °C.^[171]

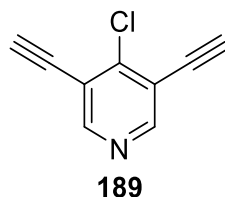
Synthesis of 4-Chloro-3,5-bis((trimethylsilyl)ethynyl)pyridine (**188**)



A solution of copper(I) iodide (14 mg, 0.07 mmol), bis(triphenylphosphine)palladium(II) dichloride (52 mg, 0.07 mmol) and 3,5-dibromo-4-chloropyridine (200 mg, 0.74 mmol) in diisopropylamine (10 mL) was freeze thaw degassed. To this trimethylsilylacetylene (0.25 mL, 1.76 mmol) was added dropwise over a period of 5 min and the reaction mixture heated to reflux for 72 h. The reaction mixture was concentrated under reduced pressure and the residue was subjected to automated flash column chromatography combiflash Rf (silica, 0-10% hexane/EtOAc, 20 min). This gave 4-chloro-3,5-bis((trimethylsilyl)ethynyl)pyridine **188** as a colourless oil in a 95% yield (217 mg).

$R_f = 0.56$ (Hexane/EtOAc [9:1]); $^1\text{H NMR}$ (300 MHz, CDCl_3) δ 8.52 (s, 2H, Py-*H*), 0.27 (s, 18H, CH_3); $^{13}\text{C NMR}$ (101 MHz, CDCl_3) δ 152.4, 146.9, 120.8, 104.9, 97.9; MS EI^+ m/z , 307.2 ($[\text{M}]^+$, 27%), 305.1 (52, $[\text{M}]^+$), 292.1 (62, $[\text{M}-\text{CH}_3]^+$), 290.1 (100, $[\text{M}-\text{CH}_3]^+$).

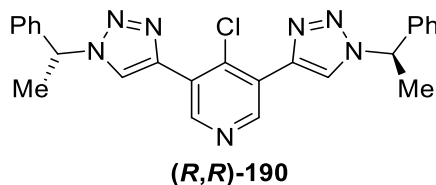
Synthesis of 4-Chloro-3,5-diethynylpyridine (**189**)



To a solution of 4-chloro-3,5-bis((trimethylsilyl)ethynyl)pyridine **188** (110 mg, 0.36 mmol) in THF/MeOH (4:2, 6 mL) was added TBAF in THF (1 M, 1.43 mL, 1.43 mmol). The reaction was stirred at rt for 30 min at which point the reaction mixture was concentrated under reduced pressure. The residue was diluted with DCM (20 mL) and washed sequentially with water (20 mL) and brine (20 mL), the organic fraction was dried over MgSO_4 , filtered and concentrated under reduced pressure. The residue was subjected to automated flash column chromatography combiflash R_f (0-10% hexane/EtOAc gradient, 15 min). This gave 4-chloro-3,5-diethynylpyridine **189** as a colourless oil in a >99% yield (68 mg).

$R_f = 0.24$ (Hexane/EtOAc [9:1]); $^1\text{H NMR}$ (300 MHz, CDCl_3) δ 8.62 (s, 2H, Py-*H*), 3.54 (s, 2H, CCH); $^{13}\text{C NMR}$ (101 MHz, CDCl_3) δ 152.9, 147.1, 119.7, 86.1, 76.7; TOF MS EI^+ m/z , 163.0 ($[\text{M}]^+$, 44%), 161.0 (100, $[\text{M}]^+$), 99.0 (31), 98.0 (29); HRMS Calculated for $\text{C}_9\text{H}_4\text{NCl}^{35+}$ = 161.0027 Found = 161.0027.

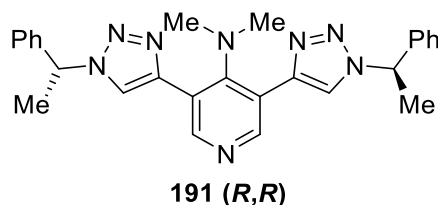
Synthesis of 4-Chloro-3,5-bis(1-((*R*)-1-phenylethyl)-1*H*-1,2,3-triazol-4-yl)pyridine ((*R,R*)-190**)**



To a solution of 4-chloro-3,5-diethynylpyridine **189** (30 mg, 0.18 mmol) and (*R*)-(1-azidoethyl)benzene (68 mg, 0.46 mmol) in methanol (5 mL) was added NaAsc (36 mg, 0.18 mmol) and CuSO₄·5H₂O (5 mg, 0.018 mmol). The reaction mixture was stirred for 24 h at 50 °C, after which time the reaction mixture was added to a solution of 4-Chloro-3,5-diethynylpyridine (**179**, 30 mg, 0.18 mmol) and (*R*)-(1-azidoethyl)benzene (68 mg, 0.46 mmol) in methanol (5 mL) and stirred for 24 h at 50 °C. The reaction mixture was then quenched with the addition of 5% v/v aqueous ammonia solution (10 mL) and extracted with ethyl acetate (3 x 25 mL). The organic extracts were combined, dried over MgSO₄, filtered and the solvent was removed under reduced pressure. The residue was purified by column chromatography (0-100% hexane/EtOAc gradient, 15 min). This gave 4-Chloro-3,5-bis(1-((*R*)-1-phenylethyl)-1*H*-1,2,3-triazol-4-yl)pyridine **190** as a cream solid in a 29% yield (24 mg).

¹H NMR (400 MHz, CDCl₃) δ 9.24 (s, 2H, Py-*H*), 7.99 (s, 2H, Triazole-*H*), 7.44 – 7.26 (m, 10H, Ar-*H*), 5.90 (q, *J* = 7.1, 2H, CH), 2.06 (d, *J* = 7.1, 6H, CH₃); ¹³C NMR (101 MHz, CDCl₃) δ 149.7, 141.5, 139.6, 137.6, 129.1, 128.7, 126.5, 126.1, 122.9, 60.6, 21.4; TOF MS ESI⁺ *m/z*, 674.3 (50%), 673.30 (57), 672.3 (100), 668.4 (37), 480.2 (15, [M+H]⁺), 478.2 (48, [M+H]⁺), 456.2 [M+H]⁺; HRMS ESI⁺ Calculated for C₂₅H₂₂N₇³⁵ClNa⁺ = 478.1517 Found = 478.1519.

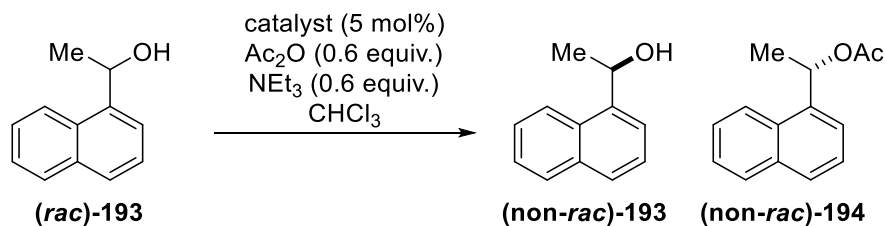
Synthesis of *N,N*-Dimethyl-3,5-bis(1-((*R*)-1-phenylethyl)-1*H*-1,2,3-triazol-4-yl)pyridin-4-amine ((*R,R*)-191)



Chloropyridine derivative (**(*R,R*)-190**) (24 mg, 0.052 mmol) was added to 40% dimethylamine in water (4 mL) and heated in a microwave reactor for 60 h at 150 °C. The solvent was removed under reduced pressure and the solid residue was dissolved in CH₂Cl₂ (10 mL), washed with saturated aqueous NaHCO₃ (2 x 10 mL). The organic fraction was dried over MgSO₄, filtered and the solvent removed under reduced pressure to afford *N,N*-dimethyl-3,5-bis(1-((*R*)-1-phenylethyl)-1*H*-1,2,3-triazol-4-yl)pyridin-4-amine (**(*R,R*)-191**) as a clear oil in a 57% yield (14 mg).

¹H NMR (400 MHz, CDCl₃) δ 8.71 (s, 2H, Py-*H*), 7.59 (s, 2H, Triazole-*H*), 7.44 – 7.28 (m, 10H, Ar-*H*), 5.89 (q, *J* = 7.1, 2H, CH), 2.37 (s, 6H, N(CH₃)₂), 2.06 (d, *J* = 7.1 Hz, 6H, CHCH₃); ¹³C NMR (101 MHz, CDCl₃) δ 154.9, 151.3, 143.8, 139.9, 137.9, 129.1, 128.6, 126.4, 121.4, 60.4, 42.9, 21.4; MS AP⁺ *m/z*, 466.3 (21%), 465.3 (100, [M+H]⁺); HRMS AP⁺ Calculated for =.C₂₇H₂₉N₈⁺ = 465.2514 Found = 465.2510; [α]_D^{29.0} 29.0° (c = 0.4, CHCl₃).

Catalysis Screening Reaction Preparation



Acetic anhydride (5.9 μL , 63 μmol , 0.60 equiv.) was added to a solution of catalyst (5.3 μmol , 0.05 equiv.), trimethylamine (8.8 μL , 63 μmol , 0.60 equiv.) and 1-(1-Naphthyl)ethanol (18.1 mg, 106 μmol , 1.00 equiv.) in chloroform (1.5 mL) at room temperature and shaken. A 2 μL aliquot was taken every 58 min and analysed by GC using a chiral stationary phase.

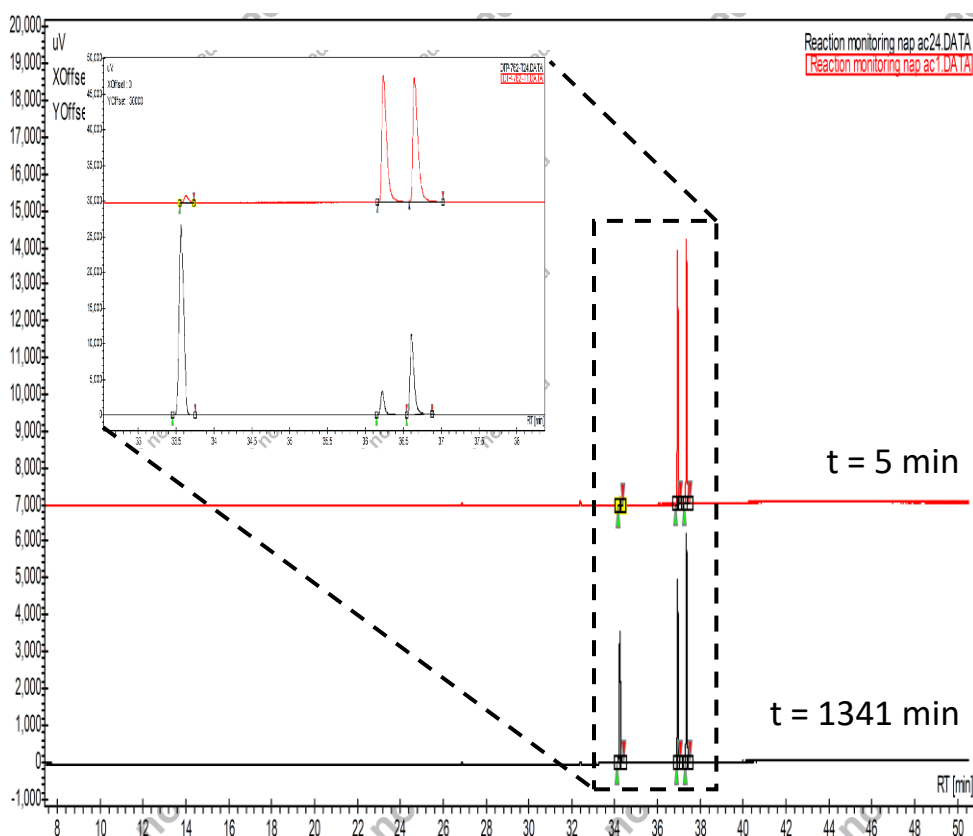


Figure 45 - Representative GC trace for selectivity factor determination for the resolution of 1-(1-naphthyl)ethanol

GC Parameters

Column

Varian WCOT Fused Silica 25M x 0.25 MM Coating CP CHIRASIL-DEX CB DF=0.25

Injector

Sample penetration depth - 90%

Washes - 9 at 8 μ L

Draw up speed - 5 μ L/s

Injector oven temperature - 260 °C

Splitter - 500

Oven

Stabilisation time - 0.5 min

Start temp - 50 °C

Ramp rate - 3.7 °C/min

Max temp - 200 °C

Hold max temp - 10 min

Run length - 50.54 min

Column flow - 1.0 mL/min

Detector

Set point - 300 °C

He flow - 25 mL/min

H₂ flow - 30 mL/min

Air flow - 300 mL/min

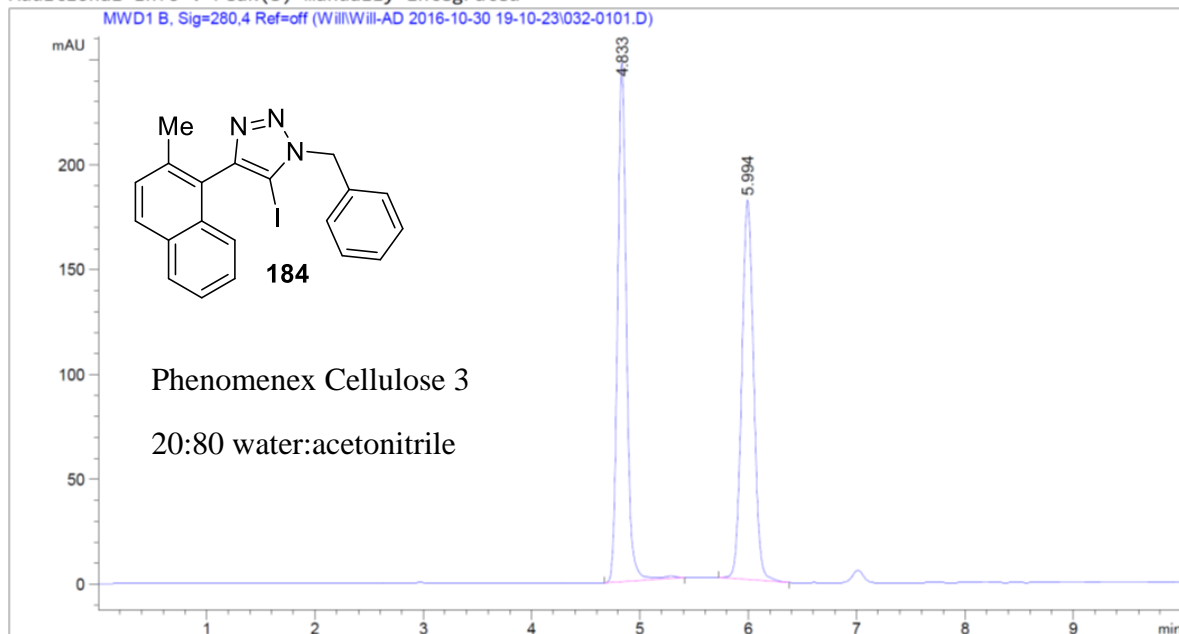
Acquisition frequency 20.0 Hz

7.4.2 Chromatography Chapter 4

7.4.2.1 Chiral HPLC Trace of Compound 184

Data File C:\Chem32\1\Data\Will\Will-AD 2016-10-30 19-10-23\032-0101.D
Sample Name: WB6-9

```
=====
Acq. Operator   : SYSTEM                      Seq. Line :    1
Acq. Instrument : LC                        Location  :   32
Injection Date  : 10/30/2016 7:11:16 PM      Inj       :    1
                                           Inj Volume: 5.000 µl
Different Inj Volume from Sample Entry! Actual Inj Volume : 2.000 µl
Acq. Method     : C:\Chem32\1\Data\Will\Will-AD 2016-10-30 19-10-23\Oxindole5050.M
Last changed    : 10/30/2016 7:18:59 PM by SYSTEM
                 (modified after loading)
Analysis Method : C:\Chem32\1\Data\Will\Will-AD 2016-10-30 19-10-23\Oxindole5050.M (Sequence
                 Method)
Last changed    : 10/30/2016 7:21:19 PM by SYSTEM
Additional Info  : Peak(s) manually integrated
=====
```



```
=====
Area Percent Report
=====
```

```
Sorted By      : Signal
Multiplier     : 1.0000
Dilution       : 1.0000
Use Multiplier & Dilution Factor with ISTDs
```

Signal 1: MWD1 B, Sig=280,4 Ref=off

Peak #	RetTime [min]	Type	Width [min]	Area [mAU*s]	Height [mAU]	Area %
1	4.833	BV R	0.0889	1420.58875	247.68842	50.7631
2	5.994	BB	0.1188	1377.87805	181.02312	49.2369

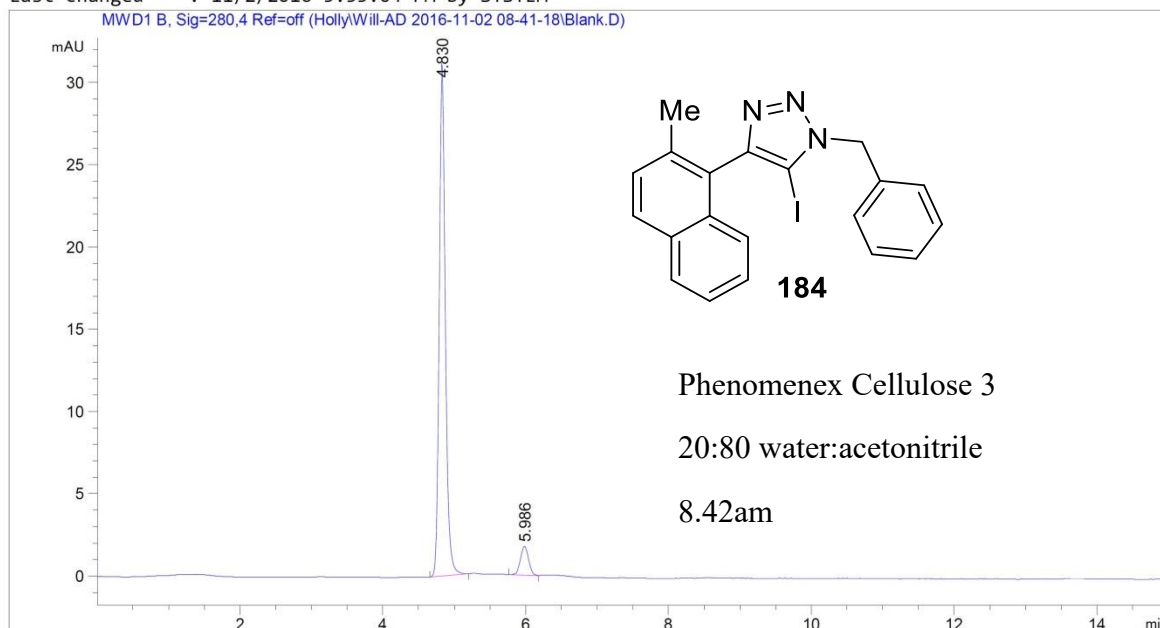
Totals : 2798.46680 428.71153

7.4.2.2 Recovered Enantioenriched Sample of 184 Following HPLC Separation

Data File C:\Chem32\1\Data\Holly\Will-AD 2016-11-02 08-41-18\Blank.D
 Sample Name: WB6-9

```

=====
Acq. Operator   : SYSTEM                      Seq. Line :    1
Acq. Instrument : LC                        Location  :    4
Injection Date  : 11/2/2016 8:42:20 AM      Inj       :    1
                                           Inj Volume: 5.000 µl
Different Inj Volume from Sample Entry! Actual Inj Volume : 20.000 µl
Acq. Method     : C:\Chem32\1\Data\Holly\Will-AD 2016-11-02 08-41-18\Oxindole5050.M
Last changed    : 11/2/2016 8:41:18 AM by SYSTEM
Analysis Method : C:\Chem32\1\Data\Holly\Will-AD 2016-11-02 08-41-18\Oxindole5050.M (Sequence
Method)
Last changed    : 11/2/2016 5:55:04 PM by SYSTEM
  
```



Area Percent Report

```

Sorted By      : Signal
Multiplier     : 1.0000
Dilution       : 1.0000
Do not use Multiplier & Dilution Factor with ISTDs
  
```

Signal 1: MWD1 B, Sig=280,4 Ref=off

Peak #	RetTime [min]	Type	Width [min]	Area [mAU*s]	Height [mAU]	Area %
1	4.830	BB	0.0938	191.89308	31.17759	93.3859
2	5.986	BB	0.1230	13.59100	1.74198	6.6141

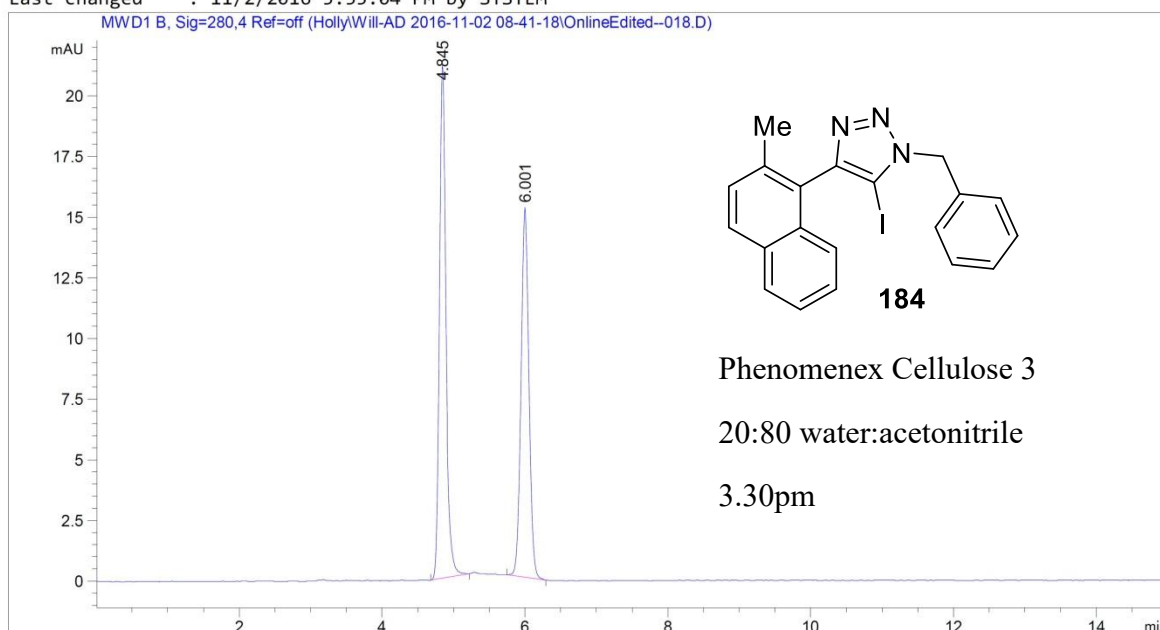
Totals : 205.48409 32.91958

7.4.2.3 Enantioenriched Sample of 184 After Being Left at Room Temperature

Data File C:\Chem32\1\Data\Holly\Will-AD 2016-11-02 08-41-18\OnlineEdited--018.D
 Sample Name: WB6-9

```

=====
Acq. Operator   : SYSTEM                      Seq. Line :   18
Acq. Instrument : LC                        Location  :    4
Injection Date  : 11/2/2016 3:30:34 PM      Inj       :   18
                                           Inj Volume: 5.000 µl
Different Inj Volume from Sample Entry! Actual Inj Volume : 20.000 µl
Acq. Method     : C:\Chem32\1\Data\Holly\Will-AD 2016-11-02 08-41-18\Oxindole5050.M
Last changed    : 11/2/2016 8:41:18 AM by SYSTEM
Analysis Method : C:\Chem32\1\Data\Holly\Will-AD 2016-11-02 08-41-18\Oxindole5050.M (Sequence
Method)
Last changed    : 11/2/2016 5:55:04 PM by SYSTEM
  
```



Area Percent Report

```

Sorted By      :      Signal
Multiplier     :      1.0000
Dilution       :      1.0000
Do not use Multiplier & Dilution Factor with ISTDs
  
```

Signal 1: MWD1 B, Sig=280,4 Ref=off

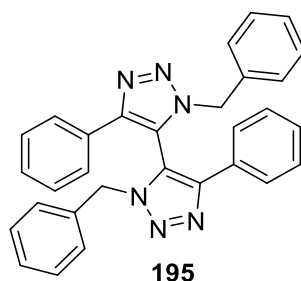
Peak #	RetTime [min]	Type	Width [min]	Area [mAU*s]	Height [mAU]	Area %
1	4.845	BB	0.0955	133.12679	21.13866	52.7164
2	6.001	BB	0.1213	119.40708	15.26199	47.2836

Totals : 252.53387 36.40065

7.5 Experimental Chapter 5

7.5.1 Synthesis

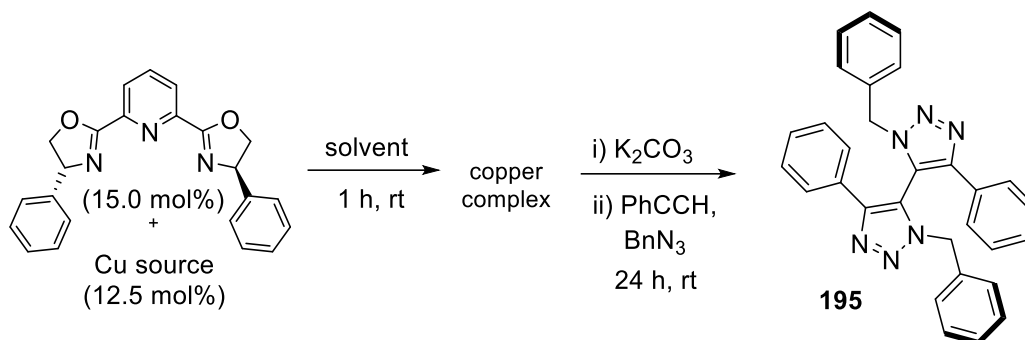
Synthesis of 3,3'-dibenzyl-5,5'-diphenyl-3H,3'H-4,4'-bi(1,2,3-triazole) (**195**)



Phenylacetylene (0.102 g, 1.0 mmol) was added to a stirred solution of benzyl azide (0.133 g, 1.0 mmol) in acetonitrile (1.5 mL) and aqueous Na₂CO₃ (2.0 N, 1.5 mL). To this solution was added a solution of copper sulfate (1.0 N, 0.1 mL) followed by copper powder (0.064 mg, 1.0 mmol). The resulting solution was stirred for 18 h at rt. The reaction mixture was then extracted with EtOAc (3 x 20 mL), the combined organic fractions were then concentrated under reduced pressure. The crude material was purified by automated flash column chromatography combiflash Rf (0-100% water/acetonitrile gradient, 20 min, C18), following chromatography slow evaporation from EtOAc was used to recover a single pure crystal of 3,3'-dibenzyl-5,5'-diphenyl-3H,3'H-4,4'-bi(1,2,3-triazole) **195** for analytical analysis in a 2% yield (8 mg).

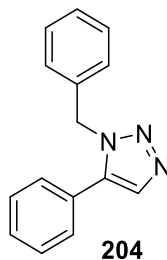
Characterisation data were in agreement with reported literature values.^[134] ¹H NMR (400 MHz, CDCl₃) δ 7.47 – 7.39 (m, 4H), 7.25 – 7.05 (m, 12H), 6.83 – 6.74 (m, 4H), 4.72 – 4.58 (ABq, Δδ_{AB} = 0.06, *J* = 14.7, 4H, CH₂); ¹³C NMR (101 MHz, CDCl₃) δ 147.84, 132.95, 129.28, 128.97, 128.82, 128.78, 128.72, 128.20, 125.83, 119.91, 52.70; MS ESI⁺ *m/z*, 469.2 [M+H]⁺, 491.2 [M+Na]⁺.

Representative Asymmetric Bis(triazole) Formation



A solution of PhPyBox **L1** (6.7 mg, 0.018 mmol, 15.0 mol%) and CuCl (1.5 mg, 0.015 mmol, 12.5 mol%) in methanol (5 mL) was stirred at rt for 1 h. After this K₂CO₃ (17 mg, 0.12 mmol, 1 equiv.) was added and the reaction mixture stirred for a further 10 minutes, to this solution was added phenylacetylene (13 mg, 0.12 mmol, 1 equiv.) and benzyl azide (32 mg, 0.24 mmol, 2 equiv.) The reaction mixture was stirred at rt for 24 h. The reaction was quenched by the addition of aqueous ammonia solution (5% v/v, 5 mL) and extracted with EtOAc (3 x 25 mL). The combined organic extracts were dried over MgSO₄ and concentrated under reduced pressure. The recovered material was subjected to chiral HPLC analysis without further purification (Phenomenex Cellulose 1 50:50 water/acetonitrile).

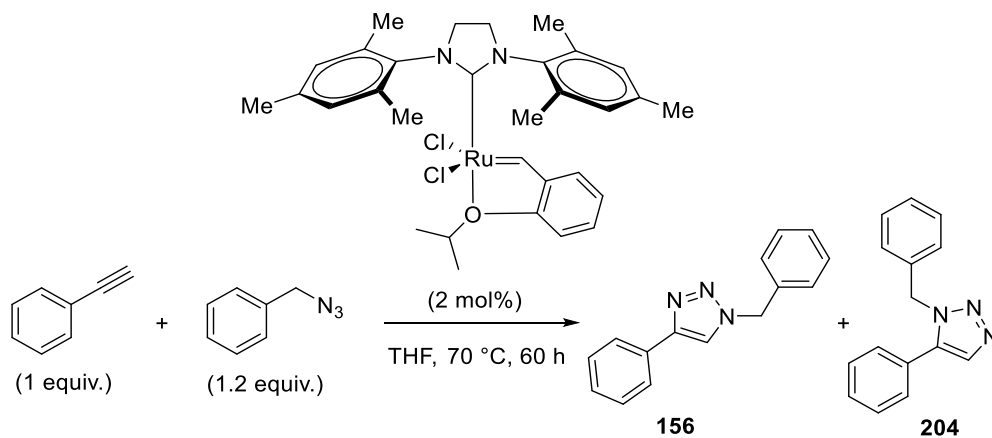
Synthesis of 1-benzyl-5-phenyl-1*H*-1,2,3-triazole (**204**)



To a solution of phenyl acetylene (40 mg, 0.39 mmol) and benzyl azide (65 mg, 0.49 mmol) in THF (2 mL) was added $\text{Cp}^*\text{RuCl}_2(\text{PPh}_3)_2$ (7.8 mg, 0.0098 mmol). The reaction mixture was heated at 70 °C and stirred for 24 h. The reaction mixture was then quenched by the addition of water (50 mL) and extracted with Et_2O (3 x 25 mL). The combined organic extracts were dried over MgSO_4 and concentrated under reduced pressure. The crude material was stirred with hexane (20 mL) and filtered. This gave 1-benzyl-5-phenyl-1*H*-1,2,3-triazole **204** as a colourless crystalline solid in a 51% yield (48 mg).

Characterisation data were in agreement with reported literature values.^[172] ^1H NMR (400 MHz, CDCl_3) δ 7.74 (s, 1H, Triazole *CH*), 7.47 – 7.36 (m, 3H, *Ar-H*), 7.31 – 7.21 (m, 4H, *Ar-H*), 7.10 – 7.04 (m, 2H, *Ar-H*), 5.55 (s, 2H, CH_2); ^{13}C NMR (101 MHz, CDCl_3) δ 138.16, 135.52, 133.29, 129.51, 128.95, 128.90, 128.83, 128.15, 127.16, 126.95, 51.82; MS ESI⁺ m/z , 258.1 ($[\text{M}+\text{Na}]^+$, 31%), 236.1 (100, $[\text{M}+\text{H}]^+$).

Representative Catalytic Reaction

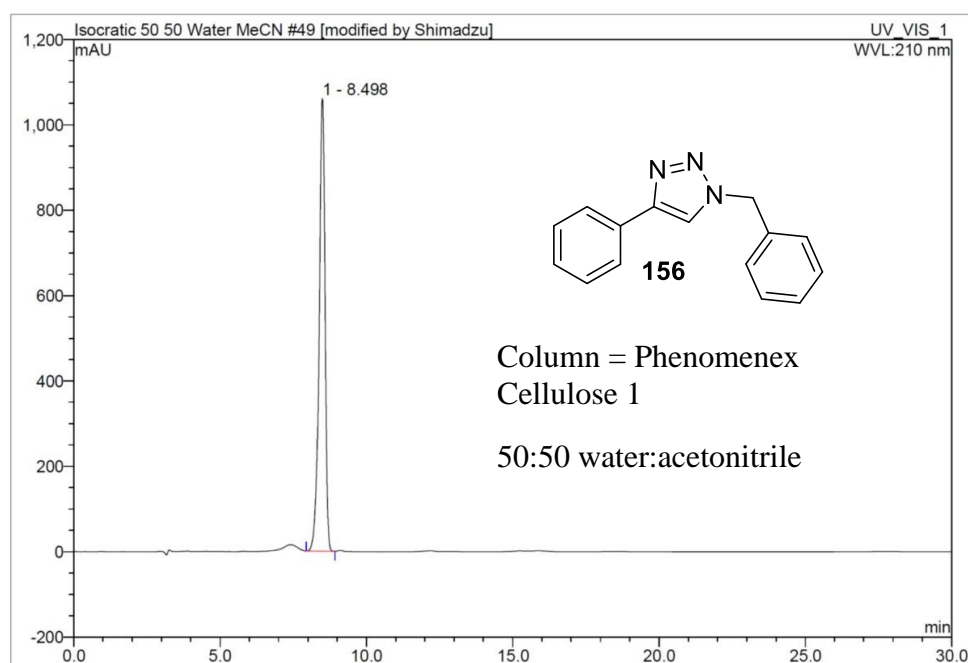


Under an atmosphere of nitrogen, to a solution of Hoveyda-Grubbs 2nd generation catalyst (3.8 mg, 2 mol%) in THF (2 mL) was added benzyl azide (50 mg, 0.38 mmol, 1.2 equiv.) and phenyl acetylene (32 mg, 0.31 mmol, 1.0 equiv.). The reaction mixture was stirred for 24 h at 70 °C. The reaction mixture was then concentrated under reduced pressure and the residue analysed by ¹H NMR spectroscopy to measure product distribution.

7.5.2 Chromatography Chapter 5

7.5.2.1 HPLC Trace of Compound 156

49 WB-MonoTriazole			
Sample Name:	WB-MonoTriazole	Injection Volume:	5.0
Vial Number:	1_3	Channel:	UV_VIS_1
Sample Type:	unknown	Wavelength:	210
Control Program:	Isocratic 50 50 water MeCN	Bandwidth:	n.a.
Quantif. Method:	Isocratic 50 50 water MeCN	Dilution Factor:	1.0000
Recording Time:	3/12/2015 11:51	Sample Weight:	1.0000
Run Time (min):	30.00	Sample Amount:	1.0000



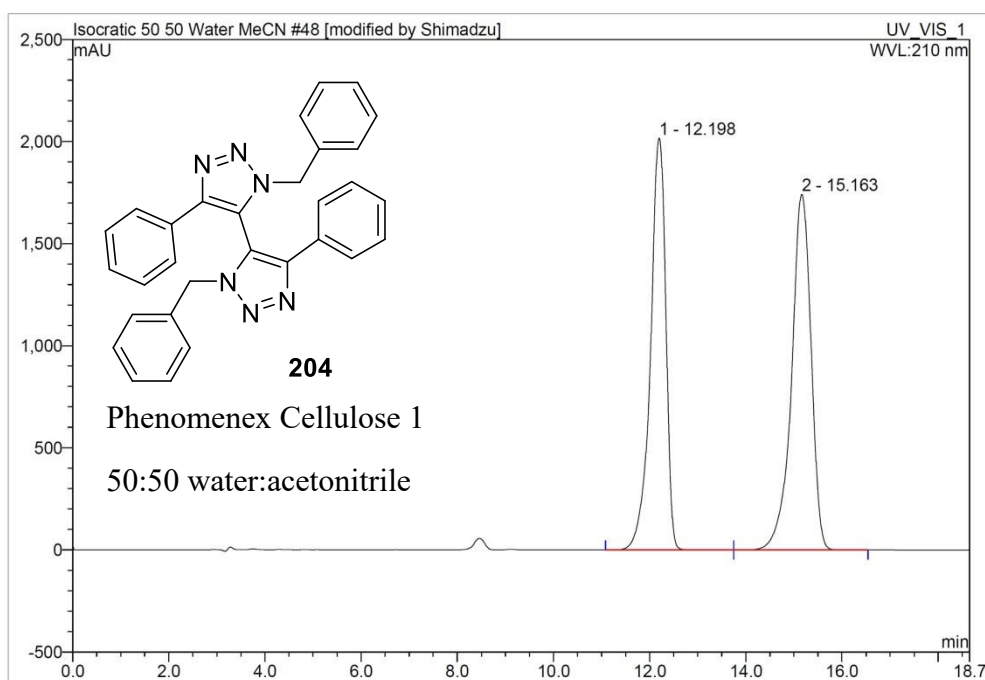
No.	Ret.Time min	Peak Name	Height mAU	Area mAU*min	Rel.Area %	Amount	Type
1	8.50	n.a.	1060.359	247.629	100.00	n.a.	BMB*
Total:			1060.359	247.629	100.00	0.000	

7.5.2.2 Chiral HPLC Trace of Compound 204

Operator:Shimadzu Timebase:LC_System2 Sequence:Isocratic 50 50 Water MeCN

Page 1-1
5/12/2016 4:29 PM

48 WB-BisTriazole			
Sample Name:	WB-BisTriazole	Injection Volume:	5.0
Vial Number:	1_2	Channel:	UV_VIS_1
Sample Type:	unknown	Wavelength:	210
Control Program:	Isocratic 50 50 water MeCN	Bandwidth:	n.a.
Quantif. Method:	Isocratic 50 50 water MeCN	Dilution Factor:	1.0000
Recording Time:	3/12/2015 11:30	Sample Weight:	1.0000
Run Time (min):	18.65	Sample Amount:	1.0000



No.	Ret.Time min	Peak Name	Height mAU	Area mAU*min	Rel.Area %	Amount	Type
1	12.20	n.a.	2018.010	744.141	47.56	n.a.	BMb
2	15.16	n.a.	1742.130	820.476	52.44	n.a.	bMB
Total:			3760.140	1564.616	100.00	0.000	

8 Appendix 2 Crystal Structure Data

WB2-NH_Gaussian (93).

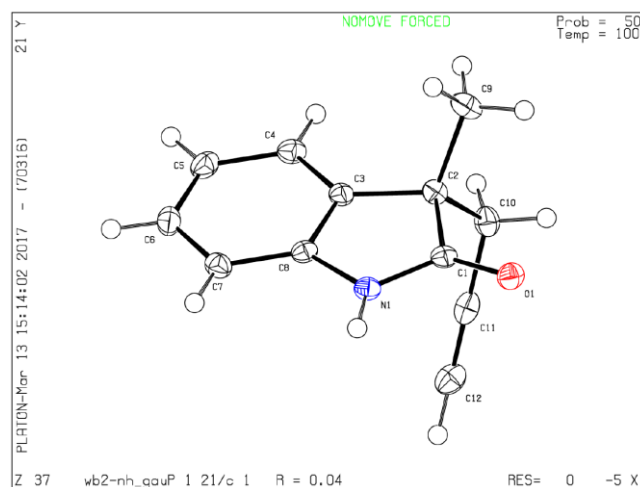


Table 1 Crystal data and structure refinement for WB2-NH_Gaussian (93).

Identification code	WB2-NH_Gaussian
Empirical formula	C ₁₂ H ₁₁ NO
Formula weight	185.23
Temperature/K	100.01(10)
Crystal system	monoclinic
Space group	P2 ₁ /c
a/Å	10.4519(2)
b/Å	7.22206(17)
c/Å	12.9528(3)
α/°	90.0
β/°	97.641(2)
γ/°	90.0
Volume/Å ³	969.06(4)
Z	4
ρ _{calc} /cm ³	1.2695
μ/mm ⁻¹	0.020
F(000)	392.2
Crystal size/mm ³	0.3826 × 0.1898 × 0.0965
Radiation	Mo Kα (λ = 0.71073)
2θ range for data collection/°	6.34 to 52.74
Index ranges	-13 ≤ h ≤ 14, -9 ≤ k ≤ 9, -16 ≤ l ≤ 17
Reflections collected	16037
Independent reflections	1978 [R _{int} = 0.0292, R _{sigma} = 0.0221]
Data/restraints/parameters	1978/0/127
Goodness-of-fit on F ²	1.055
Final R indexes [I ≥ 2σ (I)]	R ₁ = 0.0382, wR ₂ = 0.0931
Final R indexes [all data]	R ₁ = 0.0444, wR ₂ = 0.0976
Largest diff. peak/hole / e Å ⁻³	0.32/-0.23

Experimental

Single crystals of C₁₂H₁₁NO [WB2-NH_Gaussian] were grown by evaporation from acetonitrile. A suitable crystal was selected and run on a SuperNova, Dual, Cu at zero, Atlas diffractometer. The crystal was kept at 100.01(10) K during

data collection. Using Olex2 [1], the structure was solved with the ShelXS [2] structure solution program using Direct Methods and refined with the olex2.refine [3] refinement package using Gauss-Newton minimisation.

1. Dolomanov, O.V., Bourhis, L.J., Gildea, R.J., Howard, J.A.K. & Puschmann, H. (2009), *J. Appl. Cryst.* 42, 339-341.
2. Sheldrick, G.M. (2008). *Acta Cryst. A*64, 112-122.
3. Bourhis, L.J., Dolomanov, O.V., Gildea, R.J., Howard, J.A.K., Puschmann, H. (2015). *Acta Cryst. A*71, 59-75.

Crystal structure determination of [WB2-NH_Gaussian]

Crystal Data for $C_{12}H_{11}NO$ ($M=185.23$ g/mol): monoclinic, space group $P2_1/c$ (no. 14), $a = 10.4519(2)$ Å, $b = 7.22206(17)$ Å, $c = 12.9528(3)$ Å, $\beta = 97.641(2)^\circ$, $V = 969.06(4)$ Å³, $Z = 4$, $T = 100.01(10)$ K, $\mu(\text{Mo K}\alpha) = 0.020$ mm⁻¹, $D_{\text{calc}} = 1.2695$ g/cm³, 16037 reflections measured ($6.34^\circ \leq 2\theta \leq 52.74^\circ$), 1978 unique ($R_{\text{int}} = 0.0292$, $R_{\text{sigma}} = 0.0221$) which were used in all calculations. The final R_1 was 0.0382 ($I \geq 2\sigma(I)$) and wR_2 was 0.0976 (all data).

Refinement model description

Number of restraints - 0, number of constraints - 19.

Details:

1. Fixed Uiso
At 1.2 times of:
All C(H) groups, All C(H,H) groups, All N(H) groups
At 1.5 times of:
All C(H,H,H) groups
- 2.a Secondary CH2 refined with riding coordinates:
C10 (H10a, H10b)
- 2.b Aromatic/amide H refined with riding coordinates:
C4 (H4), C5 (H5), C6 (H6), C7 (H7), N1 (H1)
- 2.c Idealised Me refined as rotating group:
C9 (H9a, H9b, H9c)
- 2.d :
C12 (H12)

AD-OxindoleBn2_Gaussian (94)

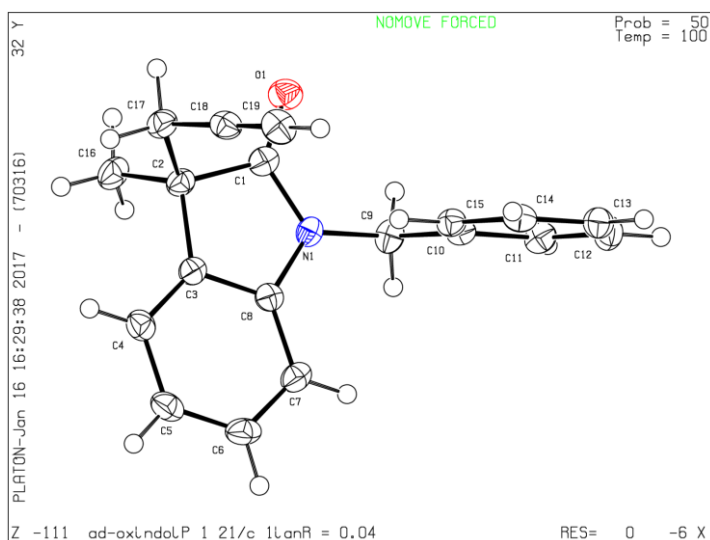


Table 1 Crystal data and structure refinement for AD-OxindoleBn2_Gaussian (94).

Identification code	AD-OxindoleBn2_Gaussian
Empirical formula	C ₁₉ H ₁₇ NO
Formula weight	275.33
Temperature/K	100.01(10)
Crystal system	monoclinic
Space group	P2 ₁ /c
a/Å	8.6271(4)
b/Å	11.5588(6)
c/Å	14.9815(8)
α/°	90
β/°	94.519(5)
γ/°	90
Volume/Å ³	1489.31(13)
Z	4
ρ _{calc} /cm ³	1.228
μ/mm ⁻¹	0.590
F(000)	584.0
Crystal size/mm ³	0.3024 × 0.2501 × 0.105
Radiation	CuKα (λ = 1.54184)
2θ range for data collection/°	9.676 to 140.12
Index ranges	-10 ≤ h ≤ 10, -6 ≤ k ≤ 14, -17 ≤ l ≤ 18
Reflections collected	5108
Independent reflections	2819 [R _{int} = 0.0221, R _{sigma} = 0.0357]
Data/restraints/parameters	2819/0/191
Goodness-of-fit on F ²	1.026
Final R indexes [I ≥ 2σ (I)]	R ₁ = 0.0436, wR ₂ = 0.1051
Final R indexes [all data]	R ₁ = 0.0507, wR ₂ = 0.1109
Largest diff. peak/hole / e Å ⁻³	0.30/-0.28

Experimental

Single crystals of C₁₉H₁₇NO [AD-OxindoleBn2_Gaussian] were grown from evaporation from acetonitrile. A suitable crystal was selected and run on a SuperNova, Dual, Cu at zero, Atlas diffractometer. The crystal was kept at

100.01(10) K during data collection. Using Olex2 [1], the structure was solved with the ShelXS [2] structure solution program using Direct Methods and refined with the ShelXL [3] refinement package using Least Squares minimisation.

1. Dolomanov, O.V., Bourhis, L.J., Gildea, R.J., Howard, J.A.K. & Puschmann, H. (2009), *J. Appl. Cryst.* 42, 339-341.
2. Sheldrick, G.M. (2008). *Acta Cryst.* A64, 112-122.
3. Sheldrick, G.M. (2015). *Acta Cryst.* C71, 3-8.

Crystal structure determination of [AD-OxindoleBn2_Gaussian]

Crystal Data for $C_{19}H_{17}NO$ ($M = 275.33$ g/mol): monoclinic, space group $P2_1/c$ (no. 14), $a = 8.6271(4)$ Å, $b = 11.5588(6)$ Å, $c = 14.9815(8)$ Å, $\beta = 94.519(5)^\circ$, $V = 1489.31(13)$ Å³, $Z = 4$, $T = 100.01(10)$ K, $\mu(\text{CuK}\alpha) = 0.590$ mm⁻¹, $D_{\text{calc}} = 1.228$ g/cm³, 5108 reflections measured ($9.676^\circ \leq 2\theta \leq 140.12^\circ$), 2819 unique ($R_{\text{int}} = 0.0221$, $R_{\text{sigma}} = 0.0357$) which were used in all calculations. The final R_1 was 0.0436 ($I > 2\sigma(I)$) and wR_2 was 0.1109 (all data).

Refinement model description

Number of restraints - 0, number of constraints - unknown.

Details:

1. Fixed Uiso
At 1.2 times of:
All C(H) groups, All C(H,H) groups
At 1.5 times of:
All C(H,H,H) groups
- 2.a Secondary CH2 refined with riding coordinates:
C9(H9A,H9B), C17(H17A,H17B)
- 2.b Aromatic/amide H refined with riding coordinates:
C4(H4), C5(H5), C6(H6), C7(H7), C11(H11), C12(H12), C13(H13), C14(H14), C15(H15)
- 2.c Idealised Me refined as rotating group:
C16(H16A,H16B,H16C)
- 2.d :
C19(H19)

This report has been created with Olex2, compiled on 2017.01.04 svn.r3372 for OlexSys. Please [let us know](#) if there

WS09A1(105 (R))

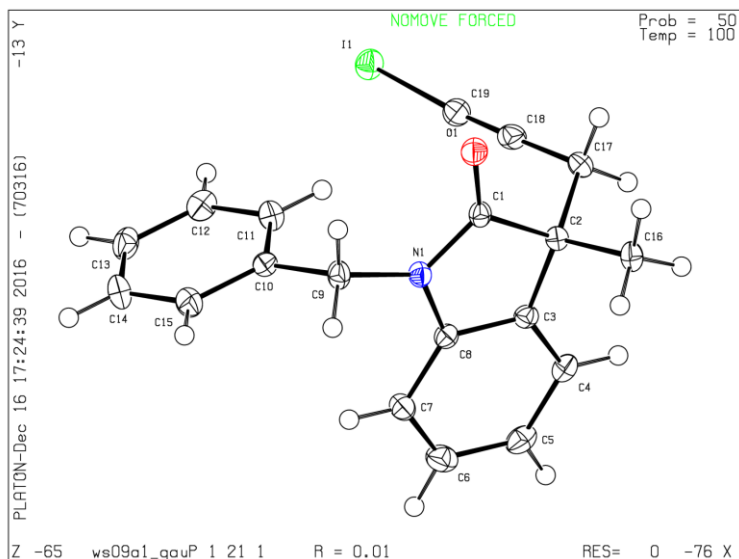


Table 1 Crystal data and structure refinement for WS09A1 ((R)-107).

Identification code	WS09A1
Empirical formula	C ₁₉ H ₁₆ NOI
Formula weight	401.23
Temperature/K	100.01(10)
Crystal system	monoclinic
Space group	P2 ₁
a/Å	8.37264(5)
b/Å	10.80933(9)
c/Å	9.22608(7)
α/°	90
β/°	98.2372(6)
γ/°	90
Volume/Å ³	826.371(10)
Z	2
ρ _{calc} /cm ³	1.612
μ/mm ⁻¹	15.222
F(000)	396.0
Crystal size/mm ³	0.2257 × 0.1482 × 0.1469
Radiation	Cu Kα (λ = 1.54184)
2θ range for data collection/°	9.686 to 148.83
Index ranges	-10 ≤ h ≤ 10, -13 ≤ k ≤ 13, -11 ≤ l ≤ 11
Reflections collected	28787
Independent reflections	3356 [R _{int} = 0.0260, R _{sigma} = 0.0112]
Data/restraints/parameters	3356/1/200
Goodness-of-fit on F ²	1.088
Final R indexes [I >= 2σ (I)]	R ₁ = 0.0145, wR ₂ = 0.0383
Final R indexes [all data]	R ₁ = 0.0145, wR ₂ = 0.0383
Largest diff. peak/hole / e Å ⁻³	0.40/-0.34
Flack parameter	-0.018(3)

Experimental

Single crystals of C₁₉H₁₆NOI [WS09A1] were grown by crystallization from ethyl acetate. A suitable crystal was selected and run on a SuperNova, Dual, Cu at zero, Atlas diffractometer. The crystal was kept at 100.01(10) K during data collection. Using Olex2 [1], the structure was solved with the ShelXS [2] structure solution program using Patterson Method and refined with the ShelXL [3] refinement package using Least Squares minimisation.

1. Dolomanov, O.V., Bourhis, L.J., Gildea, R.J., Howard, J.A.K. & Puschmann, H. (2009), *J. Appl. Cryst.* 42, 339-341.
2. Sheldrick, G.M. (2008). *Acta Cryst.* A64, 112-122.
3. Sheldrick, G.M. (2015). *Acta Cryst.* C71, 3-8.

Crystal structure determination of [WS09A1]

Crystal Data for C₁₉H₁₆NOI (*M* = 401.23 g/mol): monoclinic, space group P2₁ (no. 4), *a* = 8.37264(5) Å, *b* = 10.80933(9) Å, *c* = 9.22608(7) Å, β = 98.2372(6)°, *V* = 826.371(10) Å³, *Z* = 2, *T* = 100.01(10) K, μ (Cu K α) = 15.222 mm⁻¹, *D*_{calc} = 1.612 g/cm³, 28787 reflections measured (9.686° ≤ 2 θ ≤ 148.83°), 3356 unique (*R*_{int} = 0.0260, *R*_{sigma} = 0.0112) which were used in all calculations. The final *R*₁ was 0.0145 (*I* > 2 σ (*I*)) and *wR*₂ was 0.0383 (all data).

Refinement model description

Number of restraints - 1, number of constraints - unknown.

Details:

1. Fixed Uiso
At 1.2 times of:
All C(H) groups, All C(H,H) groups
At 1.5 times of:
All C(H,H,H) groups
- 2.a Secondary CH₂ refined with riding coordinates:
C9(H9a,H9b), C17(H17a,H17b)
- 2.b Aromatic/amide H refined with riding coordinates:
C4(H4), C5(H5), C6(H6), C7(H7), C11(H11), C12(H12), C13(H13), C14(H14),
C15(H15)
- 2.c Idealised Me refined as rotating group:
C16(H16a,H16b,H16c)

This report has been created with Olex2, compiled on 2016.11.30 svn.r3356 for OlexSys.

WS09_iodide#gaussian ((rac)-107)

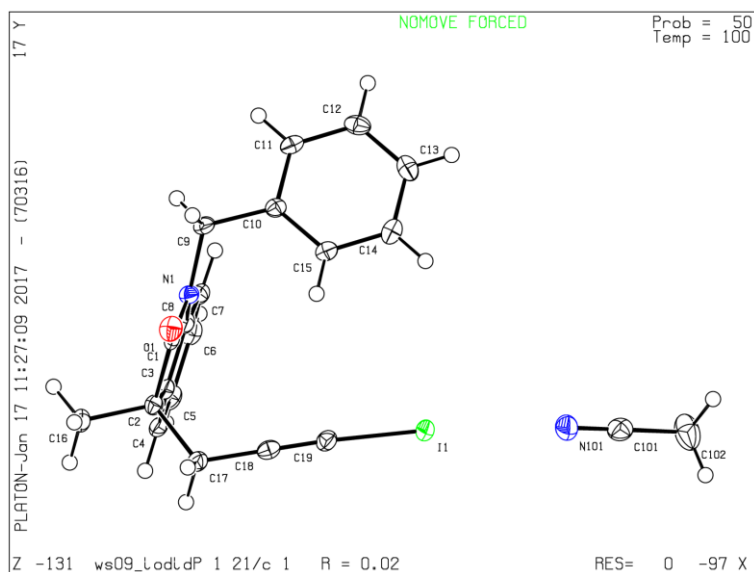


Table 1 Crystal data and structure refinement for WS09_iodide#gaussian ((rac)-107).

Identification code	WS09_iodide#gaussian
Empirical formula	C ₂₁ H ₁₉ IN ₂ O
Formula weight	442.28
Temperature/K	99.98(10)
Crystal system	monoclinic
Space group	P2 ₁ /c
a/Å	15.31276(18)
b/Å	8.17349(9)
c/Å	15.58899(17)
α/°	90
β/°	106.1831(12)
γ/°	90
Volume/Å ³	1873.79(4)
Z	4
ρ _{calc} /cm ³	1.568
μ/mm ⁻¹	13.502
F(000)	880.0
Crystal size/mm ³	0.1434 × 0.1382 × 0.0708
Radiation	CuKα (λ = 1.54184)
2θ range for data collection/°	6.01 to 140.114
Index ranges	-16 ≤ h ≤ 18, -9 ≤ k ≤ 9, -19 ≤ l ≤ 17
Reflections collected	18063
Independent reflections	3548 [R _{int} = 0.0314, R _{sigma} = 0.0216]
Data/restraints/parameters	3548/0/228
Goodness-of-fit on F ²	1.077
Final R indexes [I ≥ 2σ (I)]	R ₁ = 0.0211, wR ₂ = 0.0534
Final R indexes [all data]	R ₁ = 0.0226, wR ₂ = 0.0544
Largest diff. peak/hole / e Å ⁻³	0.53/-0.31

Experimental

Single crystals of $C_{21}H_{19}IN_2O$ [WS09_iodide#gussian] were grown by slow evaporation of acetonitrile. A suitable crystal was selected and run on a SuperNova, Dual, Cu at zero, Atlas diffractometer. The crystal was kept at 99.98(10) K during data collection. Using Olex2 [1], the structure was solved with the ShelXS [2] structure solution program using Direct Methods and refined with the ShelXL [3] refinement package using Least Squares minimisation.

1. Dolomanov, O.V., Bourhis, L.J., Gildea, R.J., Howard, J.A.K. & Puschmann, H. (2009), *J. Appl. Cryst.* 42, 339-341.
2. Sheldrick, G.M. (2008). *Acta Cryst.* A64, 112-122.
3. Sheldrick, G.M. (2015). *Acta Cryst.* C71, 3-8.

Crystal structure determination of [WS09_iodide#gussian]

Crystal Data for $C_{21}H_{19}IN_2O$ ($M = 442.28$ g/mol): monoclinic, space group $P2_1/c$ (no. 14), $a = 15.31276(18)$ Å, $b = 8.17349(9)$ Å, $c = 15.58899(17)$ Å, $\beta = 106.1831(12)^\circ$, $V = 1873.79(4)$ Å³, $Z = 4$, $T = 99.98(10)$ K, $\mu(\text{CuK}\alpha) = 13.502$ mm⁻¹, $D_{\text{calc}} = 1.568$ g/cm³, 18063 reflections measured ($6.01^\circ \leq 2\theta \leq 140.114^\circ$), 3548 unique ($R_{\text{int}} = 0.0314$, $R_{\text{sigma}} = 0.0216$) which were used in all calculations. The final R_1 was 0.0211 ($I > 2\sigma(I)$) and wR_2 was 0.0544 (all data).

Refinement model description

Number of restraints - 0, number of constraints - unknown.

Details:

1. Fixed Uiso
At 1.2 times of:
All C(H) groups, All C(H,H) groups
At 1.5 times of:
All C(H,H,H) groups
- 2.a Secondary CH2 refined with riding coordinates:
C9(H9A,H9B), C17(H17A,H17B)
- 2.b Aromatic/amide H refined with riding coordinates:
C4(H4), C5(H5), C6(H6), C7(H7), C11(H11), C12(H12), C13(H13), C14(H14), C15(H15)
- 2.c Idealised Me refined as rotating group:
C16(H16A,H16B,H16C), C102(H10A,H10B,H10C)

This report has been created with Olex2, compiled on 2017.01.04 svn.r3372 for OlexSys

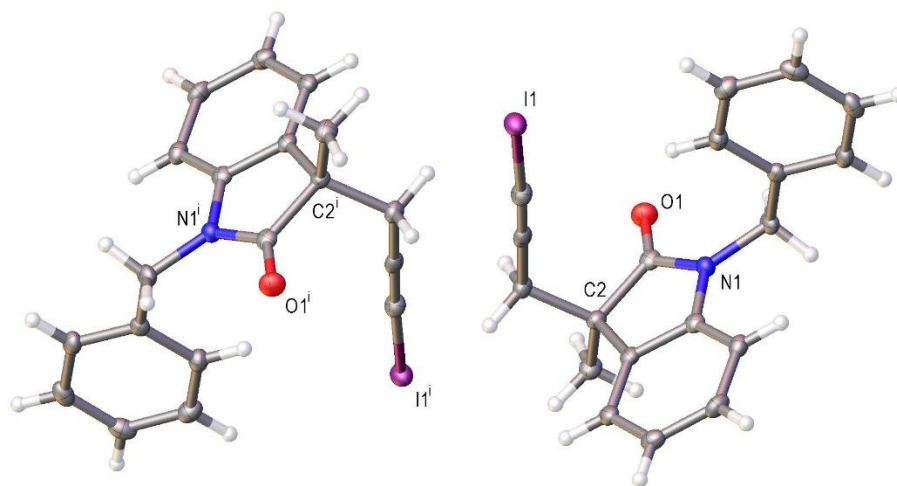


Figure 46 Selected molecules of oxindole WS09 with ellipsoids drawn at the 50 % probability level. These molecules are related by an inversion centre and are thus opposite enantiomers. Symmetry codes used to generate equivalent atoms: $i: 1-x, -y, -z$.

WB_Triazole#Gaussian (172)

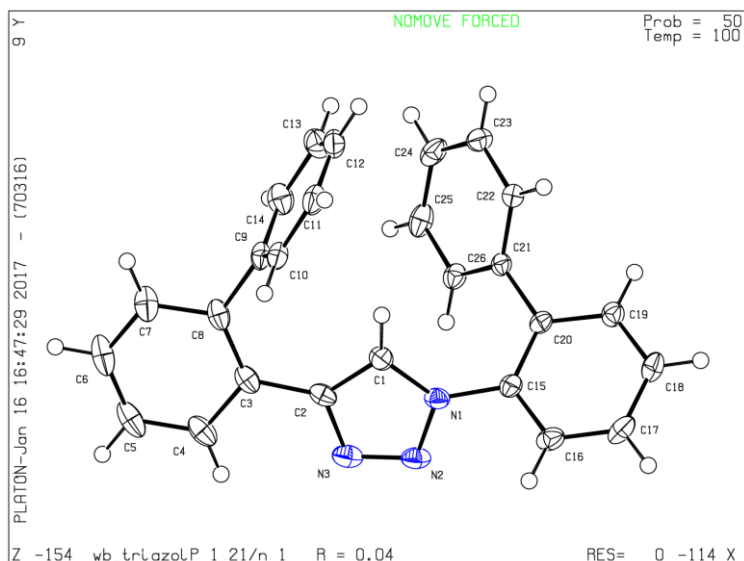


Table 1 Crystal data and structure refinement for WB_Triazole#Gaussian (172).

Identification code	WB_Triazole#Gaussian
Empirical formula	C ₂₆ H ₁₉ N ₃
Formula weight	373.44
Temperature/K	100.00(10)
Crystal system	monoclinic
Space group	P2 ₁ /n
a/Å	11.0705(4)
b/Å	11.0818(4)
c/Å	16.5372(7)
α/°	90
β/°	102.977(4)
γ/°	90
Volume/Å ³	1976.99(14)
Z	4
ρ _{calc} /cm ³	1.255
μ/mm ⁻¹	0.075
F(000)	784.0
Crystal size/mm ³	0.2501 × 0.1914 × 0.1253
Radiation	MoKα (λ = 0.71073)
2θ range for data collection/°	5.056 to 52.74
Index ranges	-13 ≤ h ≤ 12, -13 ≤ k ≤ 11, -17 ≤ l ≤ 20
Reflections collected	10775
Independent reflections	4039 [R _{int} = 0.0224, R _{sigma} = 0.0285]
Data/restraints/parameters	4039/0/262
Goodness-of-fit on F ²	1.066
Final R indexes [I ≥ 2σ (I)]	R ₁ = 0.0440, wR ₂ = 0.1027
Final R indexes [all data]	R ₁ = 0.0550, wR ₂ = 0.1100
Largest diff. peak/hole / e Å ⁻³	0.28/-0.24

Experimental

Single crystals of C₂₆H₁₉N₃ [WB_Triazole#Gaussian] were selected. A suitable crystal was selected and run on a SuperNova, Dual, Cu at zero, Atlas diffractometer. The crystal was kept at 100.00(10) K during data collection. Using Olex2 [1], the structure was solved with the ShelXS [2] structure solution program using Direct Methods and refined with the ShelXL [3] refinement package using Least Squares minimisation.

1. Dolomanov, O.V., Bourhis, L.J., Gildea, R.J, Howard, J.A.K. & Puschmann, H. (2009), *J. Appl. Cryst.* 42, 339-341.
2. Sheldrick, G.M. (2008). *Acta Cryst.* A64, 112-122.
3. Sheldrick, G.M. (2015). *Acta Cryst.* C71, 3-8.

Crystal structure determination of [WB_Triazole#Gaussian]

Crystal Data for C₂₆H₁₉N₃ (*M* = 373.44 g/mol): monoclinic, space group P2₁/n (no. 14), *a* = 11.0705(4) Å, *b* = 11.0818(4) Å, *c* = 16.5372(7) Å, β = 102.977(4)°, *V* = 1976.99(14) Å³, *Z* = 4, *T* = 100.00(10) K, μ (MoK α) = 0.075 mm⁻¹, *D*_{calc} = 1.255 g/cm³, 10775 reflections measured (5.056° ≤ 2 θ ≤ 52.74°), 4039 unique (*R*_{int} = 0.0224, *R*_{sigma} = 0.0285) which were used in all calculations. The final *R*₁ was 0.0440 (*I* > 2 σ (*I*)) and *wR*₂ was 0.1100 (all data).

Refinement model description

Number of restraints - 0, number of constraints - unknown.

Details:

1. Fixed Uiso

At 1.2 times of:

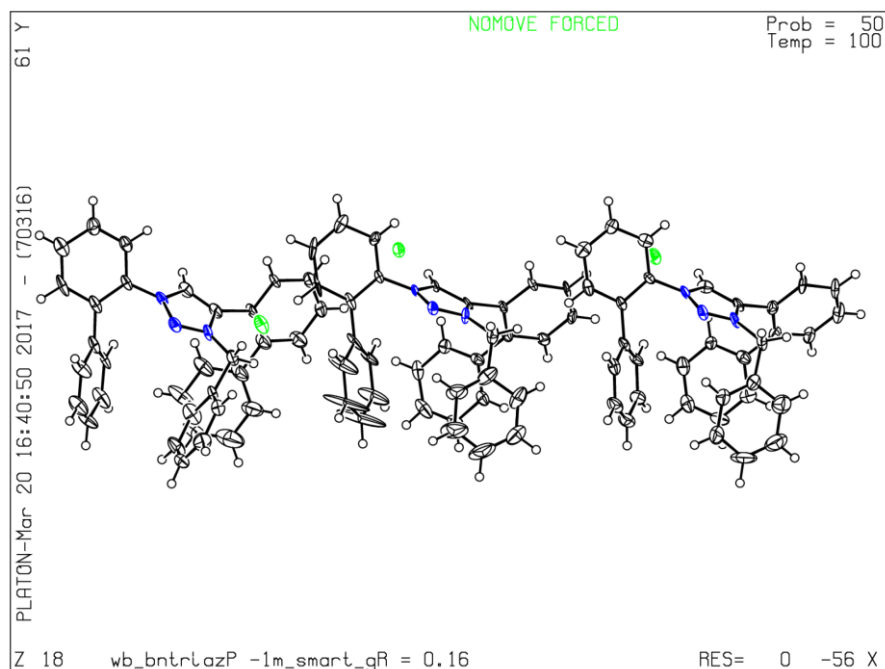
All C(H) groups

2.a Aromatic/amide H refined with riding coordinates:

C1(H1), C4(H4), C5(H5), C6(H6), C7(H7), C10(H10), C11(H11), C12(H12),
C13(H13), C14(H14), C16(H16), C17(H17), C18(H18), C19(H19), C22(H22), C23(H23),
C24(H24), C25(H25), C26(H26)

This report has been created with Olex2, compiled on 2017.01.04 svn.r3372 for OlexSys.

WB_BnTriazolium_SMART_Gaussian (178)



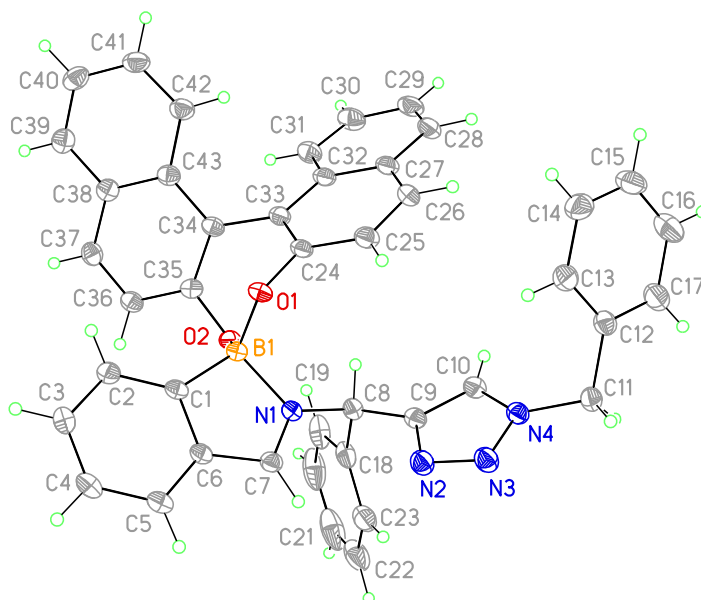
It is suspected that the dataset from **WB_BnTriazolium (178)** is not single. Several attempts were made to try to resolve the twinning and otherwise improve the data reduction, but this was not found to be possible. The structure is therefore intended for structure identification only.

Table 1 Crystal data and structure refinement for WB_BnTriazolium_SMART_Gaussian.

Identification code	WB_BnTriazolium_SMART_Gaussian
Empirical formula	BrC ₃₃ N ₃ H _{0.17}
Formula weight	518.44
Temperature/K	100.01(10)
Crystal system	triclinic
Space group	P-1
a/Å	9.6855(2)
b/Å	20.1908(5)
c/Å	21.6800(4)
α/°	104.6683(18)
β/°	96.9566(19)
γ/°	96.065(2)
Volume/Å ³	4030.09(16)
Z	6
ρ _{calc} /cm ³	1.282
μ/mm ⁻¹	2.276
F(000)	1525.0
Crystal size/mm ³	0.2986 × 0.1614 × 0.0642
Radiation	CuKα (λ = 1.54184)
2θ range for data collection/°	5.346 to 133.196
Index ranges	-11 ≤ h ≤ 11, -24 ≤ k ≤ 24, -25 ≤ l ≤ 25
Reflections collected	133692
Independent reflections	14251 [R _{int} = 0.0483, R _{sigma} = 0.0219]
Data/restraints/parameters	14251/0/1000
Goodness-of-fit on F ²	2.328
Final R indexes [I ≥ 2σ (I)]	R ₁ = 0.1555, wR ₂ = 0.4510
Final R indexes [all data]	R ₁ = 0.1604, wR ₂ = 0.4606

Largest diff. peak/hole / e Å⁻³

9.73/-1.71

wb-mecn ((R,R)-120)Table 1. Crystal data and structure refinement for **(R,R)-120**.

Empirical formula	C ₄₃ H ₃₁ B N ₄ O ₂	
Formula weight	646.53	
Temperature	100(2) K	
Wavelength	1.54184 Å	
Crystal system	orthorhombic	
Space group	P 21 21 21	
Unit cell dimensions	a = 9.4858(12) Å	□ = 90°.
	b = 16.647(2) Å	□ = 90°.
	c = 20.977(2) Å	□ = 90°.
Volume	3312.5(7) Å ³	
Z	4	
Density (calculated)	1.296 Mg/m ³	
Absorption coefficient	0.631 mm ⁻¹	
F(000)	1352	
Crystal size	0.150 x 0.100 x 0.070 mm ³	
Theta range for data collection	3.389 to 74.310°.	
Index ranges	-11 ≤ h ≤ 11, -20 ≤ k ≤ 20, -26 ≤ l ≤ 26	
Reflections collected	32887	
Independent reflections	6697 [R(int) = 0.0342]	
Completeness to theta = 67.684°	99.9 %	
Absorption correction	Semi-empirical from equivalents	
Max. and min. transmission	1.00 and 0.940	
Refinement method	Full-matrix least-squares on F ²	
Data / restraints / parameters	6697 / 0 / 452	
Goodness-of-fit on F ²	1.034	
Final R indices [I > 2σ(I)]	R1 = 0.0313, wR2 = 0.0819	
R indices (all data)	R1 = 0.0326, wR2 = 0.0831	
Absolute structure parameter	-0.2(2)	
Extinction coefficient	n/a	
Largest diff. peak and hole	0.173 and -0.199 e.Å ⁻³	

X-ray Experimental for C₄₃H₃₁N₃O₂B: Crystals grew as colorless triangular prisms by slow evaporation from acetonitrile and chloroform. The data crystal had approximate dimensions; 0.15 x 0.10 x 0.07 mm. The data were collected on an Agilent Technologies SuperNova Dual Source diffractometer using a μ -focus Cu K α radiation source ($\lambda = 1.5418\text{\AA}$) with collimating mirror monochromators. A total of 1688 frames of data were collected using ω -scans with a scan range of 1° and a counting time of 9 seconds per frame for frames collected with a detector offset of +/- 40.8° and 28 seconds per frame with frames collected with a detector offset of +/- 108.3°. The data were collected at 100 K using an Oxford Cryostream low temperature device. Details of crystal data, data collection and structure refinement are listed in Table 1. Data collection, unit cell refinement and data reduction were performed using Agilent Technologies CrysAlisPro V 1.171.37.31.^[173] The structure was solved by direct methods using SuperFlip^[174] and refined by full-matrix least-squares on F² with anisotropic displacement parameters for the non-H atoms using SHELXL-2014/7. Structure analysis was aided by use of the programs PLATON98 and WinGX. The hydrogen atoms were calculated in ideal positions with isotropic displacement parameters set to 1.2xUeq of the attached atom (1.5xUeq for methyl hydrogen atoms). The absolute configuration was determined by internal comparison to the known configuration of the binaphthalene group. The function, $\Sigma w(|F_o|^2 - |F_c|^2)^2$, was minimized, where $w = 1/[(\sigma(F_o))^2 + (0.0505*P)^2 + (0.4821*P)]$ and $P = (|F_o|^2 + 2|F_c|^2)/3$. R_w(F²) refined to 0.0831, with R(F) equal to 0.0313 and a goodness of fit, S, = 1.03. Definitions used for calculating R(F), R_w(F²) and the goodness of fit, S, are given below.^[175] $1/2$ where w is the weight given each reflection $(F) = \sigma(|F_o| - |F_c|)/\sigma|F_o|$ for reflections with $F_o > 4(\sigma(F_o))$. $S = [\Sigma w(|F_o|^2 - |F_c|^2)^2/(n - p)]^{1/2}$, where n is the number of reflections and p is the number of refined parameters. The data were checked for secondary extinction effects but no correction was necessary. Neutral atom scattering factors and values used to calculate the linear absorption coefficient are from the International Tables for X-ray Crystallography (1992). All figures were generated using SHELXTL/PC. Tables of positional and thermal parameters, bond lengths and angles, torsion angles and figures are found elsewhere.

9 Appendix 3 Undergraduate Experiment Supporting Documents

9.1 Student Experimental Procedure

Experiment Code

Rapid Determination of Enantiomeric Excess by NMR Spectroscopy

Objectives

By the end of this experiment you should be able to:

- Use volumetric pipettes to prepare solutions of accurate concentrations
- Prepare a series of solutions which can be used to produce a calibration curve
- Determine an unknown enantiomeric excess (*ee*) using a calibration curve
- Analyse an NMR spectrum using NMR processing software
- Calculate an enantiomeric excess (*ee*) from your NMR data

Time Permitted

2 practical sessions (1 session in the laboratory, 1 session in an IT Suite)

Background

Chiral molecules are important due to their prevalence in biological systems such as proteins (including structural proteins, receptors and enzymes), carbohydrates, hormones and DNA. Additionally, many pharmaceutical compounds are chiral molecules which can be synthesised as a mixture of stereoisomers, sometimes different stereoisomers can interact differently within biological systems such as the body.

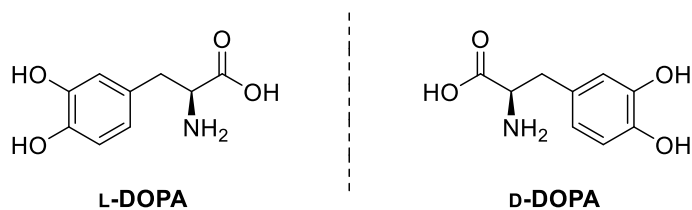
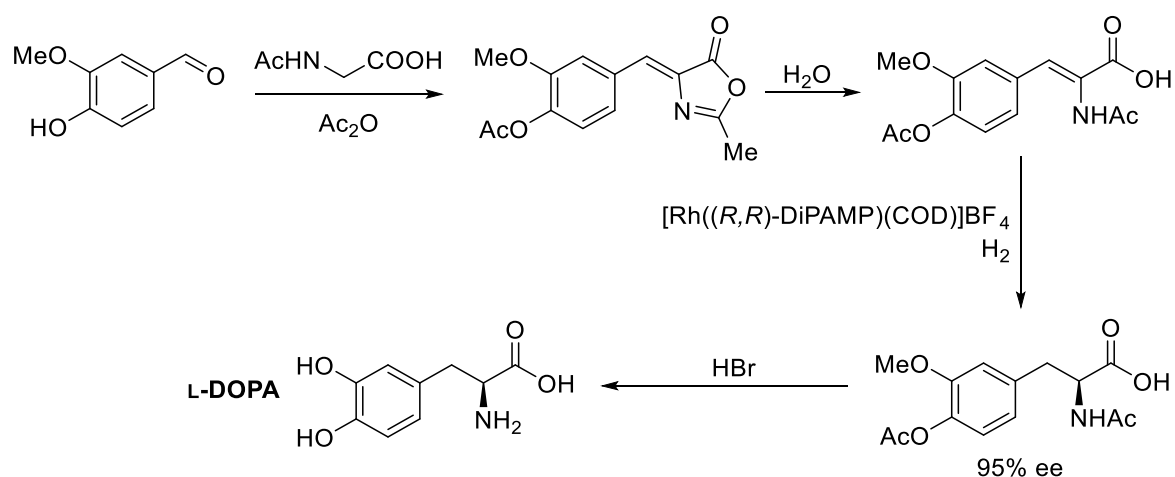


Figure 1 - Two enantiomers of DOPA

One such example of this is 2-amino-3-(3,4-dihydroxyphenyl)propanoic acid (DOPA), which is chiral; . The enantiomers (which are non-superimposable mirror images) L-DOPA and D-

DOPA are shown above (Figure 1). Whilst L-DOPA has been shown to be a useful drug in combating Parkinson's disease, its opposite enantiomer (D-DOPA) has no observable effect. Therefore, in order to make a more cost-effective and active formulation, L-DOPA alone is required. A stereoselective synthesis (a synthetic route that only produced one enantiomer) would be the most effective way to achieve this. The asymmetric synthesis of L-DOPA reported by Knowles in 1983,^[176] for which he was jointly awarded a Nobel Prize in 2001,^[177] is shown below (Scheme 1). The step in which chirality is introduced is achieved *via* asymmetric hydrogenation using a chiral ruthenium catalyst and molecular hydrogen.^[178] However, asymmetric transformations do not always give one enantiomer exclusively, i.e. a non-racemic mixture of enantiomers can be produced. This means that a method of determining the amount of each enantiomer present is required.



Scheme 1 Knowles' stereoselective synthesis of L-DOPA¹

Historically, optical rotation was used for the determination of the enantiomeric excess (*ee*). Optical rotation measures the angle of rotation of plane-polarized light by a solution of the compound. If a reference sample is available, then this can be used to determine the *ee* of an unknown sample. This has been superseded by high performance liquid chromatography (HPLC) using a chiral stationary phase. In HPLC, a sample is passed through a chiral stationary phase using a solvent as the mobile phase. For analytical HPLC this is done at high pressures, typically with small quantities of sample (<0.1 mg). Each enantiomer will interact differently with the chiral stationary phase, leading to different retention times which are usually represented as a chromatogram. The enantiomers form transient diastereoisomeric interactions with the stationary phase, where one enantiomer of the analyte forms stronger

interactions with the stationary phase, leading to difference in residence or 'retention time'.^[179]

However, HPLC can be a time-consuming process and therefore efforts have been made to develop methods which can determine the *ee* of a compound more rapidly. One technique which could be used is ¹H NMR spectroscopy, because data can be acquired quickly (less than 5 minutes per sample). However enantiomers have identical NMR spectra and therefore NMR spectroscopy cannot be used to determine the relative proportions of enantiomers in a mixture directly. Diastereoisomers have different physical and chemical properties, which means that the protons are in different magnetic environments and will produce different ¹H NMR spectra. Therefore, NMR spectroscopy can be used to measure the relative proportions of diastereoisomers in a mixture.^[179]

Thus if a mixture of enantiomers is converted into a mixture of diastereoisomers then NMR spectroscopy can be used to determine the ratio of diastereoisomers in the mixture, which can be assumed to be the same as the ratio of enantiomers (figure 2). This can only be achieved by forming derivatives with **chiral reagents of known stereochemistry**. The derivatising reagent needs to be enantiopure (a single enantiomer) because if it was not, then two pairs of diastereoisomers would be formed, each with their corresponding enantiomer, which would lead to inaccurate results.

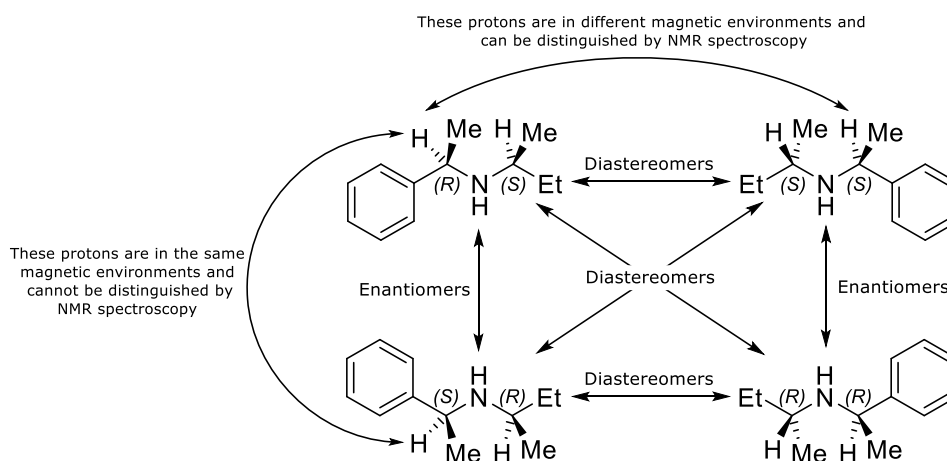
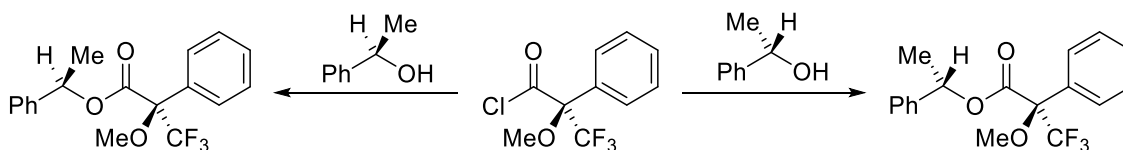


Figure 2- Demonstration of the relationship between enantiomers and diastereoisomers

There are several ways to convert an enantiomer into a pair of diastereoisomers, such as derivatization with Mosher's acid chloride (Scheme 2), the formation of ammonium salts with chiral acids such as camphor sulfonic acid, and the formation of complexes with chiral

shift reagents such as europium tris[3-(heptafluoropropylhydroxymethylene)-(+)-camphorate] (Eu(hfc)₃).



Scheme 2 Derivatisation of a chiral secondary alcohol with an enantiopure Mosher's acid chloride to form diastereoisomers

Due to the historic use of optical rotation in the field of measuring chiral integrity we determine a value called enantiomeric excess (*ee*), which is a measure of how much more of one enantiomer there is, relative to the total amount of sample.^[179] Enantiomeric excess is defined as:

$$ee = \frac{n_A - n_B}{n_A + n_B} \times 100\%$$

Where:

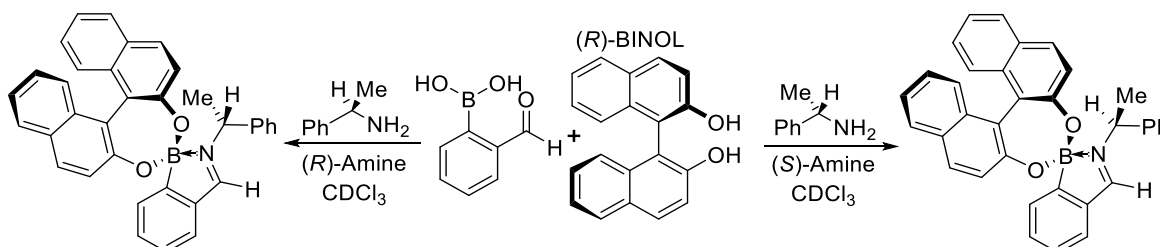
n_A = moles of major enantiomer A

n_B = moles of minor enantiomer B

Enantiomeric excess ranges in values from 0% *ee* for racemic mixtures to 100% *ee* for an enantiopure sample.

Introduction

In this experiment 2-formylphenylboronic acid (FPBA) and (*R*)-BINOL are used to form a chiral boronate ester, which then produce a pair of diastereomeric imines upon exposure to α -methylbenzylamine (MBA, a chiral amine) (Scheme 3). In aprotic solvents, this assembly is stabilised by donation of a lone pair of electrons on the nitrogen into the empty p-orbital of the boron.^[92]



Scheme 3 Assembly formation of diastereoisomers to infer the *ee* of a chiral amine

There are three key chemical concepts in this assembly; axial chirality of BINOL, the binding of boronic acids with diols and the reversible formation of stable imines from aldehydes and primary amines. Firstly, BINOL does not contain a chiral tetrahedral carbon atom,; it instead exhibits axial chirality, which is introduced through restricting the rotation of a carbon-carbon single bond between the two naphthyl units to form stable atropisomers. BINOL is important for this assembly because it is a chiral diol and boronic acids are known to bind strongly to certain diols because they form stable cyclic boronic esters. The third key concept is imine formation; – it is well studied that when exposed to an amine, an aldehyde will reversibly form an imine in equilibrium with the parent aldehyde. Imine formation is exploited in this assembly as the binding mode for the amine being studied.

For this experiment some specific terminology is used which is derived from supramolecular chemistry, these are the terms ‘host’ and ‘guest’. A host is a molecule or structure that non-covalently binds a molecule, and the guest is the compound that is bound, as illustrated in (Figure 3). According to this definition, the assembly formed in this experiment is not formally a host-guest complex, but the terminology best describes the interaction. Therefore, the BINOL-FPBA compound will be described as the host and the MBA is the guest.

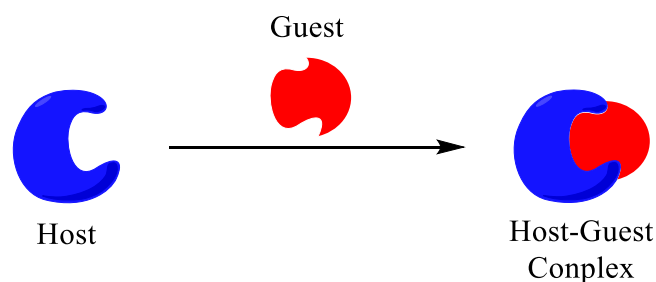


Figure 3- Theoretical example of host-guest interactions

During this experiment reactions will be performed on small scale by adding a solution of amine in CDCl_3 to a solution of FPBA and (*R*)-BINOL in CDCl_3 and the resulting complex observed by NMR spectroscopy. Therefore, in this experiment you will first make the FPBA+BINOL solution (known as the ‘host’ solution) and then solutions of (*R*)- and (*S*)-methylbenzylamine of a known enantiomeric excess (*ee*). When these two solutions are mixed together in the correct ratio, the assembly shown in scheme 3 is formed. The ratio of diastereoisomers can be determined and this will be used to construct a calibration curve.

After production of a calibration curve, you will be provided with a solution of unknown *ee* from which you will prepare NMR samples with the “host” solution. You will measure the diastereoisomeric ratio (*dr*) to determine *ee* using your calibration curve to convert spectroscopically determined values of *dr* into *ee* of your unknown amine solution.

During this experiment you will use a modified version of the calculation of *ee*. Enantiomeric excess will still use the formula defined earlier, but n_A and n_B will remain the same signal in the ^1H NMR spectroscopy rather than n_A being the major enantiomer and n_B being the minor.

$$\frac{n_A - n_B}{n_A + n_B} \times 100\%$$

n_A = moles of enantiomer A

n_B = moles of enantiomer B

This means that enantiomeric excess ranges in values from 0% *ee* for racemic mixtures to 100% *ee* for an enantiopure sample of A through to -100% *ee* for an enantiopure sample of B.

Safety & Physical Data

The hazard statements and physical data for the reagents used in this experiment are listed below:

Substance	Hazards	Physical Data
(<i>R</i>)-BINOL	Toxic if Swallowed Causes Serious Eye Irritation	RMM = 286.32 g mol ⁻¹
2-Formylphenylboronic acid (FPBA)	Causes Skin, Eye and Respiratory Irritation	RMM = 149.94 g mol ⁻¹
(<i>R</i>)- α -Methylbenzylamine	Harmful if Swallowed or by Skin Contact Causes Severe Skin Burns and Eye Damage	RMM = 121.18 g mol ⁻¹ $d = 0.94 \text{ g mL}^{-1}$
(<i>S</i>)- α -Methylbenzylamine	Harmful if Swallowed Toxic by Skin Contact Causes Severe Skin Burns and Eye Damage	RMM = 121.18 g mol ⁻¹ $d = 0.94 \text{ g mL}^{-1}$
<i>d</i> -Chloroform (CDCl ₃)	Harmful if Swallowed Causes Skin Irritation Suspected of Causing Cancer Causes Damage to Organs Through	

	Prolonged or Repeated Exposure	
4Å molecular sieves (beads)	Causes Skin, Respiratory and Serious Eye Irritation	
Acetone	Highly flammable liquid and vapour Causes serious eye irritation May cause drowsiness or dizziness	

The hazards of the diastereomeric assembly formed in this experiment needs to be considered. The assembly should be considered toxic, irritant and corrosive. Ensure that gloves are worn when handling reagents and their solutions. Gloves are to be changed immediately should any reagent or solution be spilt on them.

Procedure

First session (in the chemistry laboratory)

- In groups of five students, make 10 mL of the 'host' solution in deuterated chloroform (CDCl_3) that is 50 mM for both 2-formylphenylboronic acid (2-FPBA) and (R)-[1,1'-binaphthalene]-2,2'-diol (R-BINOL) i.e. you will make one solution which contains **both** FPBA and BINOL. (Use a 10 mL volumetric flask.)

You need to calculate the amount of FPBA and BINOL you will need. Check the results of your calculation with a demonstrator before making the solution.

This solution will need gentle warming (use a beaker of hot water) in order to fully dissolve the components. After the correct volume of CDCl_3 has been added, add enough activated 4Å molecular sieves to cover the bottom of the volumetric flask (10 should be sufficient), stopper the flask and allow the solution to dry for ten minutes with occasional swirling. This host solution will be shared among the members of the group.

- Each member of the group should make a 60 mM solution of α -methylbenzylamine (MBA) in CDCl_3 to a known *ee*. Decide as a group who is going to make which solution so that 5 different solutions are made. 7 different solutions are listed in the following table – you only need to make 5 of them.

Known ee Solutions of α -Methylbenzylamine

Known ee solution number	<i>ee</i> (%)	Concentration (mM)	Desired Volume (ml)	Volume of R-MBA (μl)	Volume of S-MBA (μl)
1	75	60	10	68	10
2	50			58	19
3	25			48	29
4	0			39	39
5	-25			29	48

6	-50			19	58
7	-75			10	68

Use a 10 mL volumetric flask. This will require using a volumetric pipette to add (*R*)- α -MBA and (*S*)- α -MBA – speak to the demonstrator if you are unsure how to use a volumetric pipette. **Use a new pipette tip every time MBA is dispensed.** After the correct volume of CDCl_3 has been added, add enough activated 4Å molecular sieves to cover the bottom of the volumetric flask (10 should be sufficient), stopper the flask and allow the solution to dry for ten minutes with occasional swirling.

- Prepare an NMR sample of known *ee* by combining 0.3 mL of the host solution with 0.3 mL of the amine solution in a vial. (Use a graduated glass pipette for this. Transfer this solution carefully over to an NMR tube using a Pasteur pipette. Cap and label the NMR tube and submit for analysis. You may wish to devise a labelling system as a group so that it is easier to analyse the spectra and avoid mix-ups. **Your group should end up with a total of 5 known *ee* NMR samples.**
- Prepare an NMR sample of unknown *ee* by combining 0.3 mL of the host solution with 0.3 mL of the unknown *ee* amine solution provided by the technician as described above. Decide as a group who is going to make which unknown solution so that a total of 5 different unknown solutions are analysed. Transfer the solution to an NMR tube, cap and label the tube and submit for analysis. **Your group should end up with a total of 5 unknown NMR samples.**
- As a final step, once you have prepared, all of your NMR samples for submission please wipe the outsides of each tube using a tissue with a small amount of acetone on it.

The NMR spectra for the samples your group have prepared will be recorded for you, and the data files will be made available for you to analyse at the start of the second session in the IT suite.

In order to prepare for the next session please take the time to read the lab manual, especially the introduction to NMR processing software given below (appendix 2) and watch the video recording on how to use the software.

Points to consider before the computer session

- What sources of error were present in carrying out the laboratory session?
- How widely applicable do you think this assembly could be. What limitations do you see in the types of substrates which could be analysed using it?

- Why did you add molecular sieves to your solutions?
- What protons are responsible for the signals observed in the ^1H NMR spectra of the starting materials?
- What signals would you expect to see in the NMR spectrum of the assembly and where would these approximately come in a ^1H NMR spectrum?

Second session (in the IT Suite)

1. Below are the NMR spectra of components used in the assembly.
2. Identify the following signals:
 - a. BINOL: alcohol protons
 - b. HOST SOLUTION: aldehyde proton of 2-formylphenylboronic acid
 - c. MBA: benzylic proton

Think carefully about these signals and what they can tell you about assembly formation.

3. Now compare the individual components to the ten spectra produced by your group.
 - a. Identify the imine protons and benzylic protons of the two diastereoisomers in each spectrum. **Take care when identifying the correct imine peaks. Compare all of the spectra to determine which peaks are of interest.**
4. Integrate the imine and benzylic peaks in all five samples of known *ee*. Use these integrations to calculate *ee*. Use the following formula:

$$ee = \frac{I_R - I_S}{I_R + I_S}$$

Where I_x is the integration of the signal. If you are unsure as to which peaks belong to *R* and *S*, use the table of known *ee* amine solutions to see which should be in excess in your spectra.

5. Construct 2 calibration curves using all five solutions of **known** *ee* – one curve using data from the imine signals and another curve using data from the benzylic signals. For each curve:
 - a. Plot the observed *ee* of the sample on the x axis (this observed *ee* was calculated from the integrations you found in step 3.)
 - b. Plot the exact (known) *ee* of the sample on the y axis.
 - c. **Calculate** the lines of best fit for your data. You can use MS Excel or Sigmaplot trend lines to do this.
6. Integrate the imine and benzylic peaks in all five samples of **unknown** *ee*. Use these integrations to calculate *ee*.
7. Now take the observed *ee*'s for the unknown samples (calculated in step 5) and use your calibration curves to determine the "true" *ee* of the samples.

The Report

For this experiment you are not expected to hand in your lab book, the mark will be 100% based on the proforma which you are required to complete. The blank proforma for this experiment is available for download through the Chemistry Canvas server.

Once completed, this should be submitted electronically via the online submission portal, which can also be found on Canvas.

For ease of processing, files uploaded must be either in Microsoft Word format or converted to PDF.

The file should be named with the experiment code followed by an underscore (“_”) followed by your name, e.g. “CODE_JBloggs.doc” or “CODE_JSmith.pdf”

All graphs should be produced in either Excel or Sigmaplot and pasted into the Word document containing your proforma, either at the end of the file or at an appropriate point.

You must ensure that the graphs are appropriately sized and labelled prior to submission.

9.2 Student Proforma

EXPERIMENT CODE

Rapid Determination of Enantiomeric Excess by NMR Spectroscopy

Student Name:

(Use block capitals)

Student ID No. (SRN)

--	--	--	--	--	--	--	--

Group:	
Date of Expt:	
Partner's Name(s):	

Assessment Criteria

This proforma is worth a total of 50 marks.

The first part of this proforma will look at the accuracy of the data you acquired and the way you have interpreted the data to produce calibration curves. Additionally, it will assess your ability to use these calibration curves to determine the *ee* of unknown solutions.

The second part of this proforma will consist of two essay style questions which will assess your ability to critically evaluate the data you have obtained.

The final part of proforma will assess your understanding of the experiment and the science behind it with a series of shorter questions.

For more information on assessment criteria, see the laboratory manual.

List the five known *ee* calibration solutions you made:

List the sample labels of your five unknown *ee* solutions:

In the box below, paste both of your calibration curves (one constructed using the integrations of the imine proton peaks, and one using the integrations of the benzylic proton peaks) from either Excel or Sigmaplot. Ensure that the equation ($y = mx + C$) and correlation coefficient (R^2) of the best-fit line is included on each graph.

10 marks

Tabulate the determined *ee* of the unknown amine samples your group used below using the integrations of both the imine and benzylic proton signals.

Unknown amine sample number	Determined <i>ee</i> of amine using benzylic proton	Determined <i>ee</i> of amine using imine proton
1		
2		
3		
4		
5		
6		
7		

10 marks

In an ideal example what would you expect the line equation for the calibration curves to be?

1 mark

What does the R^2 value of the best fit line tell you?

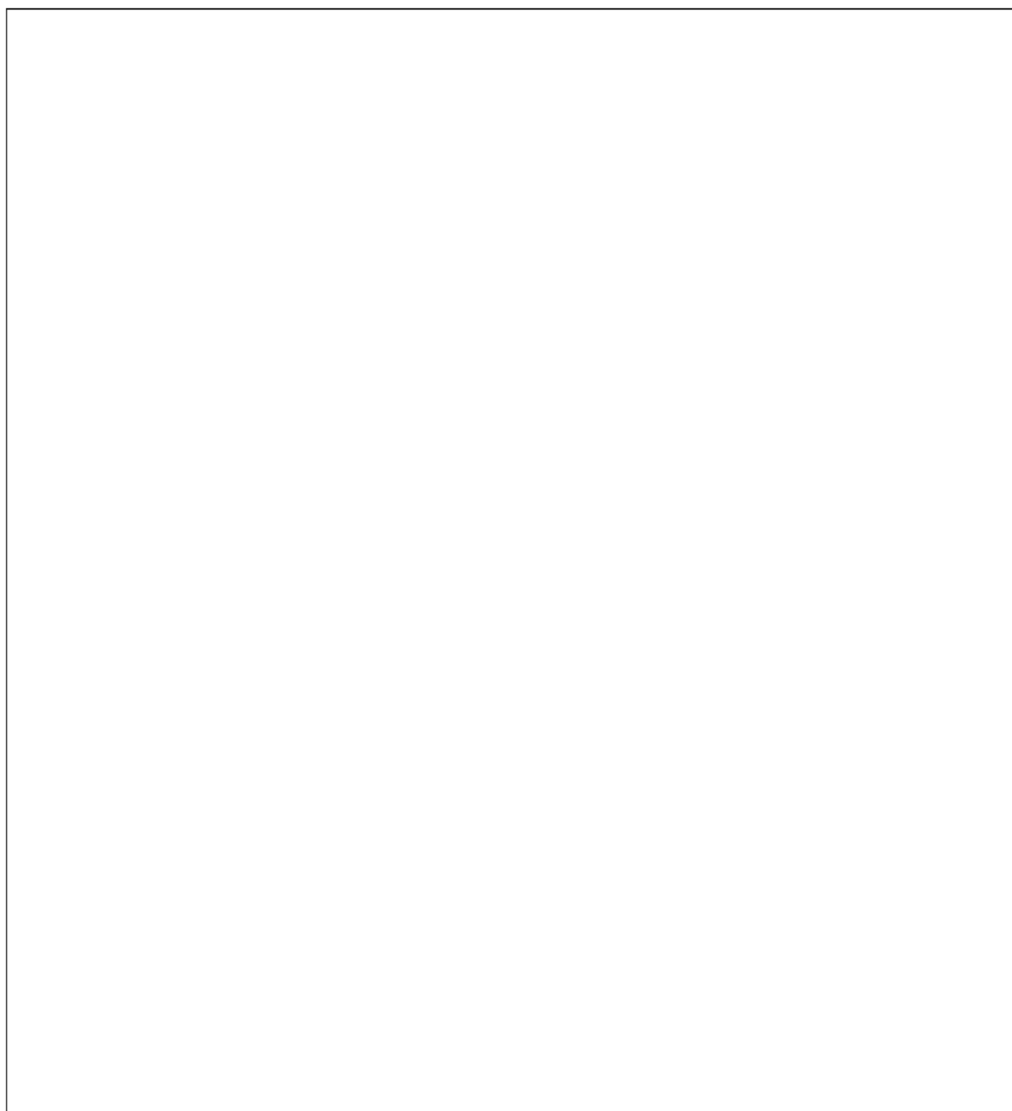
2 marks

How could you improve the quality and reliability of your calibration curves?

2 marks

Consider both of your calibration curves and discuss their accuracy and precision, ensuring that you address the following points:

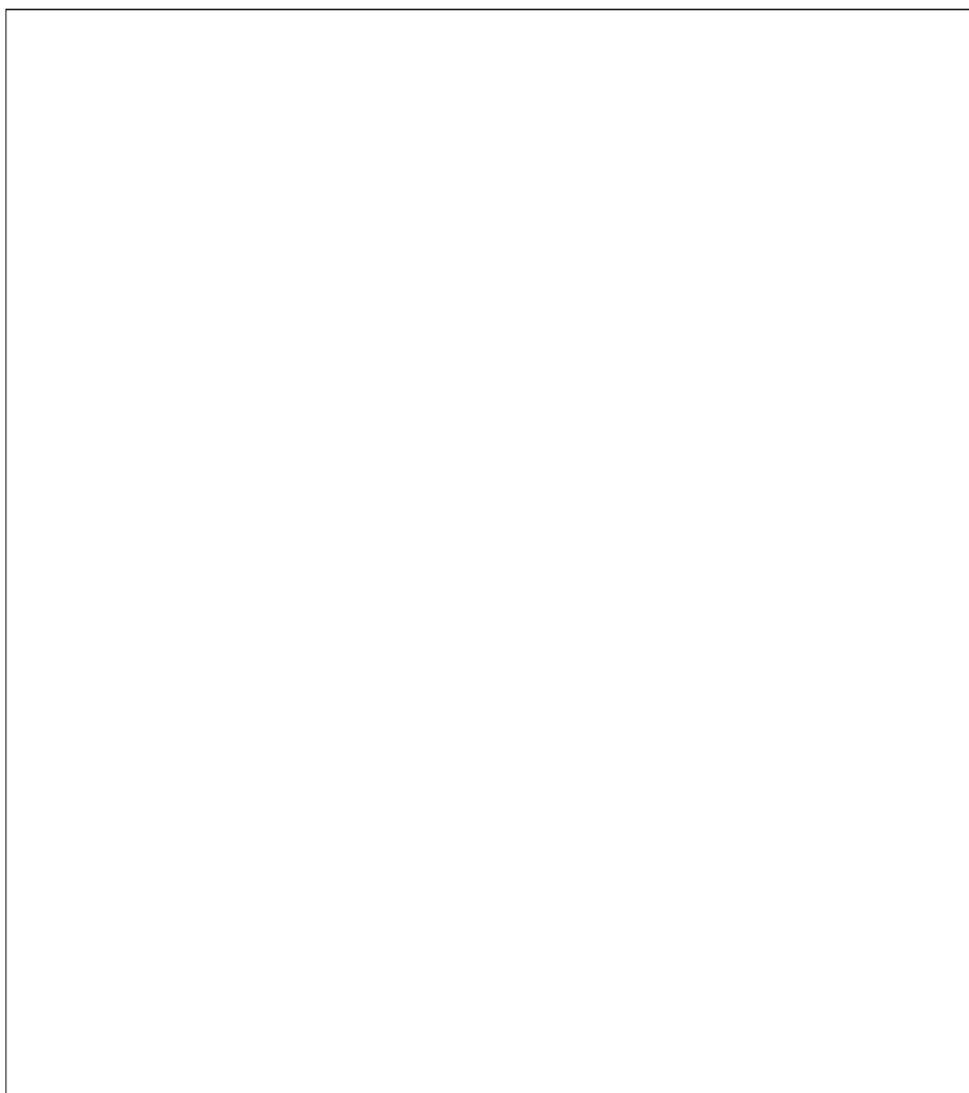
1. Quality of each calibration curve, judging by the R^2 values.
2. Anomalous points and reasoning for why they have occurred.
3. Accuracy of the individual points in the calibration curve – for example, did the sample intended to be 25% ee actually appear to be 25% ee in the NMR spectrum? If not, why not?
4. Which curve you feel will give the more accurate ee value.
5. Discuss the difference between accuracy and precision



7 marks

Consider the NMR data provided in the lab manual and also the spectra you produced:

1. Compare the NMR spectra of the starting materials (BINOL, MBA, FPBA) with the host complex produced. Are there any potential overlapping signals?
2. Are there any by-products or impurities present in the host complex NMR spectrum you recorded?
3. What effect will your answers to 1 and 2 have on the analysis of the NMR data?
4. Based on the NMR data, which signal do you think will give more accurate integrations and why?



7 marks

What is the function of molecular sieves and why are they added to this experiment? (State your literature reference)

3 marks

What sources of error were present in this experiment? How could these be overcome?

4 marks

Consider using this experimental procedure for the determination of the *ee* of other amines. Which NMR signals are general to this methodology (i.e. observed in any amine investigated) and which are specific to the use of α -methylbenzylamine?

2 marks

What are the limitations of the amines that can be studied in this experiment?

2 marks

10 References

- [1] H. C. Kolb, M. G. Finn, K. B. Sharpless, *Angew. Chem. Int. Ed.* **2001**, *40*, 2004-2021.
- [2] F. Fringuelli, O. Piermatti, F. Pizzo, L. Vaccaro, *J. Org. Chem.* **1999**, *64*, 6094-6096.
- [3] P. R. Florindo, D. M. Pereira, P. M. Borralho, C. M. P. Rodrigues, M. F. M. Piedade, A. C. Fernandes, *J. Med. Chem.* **2015**.
- [4] M. Jung, S. Lee, *Bioorg. Med. Chem. Lett.* **1998**, *8*, 1003-1006.
- [5] C. E. Hoyle, C. N. Bowman, *Angew. Chem. Int. Ed.* **2010**, *49*, 1540-1573.
- [6] M. Fiore, A. Marra, A. Dondoni, *J. Org. Chem.* **2009**, *74*, 4422-4425.
- [7] C. D. Heidecke, T. K. Lindhorst, *Chem. Eur. J.* **2007**, *13*, 9056-9067.
- [8] a) N. J. Agard, J. A. Prescher, C. R. Bertozzi, *J Am Chem Soc* **2004**, *126*, 15046-15047; b) I. Kii, A. Shiraishi, T. Hiramatsu, T. Matsushita, H. Uekusa, S. Yoshida, M. Yamamoto, A. Kudo, M. Hagiwara, T. Hosoya, *Org. Biomol. Chem.* **2010**, *8*, 4051-4055; c) L. S. Campbell-Verduyn, L. Mirfeizi, A. K. Schoonen, R. A. Dierckx, P. H. Elsinga, B. L. Feringa, *Angew. Chem. Int. Ed.* **2011**, *50*, 11117-11120; d) M. Shelbourne, X. Chen, T. Brown, A. H. El-Sagheer, *Chem. Commun.* **2011**, *47*, 6257-6259; e) J. Tummatorn, P. Batsomboon, R. J. Clark, I. V. Alabugin, G. B. Dudley, *J. Org. Chem.* **2012**, *77*, 2093-2097; f) S. Yoshida, Y. Hatakeyama, K. Johmoto, H. Uekusa, T. Hosoya, *J. Am. Chem. Soc.* **2014**, *136*, 13590-13593; g) C. G. S. Lima, A. Ali, S. S. van Berkel, B. Westermann, M. W. Paixao, *Chem. Commun.* **2015**.
- [9] a) C. W. Tornøe, C. Christensen, M. Meldal, *J. Org. Chem.* **2002**, *67*, 3057-3064; b) V. V. Rostovtsev, L. G. Green, V. V. Fokin, K. B. Sharpless, *Angew. Chem. Int. Ed.* **2002**, *41*, 2596-2599.
- [10] B. Schulze, U. S. Schubert, *Chem. Soc. Rev.* **2014**, *43*, 2522-2571.
- [11] F. Himo, T. Lovell, R. Hilgraf, V. V. Rostovtsev, L. Noodleman, K. B. Sharpless, V. V. Fokin, *J. Am. Chem. Soc.* **2005**, *127*, 210-216.
- [12] a) P. Siemsen, R. C. Livingston, F. Diederich, *Angew. Chem. Int. Ed.* **2000**, *39*, 2632-2657; b) R. D. Stephens, C. E. Castro, *J. Org. Chem.* **1963**, *28*, 3313-3315.
- [13] B. R. Buckley, S. E. Dann, H. Heaney, *Chem. Eur. J.* **2010**, *16*, 6278-6284.
- [14] V. O. Rodionov, V. V. Fokin, M. G. Finn, *Angew. Chem. Int. Ed.* **2005**, *44*, 2210-2215.
- [15] M. Ahlquist, V. V. Fokin, *Organometallics* **2007**, *26*, 4389-4391.
- [16] B. T. Worrell, J. A. Malik, V. V. Fokin, *Science* **2013**, *340*, 457-460.
- [17] C. Iacobucci, S. Reale, J.-F. Gal, F. De Angelis, *Angew. Chem. Int. Ed.* **2015**, *54*, 3065-3068.
- [18] L. Jin, D. R. Tolentino, M. Melaimi, G. Bertrand, *Sci. Adv.* **2015**, *1*.
- [19] A. Makarem, R. Berg, F. Rominger, B. F. Straub, *Angew. Chem. Int. Ed.* **2015**, *54*, 7431-7435.
- [20] M. Meldal, C. W. Tornøe, *Chem. Rev.* **2008**, *108*, 2952-3015.
- [21] S. I. Presolski, V. Hong, S.-H. Cho, M. G. Finn, *J. Am. Chem. Soc.* **2010**, *132*, 14570-14576.
- [22] E. J. Yoo, M. Ahlquist, S. H. Kim, I. Bae, V. V. Fokin, K. B. Sharpless, S. Chang, *Angew. Chem. Int. Ed.* **2007**, *46*, 1730-1733.
- [23] S. H. Cho, E. J. Yoo, I. Bae, S. Chang, *J. Am. Chem. Soc.* **2005**, *127*, 16046-16047.
- [24] L. D. Pachón, J. H. van Maarseveen, G. Rothenberg, *Adv. Synth. Catal.* **2005**, *347*, 811-815.
- [25] G. Molteni, C. L. Bianchi, G. Marinoni, N. Santo, A. Ponti, *New J. Chem.* **2006**, *30*, 1137-1139.

- [26] S. Chassaing, M. Kumarraja, A. Sani Souna Sido, P. Pale, J. Sommer, *Org. Lett.* **2007**, *9*, 883-886.
- [27] Y. M. A. Yamada, S. M. Sarkar, Y. Uozumi, *J. Am. Chem. Soc.* **2012**, *134*, 9285-9290.
- [28] H. Sharghi, R. Khalifeh, M. M. Doroodmand, *Adv. Synth. Catal.* **2009**, *351*, 207-218.
- [29] M. L. Kantam, V. S. Jaya, B. Sreedhar, M. M. Rao, B. M. Choudary, *J. Mol. Catal. A: Chem.* **2006**, *256*, 273-277.
- [30] I. S. Park, M. S. Kwon, Y. Kim, J. S. Lee, J. Park, *Org. Lett.* **2008**, *10*, 497-500.
- [31] T. Miao, L. Wang, *Synthesis* **2008**, *2008*, 363-368.
- [32] J.-c. Meng, V. V. Fokin, M. G. Finn, *Tetrahedron Lett.* **2005**, *46*, 4543-4546.
- [33] F. Zhou, C. Tan, J. Tang, Y.-Y. Zhang, W.-M. Gao, H.-H. Wu, Y.-H. Yu, J. Zhou, *J. Am. Chem. Soc.* **2013**, *135*, 10994-10997.
- [34] H. B. Kagan, *Adv. Synth. Catal.* **2001**, *343*, 227-233.
- [35] G. R. Stephenson, J. P. Buttress, D. Deschamps, M. Lancelot, J. P. Martin, A. I. G. Sheldon, C. Alayrac, A.-C. Gaumont, P. C. B. Page, *Synlett* **2013**, *24*, 2723-2729.
- [36] T. Song, L.-S. Zheng, F. Ye, W.-H. Deng, Y.-L. Wei, K.-Z. Jiang, L.-W. Xu, *Adv. Synth. Catal.* **2014**, *356*, 1708-1718.
- [37] T. Song, L. Li, W. Zhou, Z.-J. Zheng, Y. Deng, Z. Xu, L.-W. Xu, *Chem. Eur. J.* **2015**, *21*, 554-558.
- [38] M.-Y. Chen, T. Song, Z.-J. Zheng, Z. Xu, Y.-M. Cui, L.-W. Xu, *RSC Adv.* **2016**, *6*, 58698-58708.
- [39] C. Girard, H. B. Kagan, *Angew. Chem. Int. Ed.* **1998**, *37*, 2922-2959.
- [40] T. Osako, Y. Uozumi, *Org. Lett.* **2014**, *16*, 5866-5869.
- [41] T. Osako, Y. Uozumi, *Synlett* **2015**, *26*, 1475-1479.
- [42] W. D. G. Brittain, B. R. Buckley, J. S. Fossey, *ACS Catal.* **2016**, *6*, 3629-3636.
- [43] H. B. Kagan, J. C. Fiaud, in *Topics in Stereochemistry*, John Wiley & Sons, Inc., **2007**, pp. 249-330.
- [44] A. Ghanem, H. Y. Aboul-Enein, *Chirality* **2005**, *17*, 1-15.
- [45] John M. Keith, Jay F. Larrow, Eric N. Jacobsen, *Adv. Synth. Catal.* **2001**, *343*, 5-26.
- [46] S. Arai, S. Bellemin-Laponnaz, G. C. Fu, *Angew. Chem. Int. Ed.* **2001**, *40*, 234-236.
- [47] J. C. Ruble, H. A. Latham, G. C. Fu, *J. Am. Chem. Soc.* **1997**, *119*, 1492-1493.
- [48] J. Liang, J. C. Ruble, G. C. Fu, *J. Org. Chem.* **1998**, *63*, 3154-3155.
- [49] M. Binanzer, S.-Y. Hsieh, J. W. Bode, *J. Am. Chem. Soc.* **2011**, *133*, 19698-19701.
- [50] B. Tao, J. C. Ruble, D. A. Hoic, G. C. Fu, *J. Am. Chem. Soc.* **1999**, *121*, 5091-5092.
- [51] A. Peschiulli, B. Procuranti, C. J. O' Connor, S. J. Connon, *Nat Chem* **2010**, *2*, 380-384.
- [52] a) R. S. Ward, *Tetrahedron: Asymmetry* **1995**, *6*, 1475-1490; b) H. Pellissier, *Tetrahedron* **2003**, *59*, 8291-8327.
- [53] a) J. Eames, *Angew. Chem. Int. Ed.* **2000**, *39*, 885-888; b) E. Vedejs, X. Chen, *J. Am. Chem. Soc.* **1997**, *119*, 2584-2585.
- [54] G. C. Tron, T. Pirali, R. A. Billington, P. L. Canonico, G. Sorba, A. A. Genazzani, *Med. Res. Rev.* **2008**, *28*, 278-308.
- [55] G. Zhang, L. Fang, L. Zhu, D. Sun, P. G. Wang, *Biorg. Med. Chem.* **2006**, *14*, 426-434.
- [56] P. Thirumurugan, D. Matosiuk, K. Jozwiak, *Chem. Rev.* **2013**, *113*, 4905-4979.
- [57] a) R. He, Z. Yu, Y. He, L.-F. Zeng, J. Xu, L. Wu, A. M. Gunawan, L. Wang, Z.-X. Jiang, Z.-Y. Zhang, *ChemMedChem* **2010**, *5*, 2051-2056; b) X.-P. He, Q. Deng, L.-X. Gao, C. Li, W. Zhang, Y.-B. Zhou, Y. Tang, X.-X. Shi, J. Xie, J. Li, G.-R. Chen, K.

- Chen, *Bioorg. Med. Chem.* **2011**, *19*, 3892-3900; c) X.-P. He, C. Li, X.-P. Jin, Z. Song, H.-L. Zhang, C.-J. Zhu, Q. Shen, W. Zhang, L. Sheng, X.-X. Shi, Y. Tang, J. Li, G.-R. Chen, J. Xie, *New J. Chem.* **2011**, *35*, 622-631; d) C. Li, X.-P. He, Y.-J. Zhang, Z. Li, L.-X. Gao, X.-X. Shi, J. Xie, J. Li, G.-R. Chen, Y. Tang, *Eur. J. Med. Chem.* **2011**, *46*, 4212-4218; e) J.-W. Yang, X.-P. He, C. Li, L.-X. Gao, L. Sheng, J. Xie, X.-X. Shi, Y. Tang, J. Li, G.-R. Chen, *Bioorg. Med. Chem. Lett.* **2011**, *21*, 1092-1096.
- [58] a) G. Pintér, I. Bereczki, G. Batta, R. Ötvös, F. Sztaricskai, E. Róth, E. Ostorházi, F. Rozgonyi, L. Naesens, M. Szarvas, Z. Boda, P. Herczegh, *Bioorg. Med. Chem. Lett.* **2010**, *20*, 2713-2717; b) P. B. Reddy, S. K. Agrawal, S. Singh, B. A. Bhat, A. K. Saxena, H. M. S. Kumar, G. N. Qazi, *Chem. Biodivers.* **2008**, *5*, 1792-1802; c) G. C. Tron, T. Pirali, R. A. Billington, P. L. Canonico, G. Sorba, A. A. Genazzani, *Med. Res. Rev.* **2008**, *28*, 278-308.
- [59] A. H. El-Sagheer, T. Brown, *Chem. Soc. Rev.* **2010**, *39*, 1388-1405.
- [60] F. Seela, V. R. Sirivolu, P. Chittepu, *Bioconjugate Chem.* **2008**, *19*, 211-224.
- [61] A. Nuzzi, A. Massi, A. Dondoni, *QSAR Comb. Sci.* **2007**, *26*, 1191-1199.
- [62] a) W. Zhai, B. M. Chapin, A. Yoshizawa, H.-C. Wang, S. A. Hodge, T. D. James, E. V. Anslyn, J. S. Fossey, *Org. Chem. Front.* **2016**, *3*, 918-928; b) W. Zhai, L. Male, J. S. Fossey, *Chem Commun* **2017**, *53*, 2218-2221.
- [63] S. Raja, C. Satheeshkumar, P. Rajakumar, S. Ganesan, P. Maruthamuthu, *J. Mater. Chem.* **2011**, *21*, 7700-7704.
- [64] R. K. Iha, K. L. Wooley, A. M. Nyström, D. J. Burke, M. J. Kade, C. J. Hawker, *Chem. Rev.* **2009**, *109*, 5620-5686.
- [65] V. Ganesh, V. S. Sudhir, T. Kundu, S. Chandrasekaran, *Chem. Asian J.* **2011**, *6*, 2670-2694.
- [66] J.-J. Shie, Y.-C. Liu, J.-C. Hsiao, J.-M. Fang, C.-H. Wong, *Chem. Commun.* **2017**.
- [67] a) V. Aucagne, J. Berná, J. D. Crowley, S. M. Goldup, K. D. Hänni, D. A. Leigh, P. J. Lusby, V. E. Ronaldson, A. M. Z. Slawin, A. Viterisi, D. B. Walker, *J. Am. Chem. Soc.* **2007**, *129*, 11950-11963; b) R. Chinchilla, C. Nájera, *Chem. Rev.* **2014**, *114*, 1783-1826; c) G. Fang, X. Bi, *Chem. Soc. Rev.* **2015**, *44*, 8124-8173; d) A. Fürstner, *Angew. Chem. Int. Ed.* **2013**, *52*, 2794-2819; e) A. M. Lozano-Vila, S. Monsaert, A. Bajek, F. Verpoort, *Chem. Rev.* **2010**, *110*, 4865-4909.
- [68] Y.-Y. Zhu, C. Cui, N. Li, B.-W. Wang, Z.-M. Wang, S. Gao, *Eur. J. Inorg. Chem.* **2013**, *2013*, 3101-3111.
- [69] H. Nishiyama, M. Kondo, T. Nakamura, K. Itoh, *Organometallics* **1991**, *10*, 500-508.
- [70] a) L. S. Campbell-Verduyn, L. Mirfeizi, R. A. Dierckx, P. H. Elsinga, B. L. Feringa, *Chem. Commun.* **2009**, 2139-2141; b) J. F. Teichert, B. L. Feringa, *Angew. Chem. Int. Ed.* **2010**, *49*, 2486-2528.
- [71] L. Jin, E. A. Romero, M. Melaimi, G. Bertrand, *J. Am. Chem. Soc.* **2015**.
- [72] a) J. Díez, M. P. Gamasa, M. Panera, *Inorg. Chem.* **2006**, *45*, 10043-10045; b) M. Panera, J. Díez, I. Merino, E. Rubio, M. P. Gamasa, *Inorg. Chem.* **2009**, *48*, 11147-11160.
- [73] J. E. Hein, V. V. Fokin, *Chem. Soc. Rev.* **2010**, *39*, 1302-1315.
- [74] The work detailed in this section was carried out by William Brittain. Some ligand screening was carried out at the University of Utah, these ligands were kindly donated by Professor Matthew Sigman. The primary investigators of this work were Dr John Fossey and Dr Benjamin Buckley. All interpretations of the data are the work of William Brittain.
- [75] W. D. Brittain, B. R. Buckley, J. S. Fossey, *Chem Commun* **2015**, *51*, 17217-17220.

- [76] K. Tanaka, G. C. Fu, *J. Am. Chem. Soc.* **2003**, *125*, 8078-8079.
- [77] At the time of this work deuterated 2,5-hexanedione was not commercially available. However, since this solvent has become commercially available.
- [78] In this section stereochemical nomenclature to describe diastereoisomers works in this way. The first letter inside the brackets refers to the stereochemical descriptor at the oxindole stereogenic centre, the second letter within the brackets refers to stereochemical descriptor at the stereogenic centre adjacent to the triazole ring.
- [79] A. S. Thompson, G. R. Humphrey, A. M. DeMarco, D. J. Mathre, E. J. J. Grabowski, *J. Org. Chem.* **1993**, *58*, 5886-5888.
- [80] Work in this section was carried out jointly between Andrew Dalling and William Brittain. The crystal structures were solved by William Brittain with a suitable crystal of single enantiomer iodo alkyne grown by Zhenquan Sun. Unlocked NMR data was obtained by Cécile Le Duff. The primary investigators of this work were Dr John Fossey and Dr Benjamin Buckley. All interpretations of the data are the work of William Brittain.
- [81] H. H. Jo, C.-Y. Lin, E. V. Anslyn, *Acc. Chem. Res.* **2014**, *47*, 2212-2221.
- [82] H. H. Jo, X. Gao, L. You, E. V. Anslyn, M. J. Krische, *Chem. Sci.* **2015**, *6*, 6747-6753.
- [83] P. Metola, E. V. Anslyn, T. D. James, S. D. Bull, *Chem. Sci.* **2012**, *3*, 156-161.
- [84] L. You, J. S. Berman, A. Lucksanawichien, E. V. Anslyn, *J. Am. Chem. Soc.* **2012**, *134*, 7126-7134.
- [85] C.-Y. Lin, S. Lim, E. V. Anslyn, *J. Am. Chem. Soc.* **2016**, *138*, 8045-8047.
- [86] Y. Okamoto, E. Yashima, *Angew. Chem. Int. Ed.* **1998**, *37*, 1020-1043.
- [87] a) C. Dalvit, M. Flocco, S. Knapp, M. Mostardini, R. Perego, B. J. Stockman, M. Veronesi, M. Varasi, *J. Am. Chem. Soc.* **2002**, *124*, 7702-7709; b) M. T. Reetz, A. Eipper, P. Tielmann, R. Mynott, *Adv. Synth. Catal.* **2002**, *344*, 1008-1016; c) A. Chen, M. J. Shapiro, *J. Am. Chem. Soc.* **2000**, *122*, 414-415.
- [88] a) H. L. Goering, J. N. Eikenberry, G. S. Koermer, *J. Am. Chem. Soc.* **1971**, *93*, 5913-5914; b) J. Kido, Y. Okamoto, H. G. Brittain, *J. Org. Chem.* **1991**, *56*, 1412-1415; c) M. D. McCreary, D. W. Lewis, D. L. Wernick, G. M. Whitesides, *J. Am. Chem. Soc.* **1974**, *96*, 1038-1054.
- [89] a) J. A. Dale, H. S. Mosher, *J. Am. Chem. Soc.* **1973**, *95*, 512-519; b) M. E. Powell, C. D. Evans, S. D. Bull, T. D. James, P. S. Fordred, in *Comprehensive Chirality*, Elsevier, Amsterdam, **2012**, pp. 571-599.
- [90] a) J. A. Dale, D. L. Dull, H. S. Mosher, *J. Org. Chem.* **1969**, *34*, 2543-2549; b) D. L. Dull, H. S. Mosher, *J. Am. Chem. Soc.* **1967**, *89*, 4230-4230.
- [91] D. A. Allen, A. E. Tomaso, O. P. Priest, D. F. Hindson, J. L. Hurlburt, *J. Chem. Educ.* **2008**, *85*, 698.
- [92] Y. Perez-Fuertes, A. M. Kelly, J. S. Fossey, M. E. Powell, S. D. Bull, T. D. James, *Nat. Protocols* **2008**, *3*, 210-214.
- [93] a) A. M. Kelly, Y. Perez-Fuertes, J. S. Fossey, S. L. Yeste, S. D. Bull, T. D. James, *Nat. Protocols* **2008**, *3*, 215-219; b) A. M. Kelly, S. D. Bull, T. D. James, *Tetrahedron: Asymmetry* **2008**, *19*, 489-494; c) A. M. Kelly, Y. Pérez-Fuertes, S. Arimori, S. D. Bull, T. D. James, *Org. Lett.* **2006**, *8*, 1971-1974; d) Y. Pérez-Fuertes, A. M. Kelly, A. L. Johnson, S. Arimori, S. D. Bull, T. D. James, *Org. Lett.* **2006**, *8*, 609-612; e) M. E. Powell, A. M. Kelly, S. D. Bull, T. D. James, *Tetrahedron Lett.* **2009**, *50*, 876-879; f) D. A. Tickell, M. F. Mahon, S. D. Bull, T. D. James, *Org. Lett.* **2013**, *15*, 860-863; g) G. Mirri, S. D. Bull, P. N. Horton, T. D. James, L. Male, J. H.

- R. Tucker, *J. Am. Chem. Soc.* **2010**, *132*, 8903-8905; h) S. L. Yeste, M. E. Powell, S. D. Bull, T. D. James, *J. Org. Chem.* **2009**, *74*, 427-430.
- [94] B. Tang, C. D. Bray, G. Pattenden, *Org. Biomol. Chem.* **2009**, *7*, 4448-4457.
- [95] B. E. Collins, P. Metola, E. V. Anslyn, *Supramol. Chem.* **2013**, *25*, 79-86.
- [96] This work was carried out as part of an international collaboration with Professor Eric Anslyn at the University of Texas at Austin. Experimental work was carried out at the University of Birmingham and University of Texas. The experiments carried out in this section were carried out by William Brittain, Brette Chapin and Wenlei Zhai. Crystal structure was solved by Vincent Lynch. The primary investigators of this work were Dr John Fossey and Professor Eric Anslyn. All interpretations of the data are the work of William Brittain.
- [97] W. D. Brittain, B. M. Chapin, W. Zhai, V. M. Lynch, B. R. Buckley, E. V. Anslyn, J. S. Fossey, *Org. Biomol. Chem.* **2016**, *14*, 10778-10782.
- [98] O. Ramström, J.-M. Lehn, *Nat. Rev. Drug Discov.* **2002**, *1*, 26-36.
- [99] M. C. Thompson, D. H. Busch, *J. Am. Chem. Soc.* **1962**, *84*, 1762-1763.
- [100] P. T. Corbett, J. Leclaire, L. Vial, K. R. West, J.-L. Wietor, J. K. M. Sanders, S. Otto, *Chem. Rev.* **2006**, *106*, 3652-3711.
- [101] B. M. Chapin, P. Metola, V. M. Lynch, J. F. Stanton, T. D. James, E. V. Anslyn, *J. Org. Chem.* **2016**, *81*, 8319-8330.
- [102] All of the work within this section was carried out by William Brittain at the University of Texas at Austin under the supervision of Professor Eric Anslyn. All interpretations of data are the work of William Brittain.
- [103] This project was carried out as a collaboration between the University of Birmingham, University of Bath and the University of Texas at Austin. Work in this section was carried out by William Brittain, Brette Chapin, Daniel Payne, Glenn Lees, Kimberley Roper, Charles Manville, Jennifer Lloyd, Cécile Le Duff and Stephanie Lim. Academic input was given by Professor Tony James, Dr Steven Bull and Professor Eric Anslyn. The primary investigator of this work was Dr John Fossey. All interpretations of data are the work of William Brittain.
- [104] J. S. Fossey, E. V. Anslyn, W. D. G. Brittain, S. D. Bull, B. M. Chapin, C. S. Le Duff, T. D. James, G. Lees, S. Lim, J. A. C. Lloyd, C. V. Manville, D. T. Payne, K. A. Roper, *J. Chem. Educ.* **2016**, *94*, 79-84.
- [105] a) D. M. Flanigan, F. Romanov-Michailidis, N. A. White, T. Rovis, *Chem. Rev.* **2015**, *115*, 9307-9387; b) F. Glorius, *N-Heterocyclic Carbenes in Transition Metal Catalysis*, Springer Berlin Heidelberg, **2007**, pp 21-193; c) H. D. Velazquez, F. Verpoort, *Chem. Soc. Rev.* **2012**, *41*, 7032-7060.
- [106] a) F. Wang, L.-j. Liu, W. Wang, S. Li, M. Shi, *Coord. Chem. Rev.* **2012**, *256*, 804-853; b) R. C. West, A. F. Hill, *Advances in Organometallic Chemistry*, Elsevier Science, **2001**, pp. 35-55.
- [107] S. P. Nolan, *N-Heterocyclic Carbenes in Synthesis*, Wiley, **2006**, Chapters 3-13, pp. 39-393.
- [108] a) R. B. Strand, T. Solvang, C. A. Sperger, A. Fiksdahl, *Tetrahedron: Asymmetry* **2012**, *23*, 838-842; b) M. S. Kerr, J. Read de Alaniz, T. Rovis, *J. Org. Chem.* **2005**, *70*, 5725-5728.
- [109] a) R. Srinivasan, L. P. Tan, H. Wu, P.-Y. Yang, K. A. Kalesh, S. Q. Yao, *Org. Biomol. Chem.* **2009**, *7*, 1821-1828; b) I. Carvalho, P. Andrade, V. L. Campo, P. M. M. Guedes, R. Sesti-Costa, J. S. Silva, S. Schenkman, S. Dedola, L. Hill, M. Rejzek, S. A. Nepogodiev, R. A. Field, *Biorg. Med. Chem.* **2010**, *18*, 2412-2427.

- [110] a) S. Gladiali, E. Alberico, *Chem. Soc. Rev.* **2006**, *35*, 226-236; b) W. Tang, X. Zhang, *Chem. Rev.* **2003**, *103*, 3029-3070.
- [111] K. F. Donnelly, A. Petronilho, M. Albrecht, *Chem. Commun.* **2013**, *49*, 1145-1159.
- [112] a) D. Canseco-Gonzalez, M. Albrecht, *Dalton Trans.* **2013**, *42*, 7424-7432; b) D. Canseco-Gonzalez, A. Gniewek, M. Szulmanowicz, H. Müller-Bunz, A. M. Trzeciak, M. Albrecht, *Chem. Eur. J.* **2012**, *18*, 6055-6062; c) D. Canseco-Gonzalez, A. Petronilho, H. Mueller-Bunz, K. Ohmatsu, T. Ooi, M. Albrecht, *J. Am. Chem. Soc.* **2013**, *135*, 13193-13203; d) P. Mathew, A. Neels, M. Albrecht, *J. Am. Chem. Soc.* **2008**, *130*, 13534-13535; e) K. J. Kilpin, U. S. D. Paul, A.-L. Lee, J. D. Crowley, *Chem. Commun.* **2011**, *47*, 328-330.
- [113] J. M. Brunel, *Chem. Rev.* **2007**, *107*, PR1-PR45.
- [114] A. C. Spivey, P. Charbonneau, T. Fekner, D. H. Hochmuth, A. Maddaford, C. Malardier-Jugroot, A. J. Redgrave, M. A. Whitehead, *J. Org. Chem.* **2001**, *66*, 7394-7401.
- [115] J. Wu, A. S. C. Chan, *Acc. Chem. Res.* **2006**, *39*, 711-720.
- [116] L. Xu, K. H. Lam, J. Ji, J. Wu, Q.-H. Fan, W.-H. Lo, A. S. C. Chan, *Chem. Commun.* **2005**, 1390-1392.
- [117] F. Faigl, G. Tárkányi, K. Fogassy, D. Tepfenhardt, A. Thurner, *Tetrahedron* **2008**, *64*, 1371-1377.
- [118] Unpublished results by Mark Dutton.
- [119] R. Chinchilla, C. Najera, *Chem. Soc. Rev.* **2011**, *40*, 5084-5121.
- [120] G. T. Crisp, Y.-L. Jiang, *Synth. Commun.* **1998**, *28*, 2571-2576.
- [121] D. Ginsburg, R. Robinson, *Concerning Amines: Their Properties, Preparation and Reactions*, Elsevier Science, **2016**, pp. 75-78.
- [122] L. Li, G. Zhang, A. Zhu, L. Zhang, *J. Org. Chem.* **2008**, *73*, 3630-3633.
- [123] J. E. Hein, J. C. Tripp, L. B. Krasnova, K. B. Sharpless, V. V. Fokin, *Angew. Chem. Int. Ed.* **2009**, *48*, 8018-8021.
- [124] a) E. Larionov, M. Mahesh, A. C. Spivey, Y. Wei, H. Zipse, *J. Am. Chem. Soc.* **2012**, *134*, 9390-9399; b) A. C. Spivey, T. Fekner, S. E. Spey, *J. Org. Chem.* **2000**, *65*, 3154-3159; c) A. C. Spivey, D. P. Leese, F. Zhu, S. G. Davey, R. L. Jarvest, *Tetrahedron* **2004**, *60*, 4513-4525; d) J. M. Roselló, S. Staniland, N. J. Turner, J. Clayden, *Tetrahedron* **2016**, *72*, 5172-5177; e) J. D. Jolliffe, R. J. Armstrong, M. D. Smith, *Nat Chem* **2017**, advance online publication.
- [125] S. Staniland, R. W. Adams, J. J. W. McDouall, I. Maffucci, A. Contini, D. M. Grainger, N. J. Turner, J. Clayden, *Angew. Chem. Int. Ed.* **2016**, *55*, 10755-10759.
- [126] Work in this section was carried out by William Brittain. The primary investigators of this work were Dr John Fossey and Dr Benjamin Buckley.
- [127] a) G. C. Fu, *Acc. Chem. Res.* **2004**, *37*, 542-547; b) E. Vedejs, X. Chen, *J. Am. Chem. Soc.* **1996**, *118*, 1809-1810; c) T. Kawabata, M. Nagato, K. Takasu, K. Fuji, *J. Am. Chem. Soc.* **1997**, *119*, 3169-3170.
- [128] K. Kondo, K. Kan, Y. Tanada, M. Bando, T. Shinohara, M. Kurimura, H. Ogawa, S. Nakamura, T. Hirano, Y. Yamamura, M. Kido, T. Mori, M. Tominaga, *J. Med. Chem.* **2002**, *45*, 3805-3808.
- [129] A. Fürstner, M. Albert, J. Mlynarski, M. Matheu, E. DeClercq, *J. Am. Chem. Soc.* **2003**, *125*, 13132-13142.
- [130] B. C. Boren, S. Narayan, L. K. Rasmussen, L. Zhang, H. Zhao, Z. Lin, G. Jia, V. V. Fokin, *J. Am. Chem. Soc.* **2008**, *130*, 8923-8930.
- [131] 3D Models were constructed using ChemBio 3D Ultra 13.0.

- [132] Work in this section was carried out jointly between Daniel Payne and William Brittain. The primary investigator of this work was Dr John Fossey. All interpretations of the data are those of William Brittain.
- [133] Y. Angell, K. Burgess, *Angew. Chem. Int. Ed.* **2007**, *46*, 3649-3651.
- [134] C. J. Brassard, X. Zhang, C. R. Brewer, P. Liu, R. J. Clark, L. Zhu, *J. Org. Chem.* **2016**.
- [135] J. González, V. M. Pérez, D. O. Jiménez, G. Lopez-Valdez, D. Corona, E. Cuevas-Yañez, *Tetrahedron Lett.* **2011**, *52*, 3514-3517.
- [136] The work detailed in this section was carried out by William Brittain. The primary investigators of this work were Dr John Fossey and Dr Benjamin Buckley. All interpretations of the data are the work of William Brittain.
- [137] a) S. T. Nguyen, L. K. Johnson, R. H. Grubbs, J. W. Ziller, *J. Am. Chem. Soc.* **1992**, *114*, 3974-3975; b) P. Schwab, R. H. Grubbs, J. W. Ziller, *J. Am. Chem. Soc.* **1996**, *118*, 100-110; c) P. Schwab, M. B. France, J. W. Ziller, R. H. Grubbs, *Angew. Chem. Int. Ed.* **1995**, *34*, 2039-2041.
- [138] S. J. Connon, S. Blechert, *Angew. Chem. Int. Ed.* **2003**, *42*, 1900-1923.
- [139] S. Sutthasupa, M. Shiotsuki, F. Sanda, *Polym J* **2010**, *42*, 905-915.
- [140] T. J. Seiders, D. W. Ward, R. H. Grubbs, *Org. Lett.* **2001**, *3*, 3225-3228.
- [141] H. Villar, M. Frings, C. Bolm, *Chem. Soc. Rev.* **2007**, *36*, 55-66.
- [142] F. López, A. Delgado, J. R. Rodríguez, L. Castedo, J. L. Mascareñas, *J. Am. Chem. Soc.* **2004**, *126*, 10262-10263.
- [143] U. Pradere, V. Roy, T. R. McBrayer, R. F. Schinazi, L. A. Agrofoglio, *Tetrahedron* **2008**, *64*, 9044-9051.
- [144] M. Zhu, B. J. Lim, M. Koh, S. B. Park, *ACS Comb. Sci.* **2012**, *14*, 124-134.
- [145] T. Biet, T. Cauchy, N. Avarvari, *Chem. Eur. J.* **2012**, *18*, 16097-16103.
- [146] a) S. Alvarez, S. Medina, G. Domínguez, J. Pérez-Castells, *J. Org. Chem.* **2013**, *78*, 9995-10001; b) K. Kirchner, M. J. Calhorda, R. Schmid, L. F. Veiros, *J. Am. Chem. Soc.* **2003**, *125*, 11721-11729.
- [147] J. Risse, R. Scopelliti, K. Severin, *Organometallics* **2011**, *30*, 3412-3418.
- [148] K. Tonogaki, M. Mori, *Tetrahedron Lett.* **2002**, *43*, 2235-2238.
- [149] The work in this section was carried out jointly between Daniel Payne and William Brittain. The primary investigator of this work was Dr John Fossey. All interpretations of the data are the work of William Brittain.
- [150] G. C. Vougioukalakis, R. H. Grubbs, *Chem. Rev.* **2010**, *110*, 1746-1787.
- [151] R. S. Menon, A. T. Biju, V. Nair, *Beilstein J. Org. Chem.* **2016**, *12*, 444-461.
- [152] R. Kuniyil, R. B. Sunoj, *Org. Lett.* **2013**, *15*, 5040-5043.
- [153] a) E. Tayama, Y. Toma, *Tetrahedron* **2015**, *71*, 554-559; b) Y.-S. Gal, W.-C. Lee, S.-H. Jin, K. T. Lim, S.-H. Jang, W. S. Lyoo, E. Han, S. Y. Kim, *Macromol. Res.* **2007**, *15*, 267-271.
- [154] S. Zhao, X. Zhang, Y. Zhang, H. Yang, Y. Huang, K. Zhang, T. Du, *New J. Chem.* **2015**, *39*, 7734-7737.
- [155] C. Rossy, J. Majimel, M. T. Delapierre, E. Fouquet, F.-X. Felpin, *J. Organomet. Chem.* **2014**, *755*, 78-85.
- [156] S. S. Kulkarni, X. Hu, R. Manetsch, *Chem. Commun.* **2013**, *49*, 1193-1195.
- [157] S. Pramanik, P. Ghorai, *Org. Lett.* **2014**, *16*, 2104-2107.
- [158] M. K. Lakshman, M. K. Singh, M. Kumar, R. R. Chamala, V. R. Yedulla, D. Wagner, E. Leung, L. Yang, A. Matin, S. Ahmad, *Beilstein J. Org. Chem.* **2014**, *10*, 1919-1932.

- [159] C. Shao, X. Wang, J. Xu, J. Zhao, Q. Zhang, Y. Hu, *J. Org. Chem.* **2010**, *75*, 7002-7005.
- [160] L. Ye, W. He, L. Zhang, *J. Am. Chem. Soc.* **2010**, *132*, 8550-8551.
- [161] Z. Ni, L. Giordano, A. Tenaglia, *Chem. Eur. J.* **2014**, *20*, 11703-11706.
- [162] Y. Nishibayashi, M. D. Milton, Y. Inada, M. Yoshikawa, I. Wakiji, M. Hidai, S. Uemura, *Chem. Eur. J.* **2005**, *11*, 1433-1451.
- [163] B. M. Nilsson, U. Hacksell, *J. Heterocycl. Chem.* **1989**, *26*, 269-275.
- [164] D. Castagnolo, F. Dessì, M. Radi, M. Botta, *Tetrahedron: Asymmetry* **2007**, *18*, 1345-1350.
- [165] T. Kim, J. H. Song, K. H. Jeong, S. Lee, J. Ham, *Eur. J. Org. Chem.* **2013**, *2013*, 3992-3996.
- [166] D. Yuan, H. V. Huynh, *Organometallics* **2012**, *31*, 405-412.
- [167] I. T. Alt, B. Plietker, *Angew. Chem. Int. Ed.* **2016**, *55*, 1519-1522.
- [168] Y. Yamamoto, K. Matsui, M. Shibuya, *Chem. Eur. J.* **2015**, *21*, 7245-7255.
- [169] M. Juriček, K. Stout, P. H. J. Kouwer, A. E. Rowan, *Org. Lett.* **2011**, *13*, 3494-3497.
- [170] D. Lehnerr, J. M. Alzola, E. B. Lobkovsky, W. R. Dichtel, *Chem. Eur. J.* **2015**, *21*, 18122-18127.
- [171] Y. Zhang, Y. Zhang, Y. L. Sun, X. Du, J. Y. Shi, W. D. Wang, W. Wang, *Chem. Eur. J.* **2012**, *18*, 6328-6334.
- [172] L. Zhang, X. Chen, P. Xue, H. H. Y. Sun, I. D. Williams, K. B. Sharpless, V. V. Fokin, G. Jia, *J. Am. Chem. Soc.* **2005**, *127*, 15998-15999.
- [173] CrysAlisPro. Agilent Technologies (2013). Agilent Technologies UK Ltd., Oxford, UK, SuperNova CCD System, CrysAlisPro Software System, 1.171.37.31.
- [174] L. Palatinus, G. Chapuis, *J. Appl. Crystallogr.* **2007**, *40*, 786-790.
- [175] $R_w(F^2) = \{ \sum w(|F_o|^2 - |F_c|^2)^2 / \sum w(|F_o|^4) \}^{1/2}$ where w is the weight given each reflection. $R(F) = \sum (|F_o| - |F_c|) / \sum |F_o|$ for reflections with $F_o > 4(\sigma(F_o))$. $S = [\sum w(|F_o|^2 - |F_c|^2)^2 / (n - p)]^{1/2}$, where n is the number of reflections and p is the number of refined parameters.
- [176] W. S. Knowles, *Acc. Chem. Res.* **1983**, *16*, 106-112.
- [177] W. S. Knowles, *Angew. Chem. Int. Ed.* **2002**, *41*, 1998-2007.
- [178] W. S. Knowles, *J. Chem. Ed.* **1986**, *63*, 222.
- [179] A. Aitken, S. N. Kilenyi, *Asymmetric Synthesis*, Taylor & Francis, **1992**.

